CP1 DOMAIN OF LEUCYL-tRNA SYNTHETASE: DISSECTING ITS DUAL ROLES IN AMINO ACID EDITING AND RNA SPLICING

BY

JAYA SARKAR

DISSERTATION

Submitted in partial fulfillment of the requirements
for the degree of Doctor of Philosophy in Biochemistry
in the Graduate College of the
University of Illinois at Urbana-Champaign, 2012

Urbana, Illinois

Doctoral Committee:

Professor Susan A. Martinis, Chair
Professor David M. Kranz
Professor Scott K. Silverman
Associate Professor Emad Tajkhorshid

Abstract

The essential family of aminoacyl-tRNA synthetase (AARS) enzymes catalyzes the attachment of an amino acid to its cognate tRNA during ribosome-based translation of mRNA. Leucyl-tRNA synthetase (LeuRS) ensures fidelity in protein synthesis via proofreading or editing mechanisms. The editing that hydrolyzes noncognate amino acids mischarged onto $tRNA^{Leu}$ is called post-transfer editing. The hydrolytic post-transfer editing active site is located in a discretely folded polypeptide insertion called connective polypeptide 1 (CP1) that is linked to the enzyme's main body by two flexible β-strand linkers. Disruption of the CP1 domain-based editing function in LeuRS results in amino acid toxicities that compromise cell viability. A fluorescence-based *in vivo* assay was designed to quantify the effects of editing defects and hence assess the limits of mistranslation that can be borne by the cell. Sequence enabled reassembly of N and C-terminal fragments of the green fluorescence protein (GFP) were studied *in vivo* in the presence of editing defective LeuRS and noncognate amino acids.

In the yeast cytoplasmic LeuRS (ycLeuRS), the conserved post-transfer editing pocket is the target binding site for a novel class of benzoxaborole-based antimicrobials that trap $tRNA^{Leu}$ and halt protein synthesis. Resistance mutations (D487G and D487N) to the antimicrobial compound AN2690 lie outside the drug binding pocket and provided a unique opportunity to study editing mechanisms in the ycLeuRS. The Asp487 residue is located in a CP1 domain-based eukaryote-specific flexible insert called I4 that forms a 'cap' over the benzoxaborole-AMP adduct bound in the CP1 domain editing active site. Mutational and biochemical analysis at Asp487 identified a salt bridge between Asp487 and Arg316 in the hinge region of the I4 cap that is critical to tRNA deacylation. Thus, this electrostatic interaction stabilizes the cap during binding of the editing substrate for hydrolysis in the ycLeuRS.

An alternative pre-transfer editing pathway has also been identified in LeuRS and cleaves the noncognate amino acid before it is transferred to $tRNA^{Leu}$, at the stage of aminoacyl-AMP production. Co-existence of both pre- and post-transfer editing pathways was highlighted in the ycLeuRS, as has also been shown earlier for *E. coli* LeuRS. Detailed biochemical investigations on the editing activity of this enzyme revealed that ycLeuRS shifts between the two editing pathways and this shift is dictated by the chemical identity of the noncognate amino acid misactivated by the enzyme. While isoleucine is mainly cleared via the post-transfer editing route that targets Ile-$tRNA^{Leu}$, methionine is edited via the pre-transfer pathway by hydrolysis of methionyl-adenylate in ycLeuRS.

The yeast mitochondrial LeuRS (ymLeuRS) was recruited to perform an alternate cellular role of mRNA splicing. Splicing-sensitive sites have been located within and in close proximity to the CP1 domain. Remarkably, *E. coli* LeuRS supports splicing *in vivo,* although its CP1 domain appears to lack the finer adaptations for efficient splicing compared to its counterpart from the ymLeuRS. *In vitro* and *in vivo* analysis dissected functional divergences of the ymLeuRS CP1 domain that accommodate an alternate cellular role for RNA splicing at the expense of its housekeeping aminoacylation and editing function. A close look at the connecting β-strands between the CP1 domain and main body highlighted that these β-strands, as well short extensions into the enzyme main body, are indispensable to not only LeuRS's editing function, but also to its splicing activity.

To

my parents (Ma and Baba)

and

my husband (Krish)

Acknowledgements

At the very onset I would like to sincerely thank my advisor Professor Susan A. Martinis for her guidance, support and encouragement. An excellent mentor, an immaculate scientist and writer, and a wonderful human being, Susan taught me the basics and the nuances of varied aspects of science, teaching, scientific writing and presentations, and also life in general. When experiments failed, manuscripts received harsh reviews, complications swelled up in teaching a huge undergraduate class or when challenges in science and elsewhere in life seemed unsurpassable, a meeting with Susan, her charismatically encouraging words and her continuing confidence in me would leave me feeling reassured and very much capable of facing and overcoming all kinds of hurdles. I admire and respect her for her precise scientific acumen, her strength of character, her unmatched ability not to crumble at the face of the most impossible challenges and her ability to face every single day with a glowing smile and beaming confidence.

I thank my committee members, Professors Silverman, Kranz and Tajkhorshid for taking time out amidst their busy schedules for my qualifying exams, Wednesday biochemistry seminars, 6-month meeting and my defense which is to come. I am grateful to them for writing me letters of recommendation for various job/postdoctoral applications.

I would also like to express my gratitude to Professor Thomas Magliery at Ohio State University for helping me with suggestions and working tips on the GFP system. I thank Professor Rutilio Fratti at UIUC for allowing me to use his microscope set up for my GFP experiments and Terry Sasser in his lab for helping me out with the microscope operation almost every single time I used it.

Coming to my lab, I especially thank Dr. Michal Boniecki, the ‘Martinis lab encyclopedia’. All kinds of scientific queries ranging from experiment

design/troubleshooting and scientific discussions to practical bench-work tips and instrument handling would find an appropriate answer in Michal's expertise and experience. I am particularly grateful to him for sharing with me the technique of *in vivo* expression of tRNAs, which significantly facilitated my *J. Am. Chem. Soc.* publication. I also thank my other current lab mates Li Li and Hanchao Zhao and ex-lab mate Katie McTavish for the amicable environment that they maintained in the lab. Finally I would like to take this opportunity to express my gratitude to two Martinis lab alumni Drs. Yan Ling Joy Pang and Rachel Hellmann Whitaker. Both Rachel and Joy, through their friendliness and helpfulness were instrumental in making me feel at home in the Martinis lab during my initial days. These were two seniors that I could go to with any question anytime, and they would always be there to answer them with a smiling face. Joy, who was also my mentor during my rotation in the Martinis lab, was one of the reasons, besides the research and Susan that framed my decision to join this lab for my PhD. I will forever treasure the precious memories gathered during the time I overlapped with Joy and Rachel in the lab and then later on as well. I also thank a previous Martinis lab member, Ramya Raviprakash for transferring me her GFP project and then walking me through the same when I first joined the lab.

Finally coming to the pillars of strength in my life - my father (Baba) Dr. Ajit Chakraborty, my mother (Ma) Mrs. Shibani Chakraborty and my husband Dr. Krishnarjun Sarkar. Mere words of thanks will not suffice because their love, support and sacrifices for me know no boundaries and is beyond any kind of quantification. So, I would simply like to say here that I am grateful and ever indebted for parents like them and a husband like him. I dedicate this thesis to them.

Table of Contents

Abbreviations

A. aeolicus	*aquifex aeolicus*
AARS	aminoacyl-tRNA synthetase
ABD	anticodon binding domain
AlaRS	alanyl-tRNA synthetase
AMP	adenosine 5´-monophosphate
AspRS	aspartyl-tRNA synthetase
ArgRS	arginyl-tRNA synthetase
ATP	adenosine 5´-triphosphate
A76	adenosine at position 76 of tRNA
BME	β-mercaptoethanol
B. stearothermophilus	*Bacillus stearothermophilus*
C. albicans	*Candida albicans*
CGFP	C-terminal half of green fluorescent protein
CP1	connective polypeptide 1
CZGFP	C-terminal half of green fluorescent fused to a leucine zipper
D-arm	dihydrouridine arm
DHU	dihydrouridine
DNA	deoxyribonucleic acid
dNTP	deoxynucleotide triphosphate
DTT	dithiothreitol
E. coli	*Escherichia coli*
EDTA	ethylenediaminetetraacetic acid
EF-Tu	elongation factor Tu
GDP	guanosine diphosphate

GMP	guanosine monophosphate
GFP	green fluorescent protein
GluRS	glutamyl-tRNA synthetase
GlnRS	glutaminyl-tRNA synthetase
GTP	guanosine triphosphate
HEPES	4-(2-hydroxyethyl)-1-piperazineethanesulfonic acid-KOH
HisRS	histidinyl-tRNA synthetase
IleRS	isoleucyl-tRNA synthetase
IPTG	isopropyl β-D-1-thiogalactopyranoside
k_{cat}	catalytic turnover number
k_{cat} /K_M	enzyme efficiency
K_M	Michaelis constant
LB	Luria broth
LeuRS	leucyl-tRNA synthetase
LeuZ	leucine zipper
LSD	leucine-specific domain
LysRS	lysyl-tRNA synthetase
MCS	multiclonal site
MetRS	methionyl-tRNA synthetase
MIC	minimum inhibitory concentration
mRNA	messenger RNA
N. crassa	*Neurospora crassa*
NGFP	N-terminal half of green fluorescent protein
NZGFP	N-terminal half of green fluorescent fused to a leucine zipper
N73	base at position 73 of tRNA

OD	optical density
PBS	phosphate buffered saline
PCR	polymerase chain reaction
PEI	cellulose polyethyleneimine cellulose
PEG	polyethylene glycol
PP_i	pyrophosphate
P. horikoshii	*Pyrococcus horikoshii*
RNA	ribonucleic acid
S. cerevisiae	*Saccharomyces cerevisiae*
SEER	sequence enabled reassembly of proteins
SerRS	seryl-tRNA synthetase
SDS	sodium dodecyl sulfate
SDS-PAGE	sodium dodecyl sulfate polyacrylamide gel electrophoresis
T-arm	TψC arm of tRNA
TBST	tris-buffered saline and tween 20
TCA	trichloroacetic acid
ThrRS	threonyl-tRNA synthetase
TLC	thin-layer chromatography
TNF-α	tumor necrosis factor α
Tris	tris(hydroxymethyl)aminomethane
tRNA	transfer ribonucleic acid
TrpRS	tryptophanyl-tRNA synthetase
TyrRS	tyrosyl-tRNA synthetase
T. thermophilus	*Thermus thermophilus*
ValRS	valyl-tRNA synthetase

Chapter I: Introduction

I.1. Overview of Aminoacyl-tRNA Synthetases

The process of translating the genetic code into the amino acid sequence of proteins is mediated by adapter molecules called transfer RNA (tRNA) and an ancient family of enzymes called aminoacyl-tRNA synthetases (AARSs) (Nawaz, 2008). Each of the twenty naturally occurring amino acids is typically recognized by a corresponding AARS (except for lysine which can have two AARSs in some species (Lévque F., 1990)). Since the genetic code is degenerate, in most cases, there is more than one tRNA for each amino acid. The tRNAs which accept the same amino acid are called isoacceptor tRNAs (Björk, 1996). Each is recognized by a single AARS.

During the process of mRNA codon-directed protein synthesis, the AARSs catalyze the covalent attachment of the cognate amino acid to one or more of the tRNA isoacceptors. The tRNAs contain identity elements that act as molecular determinants or antideterminants for accurate recognition by the respective synthetase (Giegé, et al., 1998; Soma, et al., 1996). Studies have shown that all AARSs catalyze essentially the same reaction: ATP-dependent activation of the cognate amino acid to form an aminoacyl-adenylate intermediate, followed by transfer of the activated amino acid to the 2′- or 3′-OH of the terminal adenosine at the 3′-end of the tRNA, resulting in formation of the aminoacylated tRNA (Ibba and Söll, 2000).

Despite their common catalytic mechanism, the AARSs are divided into two classes, I and II, based on active site architectural differences and sequence and structural homologies (Table I.1, Table I.2) (Arnez and Moras, 1997; Cusack, et al., 1990; Eriani, et al., 1990; Ribas de Pouplana and Schimmel, 2001). The active site core of class I AARSs are characterized by the presence of a structural motif consisting of six-stranded parallel β sheet. The β-strands are intervened by four α helices (Figure I.1). This motif has been classified as Rossmann dinucleotide binding fold (Buehner, et al., 1974; Rossmann, et al., 1974). In addition, two

class-defining signature peptide sequences (Schimmel, 1987) 'KMSKS' (Lys-Met-Ser-Lys-Ser) (Hountondji, et al., 1986) and 'HIGH' (His-Ile-Gly-His) (Webster, et al., 1984) are also part of the active site core of class I AARSs. When present, the 'KMSKS' motif is always accompanied by the 'HIGH' motif. Although these two signature sequences are in distal

Table I.1. Classification of AARSs based on active site architectural differences and sequence and structural homology*

Class I	Class II
Ia	**IIa**
LeuRS	**SerRS**
IleRS	**ThrRS**
ValRS	**AlaRS**
MetRS	**GlyRS**
CysRS	**ProRS**
ArgRS	**HisRS**
Ib	**IIb**
GlnRS	**AspRS**
GluRS	**AsnRS**
LysRS-I	**LysRS-II**
Ic	**IIc**
TyrRS	**PheRS**
TrpRS	

*The AARSs highlighted in blue possess proofreading activities to clear misactivated and/or mischarged amino acids.

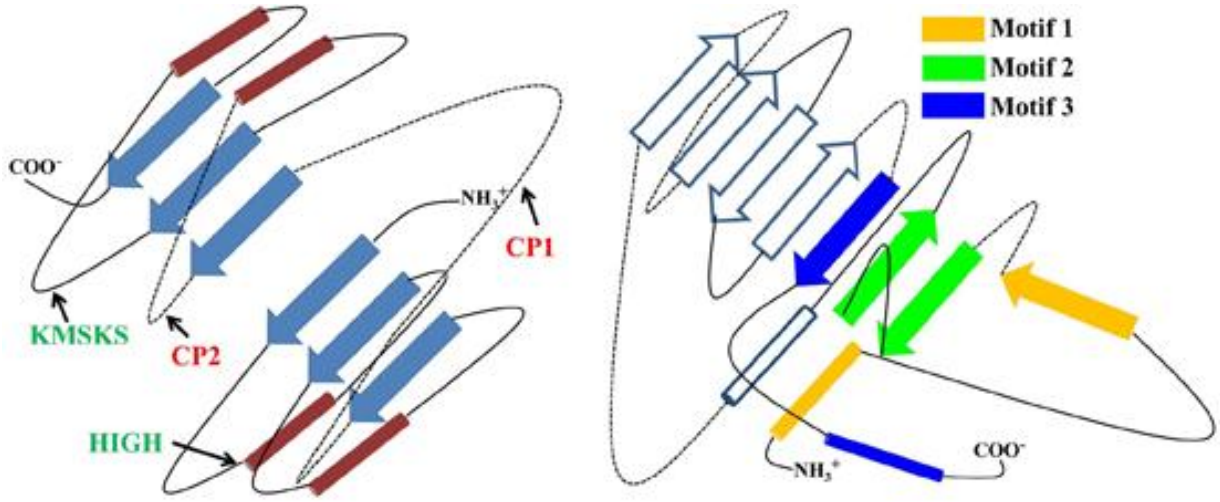

Figure I.1. Active site topologies of class I and II AARSs. (Left) Class I synthetase parallel β sheet Rossmann fold. Catalytically important conserved motifs (HIGH and KMSKS) are marked. The dashed lines represent CP1 and CP2 insertion domains. (Right) Class II synthetase antiparallel β sheet. The three characteristic motifs are highlighted. The arrows and cylinders represent β strands and α helices, respectively.

regions of the primary sequence of the Rossmann nucleotide binding fold, they fold together to comprise the active site. The HIGH and KMSKS sequences interact with ATP (Figure I.2) (Arnez and Moras, 1997; Fersht, et al., 1988; Perona, et al., 1993). Recent structural studies on TyrRS have captured snapshots of the extensive induced-fit local conformational changes within the KMSKS loop that drive the ATP-dependent activation of amino acid at the substrate binding site (Kobayashi, et al., 2005). More recent complementary structural and thermodynamic data from Charles W. Carter Jr.'s lab show that energetically favorable conformational changes within the flexible KMSKS loop lead to significantly tighter interactions between the enzyme and nucleotide uniformly in the pyrophosphate (PP_i) and adenosine binding subsites (Retailleau, et al., 2007).

On the other hand, the active site of class II AARSs present a completely different and largely unique topology consisting of eight-stranded antiparallel β sheet flanked by α helices (Figure I.1). Interestingly, the *E. coli* biotin synthetase/repressor protein (BirA) is an AARS-

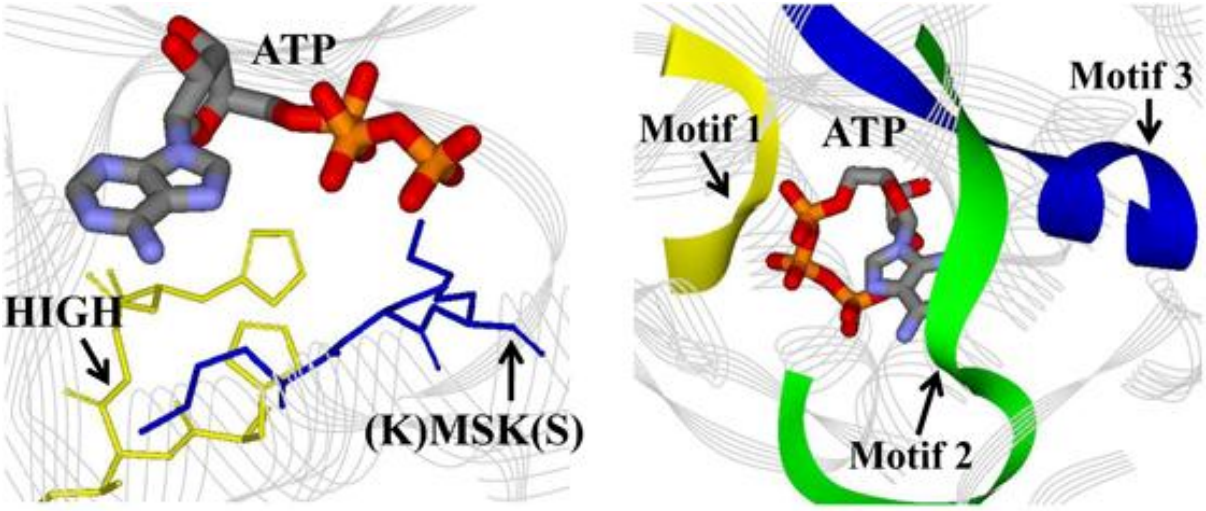

Figure I.2. Active site conserved sequences in class I and II AARSs. (Left) Crystal structure of class I GlnRS from *E. coli* in complex with ATP and $tRNA^{Gln}$ (not shown here) (PDB: 1GTR) (Perona, et al., 1993). The ATP is bound in an extended conformation and interacts with the conserved sequences HIGH and (K)MSK(S). (Right) Crystal structure of class II AspRS from yeast in complex with ATP and $tRNA^{Asp}$ (not shown here) (PDB: 1ASZ) (Cavarelli, et al., 1994). The ATP is bound in a bent conformation. The three conserved motifs 1, 2 and 3 are highlighted in yellow, green and blue, respectively.

like protein which has a domain that structurally resembles the class II seryl-tRNA synthetase (SerRS) catalytic domain (Ibba, 2005). Based on sequence homology, three motifs have been defined, in order of their occurrence (Cusack, et al., 1990; Eriani, et al., 1990). These three conserved motifs form a helix-loop-strand (motif 1), strand-loop-strand (motif 2) and strand-helix (motif 3) (Figure I.1). In the class II synthetases, the ATP is cradled at the active site by motifs 2 and 3 (Figure I.2) (Arnez and Moras, 1997; Perona, et al., 1993). Although the motifs have a conserved core, they vary in length and are conserved by as little as a single invariant residue. The sequences defining the motifs are: motif 1, gΦxxΦxxPΦΦ; motif 2, (F/Y/H)Rx(E/D)(4-12x)(R/H)xxxFxxx(D/E) and motif 3, λxΦgΦgΦeRΦΦΦΦΦ (The abbreviations are: x, variant; Φ, hydrophobic, λ, small amino acids. Lower case letters indicate that the amino acid is partially conserved).

Because class I and II AARSs each use their conserved characteristic active site sequences to bind ATP, there is little or no variation within the members of a class.

However, the ATP-binding conformation is distinct for the two classes of enzymes (Arnez and Moras, 1997). While class I synthetases bind ATP in a fully extended conformation (Perona, et al., 1993), class II synthetases bind ATP is a more compact conformation where the γ-phosphate is folded back or bent over the adenine base (Figure I.2) (Cavarelli, et al., 1994).

Distinctions in tRNA binding between the two classes of AARSs dictate different regiochemistries of the aminoacylation reaction (Arnez and Moras, 1997). Class I synthetases attach the amino acid to the 2′-OH of the ribose of the terminal adenosine, while the class II synthetases attach the amino acid at the 3′-OH of the ribose. In addition, the 3′-CCA end of the tRNA is bent in a hairpin manner into the active site in the class I GlnRS-$tRNA^{Gln}$ crystal structure (Perona, et al., 1993), while it is extended straight in the class II AspRS-$tRNA^{Asp}$ structure (Cavarelli, et al., 1994). This is because the two classes of AARSs bind tRNA distinctly. The class I enzymes approach the tRNA acceptor stem from the minor groove (Arnez and Steitz, 1996), whereas the class II enzymes approach tRNA from the major groove (Sankaranarayanan, et al., 1999). However, a generalization of the tRNA-binding pattern for all the synthetases is inappropriate since the tRNA-binding geometries are suggested mainly by AARS:tRNA crystal structures and not all synthetase crystal structures have been solved with tRNA.

It is noteworthy that unlike a class-defining amino acid-binding pocket sequence, a common tRNA-binding motif has not been identified for all the synthetases. A case in point is the eubacterial and eukaryotic LysRS which are known to be class II enzymes. However, LysRS from the archaea *Methanococcus maripaludis* is unrelated to class II AARSs (Ibba, et al., 1997). Instead, the presence of amino acid sequences similar to the Rossmann dinucleotide-binding domain classifies this LysRS as a class I synthetase (Ibba, et al., 1997).

Table I.2. Principle differences between class I and II AARSs

	Class I	Class II
Active site fold	Parallel β sheet (Rossmann fold)	Antiparallel β sheet
Conserved motifs in active site	HIGH KMSKS	Motif 1, 2, 3 (see text)
ATP conformation	Extended	Bent
tRNA-binding (acceptor stem)	Minor groove side	Major groove side
Aminoacylation site	2′-OH	3′-OH

Natural non-standard amino acids have been incorporated co-translationally to expand the genetic code in several organisms (Liu and Schultz, 2010; Sethi, et al., 2005). The strategy used in these cases is to reprogram a termination codon on the mRNA (particularly the amber codon) to encode the non-standard amino acid. An orthogonal pair of (suppressor tRNA:AARS) is one of the main requirements to design new systems. The most prominent natural example is the presence of selenocysteine (Sec) in proteins from all three domains of life. Directed by specific mRNA structural features, the amber codon-encoded selenocysteine is co-translationally incorporated with the help of amber suppressor $tRNA^{Sec}$, SerRS, selenocysteine synthase and a special elongation factor (SelB) (Leibundgut, et al., 2005). Similarly, the natural amino acid pyrrolysine (pyl) can be cotranstaionally incorporated, directed by special mRNA features and using an analogous system to selenocysteine incorporation, that is, an amber suppressor $tRNA^{Pyl}$ and an AARS-like protein PylS (Srinivasan, et al., 2002) or LysRS (Polycarpo, et al., 2003).

Genes encoding cysteinyl-tRNA synthetase (CysRS) have been detected in organisms across the three kingdoms of life, except in certain methanogenic archaea. In these

organisms, the cysteine codons are translated indirectly (Sauerwald, et al., 2005). The first step in this indirect mechanism is the formation of Sep-tRNA^{Cys} by a unique AARS called *O*-phosphoseryl tRNA synthetase (SepRS) that attaches *O*-phosphoserine (Sep) to tRNA^{Cys}. A second enzyme called SepCysS then converts Sep-tRNA^{Cys} to Cys-tRNA^{Cys} in the presence

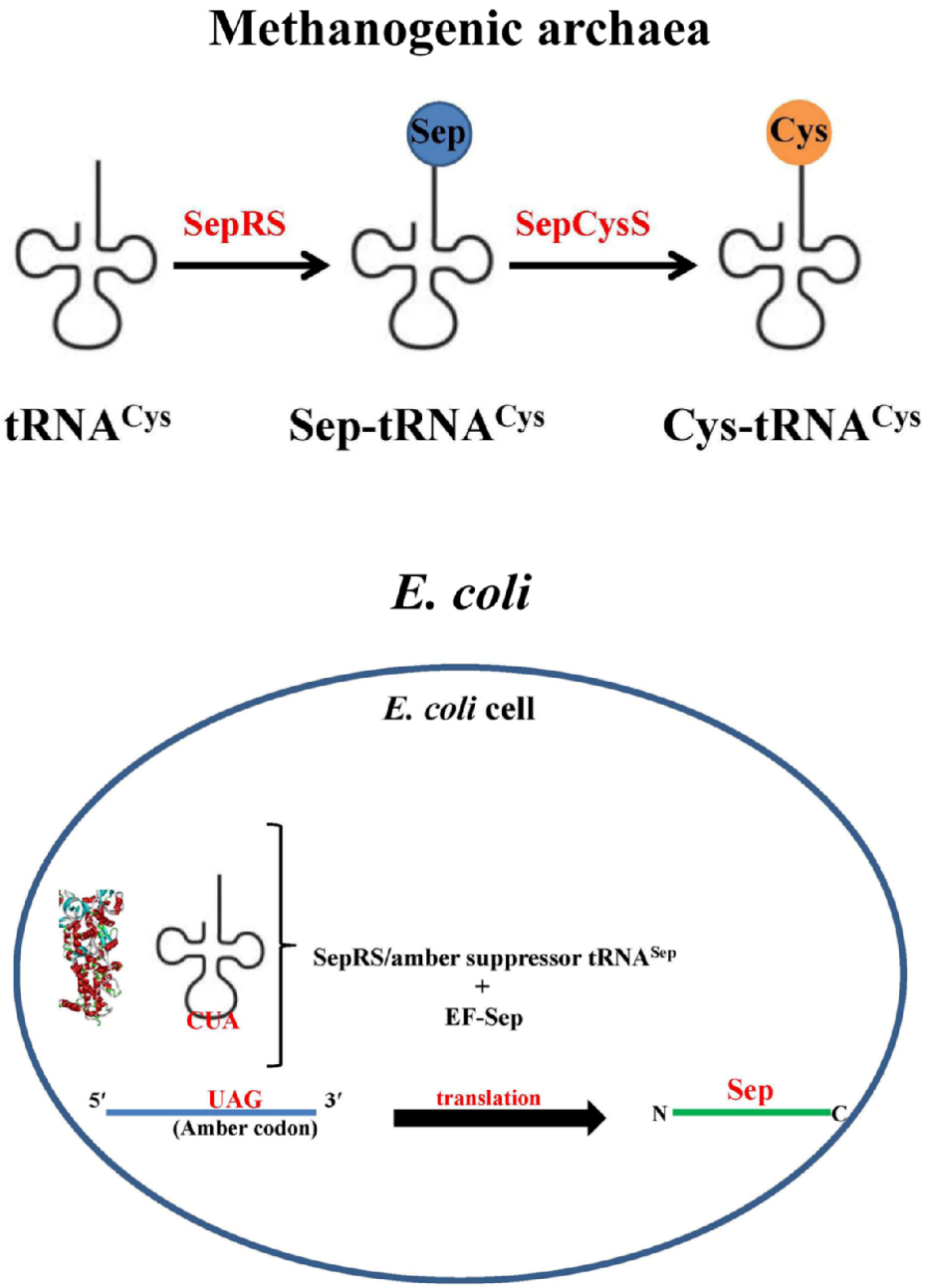

Figure I.3. Strategy for co-translational incorporation of non-standard amino acids. (Top) Indirect mechanism of cysteine codon translation in methanogenic archaea. (Bottom) Co-translational incorporation of *O*-phosphoserine (Sep) in *E. coli* proteins. Solid blue and green lines represent mRNA and polypeptide chain, respectively.

of a natural sulfate donor (Figure I.3, top). More recently, this indirect mechanism in archaea has been used to cotranslationally incorporate *O*-phsophoserine (Sep) in *E. coli* proteins (Park, et al., 2011). In this strategy, mutations in the archaeal $tRNA^{Cys}$ generated the archaeal amber suppressor $tRNA^{Sep}$. The archaeal (SepRS/amber suppressor $tRNA^{Sep}$), which then served as an orthogonal pair in *E. coli* cells was used along with a special elongation factor (EF-Sep) to co-translationally add *O*-phosphoserine (Sep) to the *E. coli* proteome (Figure I.3, bottom).

As the ancient family of AARSs evolved, several of the synthetases have acquired insertion domains or short peptides in addition to their aminoacylation catalytic domains. These insertion domains are dedicated to a variety of diverse functions. The most prominent among them is proofreading/editing during the aminoacylation reaction. In class I AARSs the hydrolytic editing domain is the conserved connective polypeptide 1 (CP1 (Starzyk, et al., 1987)) (Hou, et al., 1991; Starzyk, et al., 1987) domain) that is inserted into the Rossmann dinucleotide-binding fold of the aminoacylation active site (Lin, et al., 1996; Mursinna, et al., 2001; Schmidt and Schimmel, 1994; Starzyk, et al., 1987).

In class II synthetases, the editing domain that is responsible for hydrolytic editing is relatively more diverse in their location and structure (Beebe, et al., 2003; Wong, et al., 2002). The hydrolytic editing domain of *E. coli* threonyl-tRNA synthetase (ThrRS) exists as an additional appendage at the N-terminus (Dock-Bregeon, et al., 2000). On the other hand, based on primary structures, the ProRS family can be divided into 'prokaryotic-like' and 'eukaryotic-like' groups. The 'prokaryotic-like' group, which includes bacterial and eukaryotic mitochondrial enzymes, carries out hydrolytic editing of mischarged tRNA via a large insertion domain (INS) located between motifs 2 and 3 that constitute the aminoacylation active site (Wong, et al., 2002; Wong, et al., 2003). Surprisingly, the 'eukaryotic-like' ProRS group that includes the eukaryotic and archaeal enzymes lacks the

INS domain, but instead has a C-terminal extension that is missing from the 'prokaryotic-like' group. Some lower eukaryotes possess an N-terminal extension domain that bears weak homology to the INS domain (Ahel, et al., 2003).

Another example of an insertion domain is the anticodon binding domain (ABD). The ABD is essential to recognize the tRNA anticodon loop for most AARSs except LeuRS, SerRS, and alanyl-tRNA synthetase (AlaRS) (Asahara, et al., 1993; Giegé, et al., 1998). Significantly, the ABDs possess markedly variable structures. For example, the ABDs from glutamyl-tRNA synthetase (GluRS) (Nureki, et al., 1995) and glutaminyl-tRNA synthetase (GlnRS) (Rould, et al., 1989) are mainly comprised of α helices and β strands respectively.

I.2. Mechanism of the aminoacylation reaction

The AARSs catalyze the covalent attachment of an amino acid to the 3′-end of the cognate tRNA (Ibba and Söll, 2000). The aminoacylation reaction occurs in two steps. In the first step, the enzyme-bound amino acid is activated in an ATP-dependent fashion to form the enzyme-bound aminoacyl adenylate (AA-AMP) intermediate. In the second step, the activated amino acid is transferred to the 3′-end of the tRNA forming the charged or aminoa-

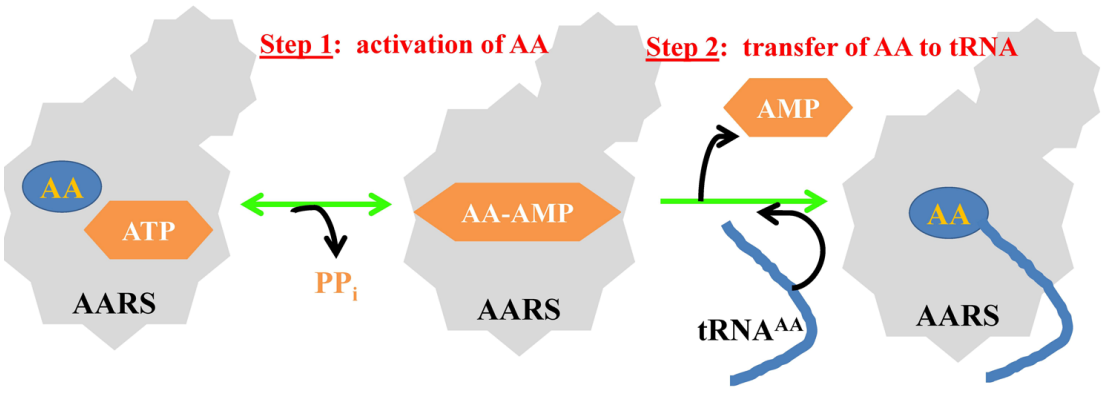

Figure I.4. Cartoon representation of the two-step aminoacylation reaction catalyzed by AARSs. Step 1 involves ATP-dependent activation of the amino acid (AA), forming the enzyme-bound aminoacyl adenylate (AA-AMP) intermediate at the synthetic active site. Step 2 entails the transfer of the activated amino acid to the 3′-end of the tRNA.

cylated tRNA (AA-tRNA^{AA}) (Figure I.4). Although the first step of amino acid activation is independent of tRNA, GluRS, GlnRS, ArgRS and LysRS-I require tRNA as a cofactor (Ibba, et al., 1996).

The first step of amino acid activation occurs by in-line nucleophilic displacement where the α-carboxylate oxygen of the amino acid attacks the α-phosphate of ATP, forming the AA-AMP intermediate. Cleavage of the phosphoanhydride linkage between the α- and the β-phosphate of ATP releases PP_i (Figure I.5). In the second step, the 2′-hydroxyl (for class I AARSs) or the 3′-hydroxyl (for class II AARSs) of the ribose of the terminal adenosine (A76) at the 3′-end of the tRNA makes a nucleophilic attack on the carboxyl carbon of the AA-AMP intermediate (Figure I.5). This cleaves the mixed anhydride bond in the adenylate, resulting in transfer of the amino acid to the 3′-end of the tRNA.

For both classes, the amino acid and ATP-binding pockets are well defined templates in which the substrates are optimally positioned for formation and stabilization of the transition state. Within this active site, specificity of a particular AARS for its cognate amino acid is determined by idiosyncratic contacts between the amino acid side chain and active site residues. The specificity of substrate recognition is further enhanced by an induced fit mechanism in which ATP-binding triggers mostly local conformational changes within the aminoacylation active site, particularly the conserved KMSKS sequence of class I synthetases (Retailleau, et al., 2007). Thus, although all AARSs catalyze the same overall two-step aminoacylation reaction, substrate binding, and stabilization of the transition state are dependent on distinct features of the active site which are class-specific.

In class I AARSs, biochemical and structural studies have shown extensive conformational rearrangements of the KMSKS and in some cases, the HIGH motif, following ATP binding, to stabilize the transition state using ATP-binding energy (First and Fersht, 1995; Kobayashi, et al., 2005). Thermodynamic data obtained from isothermal titration

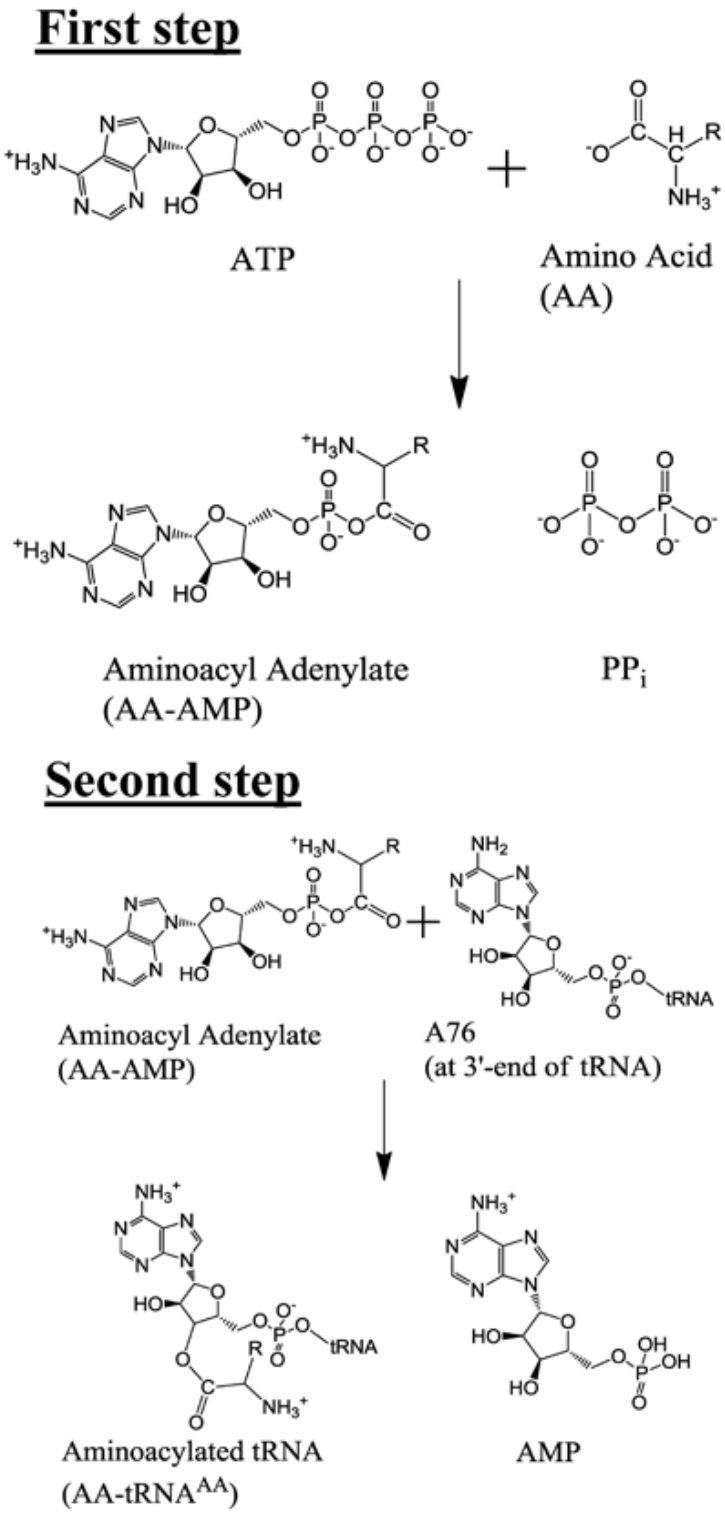

Figure I.5. Mechanism of the two-step aminoacylation reaction in class I AARSs. (Top) The first step involves a nucleophilic attack by the α-carboxyl oxygen of the amino acid at the α-phosphate of ATP, forming the aminoacyl adenylate intermediate. (Bottom) In the second step the 2′-OH of the ribose ring of terminal adenosine at the 3′-end of tRNA makes a second nucleophilic attack (for class I AARSs) at the carboxyl carbon of the aminoacyl adenylate intermediate, forming the aminoacylated tRNA.

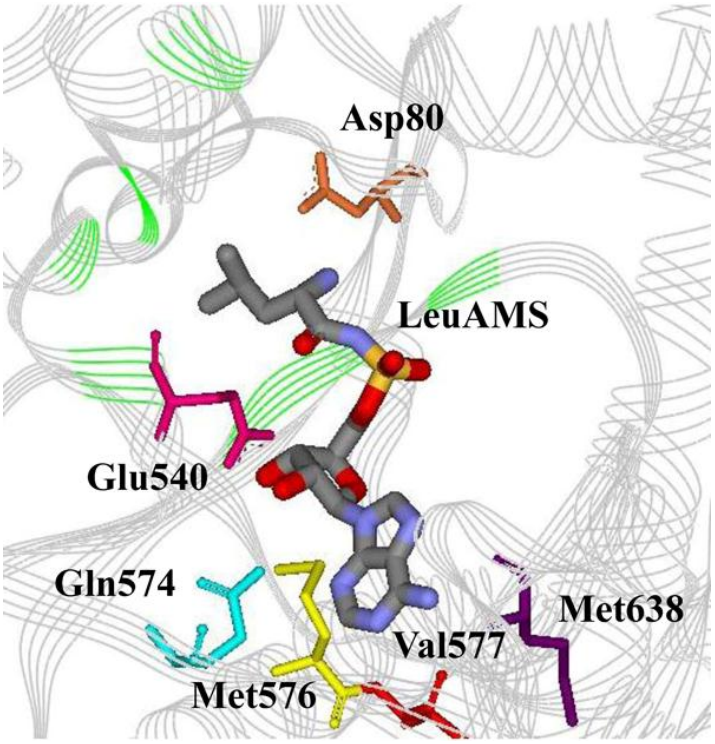

Figure I.6. Amino acid-binding pocket of LeuRS. Co-crystal structure of *T. thermophilus* LeuRS with the analog of leucyl-adenylate (5′-*O*-[*N*-(leucyl)-sulfamoyl] adenosine) (LeuAMS) bound at the aminoacylation active site (PDB: 1H3N) (Cusack, et al., 2000). Residues which H-bond with LeuAMS are shown in different colors. A largely hydrophobic pocket (Met40, Phe41, Tyr43, Phe501, Tyr507, His541 and His545) that binds the leucine side chain is highlighted in green.

calorimetry reveal that tight ATP-binding is largely driven by favorable entropy changes associated with the induced-fit assembly at the active site (Retailleau, et al., 2007). These studies also reveal a transition state in which the KMSKS signature sequence forms increasingly tighter bonds with PP_i, the leaving group, weakening linkage to the α-phosphate of ATP. The complexed structure of *T. thermophilus* LeuRS with the analog of leucyl-adenylate (5′-*O*-[*N*-(leucyl)-sulfamoyl] adenosine) (LeuAMS) at the aminoacylation active site have provided molecular details of the amino acid and ATP-binding pockets. Both the ribose and the adenine of ATP interact with the active site via multiple hydrogen bonds. The ribose is stacked on top of Met576 and is hydrogen bonded to Glu540 and Gln574, whereas the adenine base is hydrogen bonded to Gln574, Val577 and Met638 (Figure I.6) (Cusack, et

al., 2000). The α-amino group of leucine forms a hydrogen bond with the Asp80 side chain and the carbonyl oxygen of leucine interacts with His541. The leucine side chain binds in a largely hydrophobic pocket at the active site, comprised of Met40, Phe41, Tyr43, Phe501, Tyr507, His541 and His545 (Figure I.6) (Cusack, et al., 2000).

In class II AARSs, numerous structural (Cavarelli, et al., 1994) and mutational studies (Stehlin, et al., 1997) show the importance of motifs 2 and 3 in ATP and amino acid recognition and activation. The active site of these enzymes promotes amino acid activation by binding ATP and amino acid in an orientation that facilitates the reaction mechanism and stabilizes the transition state, particularly by motif 2 (Cusack, 1997). Significantly, not only is the recognition of the specific amino acid idiosyncratic to the specific synthetase, but there is also considerable variation in the magnitude of the induced-fit associated with amino acid binding. While the active sites of seryl-tRNA synthetase (SerRS) (Belrhali, et al., 1995) and aspartyl-tRNA synthetase (AspRS) (Cavarelli, et al., 1994) form a relatively rigid amino acid binding pocket, conformational changes in histidinyl-tRNA synthetase (HisRS) are much greater and have more global repercussions on movements of other domains with respect to the catalytic site (Arnez, et al., 1995). In class II synthetases, the binding of ATP in the bent conformation (Figure I.2) is dependent on the ordering of motif 2 and interactions with residues conserved in all class II synthetases. For example, in HisRS (Arnez, et al., 1995; Arnez, et al., 1997), in the absence of the adenylyl moiety of either ATP or the histidinyl-adenylate, motif 2 is poorly ordered. Consistent with other class II synthetases, the motif 2 loop in HisRS assumes an ordered β-hairpin conformation due to its main chain interactions with the adenosine base that is stacked between motifs 2 and 3 (Figure I.2).

I.3. Proofreading (Editing) pathways in AARSs

Fidelity in protein synthesis is important to the cell. Mistranslation in the proteome can result in accumulation of misfolded proteins, thus leading to neurodegenerative diseases (Lee, et al., 2006; Ross and Poirier, 2004) and eventually cell death (Karkhanis, et al., 2007). For example, editing defects in AlaRS lead to mistranslation and accumulation of misfolded proteins in neurons in mouse (Lee, et al., 2006; Nangle, et al., 2006). The accumulation of unfolded proteins is accompanied by up-regulation of cytoplasmic protein chaperones and induction of the unfolding of proteins. The mouse-model harboring the editing-defective AlaRS show a marked loss of Purkinje cells in the cerebellum and developed severe ataxia (Lee, et al., 2006).

Thus, the cell has devised multiple checkpoints to maintain translational fidelity. These are at the level of the AARSs that catalyze formation of aminoacylated tRNAs (Mascarenhas, 2008), EF-Tu, the protein that carries the aminoacylated tRNA to the ribosome (LaRiviere, et al., 2001) and the ribosome that catalyzes peptide bond synthesis (Ogle, et al., 2002; Zaher and Green, 2009). Out of these, the AARS-dependent fidelity is the first checkpoint and hence critical for the cell to ensure error-free protein synthesis by ensuring formation of the correctly charged tRNA. Several AARS-linked neurodegenerative diseases have been reported (Nangle, et al., 2007; Park, et al., 2008).

Linus Pauling, in 1957, predicted an error rate of 1 in 20 for a valine substitution in place of isoleucine by isoleucyl-tRNA synthetase (IleRS) (Pauling, 1958). However, *in vivo* error rate measurement for a valine substitution in place of isoleucine, reported an estimate of

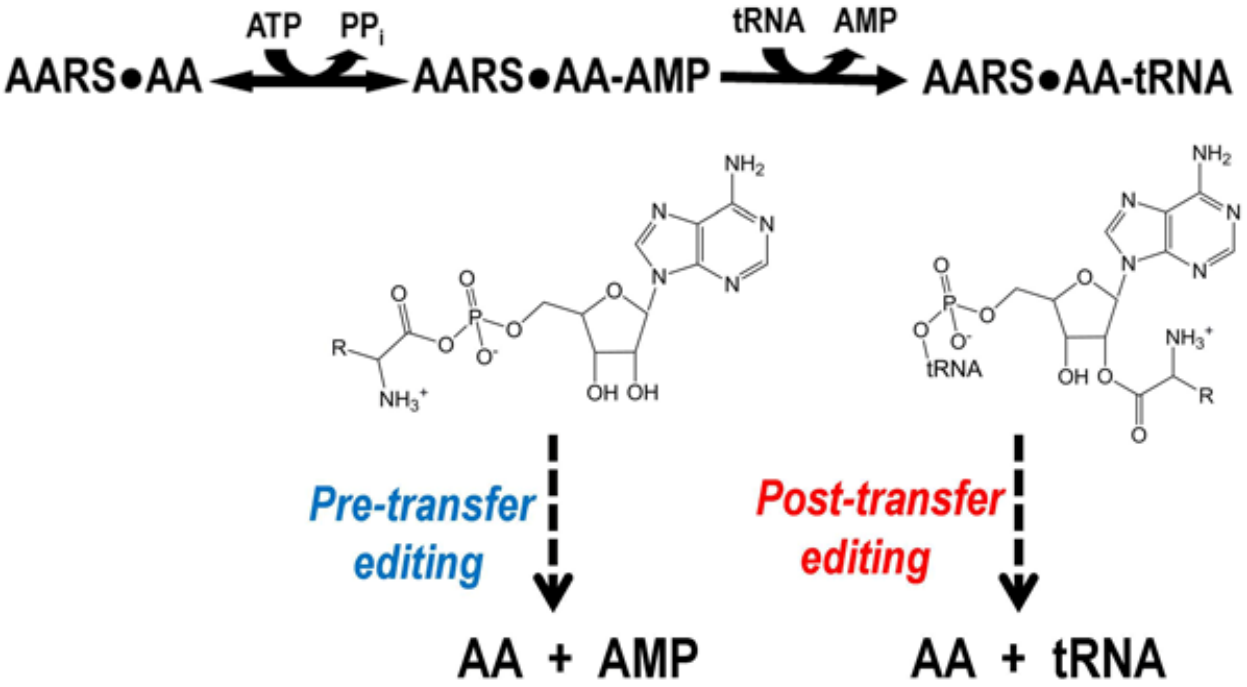

Figure I.7. Scheme showing pre- and post-transfer editing pathways. The aminoacyl adenylate (AA-AMP) is the substrate for pre-transfer editing, while the mischarged tRNA (AA-tRNA) is the substrate for post-transfer editing.

approximately 1 in 3000 (Loftfield, 1963). Such an increase in fidelity clearly indicated that molecular recognition of amino acids extends beyond initial substrate discrimination at the aminoacylation active site of AARSs. Baldwin and Berg showed that although *E. coli* IleRS catalyzed formation of both the noncognate valyl-adenylate (Val-AMP) and the cognate isoleucyl-adenylate (Ile-AMP), addition of $tRNA^{Ile}$ only led to formation of Ile-$tRNA^{Ile}$ and not Val-$tRNA^{Ile}$ (Baldwin and Berg, 1966). It was later reported that for *E. coli* IleRS, the noncognate Val-AMP was hydrolyzed (proofread), thereby avoiding valine mischarging to $tRNA^{Ile}$ (Fersht and Dingwall, 1979a). Thus, the concept of 'editing' or 'proofreading' was introduced for AARSs to explain how they maintain the high degree of fidelity in protein synthesis.

The hydrolysis pathway that targets the mixed anhydride linkage in the adenylate (AA-AMP) is called 'pre-transfer' editing, while the hydrolysis pathway that cleaves the

aminoacyl ester bond in the (mis)charged tRNA (AA-tRNA) is termed ‘post-transfer’ editing (Figure I.7). Out of the twenty standard AARSs, nine enzymes are known to possess editing activities. These include the class I AARSs, LeuRS (Englisch, et al., 1986; Mursinna, et al., 2004), IleRS (Baldwin and Berg, 1966), valyl-tRNA synthetase (ValRS) (Fersht and Kaethner, 1976) and methionyl-tRNA synthetase (MetRS) (Fersht and Dingwall, 1979b) and the class II AARSs AlaRS (Tsui and Fersht, 1981), PheRS (Yarus, 1972), ProRS (Beuning and Musier-Forsyth, 2000), ThrRS (Dock-Bregeon, et al., 2004), and LysRS (Jakubowski, 1999).

I.3.A. Post-transfer editing

To explain the high level of amino acid discrimination achieved by the AARSs, Fersht proposed the ‘double sieve’ model of fidelity (Fersht, 1977a). Some of the AARSs face the challenge of discriminating between structurally similar amino acids. For example, the LeuRS aminoacylation active site misactivates and mischarges structurally similar standard amino acids isoleucine, methionine and valine as well as nonstandard metabolic intermediates with amino acid backbones such as norvaline, norleucine and α-aminobutyrate (Figure I.8). The double sieve model predicts that one enzyme active site may not completely discriminate between leucine and the noncognate amino acids, but two separate active sites with distinct strategies for substrate recognition significantly enhance fidelity (Fersht, 1977a). The aminoacylation active site of an AARS would form the adenylate (AA-AMP) by activating cognate amino acid and also the structurally similar smaller noncognate amino acids that fit the amino acid-binding pocket to a lesser extent, thereby acting as a ‘coarse sieve’. The second active site that would provide the ‘fine sieve’ would bind the misactivated amino acid, while excluding the cognate amino acid.

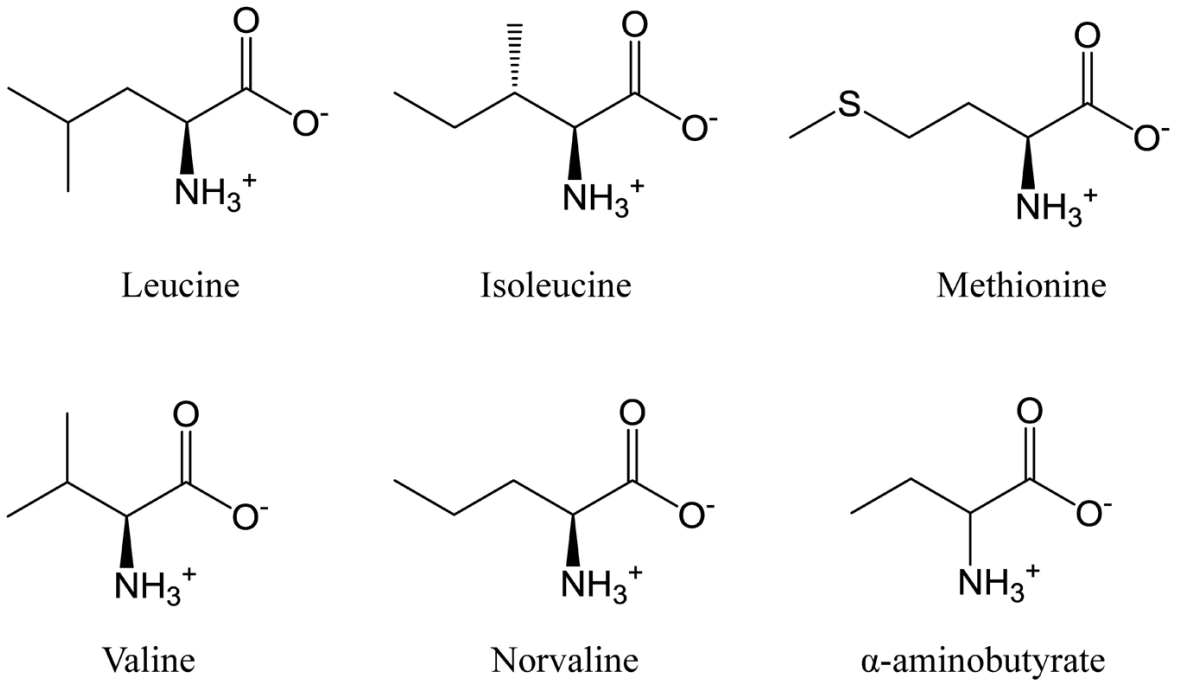

Figure I.8. Structurally similar isosteric standard amino acids and biosynthetic intermediates (norvaline and α-aminobutyrate) that are activated or misactivated by LeuRS.

For the class I AARSs, LeuRS, IleRS and ValRS, the editing active site that catalyzes post-transfer editing is housed in the homologous CP1 domain. Isolated CP1 domains from LeuRS, IleRS and ValRS clear noncognate amino acids from the respective mischarged tRNAs (Betha, et al., 2007; Lin, et al., 1996). Co-crystal structure of LeuRS with the post-transfer editing substrate analog 2′-(L-norvalyl) amino-2′-deoxyadenosine (Nva2AA) bound at the editing site in the CP1 domain (Figure I.9, left) (Lincecum, et al., 2003) as well as biochemical and computational studies (Mursinna, et al., 2001; Mursinna, et al., 2004; Mursinna, 2002) have provided molecular details of the post-transfer editing pocket in the CP1 domain. In LeuRS, the amino acid-binding pocket in the CP1 domain-based editing site has been precisely located to a threonine-rich peptide (highlighted in green in Figure I.9, left) (Lincecum, et al., 2003; Mursinna, et al., 2001). Within this pocket, a highly conserved threonine residue (Thr252 in *E. coli* and *T. thermophilus*; Thr319 in *S. cerevisiae* LeuRS

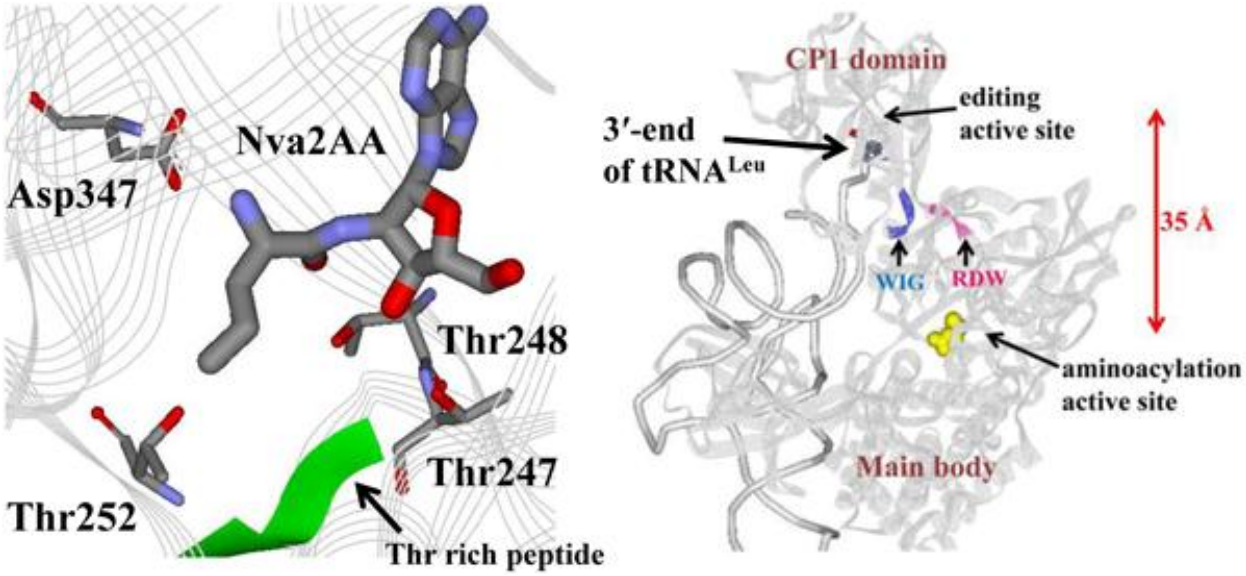

Figure I.9. CP1-based editing active site of LeuRS. (Left) Post-transfer editing substrate analog 2′-(L-norvalyl)amino-2′-deoxyadenosine (Nva2AA) bound at the editing site in the CP1 domain of *T. thermophilus* LeuRS. Editing pocket residues that make critical contacts with the substrate are highlighted, including the threonine-rich peptide (green) that lines the base of the pocket. (PDB: 10BC) (Lincecum, et al., 2003). (Right) Crystal structure of the *T. thermophilus* LeuRS in complex with $tRNA^{Leu}$ in the post-transfer editing conformation. The terminal A76 at the 3′-end of the tRNA is shown to be positioned at the editing active site in the CP1 domain. The conserved N-terminal 'WIG' peptide and the C-terminal 'RDW' peptide of LeuRS, which have critical contacts with the tRNA are highlighted in blue and pink, respectively. Leucine (yellow) is bound at the aminoacylation active site (PDB: 2BYT) (Tukalo, et al., 2005).

(Figure I.9, left) acts as the discriminator that blocks leucine from entering the editing pocket, while allowing the noncognate amino acid side chains to gain access into the editing pocket (Mursinna, et al., 2001). In this peptide, two conserved threonine residues (Thr247 and Thr248 in *T. thermophilus* LeuRS, Figure I.9, left) in total form three hydrogen bonds to the ribose moiety of Nva2AA (Lincecum, et al., 2003). Biochemical studies have shown that these two threonine residues collaborate to maintain a functional post-transfer editing active site in the CP1 domain of LeuRS (Zhai and Martinis, 2005). The Nva2AA post-transfer editing substrate analog is held in place by hydrogen bonding between the norvaline moiety and the universally conserved Asp347.

The CP1 domain-based editing active site is about ~35 Å distant from the aminoacylation active site, as revealed by crystal structures (Cusack, et al., 2000; Fukai, et al., 2000; Nureki, et al., 1998; Silvian, et al., 1999; Tukalo, et al., 2005). In the co-crystal structure of LeuRS and $tRNA^{Leu}$ in the editing conformation (Tukalo, et al., 2005), the 3′-CCA end of the tRNA is positioned in the editing site of the CP1 domain (Figure I.9, right). Thus, it is hypothesized that the (mis)charged 3′-end of the tRNA translocates from the aminoacylation active site in the enzyme main body to the editing active site in the CP1 domain. Indeed a 'translocation peptide' has been defined in *E. coli* LeuRS (Hellmann and Martinis, 2009). Mutations within this peptide abolish or impede translocation of the 3′-end of the (mis)charged tRNA. Translocation of the tRNA 3′-end is accompanied by a ~35° rotation of the CP1 domain that brings it in close proximity to the aminoacylation active site in the main body (Tukalo, et al., 2005). Two conserved motifs (WIG on the N-terminus and RDW on the C-terminus, Figure I.9, right) in the flexible β strands facilitate the movement of the CP1 domain (Mascarenhas and Martinis, 2008; Mascarenhas and Martinis, 2009; Tukalo, et al., 2005). The flexible β-strand linkers in LeuRS are also required for viable editing activity of the isolated CP1 domain (Betha, et al., 2007). MetRS is highly homologous to class I LeuRS, IleRS and ValRS, but possesses a very small CP1 domain that lacks an editing function. Biochemical studies indicate that MetRS hydrolyzes mischarged tRNA within the synthetic active site. The hydrolysis active site is however molecularly partitioned from the aminoacylation active site (Gruic-Sovulj, et al., 2007; Kim, et al., 1993).

In class II AARSs, the editing domains are structurally unrelated. The bacterial N-terminal N2 domain of ThrRS is responsible for post-transfer editing (Dock-Bregeon, et al., 2000). The ThrRS N2 domain is conserved in most bacterial and eukaryotic cytoplasmic enzymes, but is absent in archaeal and eukaryotic mitochondrial enzymes. The editing domain of AlaRS is only weakly related to the bacterial ThrRS N2 domain (Beebe, et al.,

2003; Dock-Bregeon, et al., 2000; Dock-Bregeon, et al., 2004). In bacterial ProRS, a novel insertion domain (INS) confers post-transfer editing (Wong, et al., 2002), while PheRS has another distinct editing domain (Roy and Ibba, 2006).

The post-transfer editing pathway in class II ProRS introduces a novel concept of a 'triple sieve' model for proofreading. Bacterial ProRS relies on an additional free-standing protein (*Haemophilus influenza* Ybak) to clear micharged amino acids in *trans* (An and Musier-Forsyth, 2005; Ruan and Soll, 2005). ProRS misactivates both alanine and cysteine at the aminoacylation active site (first sieve). The post-transfer editing INS domain of ProRS (second sieve) is responsible for hydrolyzing Ala-tRNA^{Pro} in *cis* (Wong, et al., 2002). However, the INS domain of bacterial ProRS lacks a Cys-tRNA^{Pro} specific hydrolytic activity (Ahel, et al., 2002; An and Musier-Forsyth, 2005). In bacteria, Cys-tRNA^{Pro} is instead cleared by the free-standing protein Ybak through formation of a novel Ybak•synthetase•tRNA ternary complex (An and Musier-Forsyth, 2005; Ruan and Soll, 2005). Thus, the free-standing protein introduces a 'third sieve' in the ProRS system. Interestingly, an INS editing domain paralog, ProX from the bacterium *Clostridium sticklandii* has been reported to hydrolyze Ala-tRNA^{Pro} but not Cys-tRNA^{Pro} (Ahel, et al., 2003). The ProRS from this species does not have an INS domain.

I.3.B. Pre-transfer editing

Editing pathways that preferentially hydrolyze noncognate adenylate AA-AMP prior to amino acid transfer to tRNA is referred to as pre-transfer editing (Figure I.7). Several models or mechanisms have been proposed for pre-transfer editing (Figure I.10). This includes enzyme-catalyzed hydrolysis of the noncognate adenylate in the aminoacylation active site where it is formed ('enzymatic hydrolysis', pathway 1 in Figure I.10). Alternately,

the noncognate adenylate which is significantly less stably bound by the enzyme as compared to the cognate adenylate (Hati, et al., 2006)] may be released into solution and non-enzymati-

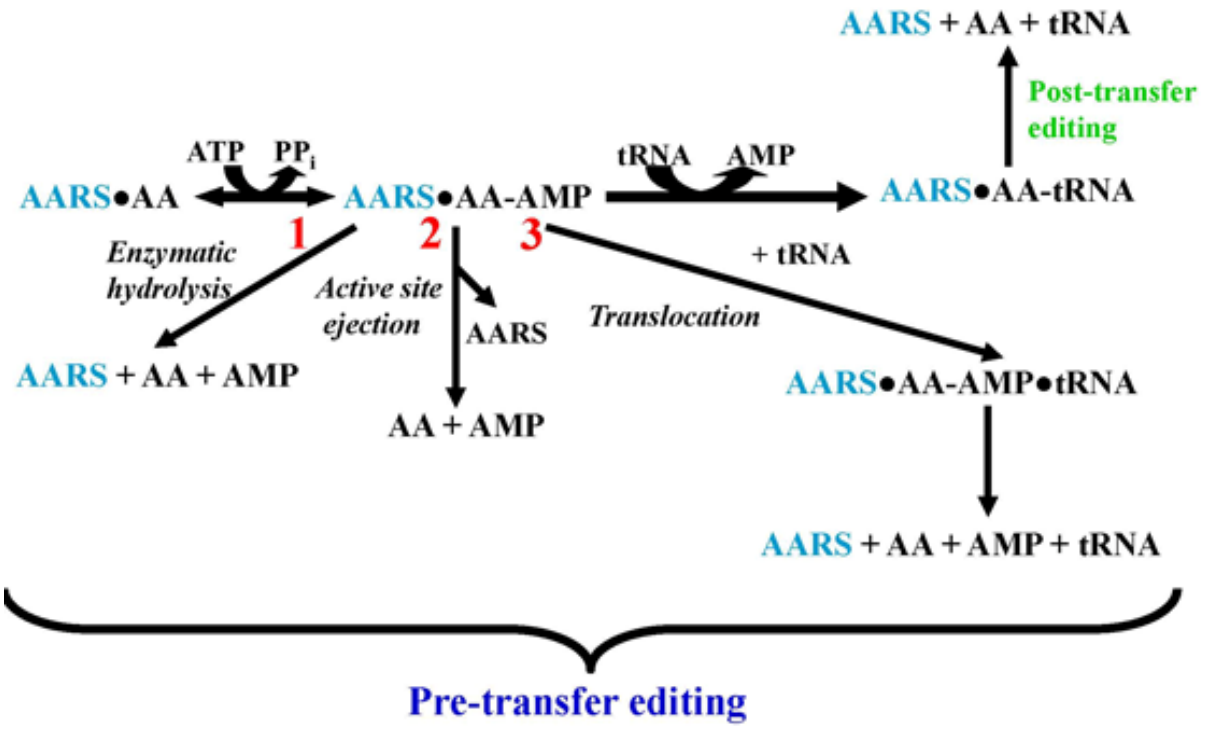

Figure I.10. Scheme showing possible pre- and post-transfer editing pathways. Abbreviations are: aminoacyl-tRNA synthetase (AARS), amino acid (AA), aminoacyl-adenylate (AA-AMP) and aminoacylated tRNA (AA-tRNA).

cally hydrolyzed ('active site ejection', pathway 2 in Figure I.10). If the rate of the adenylate release is faster than the rate of aminoacyl transfer, this pathway has been referred to as 'kinetic proofreading' (Hopfield, 1974). Pre-transfer editing via these two routes is largely independent of tRNA, although stimulation in the presence of tRNA has been also reported in some cases. Another view of the pre-transfer mechanism is referred to as the 'translocation model'. Based on fluorescence probe studies in class I IleRS, this model suggests that the noncognate adenylate (Val-AMP) is formed in the aminoacylation active site and then actively translocated to the editing site in the CP1 domain, in a tRNA-dependent manner, where it is hydrolyzed (pathway 3, Figure I.10) (Hendrickson, et al., 2002; Nomanbhoy, et

al., 1999). However, this model requires the formation of a misaminoacylated tRNA as an obligatory intermediate, followed by post-transfer editing. The post-transfer editing event primes or initiates conformational changes that facilitate translocation of the noncognate adenylate from the synthetic to the editing active site in the CP1 domain, followed by subsequent rounds of pre-transfer hydrolysis of the noncognate adenylate (Bishop, et al., 2002; Nomanbhoy, et al., 1999; Nordin and Schimmel, 2003).

There has also been evidence for the selective release and enzymatic hydrolysis pre-transfer pathways in different AARSs. The bacterial *Aquifex aeolicus* LeuRS has been reported to possess a norvaline-specific tRNA-independent pre-transfer editing activity, that is primarily enzyme catalyzed in the aminoacylation active site (Zhu, et al., 2009). In *E. coli* LeuRS, a tRNA-dependent pre-transfer editing activity within the aminoacylation active site is unmasked when the entire CP1 domain is deleted (Boniecki, et al., 2008). Similarly, in GlnRS, which is a non-editing class I AARS and lacks a spatially separated editing domain, evidence has been provided for a pre-transfer editing-like reaction within the synthetic active site (Gruic-Sovulj, et al., 2005). In ProRS, tRNA-independent pre-transfer editing has been reported against Ala-AMP (Beuning and Musier-Forsyth, 2000). In this case, the noncognate adenylate is primarily hydrolyzed on the enzyme (pathway 1, Figure I.10) (Splan, et al., 2008), with solution hydrolysis following selective release from the enzyme active site constituting a minor pathway (pathway 2, Figure I.10) (Hati, et al., 2006).

The location of the active site of pre-transfer editing has been a disputed issue in the field. As mentioned above, the aminoacylation active site has been implicated to have a critical role in both enzymatic hydrolysis of the adenylate as well as in selective release into solution (Boniecki, et al., 2008; Hati, et al., 2006). On the other hand, the pre-transfer model that comprises of translocating the adenylate from the enzyme main body to the CP1 domain indicates the latter as the site of pre-transfer. This is further supported by structural studies in

IleRS (Fukunaga and Yokoyama, 2006) and LeuRS (Lincecum, et al., 2003), which show that respective pre-transfer editing substrate analogs (NvaAMS and ValAMS) bind at sites highly overlapping with the site where the post-transfer editing substrate analogs bind. In fact, in the LeuRS CP1 domain, pre- and the post-transfer editing substrate analogs bind in the same threonine-rich peptide pocket (Figure I.9, left) (Lincecum, et al., 2003). Moreover, both the substrates are stabilized in the editing pocket by the universally conserved aspartic acid (Asp347 in *T. thermophilus* LeuRS) (Figure I.9, left) via hydrogen bonding (Lincecum, et al., 2003).

I.3.C. Coexistence of multiple editing pathways for an AARS

Many AARSs possess both pre- and post-transfer editing activities (Boniecki, et al., 2008; Martinis and Boniecki, 2010; Williams and Martinis, 2006). As an example, although class I IleRS (Fersht, 1977b) and yeast cyotoplasmic LeuRS (ycLeuRS) (Englisch, et al., 1986) have been proposed to maintain fidelity via pre-transfer pathways, both enzymes also possess a fully functional post-transfer editing activity within their homologous CP1 domains (Eldred and Schimmel, 1972; Lincecum, et al., 2003). The class II ProRS can not only edit Ala-tRNA^{Pro} by post-transfer editing catalyzed by the INS editing domain (Wong, et al., 2002), but also hydrolyze Ala-AMP via pre-transfer editing (Beuning and Musier-Forsyth, 2000). In addition, ProRS also depends on a third free-standing editing protein Ybak to clear Cys-tRNA^{Pro} (An and Musier-Forsyth, 2005).

The partitioning between the two pathways and predominance of one over the other could depend on distinct set of molecular determinants within the enzyme active site, the amino acid substrate and also other cellular cues (Boniecki, et al., 2008; Martinis and Boniecki, 2010; Sarkar and Martinis, 2011). The human cytoplasmic LeuRS (hcLeuRS) activates either one pathway against nonstandard biosynthetic intermediates, dictated by the

identity of the noncognate amino acid – while α-aminobutyrate is cleared by pre-transfer editing, norvaline is cleared by the post-transfer pathway (Chen, et al., 2011). In *E. coli* LeuRS, CP1-based mutations that selectively deactivate post-transfer editing or complete deletion of the CP1 domain activated an inherent aminoacylation active site-associated pre-transfer editing (Chen, et al., 2001; Williams and Martinis, 2006). Thus, clearly evolution has driven the AARS family towards possessing multiple checkpoints in order to ensure the highest level of fidelity in translation.

I.4. Structural overview of leucyl tRNA synthetase (LeuRS)

To date several crystal structures of LeuRS have been solved with or without $tRNA^{Leu}$ and in different conformations during the aminoacylation reaction (Cusack, et al., 2000; Fukunaga and Yokoyama, 2005a; Lincecum, et al., 2003; Rock, et al., 2007; Tukalo, et al., 2005) (Table I.3). This array of structural data shows that architectural features of LeuRS are consistent with other class I synthetases. The aminoacylation active site contains the Rossmann dicnucleotide-binding fold and also the catalytically important conserved sequences of HIGH and KMSKS (Figure I.11). Comparison of native LeuRS and leucyl-adenylate analog-bound enzyme shows that considerable local conformational changes within the aminoacylation active site accompany the binding of the adenosine moiety for amino acid activation (Cusack, et al., 2000). In particular, these changes involve the concerted dynamics of the HIGH and KMSKS loops towards the leucine-binding site which itself is very little perturbed.

Table I.3. Compilation of solved crystal structures of LeuRS

PDB ID	Reference	Structure Description
1H3N	Cusack et al. 2000	*T. thermophilus* LeuRS complexed with a sulfamoyl analog of leucyl-adenylate
1OBH	Lincecum et al. 2003	*T. thermophilus* LeuRS complexed with a pre-transfer editing substrate analogue in both synthetic active site and editing site
2BTE, 2BYT	Tukalo et al. 2005	*T. thermophilus* LeuRS complexed with a $tRNA^{Leu}$ transcript in the post-editing conformation and a post-transfer editing substrate analogue
1WZ2	Fukunaga and Yokoyama 2005	*P. horikoshii* LeuRS complexed with a $tRNA^{Leu}$ transcript in the aminoacylation conformation
2V0C, 2V0G	Rock et al. 2007	*T. thermophilus* LeuRS complexed with a sulfamoyl analogue of leucyl-adenylate in the synthetic site and an adduct of AMP with 5-fluoro-1,3-dihydro-1-hydroxy-2,1-benzoxaborole (AN2690) in the editing site
2WFE	Seiradake et al. 2009	*C. Albicans* cytosolic LeuRS CP1 editing domain
2WFG	Seiradake et al. 2009	*C. Albicans* cytosolic LeuRS CP1 editing domain bound to a benzoxaborole-AMP adduct
2WFD	Seiradake et al. 2009	Human cytosolic LeuRS CP1 editing domain

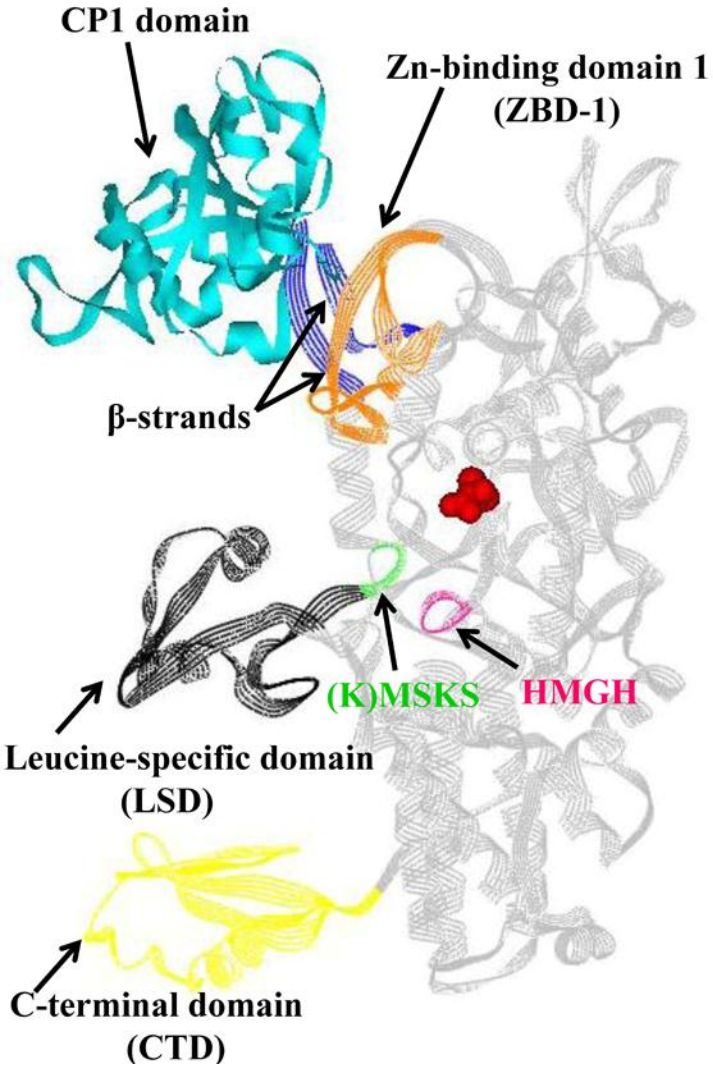

Figure I.11. Crystal structure of the *T. thermophilus* LeuRS with $tRNA^{Leu}$ in the editing conformation (PDB: 2BYT) (Tukalo, et al., 2005). For clarity, $tRNA^{Leu}$ is not shown here. The catalytic main body (grey) houses the aminoacylation active site that binds leucine (red) and ATP. Various appendages are inserted at specific points in the core main body of the enzyme, some of which fold into discrete domains, as highlighted. The CP1 domain is highlighted in cyan, the LSD in black, the CTD in yellow, the ZBD-1 in orange and the β-strand linkers in blue. The catalytically important '(K)MSKS' and 'HMGH' within the Rossmann fold are also marked.

Similar to the homologous IleRS and ValRS, the aminoacylation active site of LeuRS is split by a polypeptide insertion (approximately 180 amino acids) that discretely folds into a globular domain, called the CP1 domain (Figure I.11; Figure I.12) (Cusack, et al., 2000; Hou, et al., 1991; Starzyk, et al., 1987). The CP1 domain of LeuRS houses the editing active site which clears misaminoacylated tRNAs (Mursinna, et al., 2004). A more novel function of

the LeuRS CP1 domain is in mitochondrial intron RNA splicing in the yeast mitochondrial enzyme (Rho, et al., 2002). The bulk of the CP1 domain has little or no connection with the LeuRS main body, except for two flexible β-strands (Cusack, et al., 2000). The flexible β-strands facilitate rotations of the CP1 domain with respect to the main body during the various stages of the aminoacylation reaction (Fukunaga and Yokoyama, 2005a; Tukalo, et al., 2005). In *E. coli* LeuRS, the β-strands are critical to the hydrolytic editing activity of the protein (Betha, et al., 2007). They are hypothesized to specifically interact with the tRNA for post-transfer editing of misacylated $tRNA^{Leu}$.

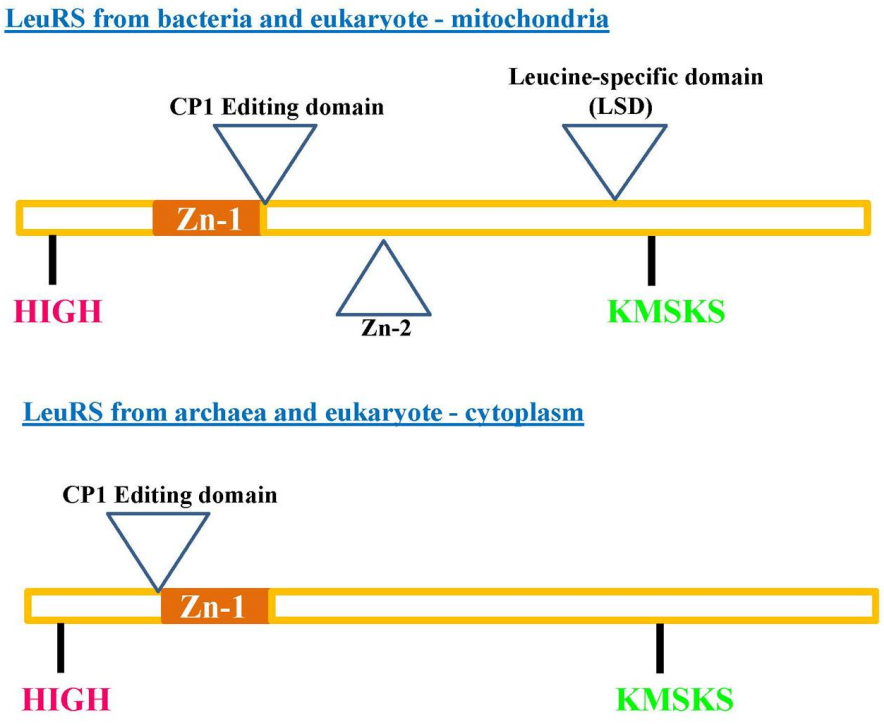

Figure I.12. Cartoon representation of the different positions of various insertion domains in LeuRS. (Top) Bacterial and eukaryotic-mitochondrial LeuRS. (Bottom) Archaeal and eukaryotic-cytoplasmic LeuRS. The figure has been adapted from Cusack et al. 2000.

In prokaryote-like LeuRSs, another small domain inserted into the catalytic main body is the leucine-specific domain (LSD; approximately 50 amino acids), inserted just prior

to the KMSKS loop (Figure I.11; Figure I.12) Although the LSD is not highly conserved in sequence or length, when present it has been shown to be critical to aminoacylation of $tRNA^{Leu}$ (Vu and Martinis, 2007). For example, while *T. thermophilus* LeuRS has one of the largest modules for LSD, it is completely missing in organisms such as *B. subtilis*, *H. pylori* and *P. horikoshii*.

The C-terminal domain (CTD) of *T. thermophilus* LeuRS is approximately 60 amino acids long and consists of a compact α-β bundle, common to other class Ia enzymes (Cavarelli, et al., 1998; Mechulam, et al., 1999; Nureki, et al., 1998). Unlike other members of class I AARSs, LeuRS does not use its CTD to recognize specific bases on the tRNA anticodon (Asahara, et al., 1993; Soma, et al., 1999). However, for the *S. cerevisiae* cytoplasmic LeuRS, the tRNA anticodon base recognition is critical (Soma, et al., 1996).

LeuRS also contains two inserted zinc-binding modules (Zn-1 and Zn-2) (Figure I.11; Figure I.12). Sequence alignments suggest that LeuRSs from archaea and cytoplasm of eukaryotes lack the Zn-2 domain (Cusack, et al., 2000). An interesting feature of LeuRS is the species-dependent variability in the point of insertion of the CP1 domain with respect to the Zn-1 domain. Comparison of primary sequences show that the CP1 domain is inserted between the two halves of the Zn-1 binding site for archaeal and eukaryotic cytoplasmic LeuRSs (Fig I.12, bottom), as also for IleRS and ValRS. Whereas, bacterial and eukaryotic mitochondrial LeuRSs have the CP1 domain inserted after the Zn-1 domain (Figure I.12, top) (Cusack, et al., 2000). Comparison of various *Pyrococcus* and *Thermus* LeuRS-$tRNA^{Leu}$ complexes highlights the importance of both an ordered closed conformation as well as the mobility of the Zn-1 domain (Tukalo, et al., 2005). The closed conformation is sterically incompatible for entry of the 3´-end of the tRNA into the catalytic site. However, in the absence of tRNA, this ordered packing of the Zn-1 domain over the leucyl-adenylate bound in the active site may provide additional protection to the adenylate from premature

hydrolysis. On the other hand, upon tRNA binding, coordinated reorientations of the Zn-1 domain and the CP1 domain would be required to allow aminoacylation. Similarly, flexibility of the Zn-1 domain would also be critical for translocation of the 3´-end of the tRNA from the aminoacylation to the editing active site.

I.5. Recognition of tRNA by AARS in aminoacylation and editing

Accurate AARS:tRNA pairing relies on identity elements within the tRNA that are recognized by the corresponding synthetase. AARSs mostly interact with one or more of the following: the discriminator base N73, the acceptor stem, and the anticodon (Figure I.13). In addition, interactions of the AARS with the variable loop and the D arm (Larkin, 2002) of the

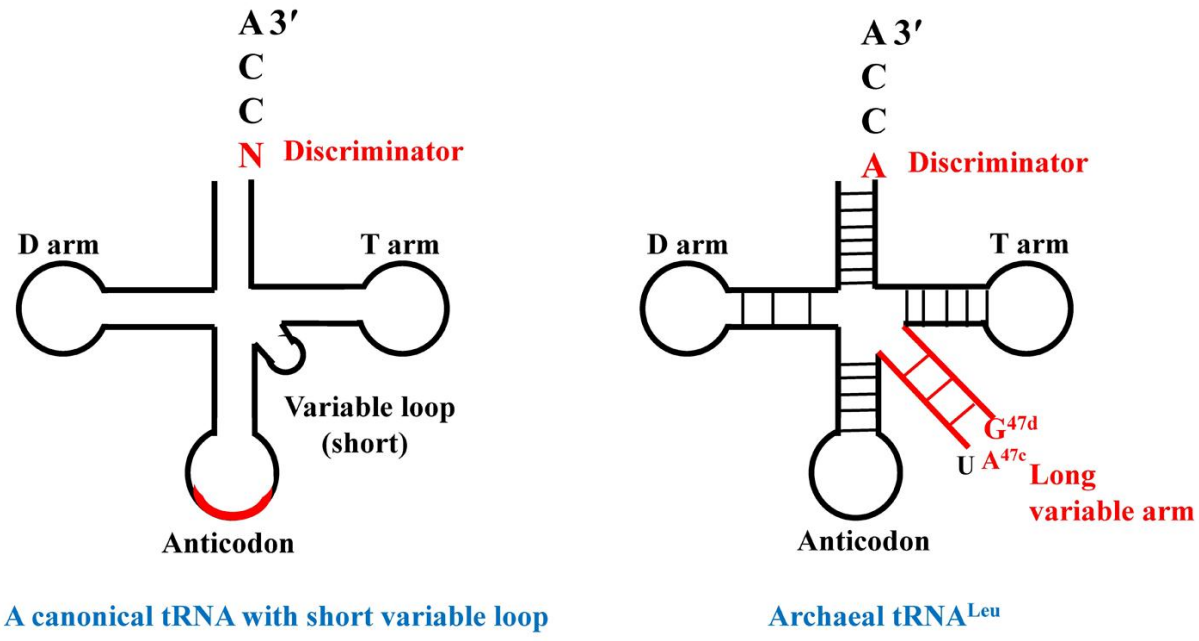

Figure I.13. Cloverleaf representations of tRNA. A canonical tRNA with a short variable loop (left) and archaeal $tRNA^{Leu}$ (right). Dashes represent base pairs. The AARS recognition identity elements are highlighted in red in both. The archaeal LeuRS uses the long variable arm and the discriminator base A for $tRNA^{Leu}$ recognition.

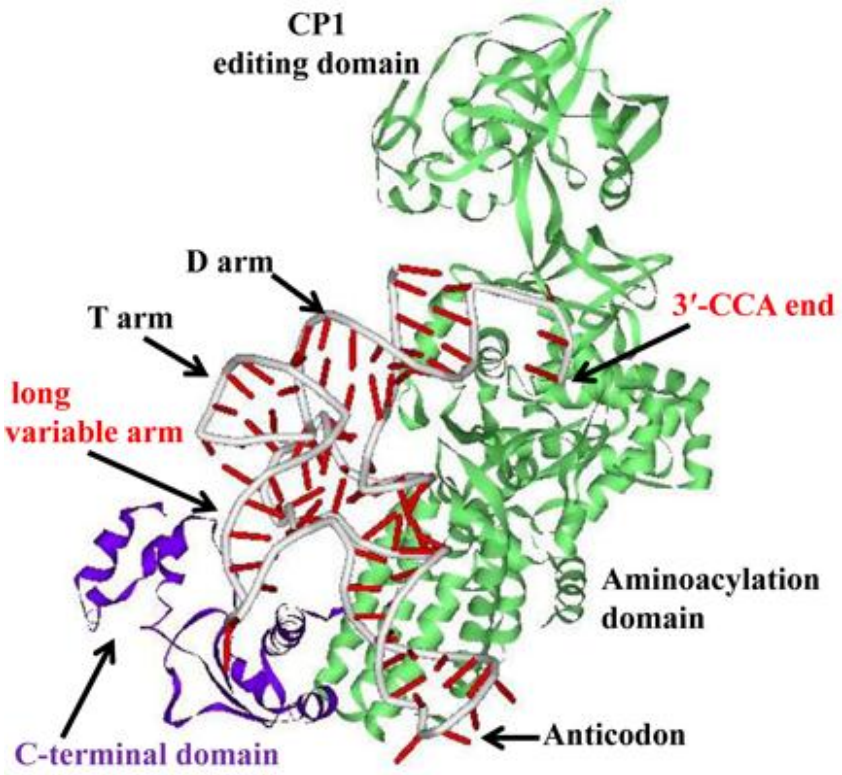

Figure I.14. *P. horikoshii* LeuRS in complex with $tRNA^{Leu}$ in the aminoacylation conformation (PDB: 1WZ2) (Fukunaga and Yokoyama, 2005a). The C-terminal domain of LeuRS (highlighted in purple) interacts with the long variable arm of $tRNA^{Leu}$ and the 3′-CCA end of the tRNA is seen in the aminoacylation active site.

tRNA has also been observed. Furthermore, structural elements unique to particular tRNAs such as G3:U70 wobble pair of $tRNA^{Ala}$ (McClain, et al., 1988; McClain and Foss, 1988) and the 15:48 tertiary base pair in $tRNA^{Cys}$ (Hou, et al., 1991; Hou, et al., 1993) have also been shown to act as strong recognition determinants in cognate aminoacylation. Occasionally, modified nucleotides can act as determinants, for example lysidine in *E. coli* $tRNA^{Ile}$ (Muramatsu, et al., 1988), 5-[(methylamino)methyl]-2-thiouridine *in E. coli* $tRNA^{Glu}$ (Sylvers, et al., 1993) and inosine in yeast $tRNA^{Ile}$ (Senger, et al., 1997). Another aspect of tRNA recognition by the synthetase is that in some tRNA:AARS pairs, the tRNA identity elements are the same for aminoacylation and editing, such as in ValRS (Tardif and Horowitz, 2002). In contrast in IleRS, the $tRNA^{Ile}$ elements that impact aminoacylation are distinct from the ones that are required for overall editing (Hale, et al., 1997). Although a

general set of recognition elements have been identified, the specific recognition elements vary between different AARS:tRNA pairs.

LeuRS recognizes up to six $tRNA^{Leu}$ isoacceptor molecules, each with a different anticodon. Idiosyncratic recognition features are required for LeuRS/$tRNA^{Leu}$ pair from different species. For bacterial LeuRSs, the discriminator base A73 (Asahara, et al., 1993; Larkin, 2002), the configuration of the D loop and the Levitt base pair, A15:U48 (Asahara, et al., 1998; Larkin, 2002) are crucial identity elements for efficient leucylation. Recognition of $tRNA^{Leu}$ by LeuRS is unique in a number of ways. Firstly, although most AARSs use the tRNA anticodon as a recognition element, LeuRS (along with SerRS (Biou, et al., 1994; Borel, et al., 1994) and AlaRS (Francklyn and Schimmel, 1989) do not depend on the tRNA anticodon as an identity element (Asahara, et al., 1993; Breitschopf, et al., 1995; Larkin, 2002). The one known exception is *S. cerevisiae* cytoplasmic LeuRS where the $tRNA^{Leu}$ anticodon is an important recognition element (Soma, et al., 1996). A second unusual feature of most $tRNA^{Leu}$ is that they contain an extra-long variable loop (Figure I.13) (type II tRNA) (along with $tRNA^{Tyr}$ and $tRNA^{Ser}$). The long variable loop is an important identity element in archaeal (Figure I.14) (Fukunaga and Yokoyama, 2005b) and human cytoplasmic (Breitschopf, et al., 1995) LeuRS, but not for *E. coli* (Asahara, et al., 1993) and *S. cerevisiae* cytoplasmic (Soma, et al., 1996) LeuRS. These observations also suggest that LeuRSs from different species have evolved to identify $tRNA^{Leu}$ using different identity elements. The anticodon of the tRNA does not contact the LeuRS (Figure I.14).

The co-crystal structure of *P. horikoshii* LeuRS and $tRNA^{Leu}$ (Figure I.14; Figure I.15) (Fukunaga and Yokoyama, 2005a) have precisely identified the interactions between the different domains of LeuRS and the $tRNA^{Leu}$ in the aminoacylation conformation. The *P. horikoshii* $tRNA^{Leu}$ assumes an L-shaped structure with a protruding long variable arm. The elements on the $tRNA^{Leu}$ that are recognized by this LeuRS include the discriminator base

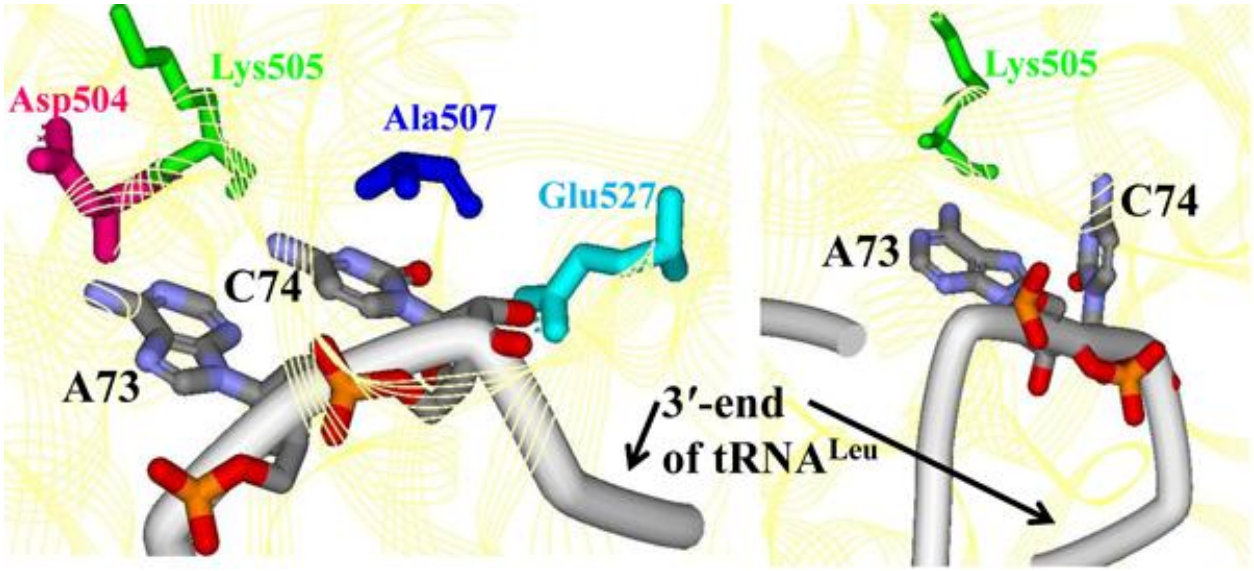

Figure I.15. Two modes of discrimination of discriminator base A73 and of C74. (Left) *P. horikoshii* LeuRS in complex with tRNA^{Leu} in the 'aminoacylation' state. The 3′-CCA end of the tRNA^{Leu} is in the aminoacylation active site. (Right) *P. horikoshii* LeuRS in complex with tRNA^{Leu} in the 'intermediate' state during transition from the aminoacylation to the editing conformation. The 3′-CCA end of the tRNA^{Leu} is partially relocated to the CP1 editing domain (PDB: 1WZ2) (Fukunaga and Yokoyama, 2005a).

A73 and the long variable arm (highlighted in red in Figure I.13). The LeuRS interacts with the tip of the long variable arm (A47c and G47d) (Figure I.13) via its C-terminal domain (Figure I.14). In this structure (Fukunaga and Yokoyama, 2005a), Fukunaga and co-workers identified two different complexes – the 'aminoacylation' complex (Figure I.15, left) in which the 3′-CCA end of tRNA^{Leu} is in the aminoacylation active site; and the 'intermediate' complex (Figure I.15, right) in which the 3′-CCA end of tRNA^{Leu} is partially turned away towards the CP1 editing domain. Interestingly, they captured two different modes of recognition of the A73 discriminator base by the LeuRS. In the aminoacylation complex, the bases A73 and C74 stack together and the discriminator base A73 hydrogen bonds with Asp504, Lys505, Ala507 and Glu527 (Figure I.15). In contrast, in the intermediate complex, the bases A73 and C74 are perpendicular to each other and Lys505 instead of hydrogen bonding with C74 now hydrogen bonds with A73 (Figure I.15). In both complexes however,

the terminal bases C75 and A76 interact only with the Rossmann fold in the aminoacylation active site.

The bacterial LeuRSs do not use the long variable arm of $tRNA^{Leu}$ as an identity element (Asahara, et al., 1993). The accompanying co-crystal structure of the *T. thermophilus* LeuRS in complex with $tRNA^{Leu}$ in the editing conformation (Tukalo, et al., 2005) showed that the 3′-end of the tRNA is positioned in the CP1-based editing active site and that neither the long variable loop nor the anticodon loop makes any contact with the bacterial LeuRS (Figure I.11). The 3′-end showed interactions with the universally conserved aspartic acid (Asp347) and the threonine-rich peptide as in the previous complexed structure of *T. thermophilus* LeuRS and the post-transfer editing substrate analog Nva2AA (Figure I.11) (Lincecum, et al., 2003). The C-terminal domain of LeuRS is critical even in the editing conformation as it forms direct contacts with the G19:C56 tertiary base pair. Overall, this structure suggested that contact areas between LeuRS and $tRNA^{Leu}$ are rather limited and much less in the editing conformation as compared to the aminoacylation conformation, consistent with the need to transition to an exit complex and product release.

I.6. Protein-assisted RNA splicing

I.6.A. Overview of the multiple alternate cellular functions of AARSs

Throughout evolution, AARSs acquired new cellular functions, that are not linked to protein synthesis, thus making this classic family of enzymes truly versatile with a broad repertoire of activities (Martinis, et al., 1999). Such functional expansion in some of the eukaryotic AARS can be traced back to the progressive addition of new protein domains to their overall structure (Guo, et al., 2010). Alternate functions of AARSs include protein-assisted splicing of intron RNAs by *S. cerevisiae* mitochondrial LeuRS and *Neurospora crassa* mitochondrial TyrRS (Lambowitz and Perlman, 1990), translational regulation by

ThrRS (Romby, et al., 1996) and transcriptional regulation by AlaRS (Putney and Schimmel, 1981). *E. coli* ThrRS binds to its own mRNA leader sequence and prevents the 30S ribosomal subunit from binding to the ribosome-binding sequence of the mRNA, thereby blocking synthesis of the protein (Romby, et al., 1996). *E. coli* AlaRS binds to a palindromic sequence flanking the transcriptional start site of its own gene, thereby repressing transcription. In human TyrRS, two specifically acquired peptides or domains, Glu-Leu-Arg (ELR) peptide and the endothelial monocyte-activating polypeptide II (EMAPII)-like domain act in concert in receptor-mediated signaling pathways involved in angiogenesis (Wakasugi, et al., 2002a; Wakasugi, et al., 2002b). Human TyrRS has been shown to be specifically secreted under apoptotic conditions and cleaved to generate two cytokines fom its N- and C-terminal halves (Wakasugi and Schimmel, 1999). The EMAP-II-like human TyrRS C-terminal domain exhibits monocyte chemotaxis acitivity and also stimulates tissue necrosis factor α (TNFα) production (Wakasugi and Schimmel, 1999). The human TrpRS has been reported to be a potent angiostatic factor (Wakasugi, et al., 2002b), in which the activity is regulated by an acquired WHEP domain of the synthetase. Under proliferative conditions, human MetRS is transported into the nucleus to stimulate rRNA synthesis in the nucleoli (Ko, et al., 2000).

I.6.B. Secondary structure of group I introns

Group I introns are present in tRNA, rRNA and protein-coding genes, particularly abundant in fungal and plant mitochondrial DNAs (Palmer and Logsdon, 1991). Group I introns can catalyze their own splicing, but are assisted by protein factors, particularly *in vivo* (Burke, 1988; Lambowitz and Perlman, 1990). The boundaries of group I introns are defined by a U residue at the 3′-end of the 5′ exon (the 5′-splice site) and a G residue at the 3′-end of

the intron (the 3′ splice site) (Figure I.16). Just like protein enzymes, the folding of group I introns into their catalytically active characteristic secondary and tertiary structure results in

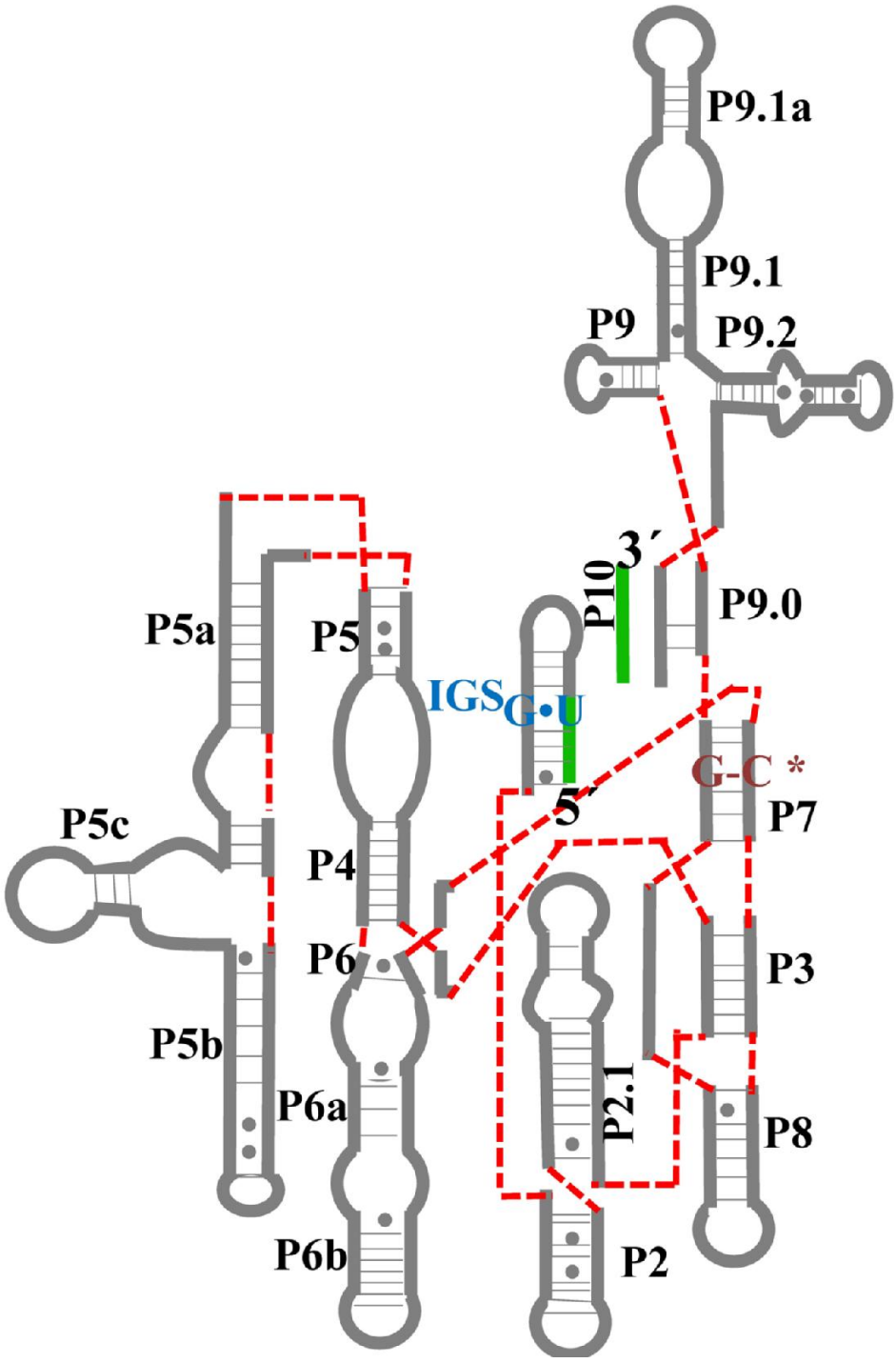

Figure I.16. Conserved secondary structure of group I intron. The 3´- and 5´-flanking exon sequences are shown in green. Dashes indicate base pairs and dots indicate wobble base pairs. Dashed red lines indicate continuity of intron strand. Tertiary interactions have been omitted for clarity. The conserved U•G base pair in the internal guide sequence (IGS), near the 5´-splice site is highlighted in blue. The guanosine binding site is denoted by asterisk (*). The figure is adapted from (Cech, et al., 1994).

juxtaposition of key residues that are widely separated in primary structures. The self-splicing ability of group I introns arises from that they all fold into highly conserved secondary and tertiary structures that bring the guanosine and the 5′- and 3′-splice sites in close proximity (Cech, 1988).

The secondary structure of all group I introns consist of a common conserved core, made up of series of paired regions (denoted P1-P10), separated by single-stranded regions or loops (Figure I.16). P1 and P10 contain the 5′- and 3′-splice sites, respectively and are formed by base pairing between an internal guide sequence (IGS) (generally located downstream of the 5′-splice site) (Davies, et al., 1982) and the exon sequences flanking the splice sites (Figure I.16). P1s of different group I introns vary in sequence, with only one conserved base pair between the U immediately preceding the 5′-splice site and a G in the IGS (Cech, 1990). In *Tetrahymena* intron, P3, P4, P6, P7, P8 and P9 form the catalytic core of the intron required for enzymatic activity (Michel and Westhof, 1990). Extra sequences, often consisting of long open reading frames (ORFs), form stem-loop structures that do not disrupt the core, are peripheral to the core, and vary in sequence between introns. Although such peripheral regions are dispensable for catalytic activity of the intron, they are not necessarily functionally irrelevant (Cech, 1990). Rather, these peripheral regions can be critical for folding of the conserved core into a catalytically active form and are also believed to provide protein-binding sites *in vivo*. Folding of the intron as well as the self-splicing reaction requires optimal Mg^{2+} ion concentration (Cech, 1990; Sugimoto, et al., 1988). Two kinds of Mg^{2+}-binding sites on the intron have been defined. One class has specific structural roles and participates in active site chemistry, while the other class promotes the global folding of the intron (Tinoco and Bustamante, 1999).

I.6.C. Splicing mechanism of group I introns

The self-splicing of group I introns occurs via two consecutive transesterification reactions, in the presence of guanosine and Mg^{2+} ions (Cech, 1990). The first transesterification reaction is initiated by guanosine or one of its phosphorylated forms (GMP, GDP, GTP). The 3′-OH of the sugar moiety of guanosine attacks the 5′-splice site and forms a 3′,5′-phosphodiester bond to the first nucleotide of the intron and as a result, the 5′ exon is excised (Cech, 1987; Zaug, et al., 1983). The 5′ exon now terminates in a free 3′-OH. This then attacks the 3′-splice site, resulting in ligation of the exons and excision of the intron (Figure I.17) (Cech, 1987; Zaug, et al., 1983).

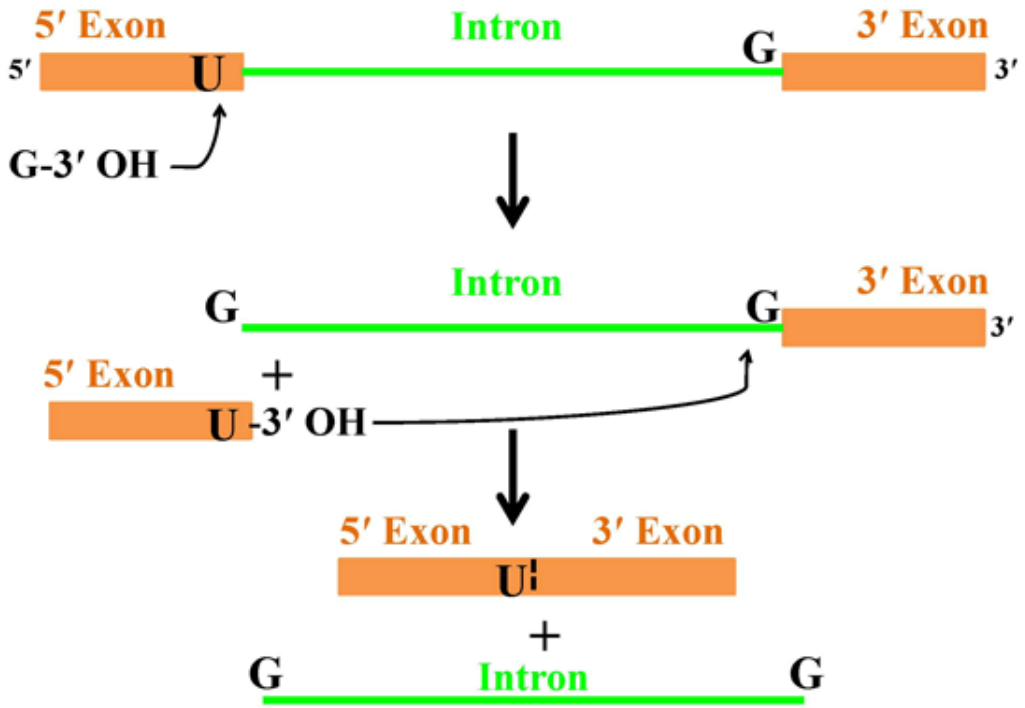

Figure I.17. Splicing mechanism of group I introns.

Group I introns have relatively low K_m values for guanosine (in the μM range) and hence can readily discriminate between guanosine and other nucleosides (Bass and Cech, 1986; Cech, 1990). Guanosine binds the intron via hydrogen bonds, interactions with the ribose hydroxyls and also base stacking interactions. A single guanosine-binding site is characterized by the presence of a conserved G•C pair in P7 (Figure I.16) (Michel, et al., 1989). However, additional interactions of the guanosine with the intron are also believed to be important.

I.6.D. Protein facilitation of group I intron splicing

Self-splicing of group I introns *in vivo* is facilitated by protein cofactors (Burke, 1988; Lambowitz and Perlman, 1990; Lambowitz, 1999). These proteins are proposed to primarily facilitate formation of the correct catalytically active intron RNA structure (Burke, 1988; Cech, 1988; Cech, 1990; Tinoco and Bustamante, 1999). The proteins that assist splicing include both intron-encoded proteins as well as nuclear-encoded proteins. One of the prominent protein facilitators among the intron-encoded proteins required for splicing of group I introns are maturases. Several group I introns in yeast mitochondrial DNA encode maturases that aid splicing of the intron that encodes them. These include the *cob*-I2, -I3 and –I4. Typically, the functioning of these maturases is intron-specific and the maturases act only in the splicing of the particular intron that encodes them (Lazowska, et al., 1980). An exception is the *cob*-I4 maturase (bI4 maturase) which functions is splicing of both the *cob*-I4 intron as well as another closely related group I intron, *cox*-I4 (De La Salle, et al., 1982; Dhawale, et al., 1981) (Figure I.18). The maturases encoded by group I introns are characterized by two repeats of the sequence motif LAGLIDADG. This motif is also characteristic of a larger family of proteins that have site-specific endonuclease activity (Perlman and Butow, 1989).

The nuclear-encoded proteins involved in splicing of group I introns include two mitochondrial AARSs. LeuRS (or NAM2) (Herbert, et al., 1988; Labouesse, 1990) and TyrRS (or CYT-18) (Akins and Lambowitz, 1987) are required for excision of group I introns from essential mitochondrial genes in yeast and *Neurospora crasssa*. The yeast mitochondrial LeuRS (ymLeuRS) is required for splicing of two closely related group I introns, bI4 and aI4α respectively from the genes encoding cytochrome *b* (*cob*) and the α subunit of cytochrome oxidase (*cox1α*) (Herbert, et al., 1988). The *Neurospora crasssa* mitochondrial TyrRS, on the other hand, is required for the splicing of a number of unrelated group I introns, such as the mitochondrial large rRNA intron as well as introns in the *cob* and ATPase 6 genes (Akins and Lambowitz, 1987; Cherniack, et al., 1990; Majumder, et al., 1989). Both LeuRS and TyrRS are believed to interact with conserved sequences or structures of group I introns.

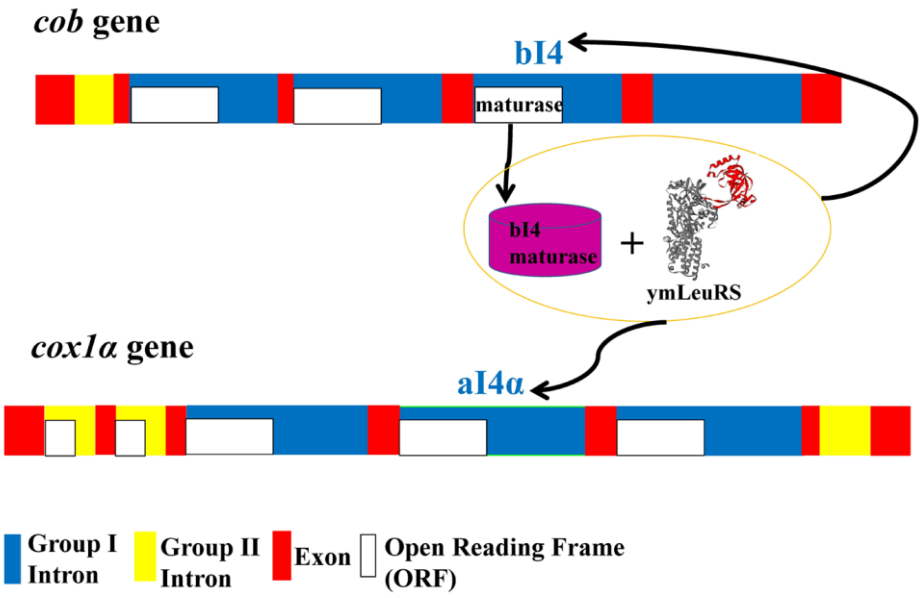

Figure I.18. Schematic representation of LeuRS-assisted splicing. The yeast mitochondrial LeuRS (ymLeuRS) facilitates the splicing of two related group I introns, bI4 and aI4α from the yeast mitochondrial *cob* and *cox1α* genes, respectively. bI4 maturase (encoded by the ORF of intron bI4) and nuclear-encoded ymLeuRS act in collaboration to aid in splicing of these two introns. (Color legend: blue – group I intron; yellow – group II intron; red – exon; and white – intron ORFs).

I.6.E. Role of AARSs in group I intron splicing

The *Neurospora crasssa* mitochondrial *cyt-18* gene encodes a protein which has both splicing as well as TyrRS aminoacylation activities. TyrRS promotes splicing of group I introns by facilitating folding of the intron into a catalytically active form (Caprara, et al., 1996; Chadee, et al., 2010; Lazowska, et al., 1980; Mannella, et al., 1979). Biochemical and

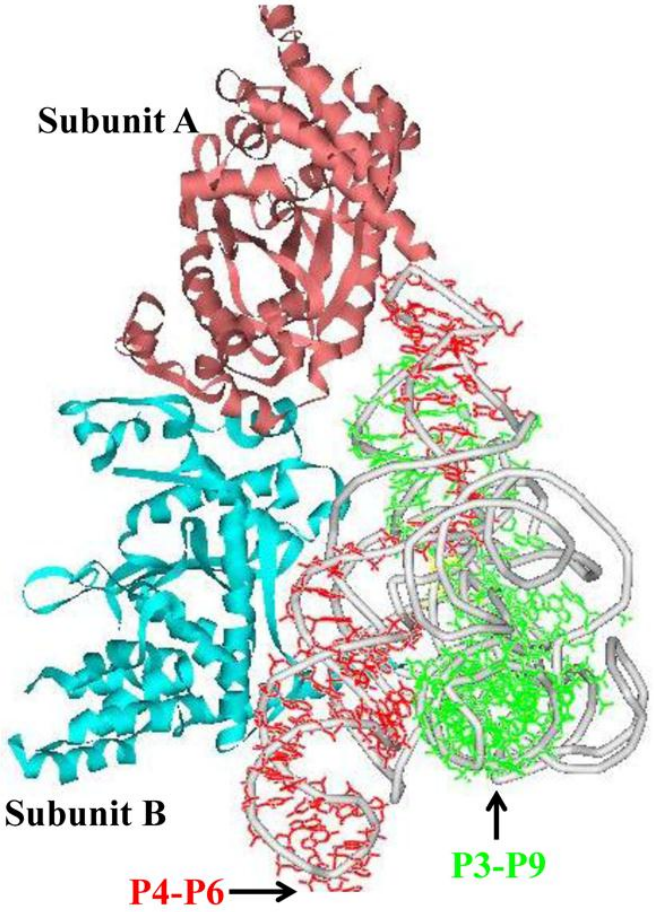

Figure I.19. Structure of *Neurospora crassa* TyrRS bound to a group I intron RNA. The P4-P6 and the P3-P9 domains of the intron are highlighted in red and green respectively (PDB: 2KJ) (Paukstelis, et al., 2008).

footprinting experiments have shown that TyrRS binds initially to the P4-P6 region of the intron, enabling formation of a scaffold for assembly of the P3-P9 domain (Caprara, et al., 1996). The binding of TyrRS to the intron RNA is believed to be a two-step process, in which the protein first recognizes primary or secondary structural features in the P4-P6

region of the unfolded intron and then makes additional contacts, concurrent with formation of tertiary structure (Caprara, et al., 1996). The structure of a TyrRS bound to a group I intron shows that the group I intron binds across the two subunits of the homodimeric protein, with the protein contacting both the P4-P6 and the P3-P9 catalytic core domains, but not the peripheral regions of the intron RNA (Figure I.19) (Paukstelis, et al., 2008). However, controrary to a previous notion, this structure suggests that the protein does not use tRNA-like features of the introns, but instead uses a distinct RNA-binding surface that is composed of an N-terminal extension absent in non-splicing bacterial TyrRSs.

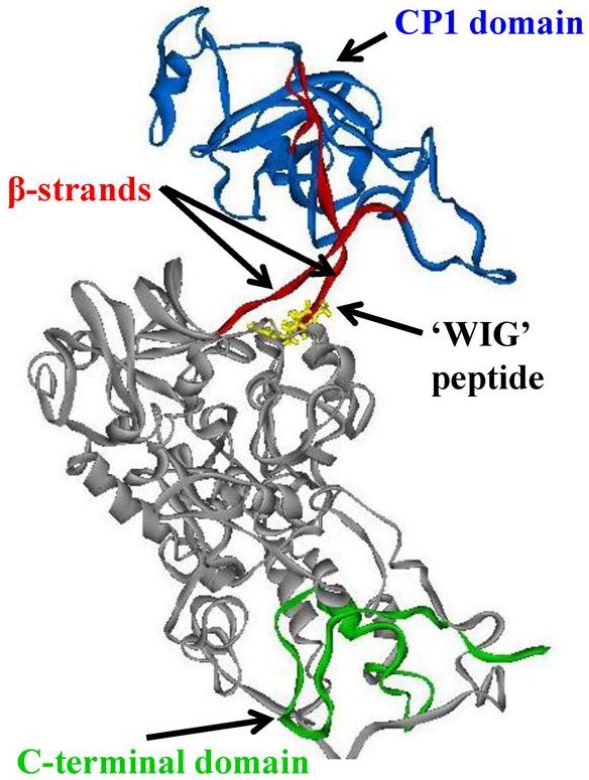

Figure I.20. Homology model of yeast mitochondrial LeuRS. The regions of the protein that impact splicing are highlighted.

The yeast mitochondrial (ymLeuRS) was implicated in RNA splicing when a suppressor mutation in LeuRS rescued RNA splicing in presence of a defective maturase

(Labouesse, et al., 1987). Splicing of *cob* and *cox* group I introns requires the collaborative functioning of the protein factors LeuRS and bI4 maturase (Figure I.18). Each of these protein factors can bind independently to the bI4 intron and stimulate RNA splicing (Rho and Martinis, 2000). Molecular determinants within LeuRS that impact splicing have been identified (Figure I.20), although the exact mechanism by which LeuRS promotes splicing of group I introns is still not clear. The CP1 editing domain of ymLeuRS, isolated from the full length enzyme, can stimulate splicing *in vivo* (Rho, et al., 2002). Regions surrounding the CP1 domain of LeuRS have also been implicated in RNA splicing. The tryptophan of the conserved WIG peptide in the N-terminal β-strand that links the CP1 domain to the LeuRS main body (Figure I.20) has been mutationally shown to impact splicing. Mutation of the tryptophan to a cysteine abolishes splicing, but maintains aminoacylation (Li, et al., 1996). A splicing-defective suppressor mutation has also been identified at the glycine of the WIG peptide in the ymLeuRS (G240S) (Figure I.20) (Labouesse, et al., 1985; Labouesse, 1990; Li, et al., 1996). In addition, the C-terminal domain of ymLeuRS is also critical in splicing and functionally diverged to accommodate the dual role of aminoacylation and splicing (Hsu, et al., 2006; Hsu and Martinis, 2008). Interestingly, LeuRSs from other organisms, such as a prokaryotic LeuRS and the human mitochondrial LeuRS can substitute for the ymLeuRS for its splicing activity (Houman, et al., 2000). This suggests that LeuRS, which unlike TyrRS has not acquired an idiosyncratic splicing-specific domain, uses its evolutionarily conserved features to interact with the intron RNA.

I.7. AARSs as antibiotic targets

The AARS family of enzymes by virtue of their universality, essentiality and diversity, have long been the focus of antibacterial drug discovery (Tao, 2000). Drug design targeting the synthetases has relied on a general chemistry platform which synthesizes analogs of the AARS substrates and intermediates. The strategy has been to find compounds that mimic the AARS substrates and also to selectively target the pathogen AARS, while sparing the human counterpart (Tao, 2000). The latter has been possible due to evolutionary divergence between prokaryotic and eukaryotic AARSs. The AARS inhibitors discovered or developed to date include mupirocin (Hughes and Mellows, 1978) and furanomycin (Tanaka, et al., 1969) against IleRS, indolmycin (Werner, et al., 1976) and chaungxinmycin (Brown, et al., 2002) against TrpRS, borrelidin (Nass, 1969) against ThrRS, AN2690 (Rock, et al., 2007) and granaticin (Ogilvie, et al., 1975) against LeuRS, cispentacin (Konishi, 1989) against ProRS and ochratoxin A (Konrad and Roschenthaler, 1977) against PheRS. Mupirocin (or pseudomonic acid), a commercially available potent inhibitor of IleRS, is a natural product of *Pseudomonas fluorescens* (Fuller, et al., 1971) and is used as a topical agent against bacteria. The tail portion of Mupirocin closely resembles the isoleucyl moiety of isoleucyl adenylate (Ile-AMP) (Figure I.21). Mupirocin binds in the vicinity of the KMSKS sequence in the aminoacylation active site of IleRS and is a bifunctional inhibitor with respect to both ATP and isoleucine (Silvian, et al., 1999; Yanagisawa, et al., 1994).

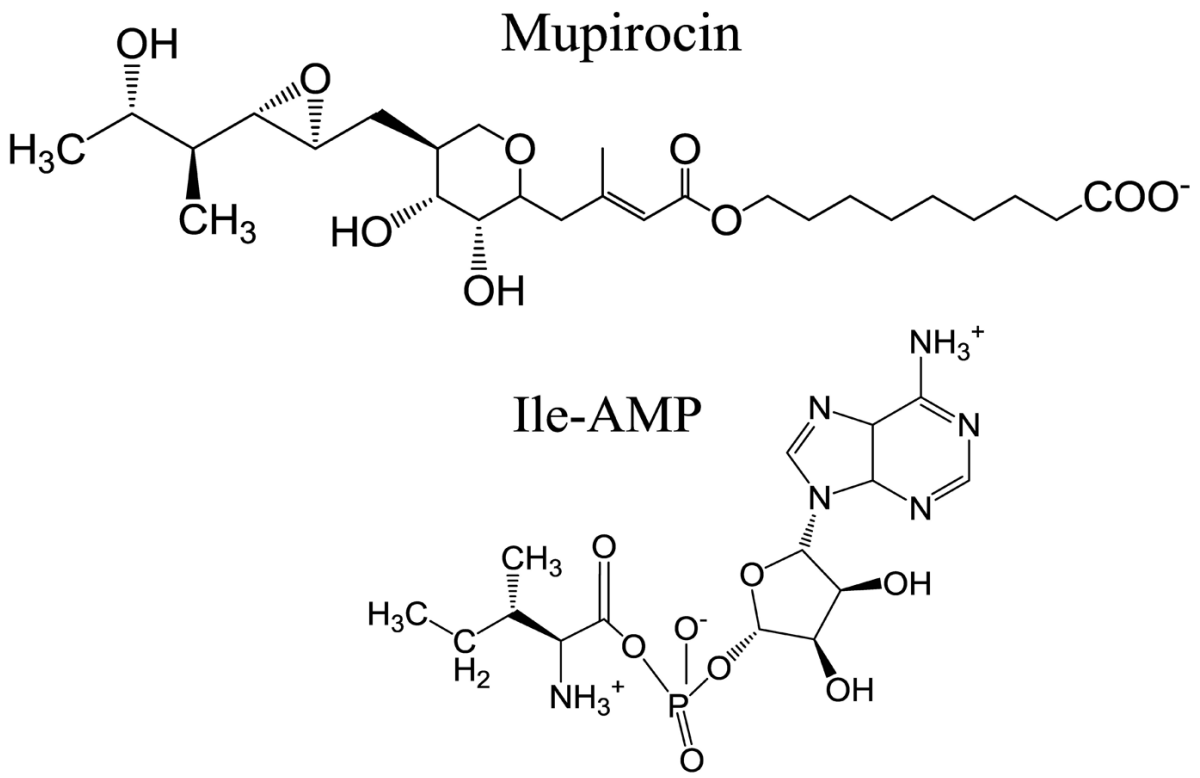

Figure I.21. Chemical structures of mupirocin and isoleucyl adenylate (Ile-AMP)

Apart from the aminoacylation active site, the editing active site is another potential binding site for inhibitors of AARSs that possess editing activity. Screening libraries of chemically synthesized boron-containing small molecules led to the discovery of a novel class of dihydrobenzoxaboroles that have broad spectrum antifungal activity (Baker, et al., 2006). Out of these benzoxaboroles, it was found that 5-fluoro-1,3-dihydroxy-2,1-benzoxaborole (AN2690) or its ethylamine derivative AN3018 (Figure I.22) inhibit protein synthesis in *Saccharomyces cerevisiae* by targeting the yeast cytoplasmic LeuRS (ycLeuRS) (Rock, et al., 2007; Seiradake, et al., 2009). The leading candidate, AN2690 is currently in clinical trials for the treatment of onychomycosis, a fungal disease of the toenail. In the editing pocket of LeuRS, AN2690 cross- links $tRNA^{Leu}$ (Figure I.23), effectively preventing release of the charged tRNA thereby rendering this essential enzyme inactive (Rock, et al., 2007). The $tRNA^{Leu}$-AN2690 adduct is formed via the boron atom of the oxaborole ring of

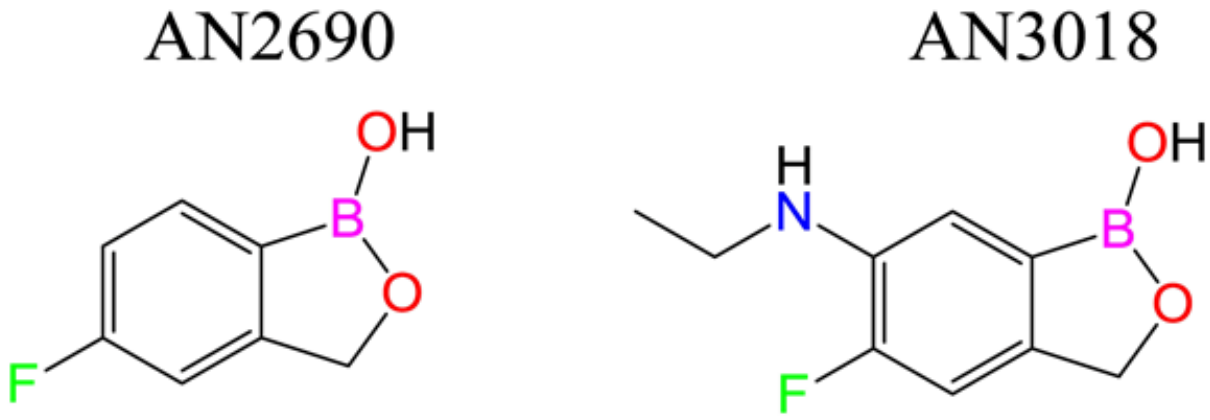

Figure I.22. Chemical structures of LeuRS inhibitors. The atom colors are: fluorine (green), boron (pink), oxygen (red) and nitrogen (blue).

AN2690 and the 2′,3′-hydroxy groups of the terminal adenosine (A76) at the 3′-end of $tRNA^{Leu}$ (Figure I.23) (Rock, et al., 2007). AN2690 occupies the noncognate amino acid-binding pocket in the editing site of the LeuRS CP1 domain (Rock, et al., 2007) and can be overlaid exactly on the post-transfer editing substrate analog (Nva2AA) (Lincecum, et al., 2003). The inactivation of LeuRS by AN2690 is reversible, but with a very slow reactivation rate, that corresponds to a long half-life for the adduct of 424 min (Rock, et al., 2007). Interestingly, spontaneously generated AN2690-resistant mutations have been identified within and outside the AN2690-binding pocket in the ycLeuRS (Rock, et al., 2007).

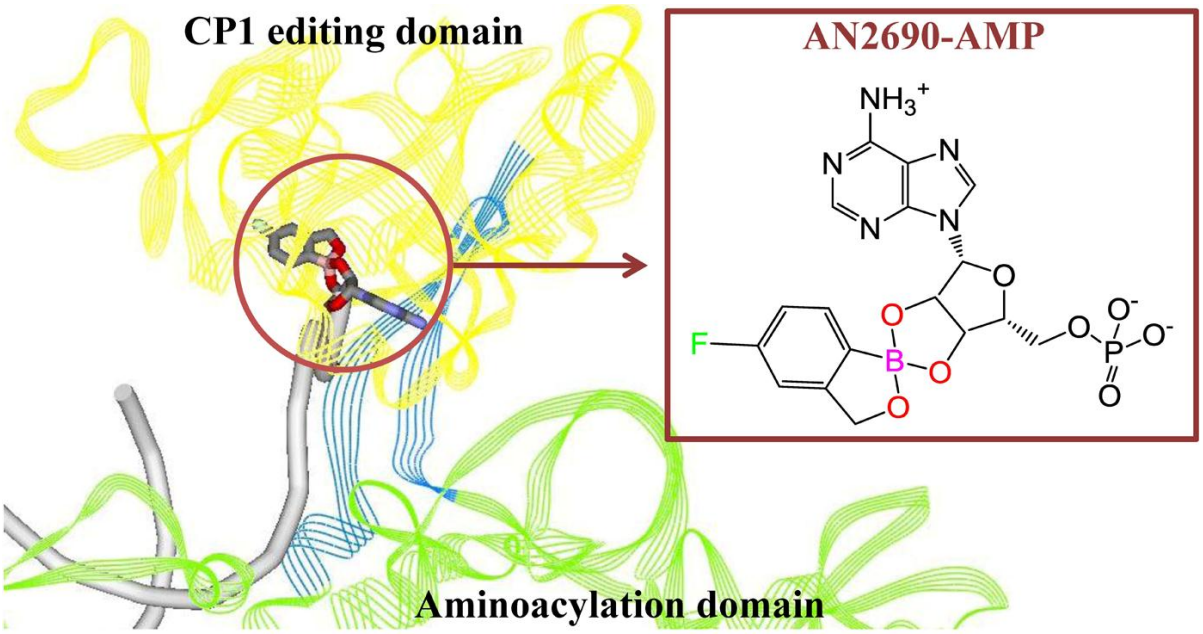

Figure I.23. *T. thermophilus* LeuRS in complex with $tRNA^{Leu}$ and AN2690. The CP1 domain of LeuRS is shown in yellow, the main body in green and the connecting β-strands are highlighted in blue. The AN2690-AMP adduct is encircled in the editing active site and its chemical structure shown in the inset (PDB: 2V0G) (Rock, et al., 2007).

I.8. AARSs-linked diseases

Specific AARSs have been implicated in the etiology of various diseases, such as autoimmune disorders, neuronal pathologies, disrupted metabolic functions and cancer (Park, et al., 2008). Charcot-Marie-Tooth (CMT) disease is characterized by muscular weakness and atrophy in the distal extremities and impaired sensation and reflexes. The CMT disease is caused by heritable mutations in genes encoding glycyl-tRNA synthetase (GlyRS) (Antonellis, et al., 2003) and TyrRS (Jordanova, et al., 2006). In GlyRS, two CMT-causing mutations are in the range of 'kissing contact' across the dimer interface of the synthetase and hamper dimer formation (Nangle, et al., 2007). Although these CMT-causing mutations in GlyRS do not affect aminoacylation, they exhibit a common defect in localization in the neurons.

Recent research hints at a possible connection between lysyl-tRNA synthetase (LysRS) and amyotrophic lateral sclerosis 1 (ALS1) (Kunst, et al., 1997). In some patients, a mutation in the Cu/Zn superoxide dismutase 1 (SOD1) is associated with ALS1 (Banci, et al., 2007). LysRS associates with the mutant SOD1 (but not the wild type) and may contribute to aggregation of SOD1, thus inducing apoptosis of motor neurons and leading to onset of neurodegeneration, the hallmark of ALS1.

It is known that several key components of the translational machinery are up- or down-regulated in various forms of cancer. MetRS, which is required for translation initiation, is increased in human colon cancer (Kushner, et al., 1976). The 3´-untranslated region (UTR) of the gene encoding MetRS contains a segement of complementary base sequence to the 3´-UTR of the C/EBP homologous protein (CHOP) that is critically involved in the onset of some tumors (Palmer, et al., 1997). Possible link between the complementarity of the 3´-UTR of these two genes is yet to be determined.

Development of leukoencephalopathy, which has brain-stem and spinal cord involvement and lactate elevation (LBSL) appears to be caused by specific mutations in the gene encoding mitochondrial aspartyl-tRNA synthetase (AspRS) (Scheper, et al., 2007). Most of these AspRS mutations are located in specific exons of the gene and can cause abnormal splicing, frame shifts or premature termination of translation.

Several of the AARSs have also been linked to autoimmune diseases. In 30% of autoimmune patients, autoantibodies against several AARSs, including HisRS, ThrRS, AlaRS, phenylalanyl-tRNA synthetase (PheRS), IleRS, GlyRS and asparaginyl-tRNA synthetase (AsnRS) have been detected. The ‘antisynthetase syndrome’ includes interstitial lung diseases (ILD) and rheumatoid arthritis, among others. In type 2 diabetic patients, a single nucleotide polymorphism of mitochondrial LeuRS was identified that caused an amino

acid substitution (H324Q) (t Hart, et al., 2005). However, the causal relationship of this mutation in LeuRS to diabetes is not yet known.

I.9. Dissecting the role of LeuRS CP1 domain in amino acid editing and splicing

The CP1 domain of LeuRS (Cusack, et al., 2000) was essentially the focus of research efforts in this thesis. Mechanistic investigations of amino acid editing, RNA splicing and drug-binding/resistance were conducted within the confines of this domain. The LeuRS CP1 domain is traditionally known for its role in post-transfer editing of mischarged tRNA (Mascarenhas, 2008) and has also been identified as the site for binding of benzoxaborole-based antimicrobial drugs (Rock, et al., 2007). Drug resistance mutations that also impacted hydrolytic editing were isolated within and surprisingly outside the conserved editing/drug-binding pocket in the LeuRS CP1 domain. One such resistance site outside the CP1-based editing pocket was specifically targeted and experiments designed to understand the impact of this residue on post-transfer editing and in the process to drug resistance. In addition, a cellular fluorescence-based assay was improvised that enables the quantification of intracellular effects of LeuRS editing defects.

LeuRS, like many other AARSs, is challenged by structural similarities between its cognate and the non cognate amino acids. As a result, it misactivates the near-cognate amino acids such as isoleucine and methionine. However, efficient editing mechanisms (Mascarenhas, 2008) in the enzyme help preserve the high level of fidelity in protein synthesis. Existence of multiple/alternate editing pathways in the ycLeuRS was investigated. Questions regarding the co-existence of these editing pathways and what cellular cues determine the shift of balance between these pathways were addressed.

The ymLeuRS has been implicated in facilitating mitochondrial RNA splicing (Labouesse, 1990). The CP1 domain, both isolated (Rho, et al., 2002) and in the context of

the full-length enzyme (Boniecki, et al., 2009), has been shown to stimulate RNA splicing. However, the detailed picture of specific molecular determinants within and around the LeuRS CP1domain was missing. In addition, questions such as how the ymLeuRS has evolved mechanistically and/or structurally to adapt to its dual roles in splicing and aminoacylation and editing were unanswered. To address these questions, dual functions of editing and RNA splicing in the LeuRS CP1 domain and the surrounding β-strand connections to the enzyme main body were investigated in an effort to isolate the overlaps and diversities between the two functions.

Chapter II: Materials and Methods

II.1. Materials

Oligonucleotide primers were synthesized by Integrated DNA Technologies (Coralville, IA). Radiolabeled amino acids and nucleotides were purchased from Amersham Pharmacia Biotech (Piscataway, NJ) or Perkin Elmer (Waltham, MA). Cloned *Pfu* DNA polymerase and dNTP mixture were obtained from Stratagene (La Jolla, CA). Restriction endonucleases and T4 DNA ligase were procured from New England Biolabs Inc. (Ipswich, MA) or Promega (Madison, WI). *E. coli* strains DH5α, BL21 (DE3) and BL21 (DE3) codon PLUS were obtained from Stratagene (La Jolla, CA), while the strain Rosetta 2 (DE3) was obtained from Novagen (Gibbstown, NJ). Crude *Saccharomyces cerevisiae* tRNA was acquired from Sigma Chemical Co. (St Louis, MO). The plasmid pGP1-2 expressing T7 RNA polymerase was generously provided by Dr. Tracy Palmer (University of East Anglia, UK).

II.2. Mutagenesis

Site directed mutagenesis was carried out via the polymerase chain reaction (PCR). Each 50 μl PCR reaction mixture contained 100 ng of template plasmid DNA, 125 ng each of forward and reverse primers, 0.05 mM dNTP mix and 0.05 U *Pfu* DNA polymerase in commercially available buffer. Under the following conditions, 25 cycles of PCR were carried out: 95 °C for 30 sec, 55 °C for 30 sec, and 68 °C for 20 min. To completely remove wild type copies of the plasmid, the final PCR mixture was restriction digested with 0.8 U *Dpn*I for 4 h at 37 °C. This restriction digested PCR mixture was used to transform *E. coli* strain DH5α. The mutation in the gene sequence was confirmed by automated DNA sequencing (UIUC Core Sequencing Facility, Urbana, IL).

II.3. Expression and purification of proteins

N-terminal six-histidine-tagged wild type or mutant proteins were expressed from the plasmids bearing the respective genes in *E. coli* strains BL21 (DE3), BL21 (DE3) codon PLUS or Rosetta 2 (DE3). A single transformant was used to inoculate 5 mL LB supplemented with required antibiotics and then incubated at 37 °C overnight. The overnight culture was used to inoculate 1 or 2 L LB (containing required antibiotics) and cells were grown at permissible temperature (30 °C or 37 °C) until the OD_{600} reached 0.6 to 0.8. Cells were then induced with 1 mM IPTG and the protein was expressed at the permissible temperature (30 °C, 37 °C or room temperature). Cells were harvested by an Avanti J-E (Beckman Coulter, Fullerton, CA) preparative centrifuge, at 6000 rpm for 15 min at 4 °C.

Cell pellets were resuspended in 8 to 10 ml of HA-I buffer [20 mM Na_2HPO_4, 10 mM tris(hydroxymethyl) aminomethane (Tris), pH 8.0, 100 mM NaCl and 5% glycerol]. This was followed by sonication on ice for 2 min at 50% amplitude and a 3 sec pulse using a Vibra Cell sonicator (Sonics, Newtown, CT). The 2 min cycle of sonication was repeated three times. The cell lysate was centrifuged at 12,000 rpm for 30 min at 4 °C. The protein-containing supernatant was mixed with 5 mL of HIS-Select Nickel Affinity Gel (Sigma-Aldrich) that had been pre-equilibrated with 30 mL of HA-I buffer. The N-terminal six-histidine-tagged protein in the supernatant was bound to the resin via gentle rocking at 4 °C for 1 h. Following binding, the resin was washed with 100 mL of HA-II buffer [20 mM Na_2HPO_4, 10 mM Tris, pH 7.0, 500 mM NaCl and 5% glycerol] containing 10 mM imidazole at 4 °C. The bound protein was then eluted from the resin using 10 mL of HA-III buffer [20 mM Na_2HPO_4, 10 mM Tris, pH 7.5, 100 mM NaCl and 5% glycerol] containing 200 mM imidazole. The eluted protein was concentrated using an Amicon Ultra centrifugal filter device (Millipore Corporation, Billerica, MA). The final protein concentration was

determined spectrophotometrically at 280 nm using the appropriate extinction coefficient, estimated by the ExPASy Protparam tool (http://ca.expasy.org/tools/protparam.html).

II.4. T7 RNA polymerase-based *in vitro* transcription of tRNA and purification

T7 RNA polymerase was expressed from the plasmid pGP1-2 (a gift from Dr. Tracy Palmer, University of East Anglia, UK) and purified as described (Pang and Martinis, 2009). *E. coli* $tRNA^{Leu}_{UAA}$, yeast mitochondrial $tRNA^{Leu}_{UAA}$ ($ymtRNA^{Leu}$) or *H. pylori* $tRNA^{Leu}_{UAG}$ were transcribed *in vitro* from the plasmids $ptDNA^{Leu}$ (Normanly, et al., 1986; Tocchini-Valentini, et al., 2000), $pYmtDNA^{Leu}$ (Rho and Martinis, 2000) or ptDNA-HP4 (Vu, 2008), respectively. Approximately 450 μg plasmid DNA were digested overnight with 25 U *Bst*NI at 60 °C, in a reaction volume of 1 mL to generate the linearized template for run-off transcription (Sampson and Uhlenbeck, 1988). Each 1 mL transcription reaction consisted of 60 μg template DNA, 40 mM Tris, 80 mg/mL PEG8000, 5 mM dithiothreitol (DTT), 50 μg/mL bovine serum albumin (BSA), 0.01% of Triton X-100, 8 μg/mL pyrophosphatase (Sigma-Aldrich), 7.5 mM each of ATP, CTP, GTP and UTP, 0.02 U/μL RNase inhibitor (Eppendorf, Hamburg, Germany), 5 mM spermidine, 30 mM $MgCl_2$ and 0.8 μM T7 RNA polymerase. The reactions were carried out at 42 °C for 3 h, followed by an a second addition of 0.8 μM T7 RNA polymerase and then incubation for another 3 h.

Transcribed tRNA was precipitated from the reaction mixtures overnight at -80 °C by adding twice the volume of 100% cold ethanol and 100 μg/mL glycogen, as an inert carrier molecule. The tRNA product was purified by electrophoresis on a denaturing 10% polyacrylamide gel, containing 8 M urea. Electrophoresis was carried out overnight at 10 mA in 1X Tris-Borate-EDTA (TBE) buffer (90 mM Tris, 90 mM boric acid and 2 mM EDTA, pH 8.0). The $tRNA^{Leu}$ band was visualized via UV shadowing and the band excised from the gel. The excised gel was crushed and soaked in 1X TBE. The tRNA was extracted

from the gel using the Elutrap electro-elution system (Whatman Inc., Florham Park, NJ). Electrophoresis was carried out in 1X TBE at 200 V for 3 h. The tRNA was then precipitated from the elution overnight at -80 °C by adding twice the volume of 100% cold ethanol and 100 μg/mL glycogen. The pellets were then washed twice with 70% ethanol, dried and resuspended in nuclease free water (Ambion Inc., Austin, TX). The concentration of the tRNA was calculated spectrophotometrically on the basis of its extinction co-efficient estimated by the online Ambion oligonucleotide calculator (http://www.ambion.com/techlib/misc/oligo_calculator.html).

II.5. Aminoacylation and misaminoacylation assay

Each aminoacylation reaction contained 60 mM Tris-HCl, pH 7.5, or 4-(2-hydroxyethy)-1-piperazineethanesulfonic acid (HEPES), pH 7.5, 10 mM $MgCl_2$, 1 mM dithiothreitol (DTT), 4 μM transcribed $tRNA^{Leu}$, 21 μM [^{3}H]-leucine (150 μCi/mL) and catalytic concentrations of enzyme. Each reaction was initiated with 4 mM ATP and carried out at room temperature or 30 °C. At various time points, 10 μL reaction aliquots were quenched on Whatman filter pads that had been pre-wet in 5% trichloroacetic acid (TCA) and then dried. The pads were then subjected to the following 10 min washes: three times with 5% TCA, and once with cold 70% ethanol. The pads were then dried under a heat lamp and quantitated for radioactivity in a liquid scintillation counter (Beckman LS 6500, Beckman Coulter, Fullerton, CA). GraphPad Prism software was used to plot data. Misaminoacylation assays were performed similarly, except that reactions contained 25 μM [^{3}H]-isoleucine (500 μCi/mL) or 50 μM [^{14}C]-isoleucine (15.9 μCi/mL).

II.6. Isolation of mischarged tRNA

Misaminoacylation of transcribed $tRNA^{Leu}$ with isoleucine was carried out by incubating the following reaction mixture at 25 °C for 3 h: 60 mM Tris, pH 7.5, 10 mM $MgCl_2$, 1 mM DTT, 8 μM transcribed $tRNA^{Leu}$, 23 μM [^{3}H]-isoleucine (300 μCi/mL), 1 μM editing defective LeuRS and 4 mM ATP. The reaction was quenched under acidic conditions with 0.18% acetic acid (Schreier and Schimmel, 1972) to stabilize the aminoacyl ester linkage between isoleucine and the terminal adenosine (A76) on $tRNA^{Leu}$. Protein was removed from the reaction mixture by phenol extraction using a 125:24:1 phenol:choloroform:isoamyl alcohol mixture (pH 4.3) (Fisher Scientific, Fair Lawn, NJ). Mischarged $tRNA^{Leu}$ was ethanol precipitated in the presence of 0.34 mg/mL glycogen at -80 °C overnight. The recovered tRNA pellet was washed twice with 70% ethanol, dried and resuspended in 50 mM KP_i (pH 5.0).

II.7. Post-transfer editing deacylation assay

Deacylation reaction mixtures contained 60 mM Tris, pH 7.0, 10 mM $MgCl_2$ and approximately 2 μM mischarged $tRNA^{Leu}$. The reactions were initiated with 1 μM enzyme. At desired time points, reaction aliquots of 5 μL were quenched on Whatman filter pads that had been pre-wet in 5% TCA and dried. Pads were washed and then quantified for radioactivity as described for the aminoacylation assays.

II.8. ATP/Inorganic pyrophosphate (PP_i) exchange assay

Reaction mixtures containing 50 mM Tris-HCl, pH 8.0 or 50 mM HEPES, pH 8.0, 10 mM $MgCl_2$, 1 mM DTT, 1 mM [^{32}P]-PP_i (100 μCi/mL), 1 mM ATP, and 1 mM leucine or 10 mM isoleucine were initiated with 1 μM enzyme. At different time intervals, reaction aliquots of 2 μL were quenched on cellulose polyethyleneimine (PEI) thin layer

chromatography (TLC) plates (Scientific Adsorbents Inc., Atlanta, GA) that were pre-run in water and dried. Reaction products were resolved on the TLC plates in 750 mM KH_2PO_4, pH 3.5 with 1 mM urea. Resolved radiolabeled bands on the TLC plate were phosphorimaged using FUJIFILM BAS Cassette 2040 (FUJIFILM Medical Systems, Stanford, CT) and images were scanned by a STORM 840 Molecular Dynamics scanner (Amersham Pharmacia Biotech, Piscataway, NJ). Images were quantified using the ImageQuant software and the resulting data plotted and analyzed using the GraphPad Prism software.

Chapter III: Characterization of Benzoxaborole-based Antifungal Resistance Mutations Demonstrates that Editing Depends on Electrostatic stabilization of the Leucyl-tRNA Synthetase Editing Cap

Adapted with permission from
Jaya Sarkar, Weimin Mao, Tommie L. Lincecum, Jr., M.R.K. Alley, and Susan A. Martinis (2011). "Characterization of benzoxaborole-based antifungal resistance mutations demonstrates that editing depends on electrostatic stabilization of the leucyl-tRNA synthetase editing cap". *FEBS Lett.*, **585**, 2986-2991.

III.1. Introduction

Aminoacyl-tRNA synthetases (AARSs) are essential to all organisms and have been pursued as promising pharmaceutical drug targets (Schimmel, 1998). Pseudomonic acid (Mupirocin) has been used for years as a topical antibiotic to selectively inhibit isoleucyl-tRNA synthetase (IleRS) via interactions with its aminoacylation active site. Recently, a novel benzoxaborole called AN2690 was discovered to block protein synthesis in yeast by binding to the editing site of cytoplasmic LeuRS (Rock, et al., 2007).

Each of the AARSs establishes the genetic code via an aminoacylation reaction that attaches a specific amino acid to its cognate tRNA, which is then delivered to the ribosome. To enhance fidelity, about half of the AARSs have evolved 'editing' or 'proofreading' mechanisms (Mascarenhas, 2008). A 'post-transfer' editing mechanism hydrolyzes the misacylated tRNA to release free uncharged tRNA and amino acid. This correction mechanism is carried out by AARSs that have hydrolytic domains or by free-standing tRNA deacylases (An and Musier-Forsyth, 2005; Fersht, 1977b; Ruan and Soll, 2005). Alternatively, 'pre-transfer' editing clears misactivated aminoacyl-adenylate (Fersht, 1977b).

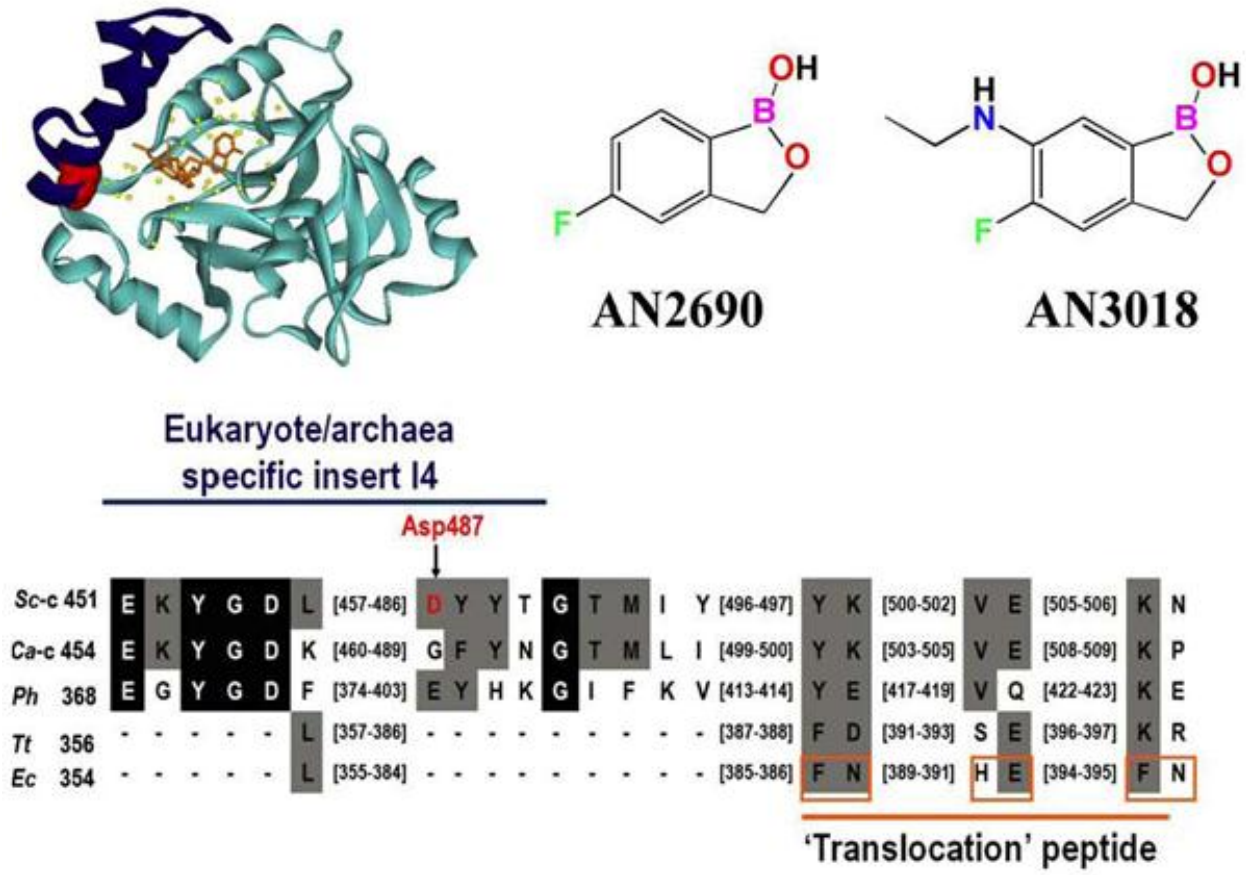

Figure III.1. Primary and tertiary structures of LeuRS I4 'cap' insert within the CP1 editing domain. (Top left) Crystal structure of *C. albicans* cytoplasmic LeuRS CP1 domain in complex with AN3018-AMP (orange) (PDB entry 2WFG) (Seiradake, et al., 2009). The I4 insert (Glu454 to Asn493 in *C. albicans*) is highlighted in blue with Gly490 (which corresponds to the Asp487 in yeast cytoplasmic LeuRS) shown in red. Yellow balls denote ordered water molecules in the editing pocket. (Top right) Chemical structures of AN2690 and AN3018. (Bottom) Multiple sequence alignment of the I4 insert within the LeuRS CP1 domain. The blue line highlights the I4 insert. The Asp487 in yeast LeuRS is indicated in red and by the arrow. The orange line indicates the putative 'translocation' peptide proposed in *Escherichia coli* LeuRS (Hellmann and Martinis, 2009). The residues boxed in orange within this peptide are proposed to impair translocation. Abbreviations are: *Thermus thermophilus* (Tt), *E. coli* (Ec), *S. cerevisiae* cytoplasmic (Sc-c), *C. albicans* cytoplasmic (Ca-c) and *P. horikoshii* (Ph).

The class I AARS canonical core of LeuRS houses the synthetic aminoacylation site. A discretely folded polypeptide insertion, called the connective polypeptide 1 (CP1) (Starzyk, et al., 1987) contains the hydrolytic editing active site (Mursinna, et al., 2001). The antifungal AN2690 forms an adduct to $tRNA^{Leu}$ in the editing pocket to trap the enzyme in a non-productive conformation (Figure III.1, top left). A series of AN2690-resistant mutations

were isolated within the CP1 domain of yeast LeuRS that localized to the hydrolytic editing active site (Rock, et al., 2007). Here, we focused on two resistance mutations at Asp487 that lie outside the hydrolytic editing active site in LeuRS, where AN2690 (Figure III.1, bottom) binds. This resistance site is downstream of conserved motifs in the primary sequence that define the editing pocket.

Sequence alignments show that Asp487 is located within an insert called I4 that is specifically found in eukaryotes and archae, but is absent in the bacteria (Figure III.1, bottom). An X-ray crystal structure of the CP1 domain from *Candida albicans* LeuRS suggests that the I4 insert forms part of a cap over the hydrolytic active site (Seiradake, et al., 2009). When closed, the I4 cap in the *C. albicans* structure sequesters an AN2690-benzoxaborole analog called AN3018 (Figure III.1, top) that is covalently linked to AMP. In this case, the AMP portion of the bound small molecule is proposed to mimic the 3´-end of a tRNA molecule that is bound in the editing site (Seiradake, et al., 2009).

Since the benzoxaborole binds in the editing site where the mischarged tRNA editing substrate binds in LeuRS (Lincecum, et al., 2003; Rock, et al., 2007), we postulated that resistance mutations at Asp487 in the I4 cap would impact hydrolytic editing. Biochemical analysis of mutations at Asp487 showed that a negatively charged residue was essential to hydrolytic editing activity. We hypothesize that Asp487 plays a critical role in facilitating the I4 cap closure over the editing active pocket during substrate binding. Our results support that electrostatic interactions between Asp487 and an arginine residue within the editing pocket facilitates the lid-like orientation of the I4 cap to stabilize bound substrate and promote editing.

III.2. Experimental methods

III.2.A. Mutagenesis

Mutations that are resistant to AN2690 were selected using the haploid *S. cerevisiae* strain (ATCC 201388) via methods that have been previously described (Rock, et al., 2007). Spontaneous ethylmethane sulfonate (EMS)-induced resistant mutants were isolated from YPD agar plates that contained concentrations of 2 μg/mL, 4 μg/mL, and 8 μg/mL AN2690.

Site directed mutagenesis was carried out via the polymerase chain reaction (PCR) as described in Chapter II. The plasmid p32YL-2-3 (Lincecum, et al., 2003) encoding the wild type *S. cerevisiae* cytoplasmic LeuRS was used as the template to introduce the desired mutations to generate the plasmids pJSycD487G, pJSycD487N, pJSycD487A, pJSycD487K, pJSycD487R and pJSycD487E encoding the mutant D487G, D487N, D487A, D487K, D487R and D487E LeuRS enzymes, respectively. Plasmids pJSycD487G, pJSycD487N and pJSycD487A were then used as templates in separate PCR reactions to introduce a second T319A mutation in each mutant protein. This created the plasmids pJSycD487G/T319A, pJSycD487N/T319A and pJSycD487A/T319A, encoding the double mutant D487G/T319A, D487N/T319A and D487A/T319A LeuRSs, respectively. Plasmid pJSycD487K was utilized as the template to introduce the second mutation R316D or R316E generating the mutant D487K/R316D or D487K/R316E LeuRSs, respectively. Similarly, plasmid pJSycD487R was utilized as the template to introduce the second mutation R316D or R316E generating the mutant D487R/R316D or D487R/R316E LeuRSs, respectively.

III.2.B. Protein expression and purification

A 2 L LB that contained 100 μg/mL ampicillin (Amp) and 34 μg/mL chloramphenicol (Cm) was inoculated with a 5 mL overnight culture and cells grown at 30 °C till OD_{600} reached ~0.8. Post induction with 1 mM IPTG, the N-terminal six-histidine tagged wild type

and mutant yeast cytoplasmic LeuRSs were expressed in *E. coli* strain Rosetta (DE3) (Novagen) at 30 °C for 45 min from the respective plasmids and purified via Ni-NTA affinity chromatography as described in Chapter II. The final protein concentration was determined spectrophotometrically at 280 nm using an extinction coefficient of 155,310 $M^{-1}cm^{-1}$, estimated by the ExPASy Protparam tool (http://ca.expasy.org/tools/protparam.html).

III.2.C. Aminoacylation and misaminoacylation assay

The aminoacylation reactions contained 60 mM HEPES, pH 7.5, 30 mM $MgCl_2$, 30 mM KCl, 1 mM DTT, 4 mg/mL *S. cerevisiae* crude tRNA, 21 µM [^{3}H]-leucine (150 µCi/mL) and catalytic concentrations of enzyme. Each reaction was initiated with 4 mM ATP. At desired time points, reaction aliquots of 10 µL were quenched and processed as described in chapter II. Kinetic parameters for the aminoacylation reaction were measured using 0.5 µM enzyme. A relatively high enzyme concentration was used for the kinetic assays due to low activity of the yeast LeuRS enzyme at lower concentrations. A range of 0.1–100 mg/mL crude yeast tRNA (Sigma) was used which corresponded to 0.05–40 µM $tRNA^{Leu}$. The 'Enzyme Kinetics analysis' module of Sigma Plot (Systat Software, Inc.) was used to calculate the kinetic parameters and error.

Misaminoacylation reactions were carried out similarly, except that the reaction mixture contained higher concentrations of 25 µM [^{3}H]-isoleucine (500 µCi/mL) or 50 µM [^{14}C]-isoleucine (15.9 µCi/mL) and 1 to 5 µM enzyme.

III.2.D. Isolation of mischarged tRNA

Misaminoacylation of *S. cerevisiae* crude tRNA with isoleucine was carried out by incubating the following reaction mixture at 30 °C for 3 h: 60 mM HEPES, pH 7.5, 30 mM $MgCl_2$, 30 mM KCl, 1 mM DTT, 4 mg/mL *S. cerevisiae* crude tRNA, 23 µM [^{3}H]-isoleucine

(300 μCi/mL), 1 μM editing defective LeuRS and 4 mM ATP. Mischarged tRNA was isolated as described in Chapter II.

III.2.E. Post-transfer editing deacylation assay

Deacylation reactions were carried out at pH 7.5 in 60 mM HEPES, 30 mM $MgCl_2$, 30 mM KCl, and approximately 2 mg/mL [^{14}C]-Ile-tRNA^{Leu} or [^{3}H]-Ile-tRNA^{Leu}. The reactions were initiated with 0.5 μM enzyme and reaction aliquots of 5 μL were quenched, processed, and analyzed as described in Chapter II.

III.2.F. ATP/Pyrophosphosphate (PP_i) exchange assay

Inorganic pyrophosphate (PP_i) exchange assays were carried out with reaction mixtures containing 50 mM HEPES, pH 8.0, 10 mM $MgCl_2$, 10 mM KCl, 1 mM DTT, 1 mM [^{32}P]-PP_i (100 μCi/mL), 1 mM ATP, and 1 mM leucine or 10 mM isoleucine were initiated with 1 μM enzyme. Aliquots of 2 μL at specific time points were analyzed via thin-layer chromatography as described in Chapter II.

III.2.G. Acid gel electrophoresis

Acid gel electrophoresis of misaminoacylation reaction products was performed in order to confirm that the amino acid is indeed present on the tRNA. Misaminoacylation reactions containing 50 mM HEPES, pH 7.5, 30 mM $MgCl_2$, 30 mM KCl, 2 mM DTT, 4 mg/mL *S. cerevisiae* crude tRNA, 20.3 μM [^{35}S]-methionine (300 μCi/mL) or 50 μM [^{14}C]-isoleucine (300 μCi/mL) and 1 μM enzyme were initiated with 4 mM ATP and incubated for 3 h at 30 °C. From each reaction, an aliquot of 10 μL was quenched with 10 μL quench buffer (100 mM NaOAc, pH 5.0, 50 mM EDTA and 8 M urea) and electrophoresed on a 10% acid acrylamide gel (pH 5.0) containing 8 M urea. The gel was

pre-equilibrated with 25 mM NaOAc, pH 5.0 and electrophoresed slowly at 5 mA in the same buffer. Upon completion of separation, the gel was dried and exposed to a phosphorimager screen (FUJIFILM BAS Cassette 2040) for 2 to 4 weeks in case of [^{14}C]-isoleucine or 2 days in case of [^{35}S]-methionine. Images were scanned by a STORM 840 Molecular Dynamics scanner and images quantified using the ImageQuant software.

III.3. Results

The antifungal LeuRS inhibitor, AN2690 binds in the CP1 domain-based editing active site of LeuRS (Rock, et al., 2007). The boron atom of AN2690 forms bonds with the *cis*-diol groups of the ribose ring at the 3´-end of $tRNA^{Leu}$ to yield a tRNA-AN2690 adduct in the editing site of LeuRS (Rock, et al., 2007) (Figure III.1, top). The AN2690-tRNA-protein complex prevents enzyme turnover, ultimately leading to an arrest in protein synthesis.

In yeast LeuRS, spontaneous resistant mutations were isolated in the presence of concentrations of AN2690 that were 4-, 8-, and 16-fold of its 0.5 µg/mL minimal inhibitory concentration (MIC) (Rock, et al., 2007). The mutants were dominant and showed an 8 to 64-fold increase in the yeast MIC. As would be expected based on target interactions, the mutant LeuRSs lacked resistance to several other known antifungal agents including amphotericin B, cerulenin, itraconazole, aculeacin A, terbinafine, tunicamycin, ciclopirox, cyclohexamide, and nikkomycin Z.

Previously, AN2690 spontaneous-resistance mutants were localized to the editing active site of yeast LeuRS, where AN2690 binds directly (Rock, et al., 2007). Herein, we focused on missense mutations to Asp487 where mutants with a cytoplasmic LeuRS bearing a glycine (D487G) or asparagine (D487N) substitution conferred an increase in the MIC of AN2690 to 32 µg/mL compared to 0.5 µg/mL for the wild-type strain. Because Asp487 is at

a site that is distal to the hydrolytic editing active site, its effect on editing or alternate mechanisms of action on the target LeuRS were not clear. The Asp487 site is separated from the primary sequence that defines the editing pocket/AN2690 binding site and it is located in an insert called I4 that is specific to the archaeal and eukaryotic enzymes (Figure III.1).

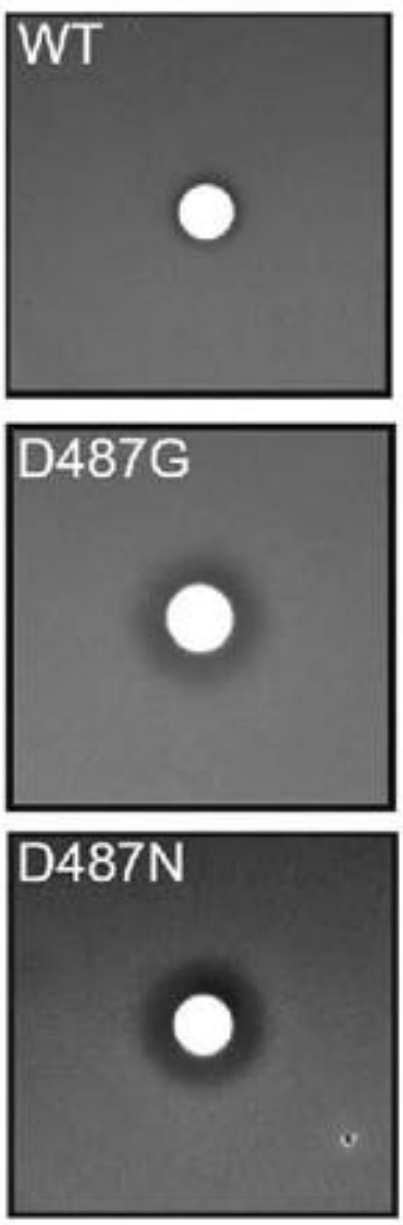

Figure III.2. Norvaline sensitivity of AN2690 resistant mutations at Asp487. The parental *S. cerevisiae* strain ATCC 201388 (Rock, et al., 2007) is labeled wild type (WT). The mutations D487G and D487N correspond to the *S. cerevisiae* resistant strains ANA325 and ANA359, respectively. The 'halo' of cell death around the central well, which incorporates 20 µL of norvaline (40 mg/mL), indicates that the resistant mutants are editing defective.

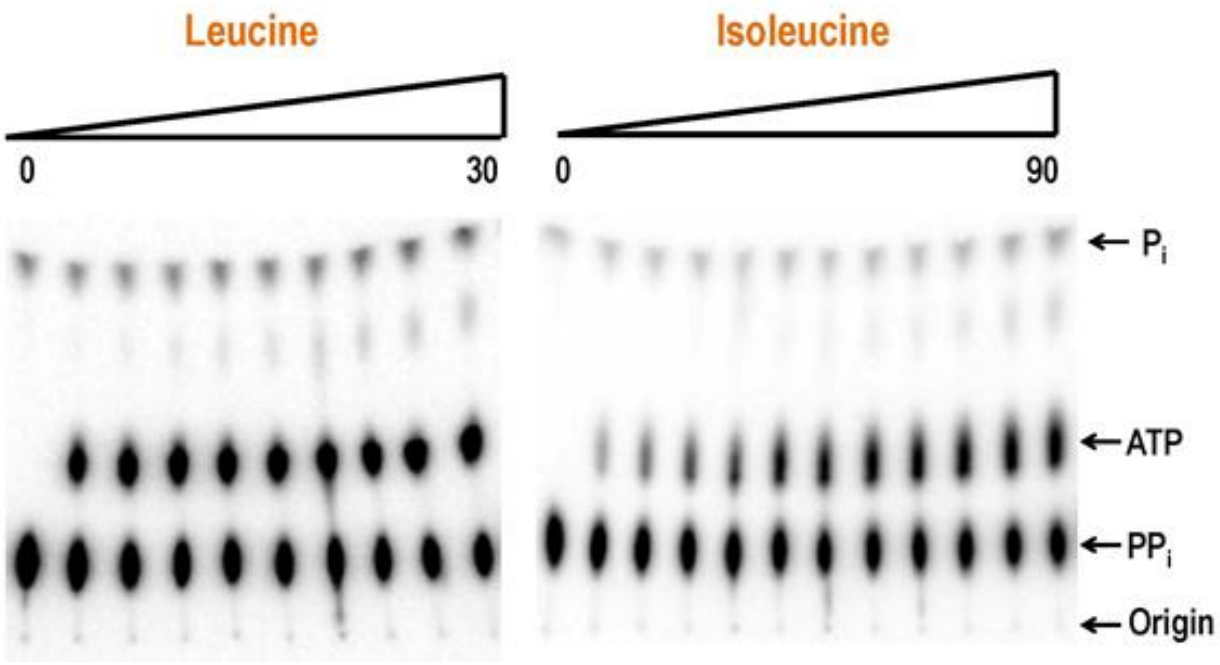

Figure III.3. Amino acid activation by wild type ycLeuRS, assessed by ATP/PP_i exchange assays. A representative reaction time course TLC-based separation of [^{32}P]-PP_i, -ATP and -P_i. Reactions containing 1 mM [^{32}P]-PP_i (100 µCi/mL), 1 mM ATP and 1 mM leucine or 10 mM isoleucine were initiated with 1 µM enzyme at 30 °C. Leucine activation reactions were carried out upto 30 min, while reactions with isoleucine upto 90 min. The TLC plates were developed in 750 mM KH_2PO_4, pH 3.5 with 1 M urea.

Comparison of the apo crystal structure of the isolated CP1 domain from *C. albicans* LeuRS and the co-crystal structure containing AN3018, an analog of AN2690 (Figure III.1, top right) (Seiradake, et al., 2009) suggests that the yeast/archeal-specific I4 helix is flexible and can close in a 'cap' like fashion over the editing site that is bound to the benzoxaborale inhibitor. The space enclosed over the editing pocket by this I4 'cap' accommodates both the substrate and a fixed network of water molecules. We hypothesized that Asp487 of the I4 insert orients the cap for substrate binding and stabilization in the editing site. Halo assays that incorporated 20 µL of norvaline (40 mg/mL) in the central well (Rock, et al., 2007) support that the LeuRS D487G and D487N are editing defective resulting in norvaline toxicities (Figure III.2).

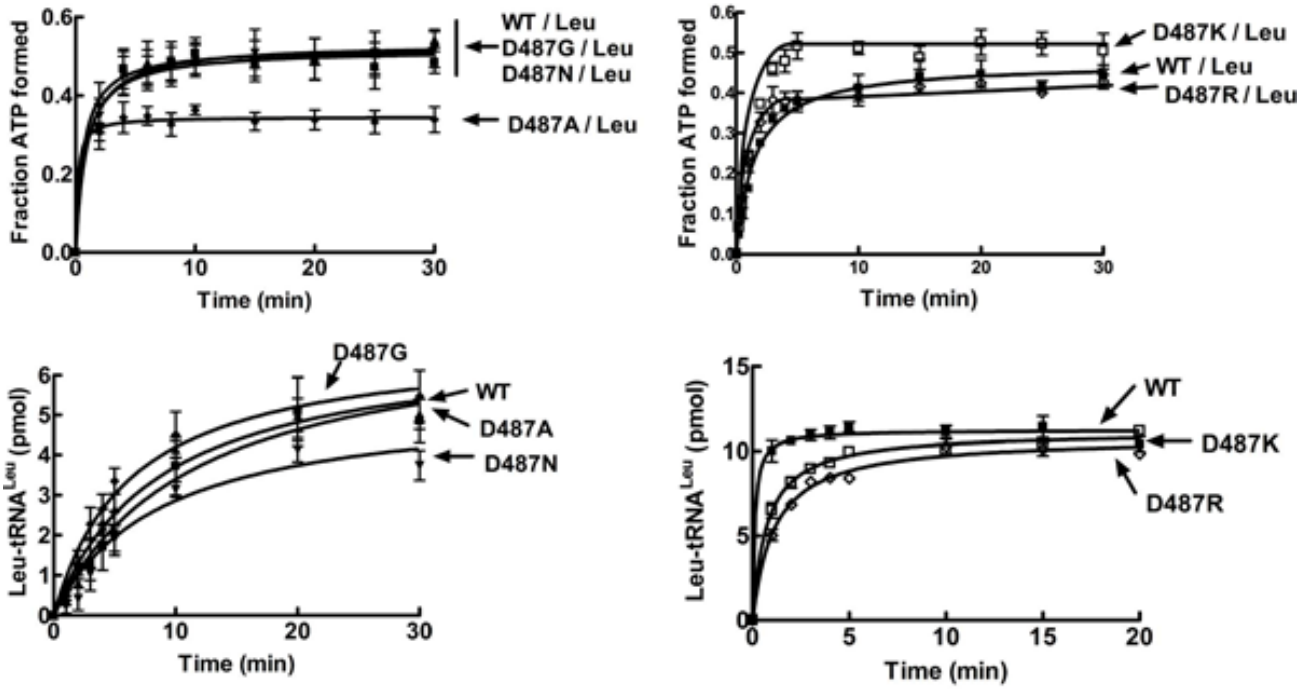

Figure III.4. Leucine activation and aminoacylation by Asp487 LeuRS mutants. (Top) Leucine-dependent pyrophosphate (PP_i) exchange reaction mixtures consisted of 1 mM PP_i (100 μCi/ml), 1 mM leucine and 1 mM ATP and were initiated with 0.5 μM enzyme. (Bottom) Aminoacylation reactions included 4 mg/ml *S. cerevisiae* crude tRNA, 0.5 μM enzyme and 21 μM [^{3}H]-leucine (150 μCi/ml) and were initiated with 4 mM ATP. Symbols are: wild type (■), D487G (▲), D487N (▼), D487A (♦), D487K (□) and D487R (◊). Error bars for each time point are a result of each reaction repeated in triplicate.

We re-created the AN2690 resistant mutations, D487G and D487N, as well as a D487A mutation in the yeast cytoplasmic LeuRS. To test the importance of a charged polar side chain in the I4 insert, we also replaced Asp487 with lysine, arginine and glutamic acid, generating the positively charged mutant D487K and D487R as well as the homologous mutant D487E LeuRSs, respectively. Leucine-dependent PP_i exchange assays showed that the resistant mutants, D487G and D487N (Figure III.3, left; Figure III.4, top left) as well as the positively charged D487K and D487R LeuRS mutants (Figure III.3, left; Figure III.4, top right) activate cognate leucine similar to the wild type enzyme. Based on its lowered plateau, the D487A mutant LeuRS exhibited slightly reduced ATP formation compared to the wild type enzyme (Figure III.4, top left).

Table III.1. Apparent kinetic parameters for $tRNA^{Leu}$ aminoacylation.[a]

LeuRS	K_M (mM)	k_{cat} (sec^{-1})	k_{cat}/K_M ($mM^{-1}sec^{-1}$)
Wild type	**0.6 ± 0.05**	**0.4 ± 0.01**	**0.7 ± 0.05**
D487G	**0.7 ± 0.10**	**0.2 ± 0.06**	**0.3 ± 0.10**
D487N	**0.4 ± 0.06**	**0.1 ± 0.01**	**0.3 ± 0.01**
D487A	**3.5 ± 0.8**	**0.3 ± 0.1**	**0.1 ± 0.01**
D487K	**1.2 ± 0.2**	**0.2 ± 0.01**	**0.2 ± 0.06**
D487R	**2.7 ± 1.2**	**0.3 ± 0.1**	**0.1 ± 0.06**

[a] $tRNA^{Leu}$ concentrations were varied as described in materials and methods.

We tested each yeast mutant LeuRS using commercially available crude yeast tRNA, since we previously determined that an *in vitro* generated yeast $tRNA^{Leu}$ transcript is a very poor substrate for its cognate LeuRS (Lincecum, et al., 2003). We hypothesize that modifications are critical in stabilizing the structure of yeast $tRNA^{Leu}$. Alternatively, they may provide an important determinant for aminoacylation by yeast LeuRS (Giegé, et al., 1998). These mutant LeuRSs aminoacylate $tRNA^{Leu}$ (Figure III.4, bottom) with approximately 2-fold reduction in k_{cat}/K_M values (Table III.1) as compared to the wild type enzyme. The decrease in the k_{cat}/K_M for the D487A and the positively charged D487 mutant LeuRSs is primarily due to an increase in K_M (Table III.1).

The Asp487 mutant LeuRSs were tested for their amino acid editing activity with yeast crude tRNA that was misaminoacylated with isoleucine using an editing-defective LeuRS. The AN2690-resistant mutants, D487G, D487N and also the D487A mutant exhibited significantly reduced deacylation activity for Ile-$tRNA^{Leu}$ (Figure III.5, top). The positively charged Asp487 mutant LeuRSs are completely defective in hydrolyzing misacylated tRNA (Figure III.5, bottom). Interestingly however, a homologous substitution at Asp487 by glutamic acid retains substantial editing activity (Figure III.5, bottom). Also as

expected, the aminoacylation activities of the LeuRS Asp487 resistance mutants were not inhibited by AN2690 (Figure III.6). The mechanism of action for AN2690 inhibition requires $tRNA^{Leu}$ binding in the editing active site for it to be trapped by the benzoxaborole.

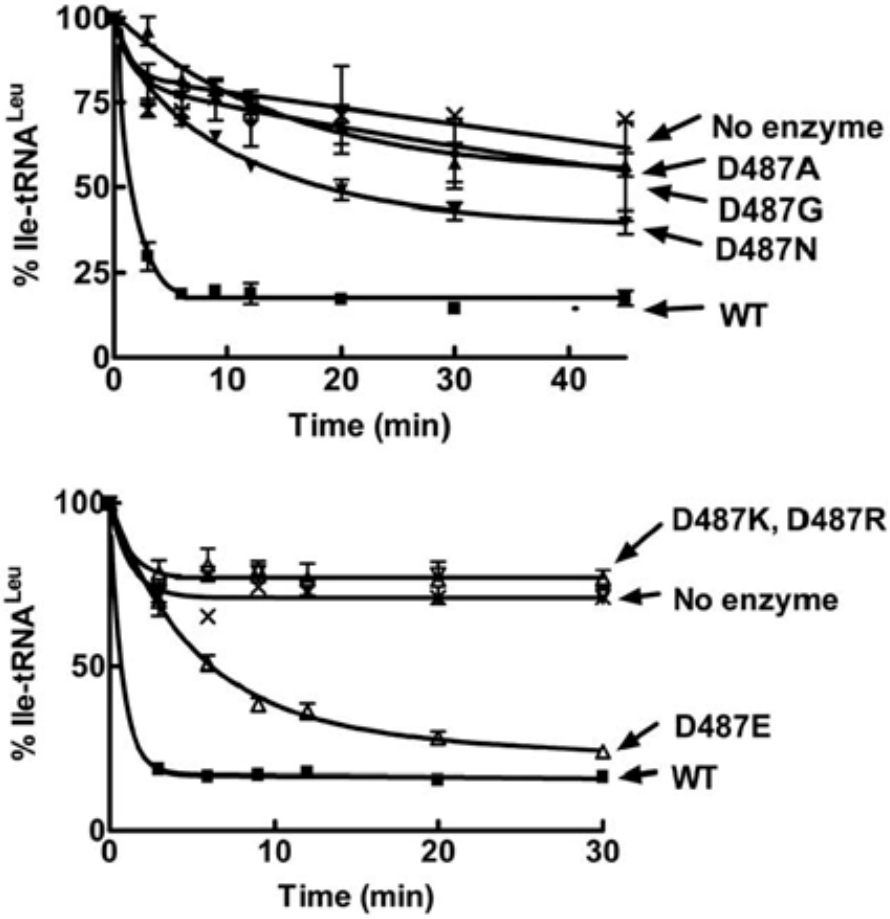

Figure III.5. Isoleucine editing activities of AN2690-resistant and charged Asp487 mutants of LeuRS. Deacylation reactions included approximately 2 mg/ml [^{14}C]-Ile-$tRNA^{Leu}$ and 0.5 µM enzyme. Symbols are: wild type (■), D487G (▲), D487N (▼), D487A (♦), D487K (□), D487R (◊), D487E (Δ) and no enzyme (x). Error bars for each time point are a result of each reaction repeated in triplicate.

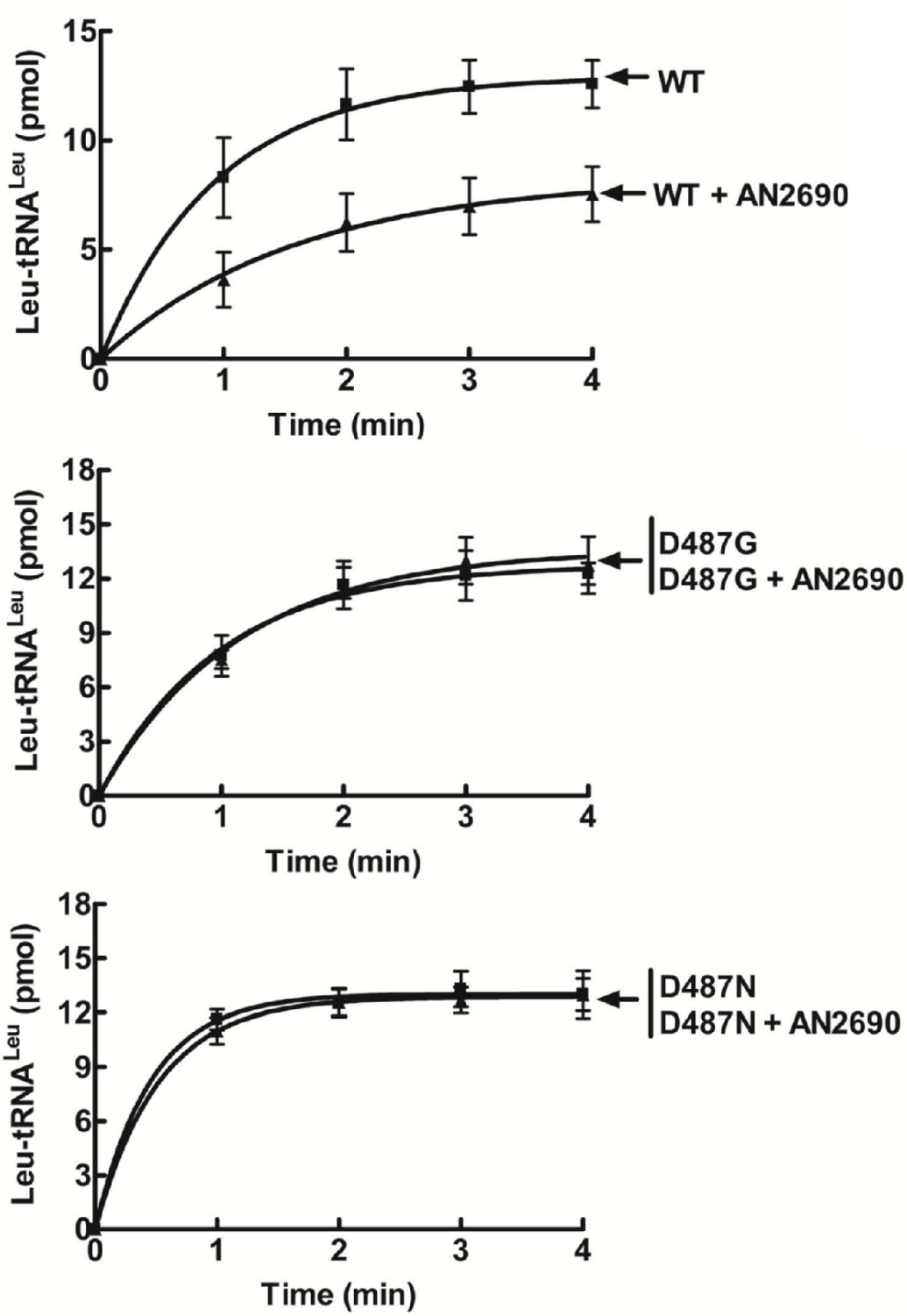

Figure III.6. Aminoacylation activities of Asp487 LeuRS resistant mutants in the presence of AN2690. Aminoacylation reactions included 4 mg/ml *S. cerevisiae* crude tRNA, 0.5 μM enzyme, 21 μM [^{3}H]-leucine (150 μCi/ml) and 0.5 mM AN2690. The reaction was incubated at 30 °C for 1 hr followed by initiation with 4 mM ATP. Symbols are: absence of AN2690 (■) and presence of AN2690 (▲). Error bars for each time point are a result of each reaction repeated in triplicate.

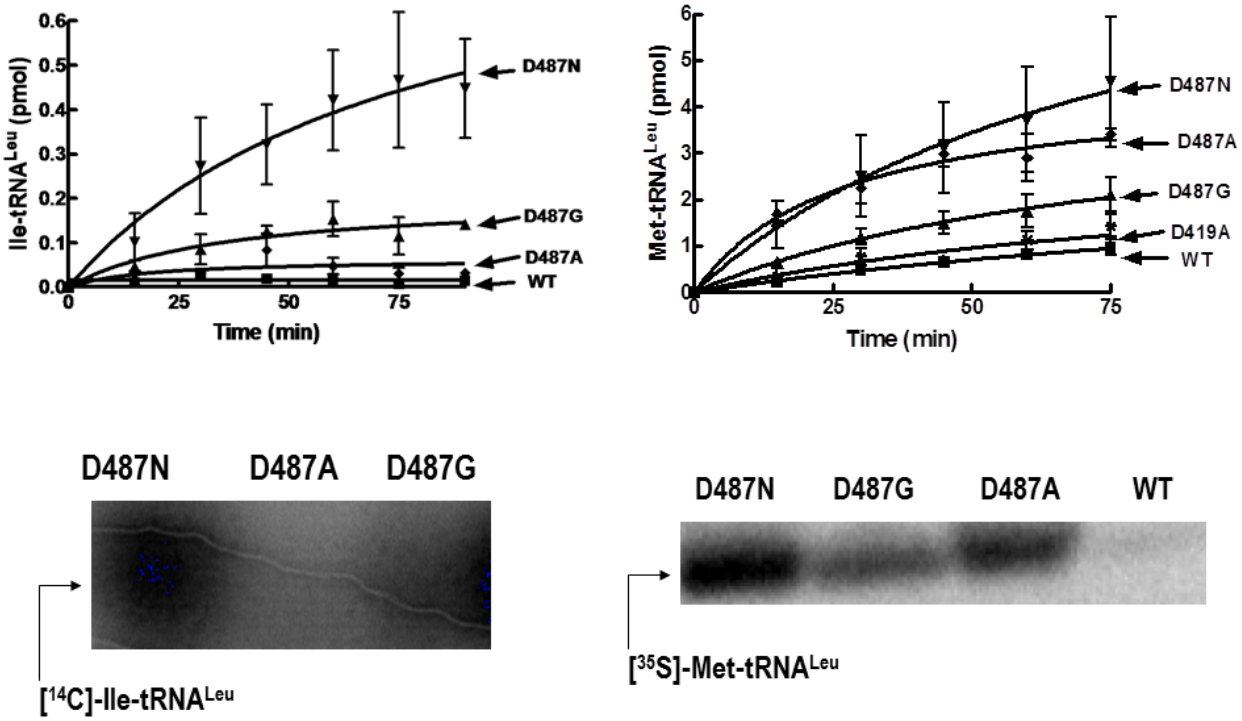

Figure III.7. Misaminoacylation activity of Asp487 LeuRS mutants. (Top) Misaminoacylation of *S. cerevisiae* crude tRNA with isoleucine or methionine. Reactions contained 8 mg/mL *S. cerevisiae* crude tRNA, 50 μM [^{14}C]-isoleucine (15.9 μCi/mL) or 20 μM [^{35}S]-methionine (10 μCi/mL) and 1 μM enzyme and were initiated with 4 mM ATP at 30 °C. Symbols are: wild type (■), D487G (▲), D487N (▼), D487A (♦) and D419A (●). Error bars for each time point are a result of each reaction repeated in triplicate. (Bottom) Acid gel analysis of misaminoacylated tRNA. Misaminoacylation reactions were carried out as mentioned above, except that 300 μCi/mL of respective radiolabeled amino acids were incorporated. Reactions were carried out for 90 min, followed by separation on denaturing polyacrylamide gel that was electrophoresed in 25 mM NaOAc, pH 5.0. Acid gel analysis confirms that the amino acid is attached to the tRNA and the enzyme is not self-labaled with the radiolabeled amino acids (Martinis and Schimmel, 1992).

The yeast cytoplasmic Asp487 LeuRS mutant editing deficiencies resulted in low accumulations of mischarged Ile-tRNA^{Leu} in misaminoacylation assays using crude yeast tRNA (Figure III.7, top; Figure III.8). These mischarging plateaus are about 8-fold lower than a strong mischarging LeuRS mutant, such as D419A which substitutes a universally conserved residue in the editing pocket that stabilizes the editing substrate via a hydrogen bond (Lincecum, et al., 2003). However, these Asp487 LeuRS mutants exhibited similar activation of isoleucine as compared to the wild type enzyme in isoleucine-dependent PP_i

exchange assays (Figure III.3, right; Figure III.9). Radiolabeled amino acids may get co-precipitated with the tRNA during TCA precipitation (see materials and methods) or remain trapped in the enzyme active site, leading to the enzyme being 'self-labeled' (Martinis and Schimmel, 1992). Under conditions when the enzyme's charging activity is weak as in case of mischarging, in order to confirm that the amino acid is indeed attached to the tRNA, products of the misaminoacylation reactions are analyzed on acidic polyacrylamide gels. Such acid gel analysis of misaminoacylation by the Asp487 resistant mutants in presence of either [^{35}S]-methionine or [^{14}C]-isoleucine show that these amino acids are indeed attached to the tRNA (Figure III.7, bottom). As would be expected, the wild type yeast LeuRS did not mischarge the crude yeast tRNA with isoleucine since LeuRS, like all other AARSs, is specific for its cognate tRNA. Recognition of $tRNA^{Leu}$ by LeuRS is facilitated by specific determinants found within the tRNA (Giegé, et al., 1998) as well as by tertiary structure formed between the D and TψC-arms of tRNA (Larkin, 2002). The yeast cytoplasmic enzyme is also unusual amongst the LeuRSs in that it relies on the anticodon of $tRNA^{Leu}$ for recognition (Soma, et al., 1996).

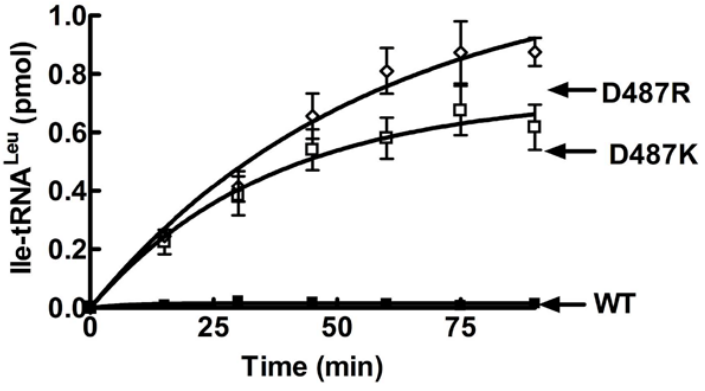

Figure III.8. Misaminoacylation activity of positively charged Asp487 mutant LeuRSs. Reactions included 4 mg/ml *S. cerevisiae* crude tRNA, 1 μM enzyme and 24 μM [^{3}H]-isoleucine (150 μCi/ml) and were initiated with 4 mM ATP. Symbols are wild type (■), D487K (□) and D487R (◊). Error bars for each time point are a result of each reaction repeated in triplicate.

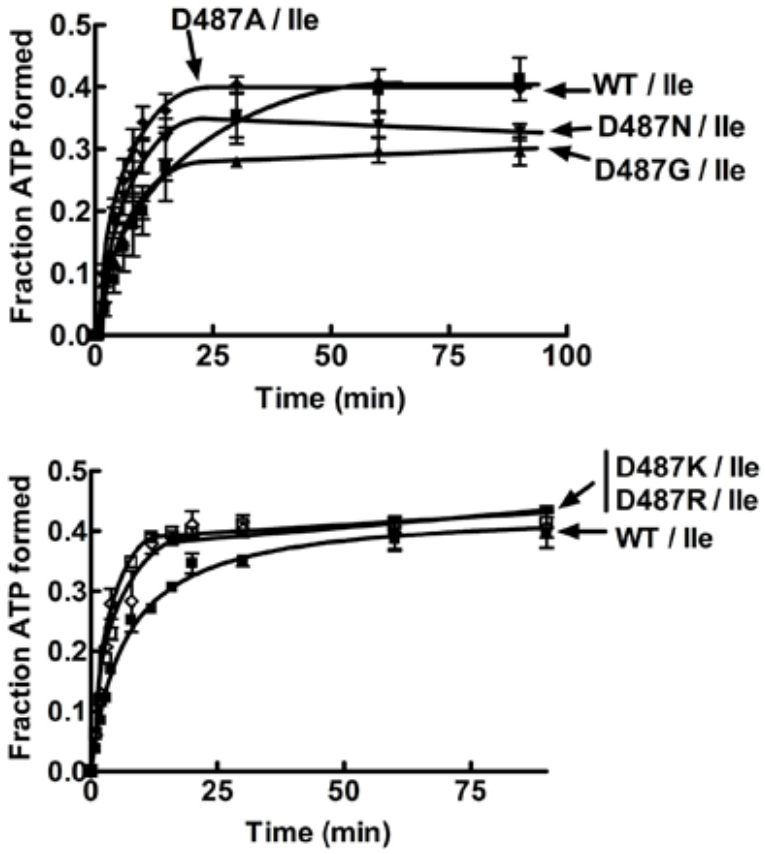

Figure III.9. Isoleucine activation by Asp487 LeuRS mutants. Isoleucine-dependent PP_i exchange assays that included 1 mM PP_i (100 μCi/ml), 10 mM isoleucine and 1 mM ATP were initiated with 0.5 μM enzyme. Symbols are wild type (■), D487G (▲), D487N (▼), D487K (□) and D487R (◊). Error bars for each time point are a result of each reaction repeated in triplicate.

Since a homologous substitution at Asp487 could restore the enzyme's hydrolytic activity, we wondered how this negative charge that is outside the editing pocket contributed towards amino acid editing. We scrutinized the X-ray crystal structure of the *C. albicans* CP1 domain in complex with the benzoxaborale AN3018 (Seiradake, et al., 2009). The *C. albicans* LeuRS CP1 domain has a glycine residue (Gly490) at the position comparable to Asp487 in *S. cerevisiae* LeuRS (Figure III.1, bottom). Ironically, a glycine at this site renders the yeast LeuRS enzyme resistant to AN2690. Nevertheless, we relied on the AN3018-bound *C. albicans* LeuRS structure as an opportunity to guide our investigation into the structure-function role of Asp487 in editing by yeast LeuRS.

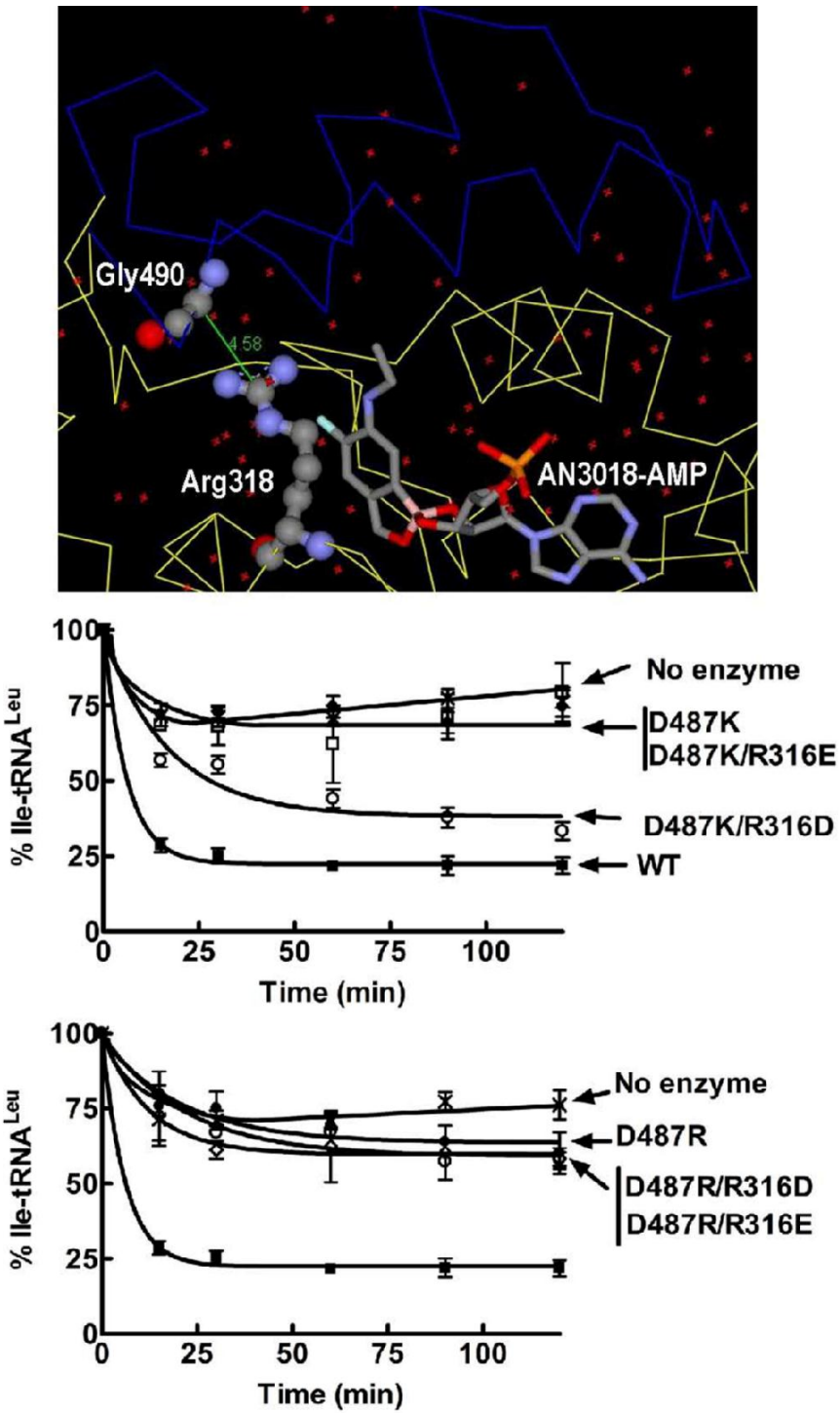

Figure III.10. Putative electrostatic interaction between the I4 insert and the editing pocket of fungal cytoplasmic LeuRS. (Top) Crystal structure of *C. albicans* cytoplasmic LeuRS CP1 domain in complex with AN3018-AMP (PDB entry 2WFG) (Seiradake, et al., 2009) highlighting the I4 insert (blue), Gly490 in the I4 insert and Arg318 in the editing pocket (analogous to Asp487 and Arg316, respectively in yeast LeuRS). (Center) and (Bottom) Hydrolytic editing activities of single charged Asp487 mutants and Asp487/Arg316 double mutants. Deacylation reactions included approximately 2 mg/ml [^{14}C]-IletRNA^{Leu} and 0.5 µM enzyme. Symbols are: wild type (■), D487K (□), D487R (◊), D487K/R316D and D487R/R316D (o), D487K/R316E and D487R/R316E (●) and no enzyme (x). Error bars for each time point are a result of each reaction repeated in triplicate.

When the I4 cap is closed over the AN3018-AMP bound editing pocket in the X-ray crystal structure of the *C. albicans* LeuRS CP1 domain, the α-carbon of Gly490 is in close proximity (~4 Å) to the guanidinium group of the arginine at position 318 (Figure III.10, top). We identified Arg316 in *S. cerevisiae* LeuRS, (corresponding to Arg318 of *C. albicans* LeuRS in the primary sequence) and hypothesized that it was also located within or near the editing pocket. Interestingly, R316I has been reported to be resistant to AN2690 in *S. cerevisiae* (Rock, et al., 2007). Although the yeast LeuRS Asp487 has a longer side chain than the Gly 490 found in *C. albicans* LeuRS that could place it closer than 4 Å to the arginine, we wondered if local rearrangements within the dynamic and diverse structures might accommodate a salt bridge between Asp487 and Arg316 in the yeast enzyme. If Asp487 at the base of the I4 cap forms an electrostatic salt-bridge with Arg316 of the yeast LeuRS editing pocket, then we postulated that it could stabilize closure of the I4 cap to sequester the bound substrate in the editing pocket.

To test this hypothesis, we mutationally swapped charges at Asp487 and Arg316 to construct the double mutants D487K/R316D, D487K/R316E and D487R/R316D, D487R/R316E. The D487K/R316D double mutant rescued hydrolytic activity of the editing-defective positively-charged D487K mutant to levels that were close to the wild type enzyme (Figure III.10, center). The D487K/R316E double mutant did not recover any hydrolytic editing activity (Figure III.10, center). We also observed that the double mutants D487R/R316D and D487R/R316E did not rescue hydrolytic editing of the editing-defective D487R mutant LeuRS (Figure III.10, bottom). This suggests that the longer side chains of glutamic acid and arginine may juxtapose the residues too close to form an effective electrostatic interaction. In lieu of an aspartate corresponding to position 487 in *C. albicans* LeuRS, (Figure III.1, bottom), the enzyme may depend on alternate residues to form an

electrostatic bridge. It is possible that Glu489, which neighbors Gly490 (Figure III.1, bottom), could form a salt bridge with Arg318.

Post-transfer editing is dependent on an intra-enzyme translocation event that moves the tRNA between the main body and the CP1 domain that are respectively responsible for aminoacylation and editing. Mutations in the *E. coli* LeuRS 'translocation peptide' (Figure III.1, bottom) appear to cause the mischarged tRNA to bypass the editing active site (Hellmann and Martinis, 2009). The eukaryotic LeuRSs lack this bacterial LeuRS translocation peptide. However, in a primary sequence alignment, Asp487 of the yeast cytoplasmic LeuRS is upstream to the N-terminus of the site that would correspond to the

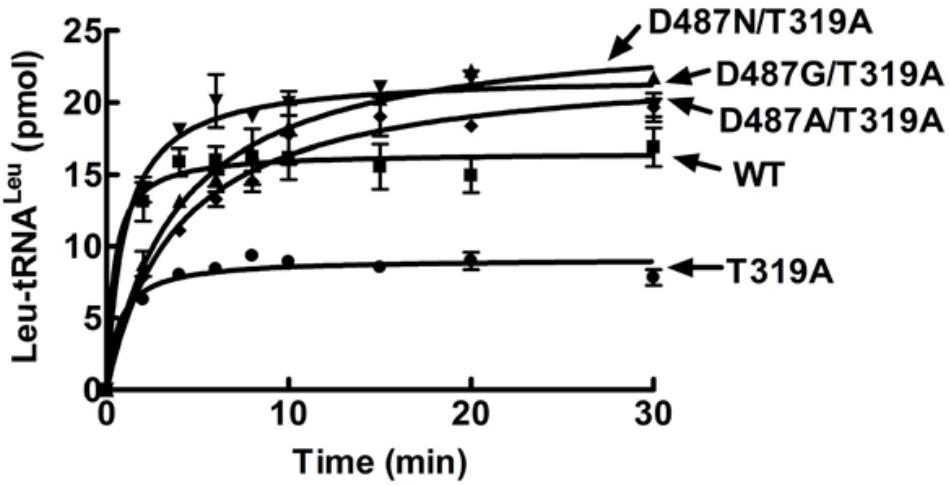

Figure III.11. Rescue of aminoacylation of editing site mutation (T319A) by Asp487 LeuRS mutants. Reactions consisted of 4 mg/ml S. cerevisiae crude tRNA, 0.5 µM enzyme and 22 µM [^{3}H]-leucine (150 µCi/ml) and were initiated with 4 mM ATP. Symbols are: wild type (■), D487G/T319A (▲), D487N/T319A (▼), D487A/T319A (♦), T319A (●) and no enzyme (x). Error bars for respective time points represent each reaction repeated in triplicate.

E. coli LeuRS translocation peptide (Figure III.1, bottom). We wondered if the Asp487 region of the I4 cap could facilitate tRNA translocation via a distinct mechanism. Previously, to test for disruptions in translocation, we relied on a conserved threonine in *E. coli* LeuRS (Thr252) which is an amino acid specificity determinant in the editing pocket that blocks

leucine from binding (Mursinna, et al., 2001). When mutated to alanine, loss of specificity confers deacylation of Leu-tRNA^{Leu}, resulting in a phenotype of weak charging activity for the T252A mutant LeuRS. Disruption of translocation would restore Leu-tRNA^{Leu} accumulation in the LeuRS mutant.

Mutation of the threonine specificity determinant in yeast LeuRS (Thr319) also results in low charging activity (Figure III.11). We combined each of the resistant mutations, D487G and D487N, with the editing site mutation T319A that uncouples specificity in the editing site of yeast LeuRS, resulting in the double mutants D487G/T319A and D487N/T319A, respectively. The Asp487 double mutants rescued aminoacylation of the T319A mutant, resulting in accumulation of Leu-tRNA^{Leu} up to wild type levels (Figure III.11). In this case, it is possible that the charged 3´-end of tRNA^{Leu} may not be stably binding at the editing pocket or alternatively, has reduced access to the editing site. We determined that the hydrolytic editing activity of the Asp487/Thr319 double mutants was significantly decreased for the correctly charged product Leu-tRNA^{Leu} (Figure III.12, top) as well as the mischarged product Ile-tRNA^{Leu} (Figure III.12, bottom) in comparison to the single T319A mutant. These results suggest that mutation of Asp487 destabilizes binding of the 3´-end of the tRNA in the editing pocket of the CP1 domain, rather than disrupting a tRNA translocation mechanism.

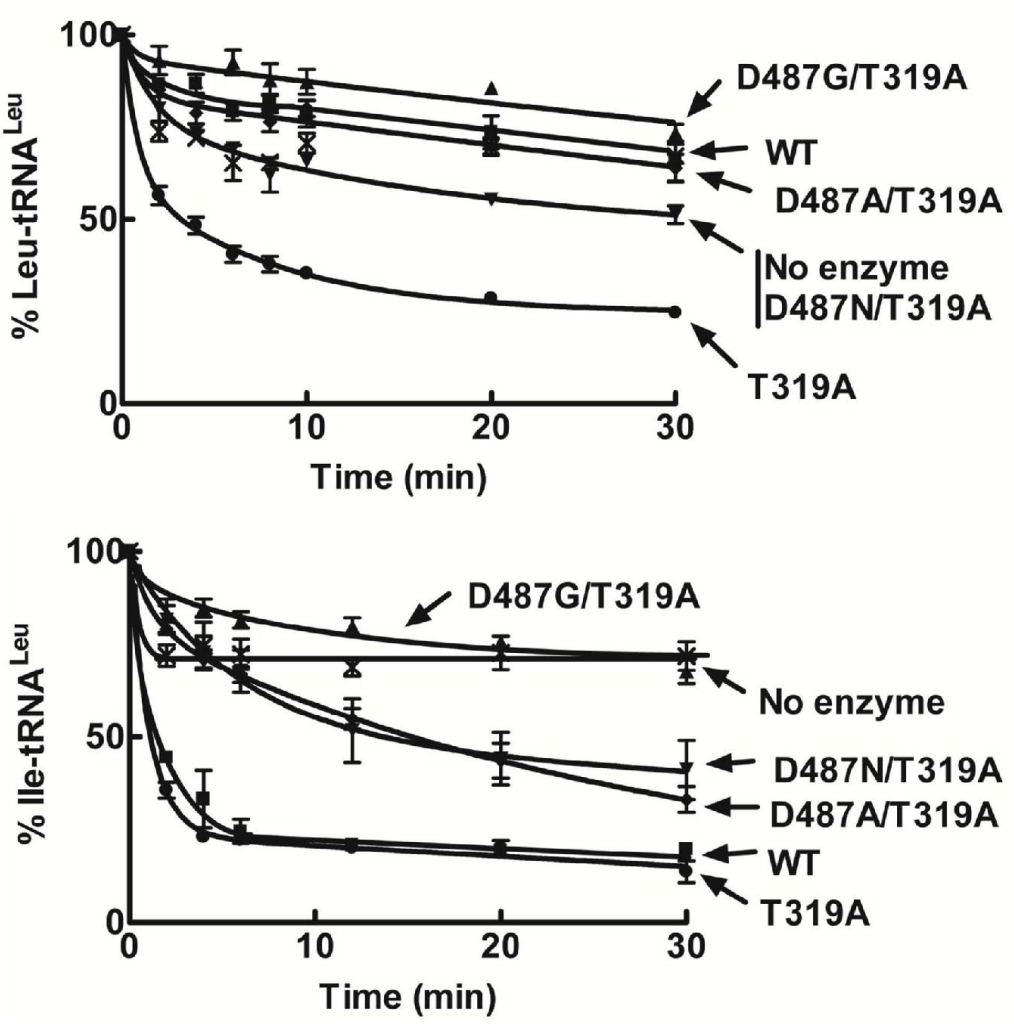

Figure III.12. Deacylation activities of Asp487/Thr319 double mutants. (Top) Deacylation of Leu-tRNA^{Leu} included approximately 2 mg/ml [^{3}H]-Leu-tRNA^{Leu} and 1 μM enzyme. (Bottom) Deacylation of Ile-tRNA^{Leu} included approximately 2 mg/ml [^{3}H]-Ile-tRNA^{leu} and 1 μM enzyme. Symbols are: wild type (■), D487G/T319A (▲), D487N/T319A (▼), D487A/T319A (♦), T319A (●) and no enzyme (x). Error bars for respective time points represent each reaction repeated in triplicate.

III.4. Discussion

The AARS family of enzymes by virtue of their essentiality and diversity, have been a focus of drug discovery to identify new antimicrobial agents. A traditional strategy has been to find compounds that selectively mimic the pathogen AARS substrates, intermediates and transition state analogs, while sparing the human counterpart (Tao, 2000). By screening

libraries of synthetic boron-containing small molecules, a new class of antifungals, the benzoxaboroles, were discovered (Baker, et al., 2006). These antifungal benzoxaboroles inhibited LeuRS in a novel way by binding in the editing pocket of the CP1 domain and trapping the tRNA in the editing conformation via an adduct with the *cis*-diols of the terminal nucleotide (Rock, et al., 2007; Seiradake, et al., 2009).

Isolation of spontaneous and EMS-generated resistant mutants to AN2690 have been reported within the editing pocket of LeuRS (Rock, et al., 2007), where the drug interacts directly with the enzyme. Each of these resistant mutants is editing defective in norvaline-dependent complementation assays (Rock, et al., 2007). Herein, we characterized resistant mutants D487G and D487N, which lie outside the editing active site. The *C. albicans* and yeast cytoplasmic CP1 domain have acquired species specific peripheral insertions, one of which (I4) appears to form a cap over the bound editing substrate (Figure III.1, top). The Asp487 lies within the I4 peripheral insert. The crystal structure of the *C. albicans* CP1 domain shows that a network of water molecules, as well as the editing substrate, are sequestered within the space enclosed by the I4 cap over the editing pocket (Seiradake, et al., 2009). We hypothesize that Asp487 in the species-specific I4 insert of the yeast LeuRS could be mechanistically important to the cap's hinge motion.

Resistance mutations highlighted that this I4 insert may be idiosyncratic, albeit an essential component of the editing mechanism in LeuRS for lower eukaryotes. Mutations at Asp487 in yeast LeuRS directly impact editing with minimal effects on aminoacylation. Charge reversals at Asp487 completely destabilize the editing activity. We scrutinized the available crystal structure information to identify a plausible electrostatic salt bridge interaction between Asp487 at the base of the I4 cap and Arg316 in the editing pocket. Significantly, a double mutation to reverse these charges rescued editing activity of the D487K LeuRS mutant, which suggests that the salt bridge was restored.

There are relatively few synthetase-tRNA contacts in the editing complex compared to the aminoacylation complex (Tukalo, et al., 2005). In addition, the yeast LeuRS active site has been suggested to be more open and accessible to water compared to its bacterial counterpart that lacks the I4 insert. The I4 cap and this salt bridge between the cap and the editing active site could stabilize substrate and inhibitor binding in a more open editing site, as well as orient enclosed water molecules. Ultimately, AN2690 crosslinks to the tRNA in the editing site resulting in a long half-life (Rock, et al., 2007). Although the fit of the AMP-benzoxaborole adduct in the editing pocket of LeuRS is complementary, only a few hydrogen bonds within the LeuRS editing active site stabilize it (Rock, et al., 2007). The AMP-benzoxaborole adduct is superimposable with a post-transfer editing substrate analog (Rock, et al., 2007). It also directly contacts the universally conserved aspartic acid residue (Asp419 in yeast LeuRS) in the editing active site that stabilizes the post-transfer editing substrate via a hydrogen bond with the α-amino group of the amino acid. However, the benzoxaborole adduct lacks a key site analogous to the amino group of an aminoacylated tRNA. Thus, a cap over the editing pocket could significantly and critically stabilize the bound editing substrate by providing or orienting either direct or water-mediated contacts between the enzyme and the substrate.

We hypothesize that, in the Asp487 mutants, stabilization of the charged 3´-end of the tRNA is compromised. De-stabilization of the bound substrate (the inhibitor or the charged 3´-end of the tRNA) at the editing site would also, at least in part, explain the resistance of D487G and D487N to AN2690, which binds in the editing pocket. We propose that Asp487, located within the I4 insert, is instrumental in inducing segmental flexibility of the I4 insert and enables the cap to sequester the mischarged tRNA substrate and/or AN2690.

Chapter IV: Amino Acid-dependent Shift in tRNA-Synthetase Editing Mechanisms

Adapted with permission from
Jaya Sarkar and Susan Anne Martinis (2011). "Amino Acid-dependent Shift in tRNA Synthetase Editing Mechanisms". *J. Am. Chem. Soc*., **133, 18510-18513**.

IV.1. Introduction

Translational machinery relies on aminoacyl-tRNA synthetases (AARSs) to attach correct amino acids to cognate tRNAs (Ibba and Söll, 2000). To ensure fidelity in protein synthesis, about half of the AARSs, including leucyl-tRNA synthetase (LeuRS), have evolved editing mechanisms against structurally similar noncognate amino acids to clear mistakes that originate in the synthetic active site (Mascarenhas, 2008). The absence of these editing mechanisms results in statistical mutations in the proteome (Li, et al., 2011).

Many aminoacyl-tRNA synthetases prevent mistranslation by relying upon proofreading activities at multiple stages of the aminoacylation reaction. Amino acid editing may occur either before (pre-transfer) (Baldwin and Berg, 1966; Fersht, 1977b) or after (post-transfer) (Eldred and Schimmel, 1972) the activated amino acid is transferred to the tRNA (Schimmel and Schmidt, 1995). Thus, pre-transfer editing targets the misactivated aminoacyl-adenylate intermediate (AA-AMP) for hydrolysis, while post-transfer editing cleaves mis-aminoacylated tRNA (AA-tRNA^{AA}) to clear the AARSs mistakes (Ling, et al., 2009). For LeuRS, the post-transfer editing active site is housed in a discrete insertion domain, called connective polypeptide 1 (CP1), that is separated from the aminoacylation active site by ~35 Å (Cusack, et al., 2000) (Figure IV.1).

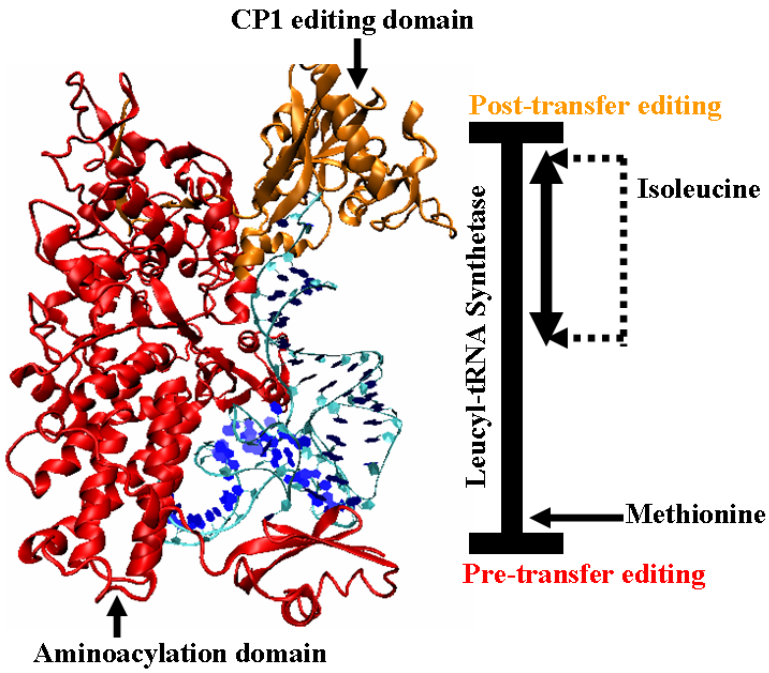

Figure IV.1. Amino-acid dependent partitioning between pre-and post-transfer editing pathways. The structure of LeuRS in complex with $tRNA^{Leu}$ (PDB: 2BYT) in the editing conformation is represented as a ribbon model, with the main body in red, the CP1 domain in orange and the tRNA in blue.

Yeast cytoplasmic LeuRS (ycLeuRS) has been proposed to have relatively poor initial substrate discrimination (Englisch, et al., 1986) and mis-activates structurally similar or isosteric standard and nonstandard amino acids such as isoleucine, methionine, norvaline, and homocysteine (Englisch, et al., 1986). An early report by Englisch *et al*. also suggested that ycLeuRS edited predominantly by a pre-transfer editing mechanism, while *E. coli* LeuRS clears mistakes exclusively by a post-transfer editing mechanism (Englisch, et al., 1986). In *E. coli* LeuRS, we have shown that the CP1 editing domain that is responsible for post-transfer editing masks a pre-transfer editing activity that is associated with the canonical aminocylation core (Boniecki, et al., 2008; Williams and Martinis, 2006). In ycLeuRS, we hypothesize that both pre- and post-transfer editing mechanisms coexist and that one predominates, similar to *E. coli* LeuRS. Here, we determined that a shift between the two AARS fidelity mechanisms can be dependent on the identity of the standard amino acids that

threaten LeuRS fidelity. A partition of fidelity mechanisms has also been reported for the human cytoplasmic LeuRS (hcLeuRS) against nonstandard biosynthetic intermediates norvaline and α-aminobutyrate (Chen, et al., 2011). This multi-step strategy for quality control could be akin to the evolution of auxiliary editing domains such as ybak to clear mischarged Cys-tRNA^{Pro} in *trans*, in addition to Ala-tRNA^{Pro} that is produced and then cleared by *cis* editing activity of prolyl-tRNA synthetase (An and Musier-Forsyth, 2005; Ruan and Söll, 2005). We show that ycLeuRS has a robust post-transfer editing activity that efficiently clears tRNA^{Leu} mischarged with isoleucine. In comparison, the enzyme's post-transfer hydrolytic activity against tRNA^{Leu} mischarged with methionine is weak. Rather, methionyl-adenylate is cleared robustly via an enzyme-mediated pre-transfer editing activity. We hypothesize that, similar to *E. coli* LeuRS, ycLeuRS has coexisting functional pre- and post-transfer editing activities. In the case of ycLeuRS, a shift between the two editing pathways is triggered by the identity of the noncognate amino acid (Figure IV.1).

IV.2. Experimental methods

IV.2.A. Expression and purification of proteins

The plasmid p32YL-2-3 (Lincecum, et al., 2003) encoding the gene for the wild type ycLeuRS was used to express the protein in *E. coli* strain Rosetta (DE3) (Novagen). Cells were grown at 30 °C till OD_{600} reached 0.6, then induced with 1 mM IPTG and the protein was expressed at 30 °C for 45 min. Protein purification was carried out as described in Chapter II, except that the bound protein was eluted in fractions from the resin using an immidazole gradient of 10 to 100 mM in HA-I. The LeuRS containing fractions were pooled and concentrated using an Amicon Ultra centrifugal filter device (Millipore Corporation, Billerica, MA). The final protein concentration was determined spectrophotometrically at

280 nm using an extinction coefficient of 155,310 $M^{-1}cm^{-1}$, estimated by the ExPASy Protparam tool (http://ca.expasy.org/tools/protparam.html).

IV.2.B. Cloning of the gene encoding yeast cytoplasmic $tRNA^{Leu}_{CAA}$ ($yctRNA^{Leu}$)

The gene fragment encoding the $yctRNA^{Leu}_{CAA}$ was amplified in a 50 µL PCR that contained 100 ng of pAMWt-25 template plasmid DNA, 125 ng each of forward [pTRC-Fw(*EcoRI*)-$yctRNA^{Leu}$] and reverse [pTRC-Rv(*BamHI*)-$yctRNA^{Leu}$] primer containing the *EcoR*I and *Bam*HI restriction sites respectively, 0.05 mM dNTP mix and 0.05 U *Pfu* DNA polymerase in commercial buffer. The PCR products were digested with *EcoR*I and *Bam*HI at 37 °C for 6 h. The restriction-digested PCR products were separated on a 2% agarose gel and gel-purified using the QIAquick gel extraction kit-250 (Qiagen Inc). The vector pTrc-99 (Martin, et al., 1993) (a gift from G. Eriani) was also cleaved with *EcoR*I and *Bam*HI, followed by gel-extraction. Gel purified restriction digests of the PCR amplified gene fragment and the vector were ligated using T4 DNA ligase at 37 °C for 15 min to yield the plasmid pJS-pTrc-(*EcoRI*)-$yctRNA^{Leu}_{CAA}$-(*BamHI*) The ligation reaction was used to transform *E. coli* strain DH5α. The gene sequence was confirmed by automated DNA sequencing (UIUC Core Sequencing Facility, Urbana).

IV.2.C. Expression and purification of $yctRNA^{Leu}_{CAA}$

The $yctRNA^{Leu}_{CAA}$ was overexpressed in *E. coli* strain DH5α harboring the plasmid pJS-pTrc-(*EcoRI*)-$yctRNA^{Leu}_{CAA}$-(*BamHI*). A single transformant was used to inoculate 6 mL LB (100 µg/mL Amp) which was incubated at 37 °C overnight. The overnight culture was used to inoculate 2 L LB (100 µg/mL Amp) and cells were grown at 37 °C until the OD_{600} reached 0.6-0.8. At this stage, cells were induced with IPTG, to a final concentration of 1 mM and the $yctRNA^{Leu}_{CAA}$ was expressed overnight at 37 °C. Cells were harvested with

an Avanti J-E preparative centrifuge (Beckman Coulter, Fullerton, CA), at 6000 rpm for 15 min at 4 °C.

Cell pellets were resuspended in 50 mL of buffer [20 mM Tris, pH 7.5; 20 mM magnesium acetate]. This was followed by two extractions with 50 mL each of phenol/Tris saturated solution (Acros Organics, New Jersey, USA) and vigorous shaking for 20 min at room temperature. The aqueous phase was collected after clarification via centrifugation at 3000 rpm for 10 min at 10 °C and then ethanol precipitated at - 80 °C overnight. The RNA was collected by centrifugation, followed by resuspension of the pellet in 500 mM Tris, pH 8.0 at 37 °C to deacylate the tRNA. The tRNA was then purified on a 10% denaturing polyacrylamide gel by electrophoresis. The concentration of tRNA was measured spectrophotometrically on the basis of its extinction co-efficient of 815,300 $M^{-1}cm^{-1}$ estimated by the online Ambion oligonucleotide calculator (http://www.ambion.com/techlib/misc/oligo_calculator.html).

IV.2.D. Misaminoacylation assay

Each misaminoacylation reaction contained 60 mM 4-(2-hydroxyethyl)-1-piperazineethanesulfonic acid (HEPES), pH 7.5, 30 mM $MgCl_2$, 30 mM KCl, 1 mM dithiothreitol (DTT), 4 μM pure yctRNA$^{Leu}_{CAA}$, 25 μM [^{3}H]-methionine (422 μCi/mL) and 1 μM enzyme. Reactions were initiated with 4 mM ATP and performed as described in Chapter II.

IV.2.E. Isolation of mischarged tRNA^{Leu}

Purified yctRNA$^{Leu}_{CAA}$ (8 μM) was misaminoacylated with isoleucine or methionine by incubating the following reaction mixture at 30 °C for 3 h in 60 mM HEPES, pH 7.5, 30 mM $MgCl_2$, 30 mM KCl, 1 mM DTT, 23.8 μM [^{3}H]-isoleucine (422 μCi/mL) or 25 μM

[^{3}H]-methionine (422 μCi/mL), 1 μM editing defective (D419A) ycLeuRS and 4 mM ATP. The reactions were performed as described in Chapter II. For each reaction, a total of six 2 μL duplicate aliquots were spotted on TCA-soaked and dried pads. Half of the pads were washed extensively (as described above) to quantitate the [^{3}H]-Ile-tRNA^{Leu} and [^{3}H]-Met-tRNA^{Leu} mischarged products (Zhai, et al., 2007).

IV.2.F. Post-transfer editing deacylation assay

Deacylation reaction mixtures were carried out at pH 7.5 in 60 mM HEPES, 10 mM $MgCl_2$, 10 mM KCl and approximately ~2 μM [^{3}H]-Ile-tRNA^{Leu} or [^{3}H]-Met-tRNA^{Leu}. The reactions were initiated with 1 μM enzyme. At desired time points, reaction aliquots of 10 μL were quenched on Whatman filter pads that had been pre-wet in 5% TCA and dried. Pads were washed and then quantified for radioactivity as described above.

IV.2.G. AMP formation assay

The formation of AMP was carried out at 30 °C in a reaction mixture containing 50 mM HEPES, pH 7.5, 20 mM $MgCl_2$, 20 mM KCl, 5 mM DTT, 0.024 U/μL inorganic pyrophosphatase, 250 μM cold ATP, 0.2 μM [α-^{32}P]-ATP (600 μCi/mL), 2.5 mM leucine or 100 mM isoleucine or 100 mM methionine. Reactions were also measured for their dependence on tRNA by incorporating 29 mg/mL crude yeast tRNA, which was measured to contain 14.5 μM tRNA^{Leu}. Reactions were initiated with 1 μM enzyme. At different time points, reaction aliquots (2.0 μL) were quenched in 8.0 μL of 200 mM sodium acetate, pH 5.0. From each quenched aliquot, 3 μL was spotted on cellulose polyethyleneimine (PEI) thin layer chromatography (TLC) plates (Scientific Adsorbents Inc., Atlanta, GA) that were pre-run in water and dried. Separation of [α-^{32}P]-ATP, [^{32}P]-AMP and [^{32}P]-AA-AMP were

achieved by developing the TLC plates in 0.1 M ammonium acetate, 5% acetic acid (Bullock, et al., 2003). Resolved radiolabeled bands on the TLC plate were phosphorimaged using FUJIFILM BAS Cassette 2040 (FUJIFILM Medical Systems, Stanford, CT) and images were scanned by a STORM 840 Molecular Dynamics scanner (Amersham Pharmacia Biotech, Piscataway, NJ). At each time point, the remaining ATP was measured as a fraction, of the total volume intensity of all the resolved spots at that time point. A known concentration of [α-^{32}P]-ATP was spotted on each TLC plate. The concentration of AMP in each separated band was calculated by comparing the volume density for each [^{32}P]-AMP spot to the volume density of the known [α-^{32}P]-ATP spot. Images were quantified using the ImageQuant software and the resulting data plotted and analyzed using the GraphPad Prism software. The observed rate constants were calculated from a linear fit of the respective data sets.

IV.2.H. Inorganic pyrophosphate (PP_i) release/ATP hydrolysis assay

ATP hydrolysis assays to monitor PP_i release were carried out at 30 °C in reactions containing 500 mM HEPES, pH 7.5, 20 mM $MgCl_2$, 20 mM KCl, 5 mM DTT, 250 μM cold ATP, 0.1 μM [γ-^{32}P]-ATP (600 μCi/mL) and 2.5 mM leucine or 100 mM isoleucine or methionine. Each reaction was initiated with 1 μM enzyme and 2.0 μL aliquots were spotted at the respective time points on cellulose PEI TLC plates, developed in 750 mM KH_2PO_4, pH 3.5 and quantitated as above.

IV.2.I. Nonenzymatic hydrolysis of AA-AMP

The rate of nonenzymatic hydrolysis of AA-AMP was calculated using an adapted chase assay (Gruic-Sovulj, et al., 2005) where a molar excess of cold ATP (25 mM) is used to eject the AA-AMP from the enzyme's active site. Enzyme synthesized AA-AMP was

allowed to form and accumulate for 10 min at 30 °C in a reaction mixture containing 50 mM HEPES, pH 7.5, 20 mM $MgCl_2$, 20 mM KCl, 5 mM DTT, 250 μM cold ATP, 0.6 μM [α-^{32}P]-ATP (1800 μCi/mL), 100 mM methionine and 5 μM enzyme. Following addition of molar excess of ATP (100 fold), hydrolysis of the AA-AMP in solution was quenched at various time points by mixing 2.0 μL reaction aliquot with 8.0 μL of 200 mM sodium acetate, pH 5.0. Separation of reaction products on TLC plates were performed and quantified as described above. The rate constants for AA-AMP hydrolysis in solution was calculated by fitting the respective data sets to the equation $y = Ae^{-kx}$, using GraphPad Prism software.

IV.3. Results

We cloned the gene for yeast cytoplasmic $tRNA^{Leu}$ ($yctRNA^{Leu}_{CAA}$) into the pTrc-99 vector (Martin, et al., 1993b) for overexpression in *E. coli*. The $yctRNA^{Leu}$ was extracted with phenol/tris saturated solution, followed by denaturing gel purification. The ycLeuRS with a six-histidine tag, was purified via affinity purification (Lincecum, et al., 2003). Using *in vitro* deacylation assays that incorporated purified $yctRNA^{Leu}$ mischarged with [^{3}H]-isoleucine, we determined that ycLeuRS has a robust post-transfer editing mechanism that clears mischarged Ile-$tRNA^{Leu}$ (Figure IV.2, top). In comparison, this yeast enzyme exhibited significantly reduced hydrolytic activity against [^{3}H]-Met-$tRNA^{Leu}$ (Figure IV.2, top). This amino-acid-dependent difference in post-transfer editing was surprising in that it contrasts with other LeuRSs that effectively deacylate $tRNA^{Leu}$ mischarged with either isoleucine or methionine (Chen, et al., 2000; Chen, et al., 2011; Karkhanis, et al., 2007; Mursinna, 2002; Zhai and Martinis, 2005; Zhai, et al., 2007). Despite its weak post-transfer editing activity, we did not observe accumulation of mischarged Met-$tRNA^{Leu}$ for wild-type ycLeuRS (Figure IV.2, bottom), as compared to an editing defective mutant (D419A) that we previously characterized (Lincecum, et al., 2003). In ycLeuRS, mutation of the universal Asp

419 to alanine disrupts overall editing (pre- and post-transfer) (Lincecum, et al., 2003). Thus, the mutant enzyme mischarges yctRNA^{Leu} with noncognate amino acids. It remains unclear how this single site impacts both pre- and post-transfer editing. Because of this striking difference in deacylation activities, we hypothesized that methionine that is misactivated by ycLeuRS is more efficiently cleared by an alternate fidelity pathway to post-transfer editing.

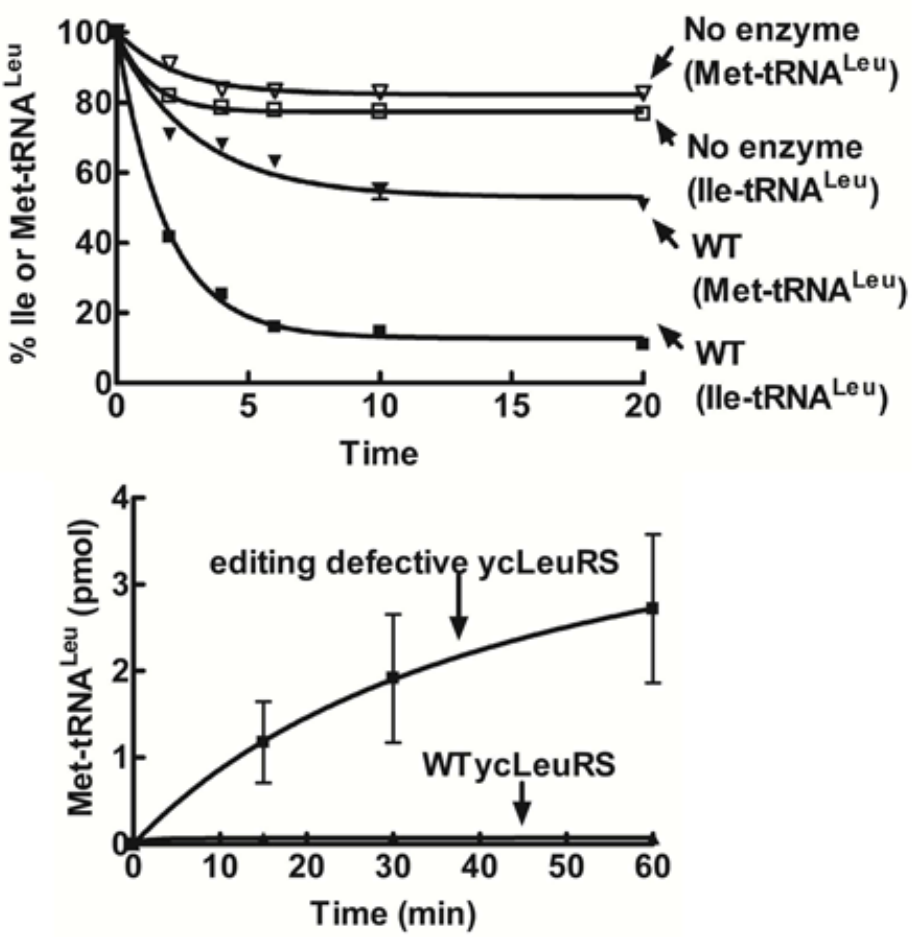

Figure IV.2. *In vitro* enzymatic activities of wild type ycLeuRS. (Top) Deacylation of [^{3}H]-Ile-tRNA^{Leu} and [^{3}H]-Met-tRNA^{Leu} by 1 μM ycLeuRS. Post-transfer hydrolytic activity against Met-tRNA^{Leu} is significantly weaker than that against Ile-tRNA^{Leu}. (Bottom) Misaminoacylation of pure yctRNA^{Leu} with 25 μM [^{3}H]-methionine (422 μCi/mL) by 1 μM wild type ycLeuRS. The wild type enzyme does not exhibit accumulation of mischarged Met-tRNA^{Leu} *in vitro*. Error bars for each time point are a result of each reaction repeated in triplicate.

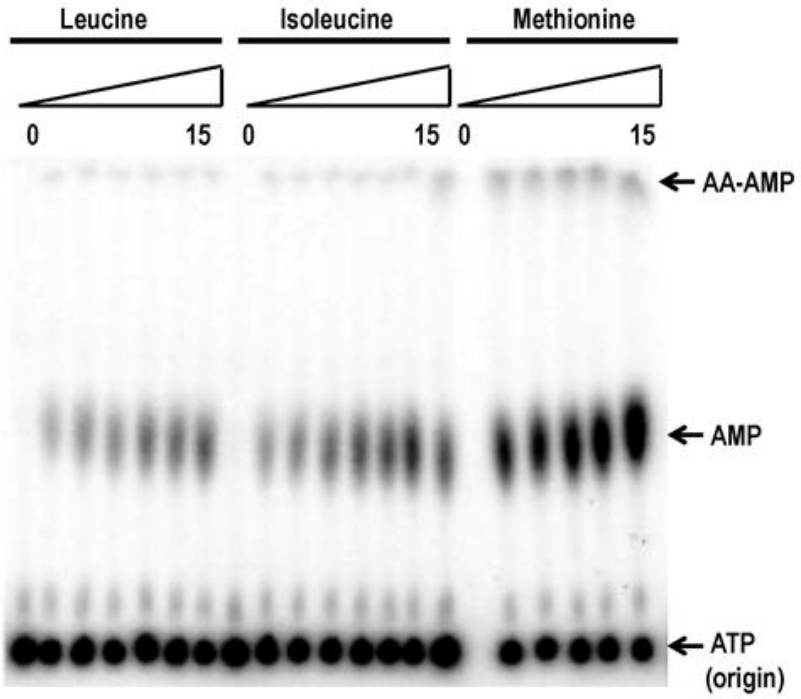

Figure IV.3. Pre-transfer editing activity of wild type ycLeuRS assessed by TLC-based AMP-formation assay, in absence of tRNA. A representattive reaction time course chromatographic separation of [^{32}P]-ATP, AMP and AA-AMP, as indicated. Reactions containing 250 μM cold ATP, 0.2 μM [α-^{32}P]-ATP (600 μCi/mL) and amino acids (2.5 mM leucine or 100 mM isoleucine or methionine) were initiated with 1 μM enzyme and carried out upto 15 min at 30 °C. Reaction products were resolved on TLC developed in 0.1 M ammonium acetate, 5% acetic acid.

Consistent with previous activation measurements of other noncognate amino acids by ycLeuRS (Englisch, et al., 1986), we measured a poor discrimination factor of 1/72 for methionine (data not shown). Since ycLeuRS lacks a robust post-transfer editing activity to clear Met-tRNA^{Leu}, we predicted that the methionyl adenylate intermediate might be cleared by pre-transfer editing. Pre-transfer editing is typically characterized by increased consumption of ATP in the presence of noncognate amino acids (Chen, et al., 2011; Dulic, et al., 2010; Hati, et al., 2006). We analyzed both ATP hydrolysis and AMP formation using TLC-based assays that utilize [α-^{32}P]-ATP to visualize separated ATP, AMP, and AA-AMP (Figure IV.3). In the absence of tRNA, ATP hydrolysis for methionine was stimulated

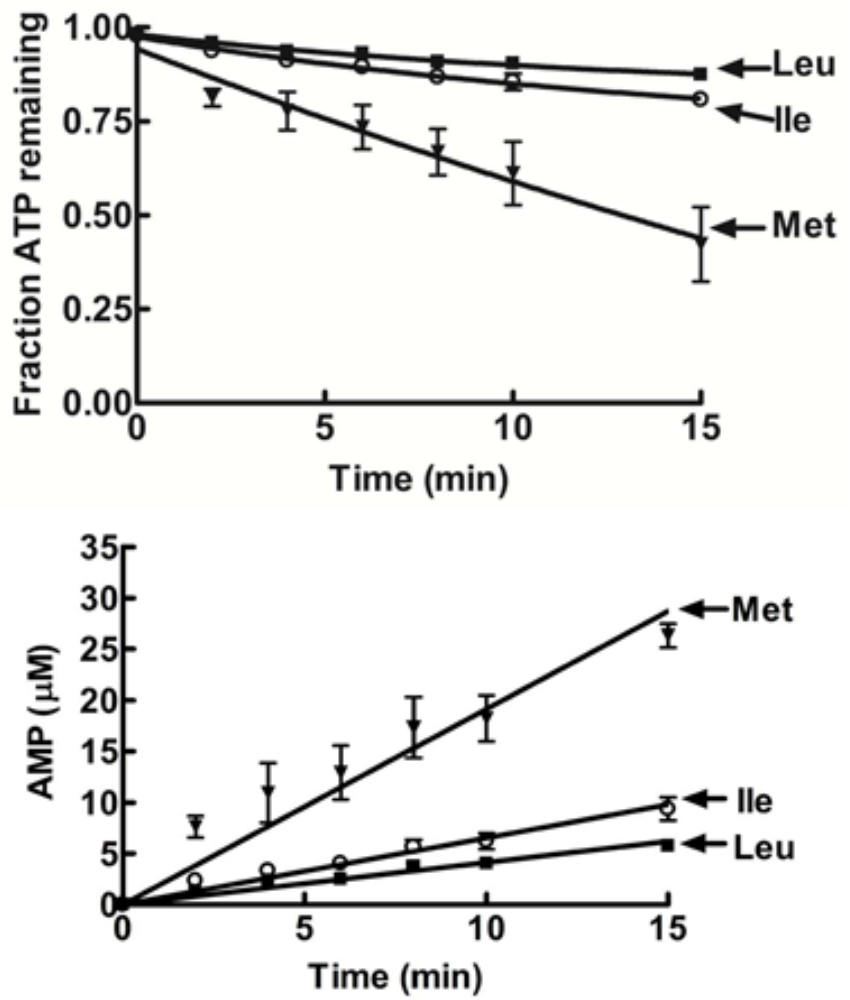

Figure IV.4. Amino acid-dependent pre-transfer editing activity of wild type ycLeuRS in absence of tRNA. (Top) ATP hydrolysis and (Bottom) AMP formation assessed by TLC-based AMP-formation aassays that enable separation and visualization of ATP, AMP and AA-AMP. Reactions containing 250 μM cold ATP, 0.2 μM [α-^{32}P]-ATP (600 μCi/mL) and amino acids (2.5 mM cognate or 100 mM noncognate) were initiated with 1 μM enzyme and carried out upto 15 min at 30 °C. Reaction products were resolved on TLC developed in 0.1 M ammonium acetate, 5% acetic acid. Error bars for each time point are a result of each reaction repeated in triplicate.

relative to cognate leucine (Figure IV.4, top), yielding an accumulation of 25 μM of AMP (Figure IV.4, bottom) with k_{obs} = 2.0 ± 0.3 min^{-1} that was 5-fold stimulated than the k_{obs} = 0.4 ± 0.01 min^{-1} for cognate leucine in tRNA-independent AMP formation assays (Figure IV.4, bottom; Table IV.1). By comparison, isoleucine-dependentAMP formation was only slightly elevated, with k_{obs} = 0.7 ± 0.1 min^{-1} in the absence of tRNA (Figure IV.4,

bottom; Table IV.1). Similar increases in AMP formation have been measured for other AARSs in the presence of noncognate amino acids as an indicator for tRNA independent pre-transfer editing activity (Table IV.2).

Table IV.1. Observed rate constants (k_{obs}) for AMP formation

Amino acid	Enzyme-dependent AMP formation k_{obs} (min^{-1})	Non-enzymatic AMP formation k_{obs} (min^{-1})	Fold-difference
Leucine	**0.4 ± 0.01**	**NA**	**NA**
Isoleucine	**0.7 ± 0.1**	**0.01 ± 0.002**	**70**
Methionine	**2.0 ± 0.3**	**0.1 ± 0.001**	**20**

Pre-transfer editing events of ycLeuRS against methionine in absence of tRNA were also measured in PP_i release assays that incorporated [γ-^{32}P]-ATP which allowed direct visualization of both ATP and PP_i released on TLC plates (Figure IV.5, top). In absence of tRNA, noncognate amino acids that are hydrolyzed at the adenylate stage are repeatedly reactivated by the synthetase, consuming ATP and hence producing PP_i in eah cycle. Thus, stimulated ATP hydrolysis and increased PP_i formation in presence of noncognate methionine, but not in presence of cognate leucine suggests robust pre-transfer editing activity of ycLeuRS against methionine in absence of tRNA (Figure IV.5, bottom).

The addition of tRNA in AMP formation assays enhanced ATP hydrolysis for methionine but failed to significantly stimulate isoleucine-dependent ATP hydrolysis (Figure IV.6), suggesting an increase in overall editing against methionine. This is consistent with early reports where tRNA addition was reported to weakly stimulate pre-transfer editing of noncognate amino acids by ycLeuRS (Englisch, et al., 1986).

Table IV.2. Rate Constants (min^{-1}) for tRNA-independent AARS pre-transfer editing activities of standard amino acids[a]

	Enzyme-dependent AMP formation	Non-enzymatic hydrolysis of AA-AMP	Fold difference	Reference
LeuRS Met	**2.0**	**0.100**	**20**	**This work**
IleRS Val	**3.2**	**0.120**	**30**	**(Dulic, et al., 2010)**
GlnRS[b]Gln	**1.5**	**0.042**	**35**	**(Gruic-Sovulj, et al., 2005)**
ProRS Ala	**27.2**	**0.113**	**240**	**(Hati, et al., 2006; Splan, et al., 2008)**
ValRS Thr	**22.2**	**0.070**	**300**	**(Dulic, et al., 2010)**

[a] For enzymatic AMP formation, kobs was reported for all systems, except IleRS and ValRS activation of valine and threonine, respectively, for which k_{cat} was reported. For non-enzymatic solution hydrolysis, k_{obs} was reported.
[b] The GlnRS-Gln system requires presence of $tRNA^{Gln}$.

Hydrolysis of AA-AMP can be catalyzed by the enzyme or depend on a selective release mechanism (Hati, et al., 2006; Splan, et al., 2008). The latter relies on enzyme ejection of adenylate intermediate into the aqueous environment for hydrolysis of noncognate AA-AMP (Hati, et al., 2006; Ling, et al., 2009; Mascarenhas, 2008). To distinguish between these two possibilities for Met-AMP hydrolysis, we performed a chase assay (Dulic, et al., 2010) using reaction conditions that were identical to the AMP formation assays described above. Enzyme-synthesized AA-AMP accumulated for 10 min was followed by addition of a large molar excess of non-radioactive ATP (25 mM) to displace AA-AMP from the synthetic active site. Enzyme-independent hydrolysis of methionyl-adenylate in solution occurred at a rate of 0.1 ± 0.001 min^{-1} (Figure IV.7, Table IV.1), which is 20-fold slower than the rate of methionine-dependent AMP formation by ycLeuRS (2.0 min^{-1}) (Table IV.1). This is consistent with other AARSs that have been proposed to edit by tRNA-independent pre-

transfer editing mechanisms (Table IV.2). We estimate that enzyme-associated hydrolysis of the methionyl-adenylate would account then for ~95% of the tRNA-independent pre-transfer editing activity of ycLeuRS against methionine. Similarly, the solution hydrolysis rate of isoleucyl-adenylate (0.01 ± 0.001 min^{-1}) (Figure IV.7, Table IV.1) was also 70-fold diminished than the overall rate of isoleucine-dependent AMP formation (Table IV.1).

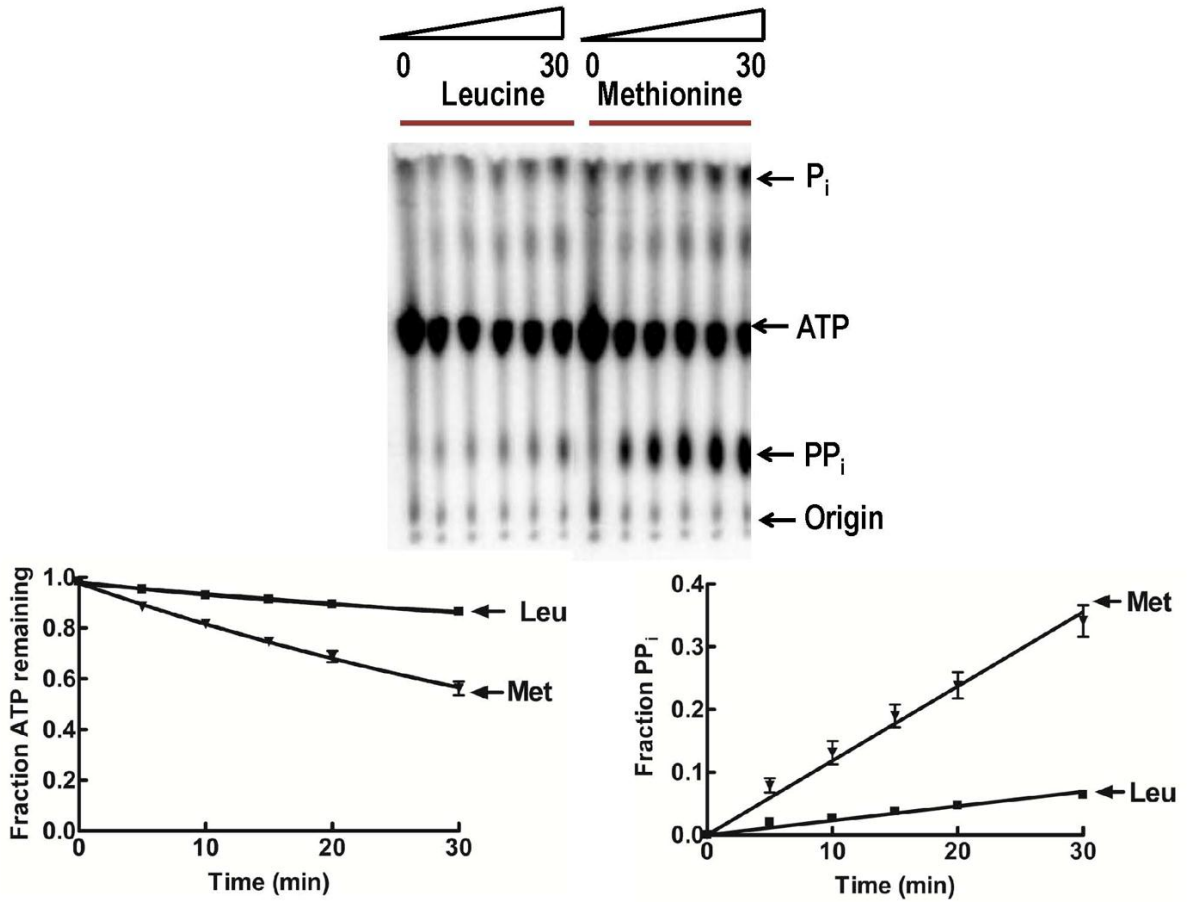

Figure IV.5. Pre-transfer editing activity of wild type ycLeuRS assessed by TLC-based PP_i release assay. (Top) Reaction time courses showing chromatographic separation of [^{32}P]-PP_i, ATP and P_i as indicated. (Bottom, left) ATP hydrolysis is enhanced by noncognate amino acid methionine. (Bottom, right) Fraction of PP_i released is stimulated by noncognate methionine. Reactions containing 250 µM cold ATP, 0.1 µM [γ-^{32}P]-ATP (600 µCi/mL) and 2.5 mM amino acids were initiated with 1 µM enzyme and carried out upto 30 min at 30 °C. Reaction products were resolved on TLC plates that were developed in 750 mM KH_2PO_4, pH 3.5. Symbols are: leucine (■), isoleucine (○), and methionine (▼). Error bars for each time point are a result of each reaction repeated in triplicate.

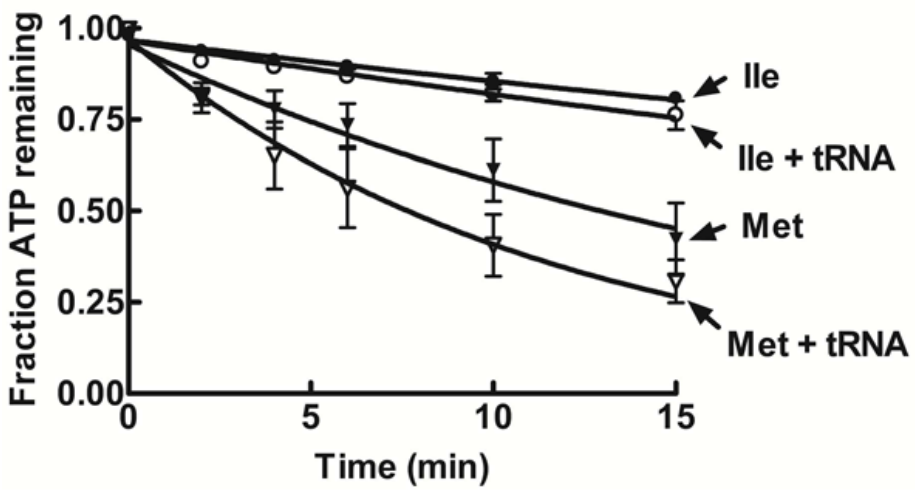

Figure IV.6. Increase in global overall editing against methionine in presence of $tRNA^{Leu}$ for wild type ycLeuRS. ATP hydrolysis was assessed in reactions containing 250 µM cold ATP, 0.2 µM [α-^{32}P]-ATP (600 µCi/mL), 100 mM noncognate amino acids and 29 mg/mL crude yeast tRNA (which was measured to contain 14.5 µM $tRNA^{Leu}$), initiated with 1 µM enzyme and carried out upto 15 min at 30 °C. Reaction products were resolved on TLC developed in 0.1 M ammonium acetate, 5% acetic acid. Error bars for each time point are a result of each reaction repeated in triplicate.

IV.4. Discussion

Adenylate hydrolysis by the homologous IleRS has been proposed to involve its translocation from the synthetic site to the CP1 domain editing site in a tRNA-dependent manner (Nomanbhoy, et al., 1999). In contrast, for *E. coli* LeuRS, a robust pre-transfer editing activity was stimulated only when the CP1 domain was deleted from the enzyme (Boniecki, et al., 2008) or when a mutation at CP1 domain-based Ala 293 was introduced (Williams and Martinis, 2006). Similarly, pre-transfer editing activity is activated in ProRS (Splan, et al., 2008) and ThrRS (Minajigi and Francklyn, 2010) mutants under circumstances where post-transfer activity was selectively inactivated. Pre-transfer editing activities that are tRNA independent have also been reported for SerRS (Gruic-Sovulj, et al., 2007), which lacks a specialized editing domain, as well as in GlnRS (Gruic-Sovulj, et al., 2005), which

apparently does not require editing activity. In addition, MetRS clears homocysteine in a pre-transfer editing cyclization mechanism to produce thiolactone in the synthetic active site (Kim, et al., 1993).

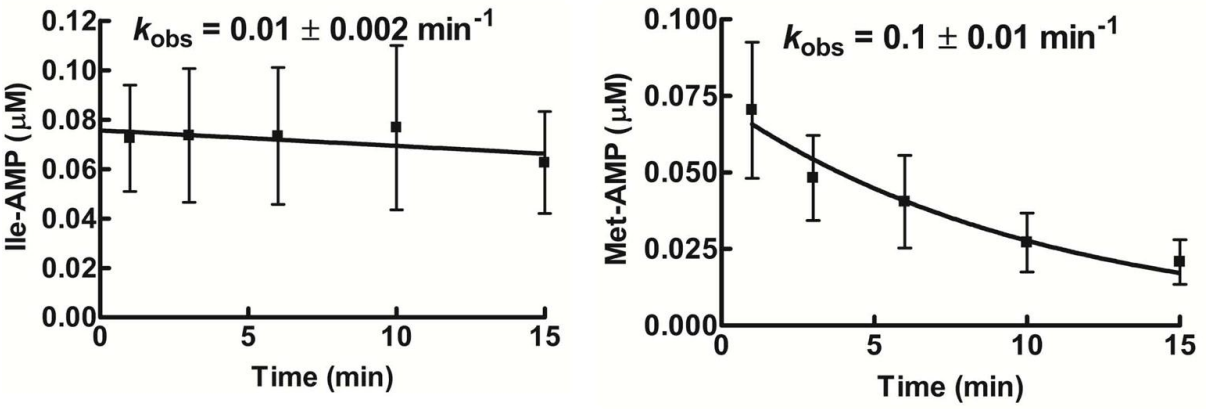

Figure IV.7. Non-enzymatic (LeuRS-independent) hydrolysis of noncognate adenylates. TLC-based ATP chase assays included 251 μM ATP (1800 μCi/mL), 100 mM isoleucine or methionine and 5 μM ycLeuRS. The AA-AMP accumulated on the enzyme was chased from the active site into solution by adding 100-fold excess of non-radioactive 25 mM ATP. Error bars for each time point are a result of each reaction repeated in triplicate.

Segregation of amino acids to different editing pathways has been reported for hcLeuRS, which edits biosynthetic intermediates (α-amino butyrate and norvaline) under *in vitro* conditions via pre- and post-transfer hydrolysis, respectively (Chen, et al., 2011). A tRNA-independent pre-transfer editing for *Aquifex aeolicus* LeuRS has also been identified to clear norvalyl-adenylate (Zhu, et al., 2009). Our results demonstrate that pre- and post-transfer editing co-exist in ycLeuRS, as also found previously for *E. coli* LeuRS (Boniecki, et al., 2008; Williams and Martinis, 2006). Methionine-stimulated ATP hydrolysis and AMP formation in the absence of tRNA as well as ATP chase experiments support that quality control for ycLeuRS is highly dependent on pre-transfer editing under *in vitro* conditions. It is possible that the inclusion of tRNA shifts the editing mechanism preference and increases overall global editing. The same conditions that incorporate isoleucine rather than

methionine suggest that the ycLeuRS relies on post-transfer editing for isoleucine clearance. Although most *in vitro* enzyme experiments fail to recapitulate the dynamic cellular environment, direct *in vitro* comparison for ycLeuRS suggests that methionine and isoleucine partition for clearance between different editing pathways (Figure IV.1). It remains possible that ycLeuRS relies on a combination of editing mechanisms, but our results support that the preference of editing pathways can be dependent on substrate identity.

We hypothesize that these two fidelity mechanisms in ycLeuRS are not redundant but are adapted to accommodate diverse specificities of the noncognate amino acids that challenge LeuRS fidelity in the cell (Karkhanis, et al., 2007; Li, et al., 2011). Under this scenario, ycLeuRS pre- and post-transfer editing sites would have evolved in a complementary way, similar to AARSs that are dependent on independent auxiliary editing domains. Thus, in the case of ycLeuRS, we propose that pre- and post-transfer editing pathways partition in a way that is dependent on the chemical structure of the noncognate amino acid to ensure that all errors are efficiently targeted for clearance by ycLeuRS. This is critical to the cell since disruptions or absence of editing activities in LeuRS can cause mistranslation and cell death (Karkhanis, et al., 2007; Li, et al., 2011).

Chapter V: Split Green Fluorescent Protein-based *in vivo* Assay to Assess Intracellular Effects of Editing Defects in LeuRS

V.1. Introduction

Dissection of a protein and its subsequent reassembly from the peptide fragments have been used to study evolution of large multidomain proteins, protein folding, role of tertiary structural elements in enzyme catalysis, macromolecular assembly and protein-protein interactions. Unassisted reconstitution of protein fragments in *trans* into functional proteins have been demonstrated for IleRS (Shiba and Schimmel, 1992) and ribonuclease (Richards and Vithayathil, 1959) among others. Oligomerization assisted reassembly of protein fragments has been demonstrated in dihydrofolate reductase (DHFR) (Pelletier, et al., 1998), ubiquitin (Karimova, et al., 1998) and β-galactosidase (Rossi, et al., 1997). Assisted reconstitution of these protein fragments is dependent upon covalent fusion to soluble independently folding and interacting domains whose interactions promote the reassembly and folding of the fragments to form the active enzyme. In addition, a viable and sensitive *in vivo* screening assay is also required to test for successful fragment reassembly.

Antiparallel leucine zipper (LeuZ)-assisted reassembly of the N-and C-terminal halves of split green fluorescent protein (GFP) was demonstrated by the Regan laboratory (Ghosh, 2000; Magliery, et al., 2005). The leucine zipper is one of the common motifs found in many gene activator/repressor DNA-binding proteins (Landschulz, et al., 1988). This includes the CCAAT-binding protein or enhancer binding protein (C/EBP), the yeast gene regulatory protein GCN4 and the transforming proteins Fos and Jun. The α-helical leucine zipper motif is characterized by the presence of a leucine residue at every seventh position, extending over a distance covering eight helical turns. The leucine zipper α helix is amphipathic with one side of the helix predominated by hydrophobic residues (particularly leucine) and the other side predominated by charged side chains and uncharged polar side chains (Landschulz, et al., 1988). In addition, leucine side chains protruding from one α-

helix interdigitate with those displayed from a similar α helix of another polypeptide, thus facilitating dimerization into a coiled coil structure (Landschulz, et al., 1988; Lupas, 1996). It has also been shown that the leucine residues in each α helix are critical for dimerization of the leucine zipper and that a general hydrophobic interface is not sufficient for 'zipping' up of the leucine zipper α helices to form the coiled coil dimer structure (Hu, et al., 1990). Generally three of the four hydrophobic positions (Ghosh, 2000) require leucine for the dimerization, as exhibited by the GCN4 leucine zipper (Hu, et al., 1990). The parallel or antiparallel orientation of the leucine zippers (with respect to the N- to C-terminus of one helix) in the coiled coil dimer is determined by the polar and ionic interactions between the charged residues flanking the hydrophobic leucine core (Lupas, 1996).

As a reporter system for reconstitution of protein fragments, GFP is an attractive tool by virtue of its autocatalytically generated fluorescence, which in turn, is dependent on its properly folded structure (Miyawaki, et al., 1997) and because it is known to express, fold and fluoresce in virtually every cell type (Tsien, 1998).

V.1.A. Sequence-enabled reassembly of split green fluorescent protein

The Regan laboratory demonstrated that the leucine zipper sequence-enabled reassembly (SEER) of split GFP resulted in refolded fluorescent GFP (Ghosh, 2000; Magliery, et al., 2005). In these work, GFP was split in a mobile loop (between residues 157 and 158) that was deduced to be not an integral part of the protein structure, to result into the N- and C-terminal halves of GFP (NGFP and CGFP, respectively) (Figure V.1). When produced in *trans* in bacteria, NGFP and CGFP did not associate to give reassembled fluorescent GFP. Strongly interacting (nM affinity) leucine zippers were fused to the C- and N-termini of NGFP and CGFP, resulting in the fusion protein fragments NZGFP and CZGFP, respectively (Figure V.1). When expressed in bacteria, the split GFP fragments reassembled,

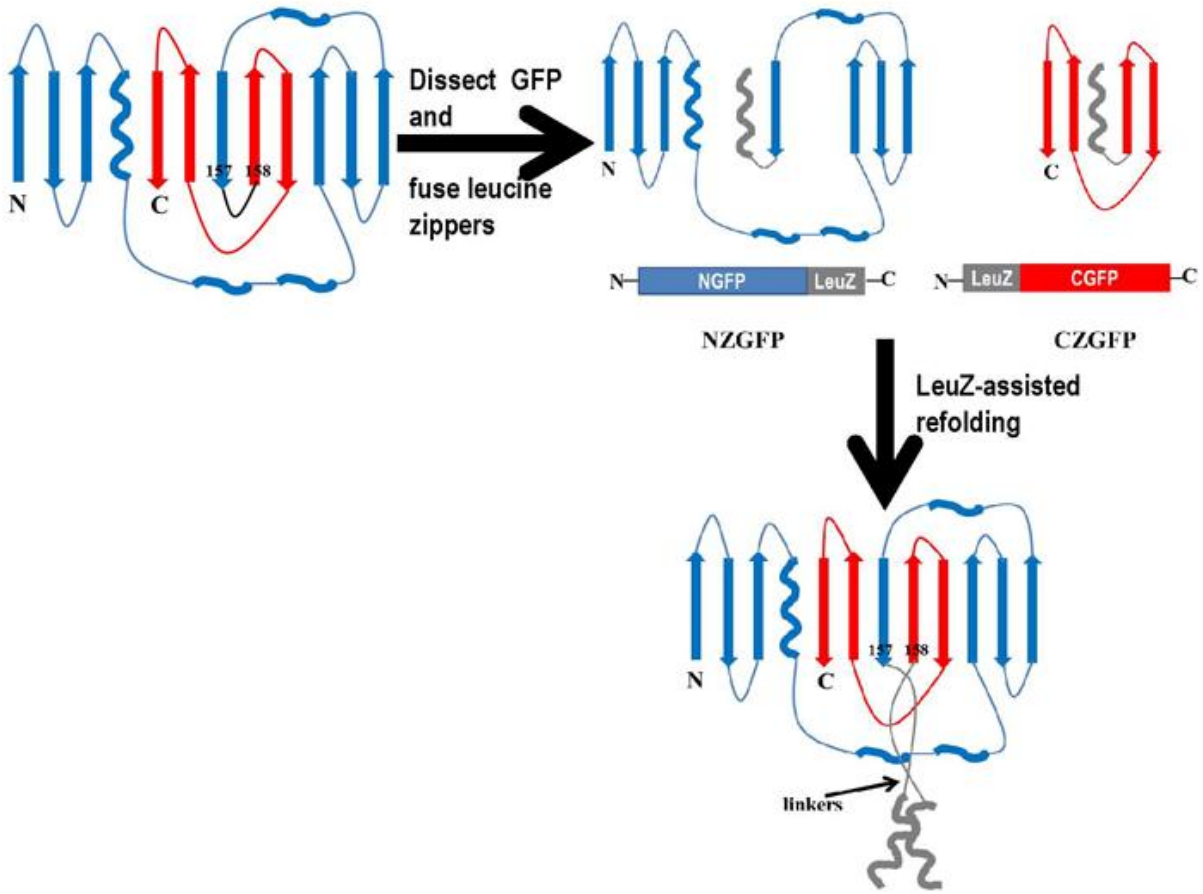

Figure V.1. Scheme showing LeuZ-assisted refolding of split GFP. Intact GFP is split in a loop between residues 157 and 158 and antiparallel leucine zippers fused to each half, resulting in the fused GFP protein fragments, NZGFP and CZGFP. When both these fragments are expressed in bacterial cells from compatible plasmids, the two GFP fragments associate via dimerization of the leucine zippers and result in fluorescence from the refolded GFP. Arrows represent β-strands, squiggles represent α-helices and curved lines represent loops. Colors are: blue for NGFP, red for CGFP and grey for leucine zippers. The figure has been adapted from (Ghosh, 2000).

forming the NZ-CZ refolded GFP complex, directed by oligomerization of the leucine zippers. This resulted in fluorescence. It was demonstrated that GFP folding from its fragments was irreversible *in vitro* and the minimum interaction (K_D) between the leucine zippers, required for this screen, was determined to be as low as approximately 1 mM. The leucine zipper peptides were designed to favor antiparallel orientation by judicious placement of charge-charge interactions that would otherwise result in clashes in the parallel orientation and by introducing a polar residue (asparagine) into the canonical hydrophobic core (Ghosh, 2000).

V.1.B. Fluorescent reporter assay to assess intracellular effects of editing defects in LeuRS

The leucine zipper-directed complementation of the N- and C-terminal GFP fragments was exploited to develop an *in vivo* assay that would assess mistranslation by detecting fluorescence changes that resulted from statistical substitutions at leucine positions in the leucine zippers. The synthetic active site of LeuRS must distinguish between structurally similar isosteric noncognate amino acids isoleucine, methionine, norvaline and valine from the cognate leucine. To preserve high level of fidelity in protein synthesis, LeuRS and other synthetases have evolved to possess robust editing or proofreading activities (Mascarenhas, 2008). The CP1 domain of LeuRS is its editing domain that is responsible for hydrolyzing $tRNA^{Leu}$ mischarged with noncognate amino acids (Betha, et al., 2007). Several conserved residues within the *E. coli* LeuRS editing active pocket in the CP1 domain have been implicated to be critical in the editing pathway, including Thr 252 (Mursinna, et al., 2001), Thr 247, Thr 248 (Zhai and Martinis, 2005) and Asp 345 (Lincecum, et al., 2003). Three mutations (Y330A, D342A and D345A) in the conserved *E. coli* LeuRS editing pocket generates an editing-defective *E. coli* LeuRS mutant (YDD LeuRS) that is unable to cleave the mischarged tRNA substrate, thereby allowing formation of mischarged $tRNA^{Leu}$ and then mistranslation at leucine codons. Such programmed manipulation of the LeuRS editing pocket that attenuate the synthetase's editing activity has been shown to yield *in vivo* incorporation of fluorinated analogs of leucine in recombinant proteins expressed in *E. coli* (Tang and Tirrell, 2001; Tang and Tirrell, 2002; Tang, et al., 2009).

We designed an *in vivo* mistranslation assay to simultaneously overexpress NZGFP fragment protein and editing-defective LeuRS as independent proteins from one plasmid. The CZGFP protein fragment was overexpressed from another plasmid in *E. coli* cells (Figure V.2). Excess noncognate amino acids were incorporated in the growth medium. We hypothesized that the editing defect in the mutant LeuRS (YDD LeuRS) would lead to

statistical substitutions of leucines in the leucine zippers fused to each of the N- and C-terminal halves of GFP, with the noncognate amino acid provided in the medium. Such substitutions would decrease/abolish dimerization of the leucine zippers to form coiled coils. The disruption of leucine zipper dimerization will hamper refolding of the N- and C-terminal halves to GFP and this will be reflected in decreased observable fluorescence. Thus, observation and quantification of fluorescence changes would provide a valuable tool in studying intracellular effects of editing defects in LeuRS. The precise extent of the impact of specific molecular determinants in editing could be deduced using this assay.

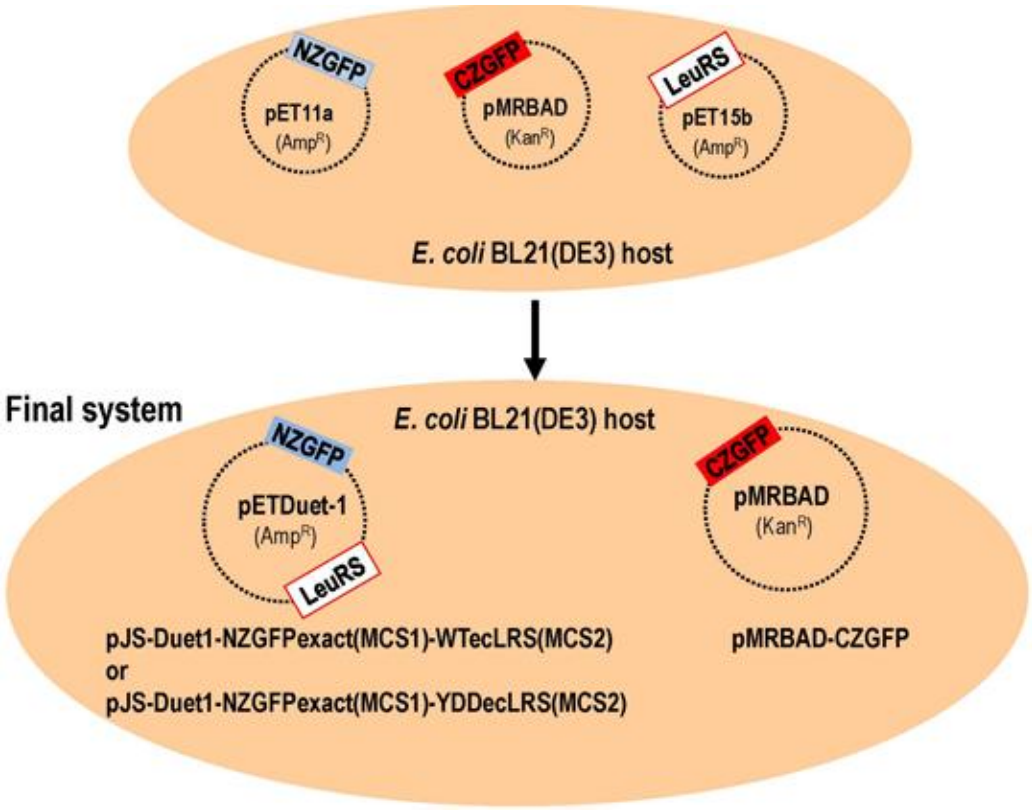

Figure V.2. Design of plasmids for *in vivo* fluorescent reporter assay in *E. coli* BL21(DE3) host cells. Genes encoding LeuRS and one of the fused GFP fragments, NZGFP were subcloned in independent multiclonal sites on pETDuet vector to result in the plasmids pJS-Duet1-NZGFPexact(MCS1)-WTecLRS(MCS2) or pJS-Duet1-NZGFPexact(MCS1)-YDDecLRS(MCS2). The other fusion fragment of GFP, CZGFP was expressed from the plasmid pMRBAD-CZGFP.

V.2. Experimental methods

V.2.A. Cloning, mutagenesis and plasmid construction

Cloning of NZGFP gene in MCS1 of pDuet-1: The gene encoding the protein fragment NZGFP was PCR-amplified in a 50 μL reaction mixture containing 100 ng of the template plasmid pET11a-NZGFP (gift from Lynne Regan), 125 ng each of the forward primer FP *Bam*HI NZGFP Ampl [5′-TTATGGATCCGGCGCGAGCAAAGG-3′] and the reverse primer RP *Eco*RI NZGFP Ampl [5′-CGAT GAATTCTTACTGCGCCAGTT C-3′], 0.05 mM dNTP mix (Stratagene, La Jolla, CA) and 0.05 U *Pfu* DNA polymerase in commercial buffer. The amplified PCR products and the vector pETDuet-1 were separately digested with *Bam*HI and *Eco*RI at 37 °C for 6 h. The restriction-digested PCR products and the vector were separated on a 1% agarose gel and gel-purified using the QIAquick gel extraction kit-250 (Qiagen Inc).

Gel purified restriction digests of the PCR amplified gene fragment and the vector were ligated using T4 DNA ligase at 16 °C overnight. Sequencing the NZGFP gene fragment in the pDuet1 vector identified a random mutation and also that the gene was out of frame. First, the random mutation in the NZGFP gene was corrected in a PCR reaction using the forward primer FP Corr T to C in clone 13 [5′-CACACAACGTTCCCATCATGGCAGAC-3′] and the reverse primer RP Corr T to C in clone 13 [5′-GTCTGCCATGATGGGAACGTTGTGTGs-3′]. Next, the NZGFP gene fragment was made in frame by a PCR reaction using the forward primer FP Insr A in cl 13 to in frame [5′-CAGCCAGGATCCAGGCGCGAGCAAAG-3′] and the reverse primer RP Insr A in cl 13 to in frame [5′-CTTTGCTCGCGCCTGGATCCTGGCTG-3′]. Thus, this resulted in the plasmid pJS-Duet1-NZGFP(MCS1), that contained the gene encoding the six histidine-tagged protein fragment NZGFP in MCS1 between the restriction sites *Bam*HI and *Eco*RI.

Since the NZGFP protein fragment expressed from the plasmid pJS-Duet1-NZGFP(MCS1) did not show fluorescence with the other half of GFP (CZGFP), the following three modifications were made in the NZGFP insert of pJS-Duet1-NZGFP(MCS1), as highlighted in Figure V.3: (1) the glycine (adjacent to the first methionine) was mutated to an alanine; (2) one serine residue was deleted; (3) the tetrad Ser-Gln-Asp-Pro, immediately following the six histidine tag, was deleted. These modifications resulted in the NZGFP gene construct within the pDuet1 vector to exactly mimic the same construct in the original system of pET11a vector (Ghosh, 2000). We speculated that these modifications would facilitate interactions of NZGFP with CZGFP and hence aid the re-folding process. First, modification 1 was made in a PCR reaction containing the template plasmid pJS-Duet1-NZGFP(MCS1), the forward primer FP NZGFP/Duet-Corr 1 [5′-GGAGATATACCATGGCCAGCCATCAC-3′] and the reverse primer RP NZGFP/Duet-Corr 1 [5′-GCTGTGGTGATGATGGTGATGGCTG-3′]. Next, modifications 2 and 3 were carried out in a single PCR reaction using the forward primer FP NZGFP/Duet-Corr 2 [5′-GCCATCACCATCATCACCACGGCGC-3′] and the reverse primer RP NZGFP/Duet-Corr 2 [5′-GTTCTTCTCCTTTGCTCGCGCCGTGG-3′]. These modifications resulted in the final plasmid pJS-Duet1-NZGFPexact(MCS1) bearing the six histidine-tagged NZGFP gene in MCS1. This plasmid was used in the further cloning steps. It is important to note here that in the process of the three above mentioned modifications, the *Bam*HI restriction site in MCS1 has been deleted.

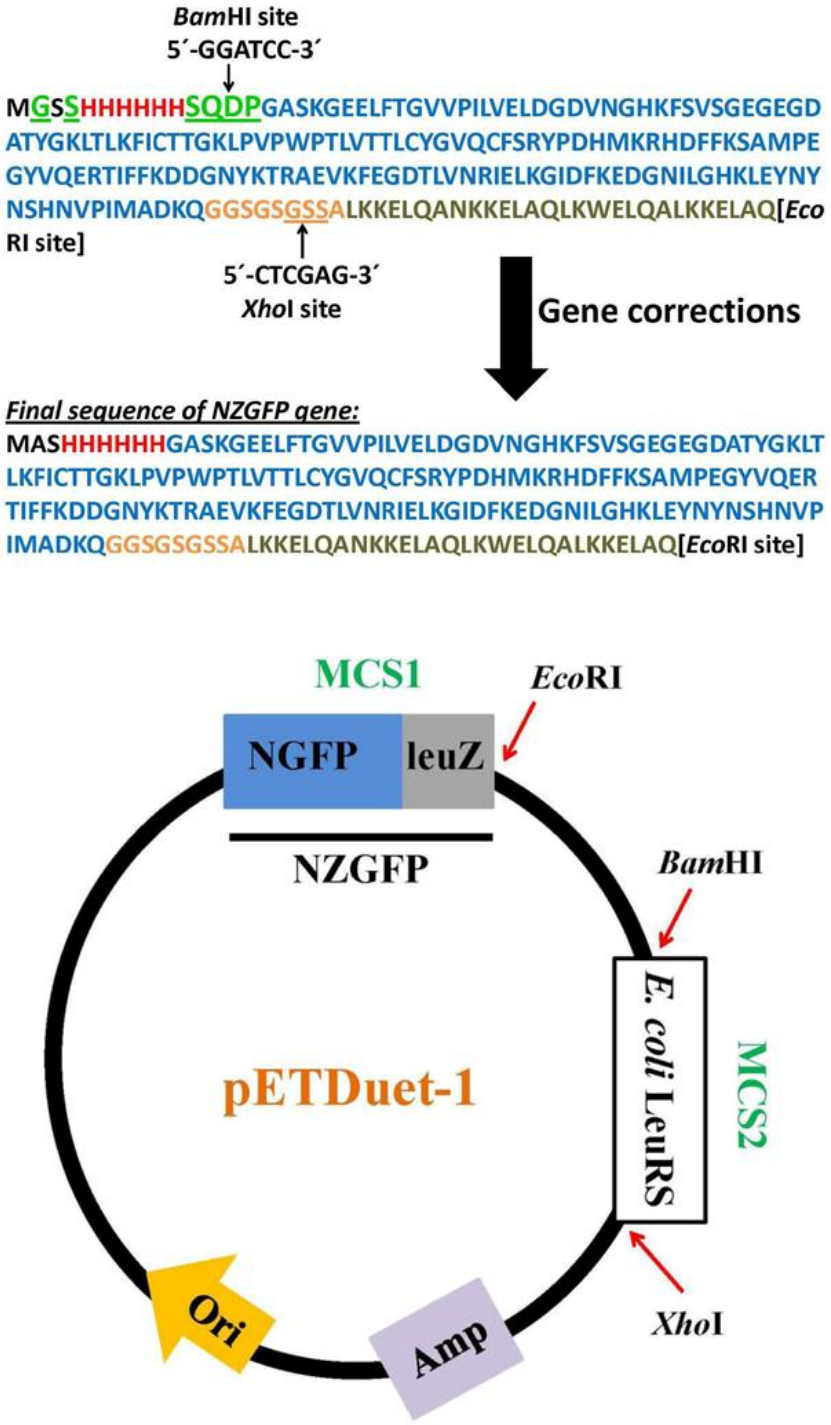

Figure V.3. Construction of the plasmid pJS-Duet1-NZGFPexact(MCS1)-WTecLRS(MCS2). (Top) Amino acid sequence of NZGFP protein fragment, the gene for which has been cloned in MCS1 of pETDuet-1 vector, using *Bam*HI and *Eco*RI restriction sites. In the final NZGFP gene sequence, the *Bam*HI restriction site has been deleted and the *Xho*I site within the NZGFP sequence has been removed by conservative mutations. The colors indicate: red, six-histidine tag; blue, NGFP sequence, grey; leucine zipper; orange, spacer between NGFP and the leucine zipper; and green, residues which have either been mutated or removed to result in the final sequence. (Bottom) The construct pJS-Duet1-NZGFPexact(MCS1)-WTecLRS(MCS2). The gene encoding NZGFP is cloned in MCS1 and that encoding LeuRS is cloned in MCS2 between *Bam*HI and *Xho*I.

Cloning of E. coli LeuRS gene in MCS2 of pJS-Duet1-NZGFPexact(MCS1): Two restriction sites were introduced into pJS-Duet1-NZGFPexact(MCS1) to produce pJS-Duet1-NZGFPexact(MCS1)-modified via two sequential PCR mutations. First, the *Bgl*II restriction site in MCS2 was mutated to a *Bam*HI site, using the forward primer FP *Bgl*II-*Bam*HI/MCS2/pD [5′-GATATACATATGGCGGATCCCAATTG-3′] and the reverse primer RP *Bgl*II-*Bam*HI/MCS2/pD [5′-CGATATCCAATTGGGATCCGCCATAT-3′]. Next, a *Xho*I restriction site in the spacer region of the NZGFP gene sequence (Figure V.3) was removed by mutations that did not alter the amino acid sequence of the gene using the forward primer FP del *Xho*I (pDuNZGFP) [5′-GGTGGCTCTGGCTCTGGTTCTTCCGC-3′] and the reverse primer RP del *Xho*I (pDuNZGFP) [5′-CTTTTTTGAGGGCGGAAGAACCAGAG-3′].

The gene encoding the full length wild type *E. coli* LeuRS was PCR-amplified in a 50 µL reaction mixture containing the template plasmid p15ec3-1 (Martinis and Fox, 1997), forward primer FP Ampl/ecLRS/*Bam*HI [5′-GATATACATATGGCGGATCCAATTG-3′] and reverse primer RP Ampl/ecLRS/*Xho*I [5′-GTAACTCGAGTTAGCCAACGACCAGA-3′] as described before in this section. The amplified insert and the plasmid vector pJS-Duet1-NZGFPexact(MCS1)-modified was separately digested with restriction enzymes *Bam*HI and *Xho*I at 37 °C for 3 h. The restriction digests were then inactivated by heating to 80 °C for 20 min. The restriction-digested plasmid vector pJS-Duet1-NZGFPexact(MCS1)-modified (8 µg) was treated with 22 U of calf intestinal phosphatase (CIP) (New England BioLabs Inc., Beverly, MA) at 37 °C for 1 h. This was followed by agarose gel separation and purification of the insert and the vector using the QIAquick gel extraction kit-250 (Qiagen Inc). Gel purified restriction digests of the PCR amplified gene fragment and the vector were ligated using T4 DNA ligase as described previously in this section. A frame shift mutation was corrected in a separate PCR reaction containing the forward primer Fwd-In fr ec-pD1(NZ+ecL) [5′-CATATGGCGGATCCGATGCAAGAGC-3′] and reverse primer

Rev-In fr ec-pD1(NZ+ecL) [5′-GCTCTTGCATCGGATCCGCCATATG-3′] yielding the final plasmid pJS-Duet1-NZGFPexact(MCS1)-WTecLRS(MCS2).

The salient features of the plasmid pJS-Duet1-NZGFPexact(MCS1)-WTecLRS(MCS2), as enumerated in Figure V.3, are: (i) The plasmid contains the NZGFP gene in MCS1. (ii) The *Bam*HI restriction site of MCS1 (that was originally used, along with the *Eco*RI site to clone the NZGFP gene) has been deleted. (iii) The *Xho*I restriction site originally present in the NZGFP sequence has been removed by conservative mutations that did not alter the amino acid sequence of NZGFP. (iv) The NZGFP gene sequence in this construct is identical to the gene sequence in the pET11a-NZGFP construct (Magliery, et al., 2005). (v) The plasmid contains the wild type *E. coli* LeuRS gene in MCS2 between the restriction sites *Bam*HI and *Xho*I.

The editing defective mutations in *E. coli* LeuRS were introduced in the plasmid pJS-Duet1-NZGFPexact(MCS1)-WTecLRS(MCS2) in two sequential PCR reactions resulting in the plasmid pJS-Duet1-NZGFPexact(MCS1)-YDDecLRS(MCS2), bearing the editing defective (YDD) *E. coli* LeuRS gene in MCS2 and the NZGFP gene in MCS1. First, the mutations D342A and D345A were constructed using the forward primer FPecD342A/D345A [5′-GTACCGGGGCACGCCCAGCGCGCCT-3′] and reverse primer RPecD342A/D345A [5′-GCAAACTCGTAGGCGGGCTGGGCGT-3′]. Next, the mutation Y330A was introduced by using the forward primer FPecY330A [5′-GTATTGATGGAGGCCGGCACGGGCG-3′] and reverse primer RPecY330A [5′-CTGCGCCCGTGCCCGCCTCCATCAA-3′]. All gene sequences and mutations were confirmed by DNA sequencing at the UIUC Core Sequencing Facility (Urbana, IL).

V.2.B. Screening of refolded NZ-CZ GFP complex

Competent *E. coli* strain BL21(DE3) cells were co-transformed with compatible pairs of plasmids (Table V.1): Positive control - plasmid pJS-Duet1-NZGFPexact(MCS1)-WTecLRS(MCS2) encoding the NZGFP fusion protein fragment and the wild type LeuRS, and plasmid pMRBAD-CZGFP, encoding the CZGFP fusion protein; Test system - plasmid pJS-Duet1-NZGFPexact(MCS1)-YDDecLRS(MCS2), encoding the NZGFP fusion protein fragment and the editing-defective YDD mutant LeuRS, and plasmid pMRBAD-CZGFP, encoding the CZGFP fusion protein; negative control - plasmid pET11a-NGFP and plasmid pMRBAD-CGFP, encoding the protein fragments NGFP and CGFP, respectively. Cells were grown overnight on LB-agar media that had 100 μg/mL Amp and 35 μg/mL kanamycin (Kan), at 37 °C.

Table V.1. Pairs of plasmids used to transform *E. coli* cells to screen re-folded NZ-CZGFP complex

System	Pairs of plasmids	Expressed proteins
Positive Control	pJS-Duet1-NZGFPexact(MCS1)-WTecLRS(MCS2) and pMRBAD-CZGFP	NZGFP, wild type *E. coli* LeuRS, and CZGFP
Test	pJS-Duet1-NZGFPexact(MCS1)-YDDecLRS(MCS2) and pMRBAD-CZGFP	NZGFP, editing-defective YDD *E. coli* LeuRS, and CZGFP
Negative Control	pET11a-NGFP and pMRBAD-CGFP	NGFP, and CGFP

A 3 mL LB culture, containing 100 μg/mL Amp and 35 μg/mL Kan was inoculated with a single colony from each plate and grown overnight at 37 °C. The proteins were expressed by plating of a 1:10,000 dilution of each saturated overnight culture on LB-agarose plates that had 100 μg/mL Amp, 35 μg/mL Kan, 10 μM IPTG and 0.2% arabinose. Cells were then grown at 30 °C overnight, followed by room temperature for 2 to 3 days.

Alternately, protein expression was induced at the log phase as follows: A 3 mL LB media containing 100 μg/mL Amp and 35 μg/mL Kan was inoculated with 50 to 100 μL of the respective overnight cultures and grown at 37 °C until the OD_{600} reached ~0.6. This was followed by induction of the log phase liquid culture with 10 μM IPTG and 0.2% arabinose, with subsequent plating of a 1:1,000 dilution of the culture on LB-agar plates that contained 100 μg/mL Amp, 35 μg/mL Kan, 10 μM IPTG and 0.2% arabinose. The cells were grown at 30 °C overnight and then at room temperature for 2 to 3 days.

Cells that fluoresced were observed with a hand-held UV transilluminator at 365 nm. Alternately, fluorescence was observed by fluorescence microscopy. Microscope slides were prepared as follows: A single fluorescent colony from the respective plate, was resuspended in 10 μL 1X phosphate buffered saline (PBS) and spread evenly on poly-D-lysine-treated microscope slides (Fischer Scientific), covered by a glass slip (Corning) and allowed to dry. The cells were then observed under the microscope (Carl Zeiss, Jena, Germany), using the GFP filter ($\lambda_{excitation}$ = 468 nm, $\lambda_{emission}$ = 505 nm) and image acquisition of the fluorescing cells was performed with the AxioVision software.

V.2.C. Fluorescent reporter assay

E. coli strain BL21 (DE3) was co-transformed with compatible pairs of plasmids as described in the previous section (Table V.1). For each set of transformations, two 1 mL overnight cell cultures were harvested separately in a table top centrifuge (Eppendorf 5417C). Each cell pellet was washed twice with 1 mL of minimal standard (MS) media (Leu^-) (Low, et al., 1971). The cell pellet was resuspended in 100 μL of MS media (Leu^-), mixed with 0.7% soft agar along with 10 μM IPTG and 0.2% arabinose and evenly plated on MS media (Leu-)-agarose plates that contained 100 μg/mL Amp and 35 μg/mL Kan. A central well was bored into each plate after the soft agarose solidified and filled with 100 to 150 μL of

100 mM of either isoleucine or norvaline. The cells were allowed to grow overnight at 30 °C and then at room temperature for 2 to 3 days. The halo of cell death or decreased fluorescence, when present, was observed by fluorescence microscopy.

V.2.D. Affinity purification of refolded NZ-CZGFP protein complex.

Fluorescing *E. coli* BL21 (DE3) cells harboring the refolded NZ-CZGFP complex were screened on solid media as described in section V.2.B. A single fluorescent colony was used to inoculate 3 mL LB (100 μg/mL Amp and 35 μg/mL Kan) and grown overnight at 30 ° C. The overnight culture was then used to inoculate 250 mL LB (100 μg/mL Amp and 35 μg/mL Kan) and grown until OD_{600} reached 0.6. Protein expression was induced during log phase (or at the overnight phase) with 10 μM IPTG and 0.2% arabinose with an overnight incubation at 30 ° C overnight, followed by room temperature for 2 to 3 days, with shaking.

Cells were harvested using an Avanti J-E preparative centrifuge (Beckman Coulter, Fullerton, CA) at 6000 rpm for 15 min at 4 °C. The cell pellet was resuspended in lysis buffer [(50 mM Tris-HCl, pH 8.0, 200 mM NaCl and 2 mM β-mercaptoethanol (BME) containing (10 mM imidazole, 0.1% triton-X-100, 1 μL DNase I, 1 μL RNase, 1mg/mL hen egg white lysozyme, 5 mM $MgCl_2$ and 0.5 mM $CaCl_2$)] (Magliery, et al., 2005; Wilson, et al., 2004) and incubated on ice for 30 min, followed by brief sonication. The protein-containing supernatant was mixed with 1 mL of HIS-Select Nickel Affinity Gel (Sigma-Aldrich) that had been pre-equilibrated with 10 mL of GFP buffer [50 mM Tris-HCl, pH 8.0, 200 mM NaCl and 2 mM BME]. The N-terminal six-histidine tagged refolded NZ-CZGFP complex in the supernatant was bound to the resin via gentle rocking at 4 °C for 1 h. Following binding, the resin was washed with 10 mL of GFP buffer containing 20 mM imidazole. The bound NZ-CZGFP protein complex was then eluted in fractions from the resin using 6 mL of GFP buffer containing 300 mM imidazole.

V.3. Results and Discussion

V.3.A. Design of *in vivo* fluorescent assay

The split-GFP complementation system (Magliery, et al., 2005) is comprised of two fragments of GFP, each fused to a leucine zipper. The NZGFP and CZGFP fragments are expressed from plasmids pET11a (Amp resistance) and pMRBAD (Kan resistance). A third plasmid (Amp resistance) expressing LeuRS was coexpressed in the *E. coli* strain BL21 (DE3). However, it was determined not to be feasible because of plasmid incompatibility and overlapping antibiotic selection marker (Figure V.2). Hence, the gene encoding the NZGFP fragment and the gene encoding LeuRS (wild type or editing defective) were cloned into one vector, pDuet-1, at two different multiclonal sites (MCS). The expression of each was under the control of the T7-*lac* promoter. This resulted in the plasmid pJS-Duet1-NZGFPexact(MCS1)-WTecLRS(MCS2) (Figure V.3), encoding NZGFP fragment and wild type LeuRS or the plasmid pJS-Duet1-NZGFPexact(MCS1)-YDDecLRS(MCS2), encoding NZGFP fragment and editing-defective LeuRS. The plasmid pMRBAD-CZGFP was used to express the CZGFP protein fragment (Figure V.2).

E. coli BL21 (DE3) cells were co-transformed with pairs of compatible plasmids for the test system, and positive and negative controls (Table V.1). The expression of the independent recombinant proteins NZGFP (or NGFP) and LeuRS was induced with 10 μM IPTG and that of CZGFP (or CGFP) was induced with 0.2% arabinose, in the background of endogenous wild type LeuRS. Cells were grown on MS media (Leu^-) in the presence of 100 mM of noncognate amino acids (isoleucine or norvaline) on plates. Decreases in fluorescence in this assay rely on statistical substitutions of leucines due to editing defects in LeuRS. Thus, it is anticipated that even in the background of the wild type LeuRS, statistical fidelity mistakes can be detected because the editing-defective mutant of LeuRS is overexpressed.

V.3.B. Expression of individual recombinant proteins and affinity purification of the refolded NZ-CZGFP complex

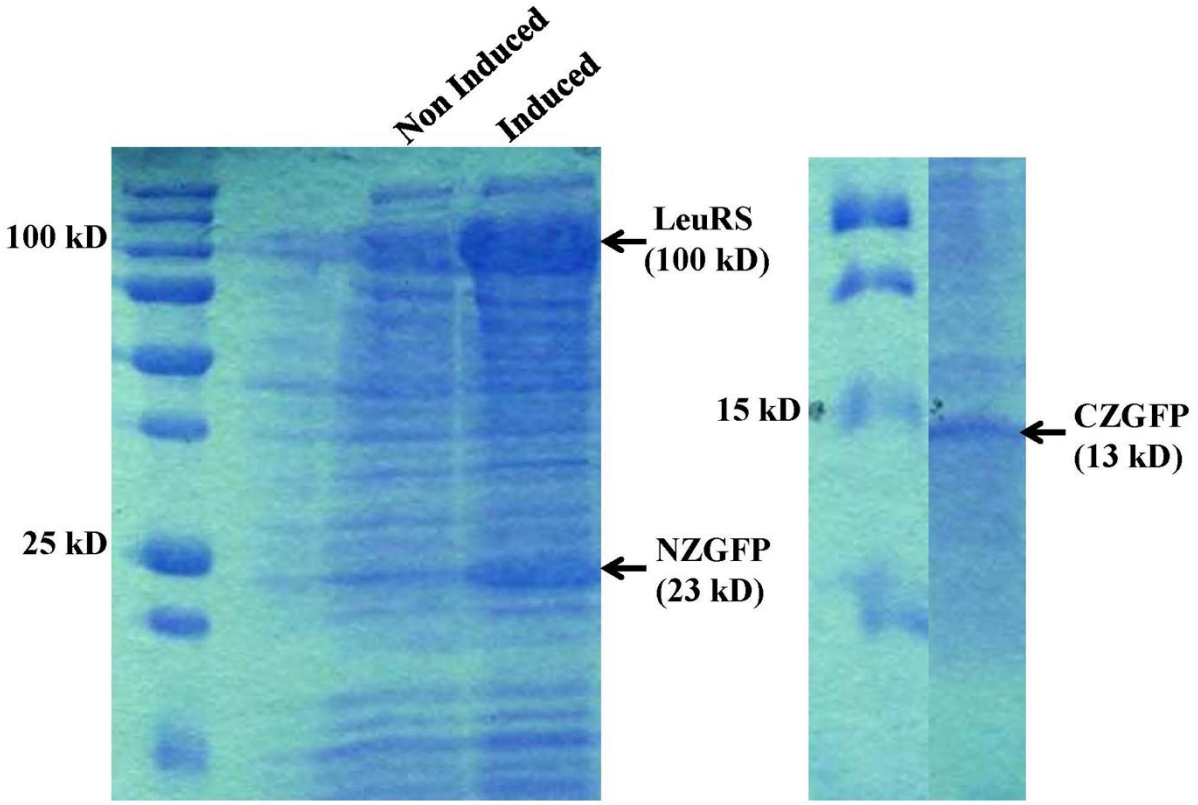

Figure V.4. SDS-PAGE analysis of expression of LeuRS and the GFP fusion fragments, NZGFP and CZGFP. (Left) Expression of LeuRS and NZGFP from the plasmid pJS-Duet1-NZGFPexact(MCS1)-WTecLRS(MCS2). (Right) Expression of CZGFP from the plasmid pMRBAD-CZGFP. The extreme left lanes in both gels represent the protein ladder. The calculated molecular weights of the protein fragments are: $(His)_6$-NZGFP, 23 kD; CZGFP, 13 kD; and *E. coli* LeuRS, 98 kD.

Small scale (3 mL culture) expressions were carried out to check the expression of the individual recombinant proteins from the respective plasmids. *E. coli* BL21 (DE3) cells were transformed with either plasmid pJS-Duet1-NZGFPexact(MCS1)-WTecLRS(MCS2), co-expressing NZGFP protein fragment and wild type LeuRS as independent proteins or with plasmid pMRBAD-CZGFP, expressing CZGFP protein fragment. Cells were grown at 37 °C and then induced with 10 μM IPTG or 0.2% arabinose when the OD_{600} reached 0.6. The cells were harvested after 3 h of protein expression at 30 °C, followed by resuspension and sonication. Analysis of the lysate by SDS-PAGE clearly showed that both the NZGFP

fragment and LeuRS were expressed from the plasmid pJS-Duet1-NZGFPexact(MCS1)-WTecLRS(MCS2) and the fragment CZGFP was expressed from the plasmid pMRBAD-CZGFP (Figure V.4).

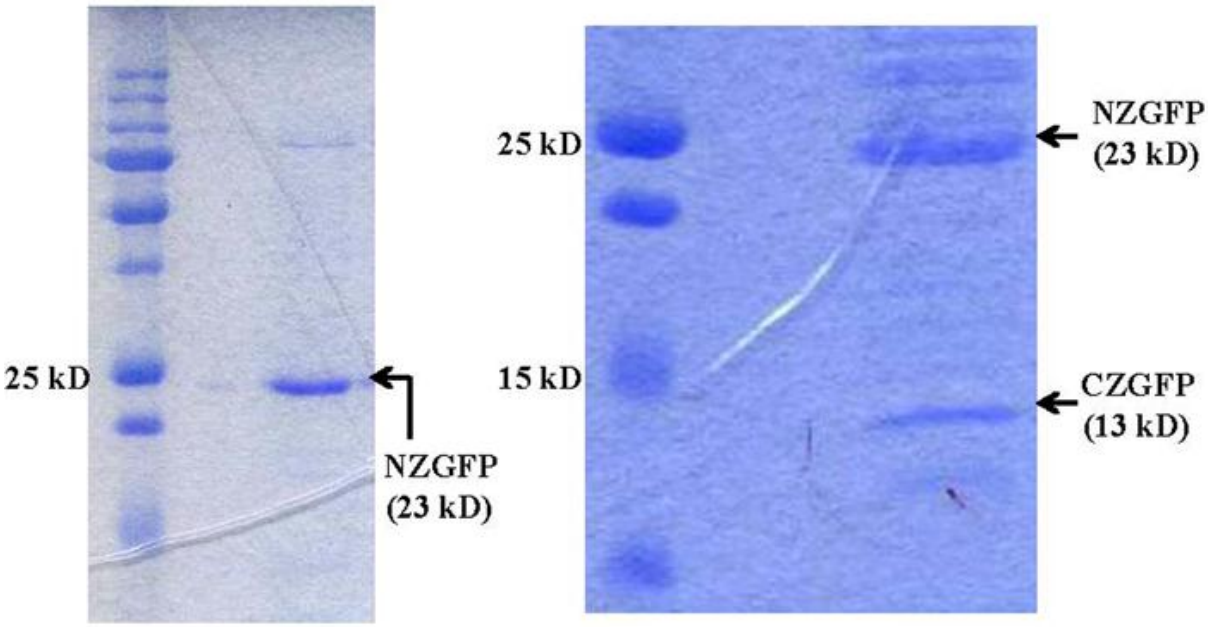

Figure V.5. Purification of re-folded GFP. Affinity purification of six-histidine-tagged GFP fragment NZGFP (left) and refolded NZ-CZGFP complex (right). The complex components NZGFP (23 kD) and CZGFP (13 kD) are visible. The extreme left lanes in both gels represent the protein ladder.

The refolded NZ-CZGFP complex was purified from cells that fluoresced using the six-histidine tag at the N-terminus of the NZGFP fragment. The purification was facilitated by the stability of the refolded GFP complex. Fluorescent cells harboring the refolded NZ-CZGFP complex were grown in liquid cultures for 2 to 4 days at room temperature or 30 °C and the six histidine-tagged GFP complex affinity purified from the soluble fraction of the cell lysate, yielding strong bands on an SDS-PAGE gel that corresponded to the complex components, $(His)_6$-NZGFP (23 kD) and CZGFP (13 kD) (Figure V.5). Cells that were

fluorescent were also visualized on MS media-agar plates either with a hand-held UV illuminator at 365 nm or under the microscope using a GFP filter (Figure V.6).

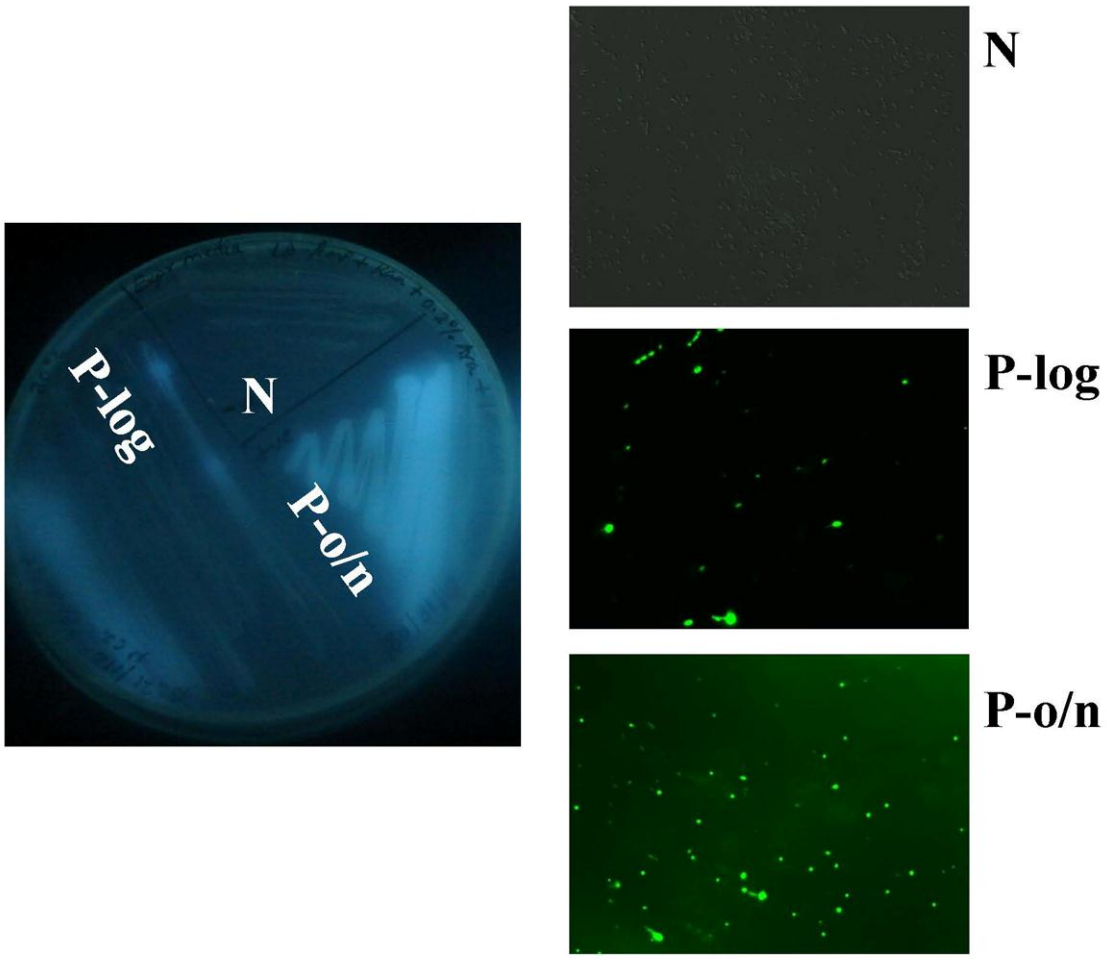

Figure V.6. Visualization of fluorescence of LeuZ-assisted refolded GFP. (Left) Fluorescence is visualized on solid MS media-agar plates using a hand-held UV illuminator at 365 nm. (Right) Fluorescing *E. coli* BL21(DE3) cells visualized under the microscope using GFP filter. Abbreviations are as follows: N, negative control- cells in which NGFP and CGFP have been coexpressed; P-log, positive control- cells in which coexpression of NZGFP, CZGFP and wild type LeuRS were induced at log phase (OD_{600} 0.6) of cell growth; P-o/n, cells in which coexpression of NZGFP, CZGFP and wild type LeuRS were induced at the overnight (13 h) phase of cell growth.

V.3.C. Editing-dependent fluorescence reporter changes

Competent *E. coli* BL21(DE3) cells were transformed with compatible pairs of plasmids (Table V.1), expressing NZGFP, CZGFP, and wild type LeuRS or editing-defective YDD LeuRS. The cellular fluorescent assay was performed with cells that expressed either

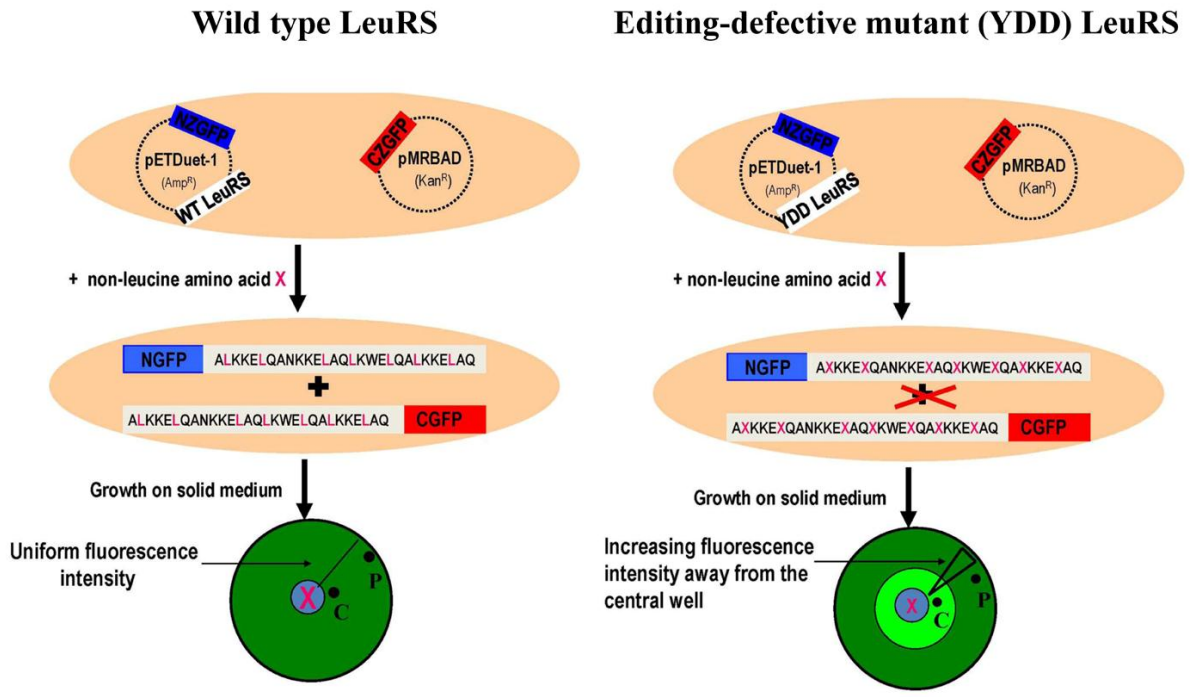

Figure V.7. Scheme of LeuRS editing-dependent *in vivo* fluorescent reporter assay. NZGFP, LeuRS (wild type – left; or editing-defective – right) and CZGFP are overexpressed simultaneously in *E. coli* BL21(DE3) cells from compatible plasmids in presence of exogenously supplied non-leucine amino acid X (isoleucine or norvaline) on solid MS media (Leu-)-agarose. The non-leucine amino acid incorporated into the central well of the MS media plate will diffuse into the solid growth medium. GFP fluorescence from cells near the central well (C) or at the periphery of the plate (P) was observed by fluorescence microscopy using a GFP filter.

wild type or editing-defective LeuRS. For both sets, cells from discrete points on the MS media-agar plate ('C', near the noncognate amino acid-containing central well; or 'P', at the periphery of the plate) (Figure V.7) were visualized under the microscope, using GFP filter. Multiple snap shots of fluorescing cells were acquired under the microscope (Figure V.8). In the presence of the wild type LeuRS and noncognate amino acid, cells from the 'C' and 'F'

points on the plate show similar fluorescence (Figure V.8, top). This suggested that leucine zipper-assisted refolding of the NZ- and CZGFP fragments has not been affected by the presence of the noncognate amino acids, as long as the wild type enzyme is present. Thus, the leucine zipper fused to each of the GFP protein fragments would be expected to have been translated error-free. Hence, enabled by the wild type leucine zipper dimerization, the N- and C-terminal halves of GFP have reassembled in a stable way to show fluorescence.

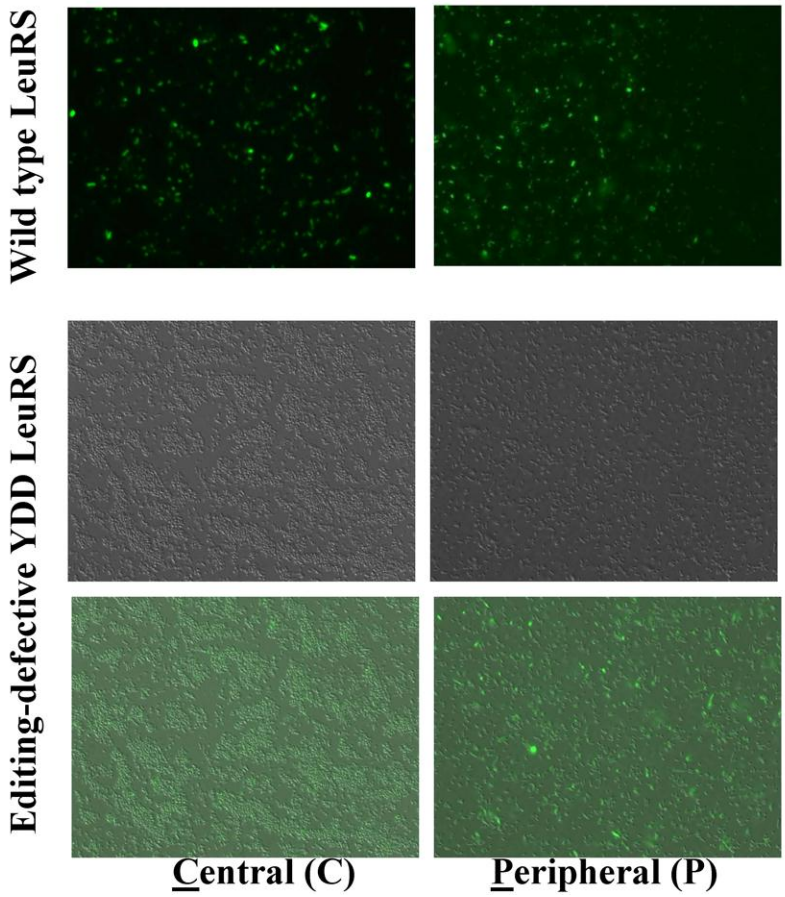

Figure V.8. LeuRS editing-dependent fluorescence changes. Miscroscope snap shots of fluorescent cells using a GFP filter, from the center (C) or periphery (P) of MS media-agar plates. (Top) Uniform fluorescence in presence of overexpressed wild type LeuRS. (Bottom) In presence of overexpressed editing-defective YDD LeuRS, the cells from the center point C are not fluorescing due to disrupted dimerization of the leucine zippers. Cells from the peripheral point P show relatively increased fluorescence. The grey images represent cells visualized by differential interference contrast (DIC) microscopy.

The editing-defective LeuRS mutant (YDD) was also overexpressed in cells that produced the GFP fragments. The center 'C' point on the MS media-agar plate showed nearly no fluorescent cells under the microscope, while the peripheral 'P' point showed relatively increased number of cells that fluoresced (Figure V.8, bottom). The absence or reduction in fluorescence suggested that overexpression of the editing-defective LeuRS, in the background of endogenous wild type LeuRS resulted in mistranslation of the leucine zippers. This impairs their dimerization and hence reassembly of the GFP fragments. The increase in fluorescence moving from the center to the periphery of the plate suggested that statistical leucine substitutions in the leucine zippers was likewise increased in cells growing near the central well that contained the non-leucine amino acid.

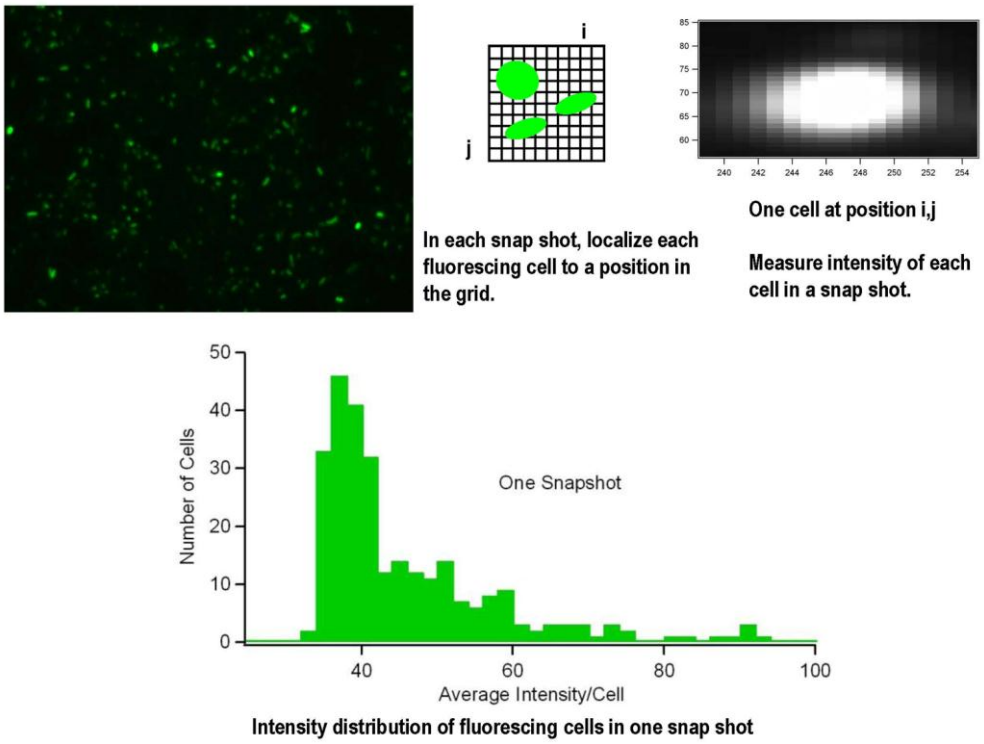

Figure V.9. Fluorescence intensity analysis of one microscope snap shot. Fluorescent *E. coli* BL21(DE3) cells coexpressing NZGFP, CZGFP and wild type LeuRS are visualized by microscopy, using GFP filter. (Top, left to right) Each snap shot is treated like a grid; each cell in the snap shot is localized to a position (i, j) in the grid and intensity measured using MATLAB. (Below) The intensity distribution of all the fluorescing cells in one snap shot.

A scheme was designed to analyze these observed fluorescence changes (Figure V.9, Figure V.10.) Cells in the area covered by the cover slip were scanned as a grid under the microscope and snap shots were captured for each cover slip, followed by fluorescence analysis of individual snap shots. In each snap shot, fluorescing cells were located to a position in the grid (i, j). Its fluorescence intensity was calculated (I_k) and then the distribution of fluorescence intensity over the cells in that snap shot were plotted (Figure V.9.). This would be followed by calculation of average fluorescence intensity per snap shot,

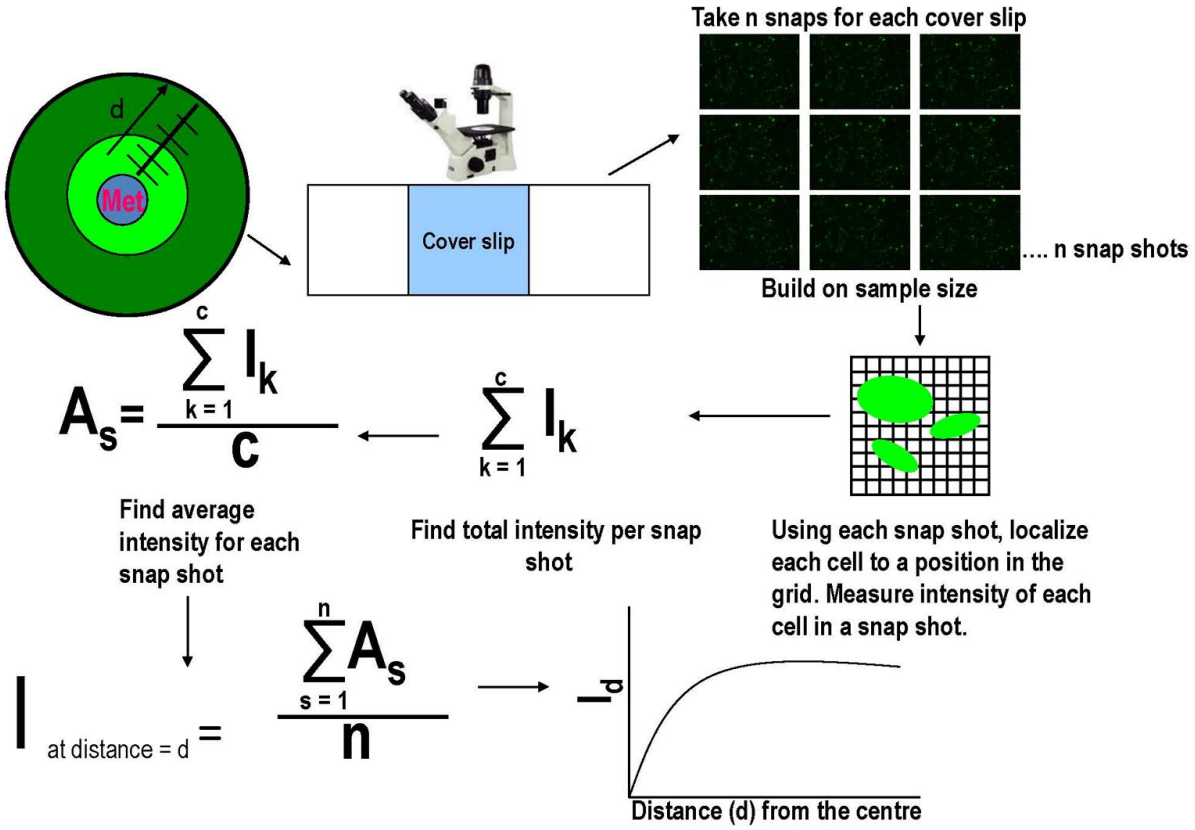

Figure V.10. Quantification of LeuRS editing-dependent fluorescence intensity changes. Cells from discrete points on the MS media-agar plate were viewed on a glass slide-cover slip under the microscope. The cover slip was scanned and multiple (n) snap shots captured for one cover slip. The intensity at a discrete distance from the central well (I_d) on the plate was calculated as the average intensity over the total n number of snap shots captured for that point. Plotting I_d versus distance from the central well (d) would give the fluorescence intensity changes of refolded GFP due to editing-defects in LeuRS.

averaging over the number of cells (c) in that snap shot (A_s) (Figure V.10.). Finally, the fluorescence intensity at a distance (d) from the noncognate amino acid-containing central well would be calculated by averaging fluorescence intensity over the total number of snap shots (n) captured for cells from that point on the plate. Cellular fluorescence intensity (averaged over the number of the cells in a snap shot and also over the number of snap shots captured for that distance/point on the plate) was plotted against the distance (d) of the point from the central well (Figure V.10.)

V.3.D. Concluding remarks

The fluorescent reporter assay to assess the effects of editing defects in LeuRS relies on fluorescence that results due to LeuZ-assisted reassembly of GFP fragments. Co-expression of the multiple protein fragments and full length proteins from compatible plasmids yielded a robust working system that monitors LeuRS editing-dependent fluorescence changes *in vivo*. This reporter assay could quantitatively analyze the fluorescence changes to gauge the cellular impact of LeuRS editing defects.

Further optimization of the experimental parameters in the fluorescent reporter assay would be required in order to capture the finer differences in fluorescence intensity changes of reassembled GFP. As an example, judicious manipulation of the noncognate amino acid concentration incorporated in the central well could lead to better observable fluorescence intensity changes, moving from the center to the periphery of the plate. Alternately, using a LeuRS-knockdown bacterial strain to perform the fluorescent reporter assays would ensure complete removal of any endogenous editing activity. Mass spectrometric analysis of the purified leucine zippers from the system that allows mistranslation due to editing defects in LeuRS will provide molecular level insights into the nature of the statistical mutations.

In short, the fluorescent reporter assay has provided a superior and more sophisticated way of investigating intracellular effects of editing defects. Previously, a similar, but non-fluorescent 'halo' assay has been utilized for studying mistranslation *in vivo* (Hellmann and Martinis, 2009; Karkhanis, et al., 2006; Sarkar, et al., 2011). However, the non fluorescent halo assay relied on an 'all or none' effect of mistranslation on cell viability. Because the current fluorescent assay monitors small changes in fluorescence intensity, it provides a tighter handle on studying the precise impact of LeuRS editing defects on cell survival. The molecular determinants of post-transfer editing in LeuRS are well established (Lincecum, et al., 2003; Mursinna, et al., 2001; Pang and Martinis, 2009; Sarkar, et al., 2011; Zhai and Martinis, 2005). Although there are multiple common *in vitro* methods to study these editing determinants, their quantitative cellular impact is largely unknown. The fluorescent reporter assay described here essentially fills in that void by providing a sensitive *in vivo* tool to quantify the impact of LeuRS edting defects on cell viability.

Chapter VI: A Specific Insert in LeuRS Enhances tRNA-Protein Interactions

VI.1. Introduction

LeuRS is a class I AARS, characterized by a Rossmann dinucleotide binding fold in the synthetic active site. The synthetic active site in class I AARSs is further marked by signature sequences 'HIGH' (Webster, et al., 1984) and 'KMSKS'(Hountondji, et al., 1986). These sequences interact with ATP (Arnez, et al., 1997; Fersht, et al., 1988; Perona, et al., 1993) and stabilize the transition state of the aminoacylation reaction by utilizing ATP binding energy for amino acid activation. Structural studies on TyrRS (Kobayashi, et al., 2005) and TrpRS (Retailleau, et al., 2007) show elaborate energetically favorable conformational flexibility within the mobile KMSKS loop associated with the ATP-dependent activation of amino acid at the synthetic active site.

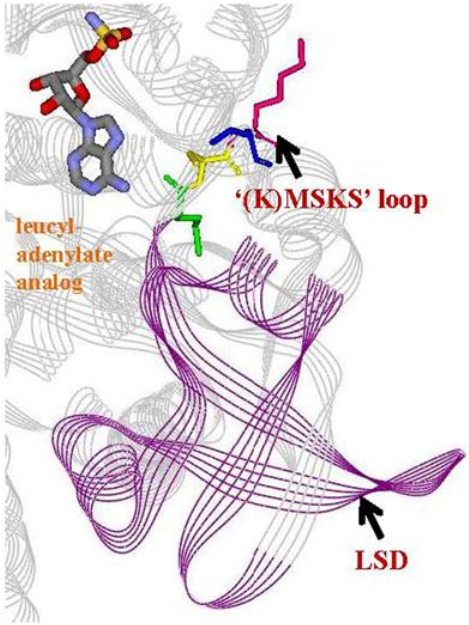

Figure VI.1. *T. thermophilus* LeuRS in complex with 5´-*O*-[*N*-(leucyl)-sulfamoyl] adenosine, a sulfamoyl analog of leucyl adenylate (LeuAMS) in the synthetic active site (Cusack, et al., 2000) (PDB: 1H3N). The LSD is inserted before the catalytically important conserved '(K)MSKS' loop.

The core of the LeuRS main body contains several appendages of varying sizes (Cusack, et al., 2000). Exclusive to LeuRS, a small domain (~50 amino acid), called the leucine-specific domain (LSD) is inserted into the catalytic core just prior to the catalytically important 'KMSKS' loop (Figure VI.1). In *T. thermophilus* LeuRS, the well-ordered LSD is comprised of five β-strands and two α-helices and is positioned at the entrance to the active site. It is connected to the enzyme's main body by flexible β-linkers, suggesting that it can re-orient during distinct stages of the aminoacylation reaction (Cusack, et al., 2000). The crystal structure of the *T. thermophilus* LeuRS in complex with $tRNA^{Leu}$ in the editing conformation shows that the LSD rotates by about 19° upon tRNA binding, although no direct contact with the tRNA has been captured in the editing conformation (Tukalo, et al., 2005). A model of $tRNA^{Leu}$ docked to the *T. thermophilus* LeuRS shows the LSD to be poised to interact with the base of the acceptor stem and the core of the tRNA (Cusack, et al., 2000).

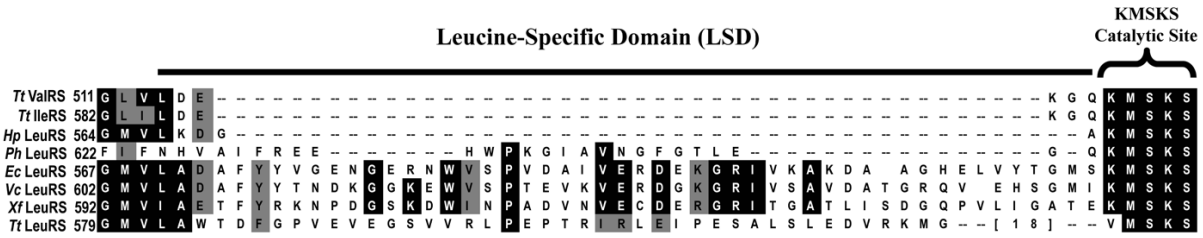

Figure VI.2. Multiple sequence alignment. The leucine-specific domain (LSD) is present in some bacterial LeuRSs, inserted prior to the 'KMSKS' loop, while is completely absent in some bacterial and archaeal LeuRSs. Abbreviations are: *Tt*, *T. thermophilus*; *Hp, H. pylori*; *Ph, Pyrococcus horikoshii*; *Ec, E. coli*; *Vc, Vibrio cholera*; and *Xf, Xylella fastidiosa*.

Although this domain is unique to prokaryote-like LeuRSs, it is neither conserved in sequence nor in length across LeuRSs from different organisms as seen in a multiple sequence alignment (Figure VI.2). While in *E. coli* LeuRS, the LSD is critical to aminoacylation (Vu and Martinis, 2007), some bacterial and archaeal LeuRSs, including the

H. pylori, *B. subtilis*, and *P. horikoshii* LeuRS completely lack the LSD (Figure VI.2). We asked why LeuRS of some organisms evolved to incorporate the LSD while others did not. For this purpose, we constructed a chimeric swap of the *E. coli* LeuRS LSD into the *H. pylori* LeuRS, which completely lacks the domain to result in the chimeric HP-LSD (Figure VI.3). Biochemical analysis of the chimeric *H. pylori* enzyme HP-LSD shows that introduction of the LSD results in tighter *E. coli* $tRNA^{Leu}$ binding and enhances aminoacylation.

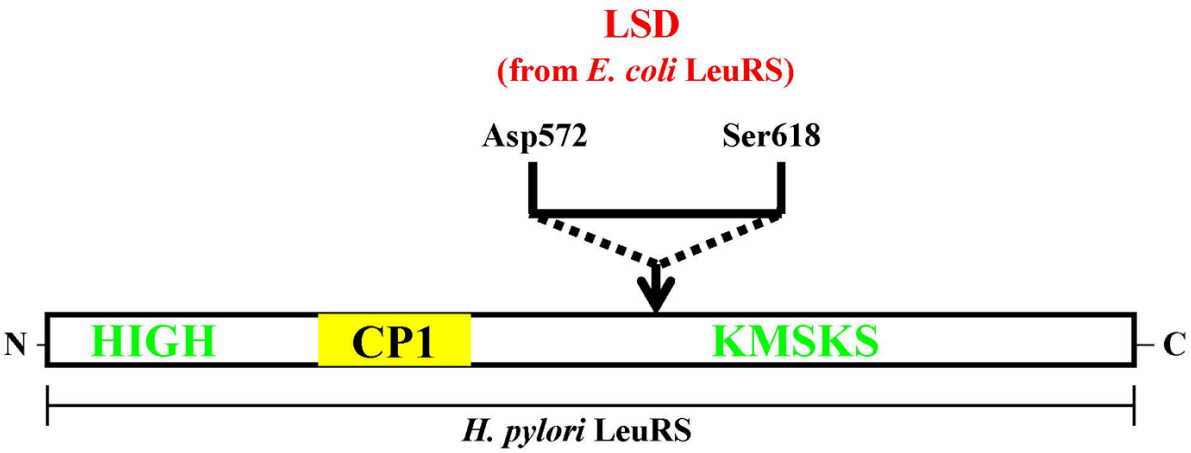

Figure VI.3. Chimeric *H. pylori* LeuRS construct (HP-LSD LeuRS) containing the *E. coli* LSD inserted prior to the 'KMSKS' loop.

VI.2. Experimental methods

VI.2.A. Cloning and plasmid construction

The gene encoding *H. pylori* LeuRS (HPLeuRS) was amplified from the genomic DNA of *H. pylori* J99 via PCR in a 50 μL reaction mixture that contained 17.3 ng of template DNA, 125 ng each of forward and reverse primers containing *Nde*I and *Bam*HI restriction sites, respectively, 0.05 mM dNTP mix and 0.05 U *Pfu* DNA polymerase in commercially available buffer. The amplified PCR product was then subcloned into the vector pET-14b

(Novagen, Gibbstown, NJ) to yield the plasmid pMTV-LeuRSHP3d. The gene encoding *H. pylori* $tRNA^{Leu}_{UAG}$ was also amplified from the genomic DNA of *H. pylori* strain J99 via PCR as described above for the pUC-19 plasmid vector (Thermo Scientific, Glen Burnie, MD) using forward and reverse primers containing *Bam*HI and *Pstn*I restriction sites, respectively, to yield the plasmid ptDNA-HP4.

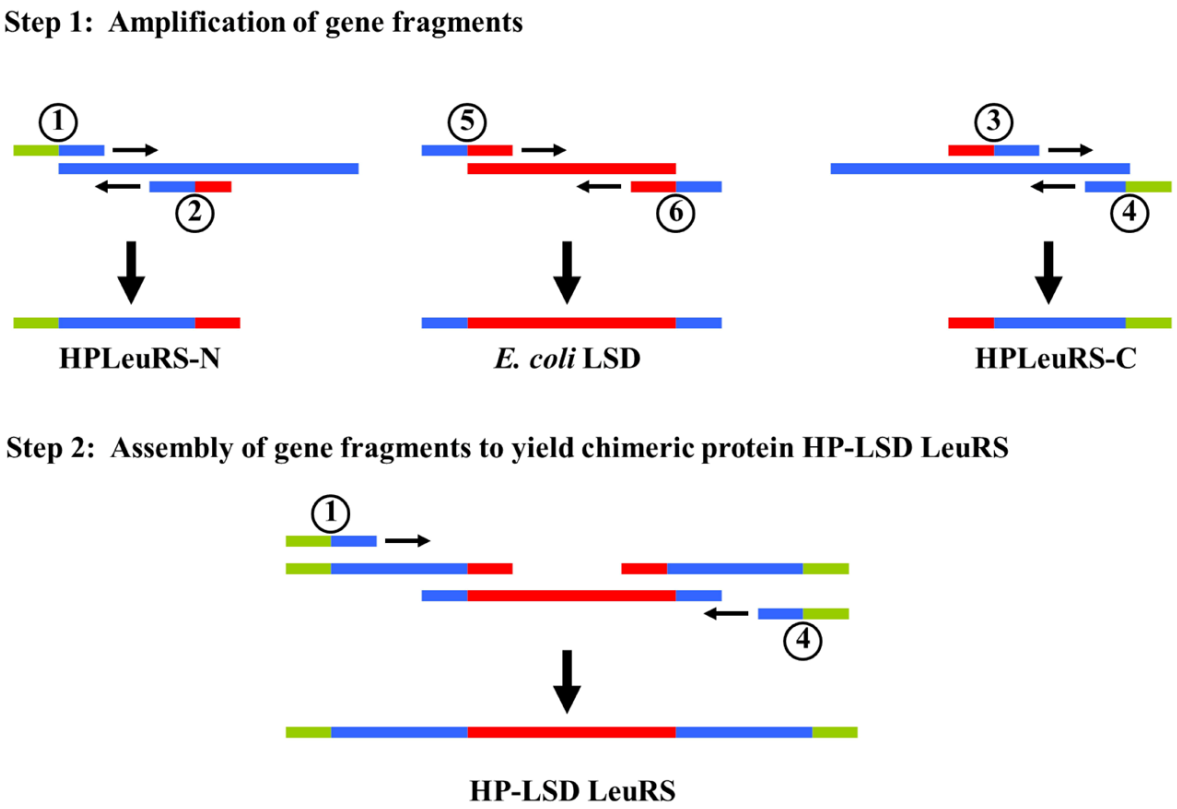

Figure VI.4. Schematic representation of overlap extension PCR (OE-PCR). In step 1, the gene encoding *H. pylori* LeuRS (blue) (HPLeuRS) was used as a PCR template to amplify the gene fragments HPLeuRS-N and HPLeuRS-C, encoding the N and C-terminus of HPLeuRS, respectively and the gene encoding the *E. coli* LeuRS (red) to amplify the gene fragment *E. coli* LSD. The circled numbers denote the primers used. Primers 1 and 4 contain the restriction sites *NdeI* at the 5′ end and *BamHI* at the 3′ end (green), respectively. Primers 2 and 3 contain overlapping DNA sequences of 18 nucleotides with the *E. coli* LeuRS gene segment encoding the LSD. Similarly, primers 5 and 6 contain overlapping sequences with the HPLeuRS gene. In step 2, the three amplified gene fragments are assembled in a PCR reaction with primers 1 and 4 to generate the complete gene fragment HP-LSD LeuRS.

Overlap extension PCR (OE-PCR) (Grandori, et al., 1997) followed by ligation-dependent PCR was used to generate the recombinant gene expressing the chimeric protein HP-LSD LeuRS. This work was performed by Hyeryoung Yoon. In the first step of OE-PCR (Figure VI.4.), in two separate PCR reactions, the gene fragments HPLeuRS-N (encoding the N-terminal half of HPLeuRS) and HPLeuRS-C (encoding the C-terminal half of HPLeuRS) were amplified via PCR using the template pMTV-LeuRSHP3d and primers 1 and 2 and primers 3 and 4 respectively. In a third PCR reaction, the gene fragment *E. coli* LSD (encoding the leucine-specific domain of *E. coli* LeuRS) was also amplified using the template p15ec3-1 (Martinis and Fox, 1997) and the primers 5 and 6. Primers 1 and 4 were designed to include the restriction sites *NdeI* and *BamHI*, respectively. Primer 2 contains overlapping DNA sequence (18 nucleotides) with the 5′ end and primer 3 with the 3′ end of the *E. coli* LeuRS gene segment encoding the LSD. Primers 5 and 6 also contain overlapping DNA sequences of 18 nucleotides with the HPLeuRS gene (Figure VI.4.). Each PCR reaction was set up as described above, except that 100 ng of template DNA was used. Under the following conditions, 30 cycles of PCR were carried out: 95 °C, 1 min; 55 °C, 1 min; 72 °C, 5 min. In the second step of the OE-PCR technique, the amplified gene fragments were joined together via PCR. Pre-amplification was carried out in a reaction mixture containing 500 ng of each of the three amplified gene fragments, HPLSD-N, HPLSD-C and *E. coli* LSD, 0.05 mM dNTP mix and 2.5 U *Pfu* DNA polymerase, without any primer for 5 cycles under similar conditions as mentioned above. This was followed by 35 cycles of PCR with primers 1 and 4 to amplify the full-length HP-LSD LeuRS gene. The amplified full-length HP-LSD LeuRS gene was then made to replace the wild type HPLeuRS gene in the plasmid pMTV-LeuRSHP3d via ligation-dependent PCR, resulting in the plasmid pHPLSD. The reaction mixture included 500 ng of pMTV-LeuRSHP3d and 200 ng of the

full-length recombinant HP-LSD LeuRS gene to act as primer, apart from the other PCR components as described above.

VI.2.B. Expression and purification of proteins

The wild type HPLeuRS and the chimera HP-LSD LeuRS were expressed from the plasmids pMTV-LeuRSHP3d and pHPLSD, respectively in *E. coli* strain BL21 (DE3) codon PLUS. A single transformant was used to inoculate 5 mL LB supplemented with 100 μg/mL Amp and 34 μg/mL Cm, followed by overnight incubation at 37 °C. The overnight culture was used to inoculate 1 L LB (100 μg/mL Amp and 34 μg/mL Cm) and cells were grown at 37 °C until the OD_{600} reached 0.6 to 0.8. Cells were then induced with 1 mM IPTG and the protein was expressed at 37 °C for 3 h. N-terminal six-histidine tagged proteins were purified via Ni-affinity chromatography as described in Chapter II. Final protein concentrations were determined spectrophotometrically at 280 nm using the respective extinction coefficients (146 x 10^3 $M^{-1}cm^{-1}$ for wild type HPLeuRS and 155.62 x 10^3 $M^{-1}cm^{-1}$ for HP-LSD LeuRS) estimated by the ExPASy Protparam tool (http://ca.expasy.org/tools/protparam.html).

VI.2.C. *In vitro* transcription and purification of $tRNA^{Leu}$

The *E. coli* $tRNA^{Leu}_{UAA}$ and the *H. pylori* $tRNA^{Leu}_{UAG}$ were transcribed *in vitro* in a T7 RNA polymerase-dependent reaction from the plasmids $ptDNA^{Leu}$ (Normanly, et al., 1986; Tocchini-Valentini, et al., 2000) and ptDNA-HP4, respectively as described in Chapter II. The concentration of the tRNA was calculated spectrophotometrically on the basis of its extinction co-efficient (840,700 and 817,500 M^{-1} cm^{-1}, for *E. coli* and *H. pylori* tRNA, respectively), as estimated by the online Ambion oligonucleotide calculator (http://www.ambion.com/techlib/misc/oligo_calculator.html).

VI.2.D. Aminoacylation assay

Each aminoacylation reaction contained 60 mM Tris-HCl, pH 7.5, 10 mM $MgCl_2$, 1 mM dithiothreitol (DTT), 4 μM transcribed $tRNA^{Leu}$, 21 μM [^{3}H]-leucine (150 μCi/mL) and 100 nM enzyme. Each reaction was initiated with 4 mM ATP. The assay was performed as described in Chapter II.

VI.2.E. Isolation of mischarged Ile-$tRNA^{Leu}$

Misaminoacylation of 8 μM *H. pylori* $tRNA^{Leu}$ with isoleucine was carried out by incubating the tRNA transcript with 60 mM Tris, pH 7.5, 10 mM $MgCl_2$, 1 mM DTT, 23 μM [^{3}H]-isoleucine (300 μCi/mL), 1 μM editing defective *E. coli* LeuRS and 4 mM ATP at 25 °C for 3 h. The mischarged tRNA was isolated as described in Chapter II.

VI.2.F. Post-transfer editing deacylation assay

Deacylation reaction mixtures contained 60 mM Tris, pH 7.5, 10 mM $MgCl_2$ and approximately 2 μM [^{3}H]-Ile-*H. pylori* $tRNA^{Leu}$. The reactions were initiated with 1 μM enzyme and were carried out at 25 °C as described in Chapter II.

VI.2.G. Leucine-dependent ATP/PP_i exchange assay

The assay was carried out as described in Chapter II. Reaction mixtures containing 50 mM Tris-HCl, pH 7.5, 10 mM $MgCl_2$, 1 mM DTT, 1 mM [^{32}P]-PP_i (100 μCi/mL), 1 mM ATP, and 1 mM leucine were initiated with 1 μM enzyme.

VI.2.H. Nitrocellulose filter binding assay

Binding of *E. coli* $tRNA^{Leu}_{UAA}$ to the wild type HPLeuRS and to the chimeric HP-LSD LeuRS were assessed in 50 μL reaction mixtures containing 60 mM Tris, pH 7.5, 10 mM $MgCl_2$, 1 mM dithiothreitol (DTT), 20 μM leucine, 0.1 μM 5′-[^{32}P]-labeled *E. coli* $tRNA^{Leu}_{UAA}$ and enzyme concentrations ranging from 0.1 to 10 μM for wild type HPLeuRS and 0.1 to 4 μM for HP-LSD LeuRS. The reactions were incubated at 37 °C for 8 min and quenched by spotting the entire 50 μL on a nitrocellulose membrane (Whatman, Dassel, Germany), pre-soaked in non-specific RNA (1 mg/mL) for 1 h and then assembled on a MINIFOLD-1 Spot Blot apparatus (Schleicher and Schuell, Keene, NH). The spots on the nitrocellulose membrane were washed with 200 μL of binding buffer (60 mM Tris, pH 7.5, 10 mM $MgCl_2$, 1 mM DTT) to remove any tRNA that is not bound to protein. The nitrocellulose membrane was phosphorimaged and radiolabeled products visualized and quantified as described in Chapter II.

VI.3. Results and Discussion

Many prokaryote-like LeuRSs bear the unique LSD insert of about 50 amino acids immediately prior to the catalytically important 'KMSKS' loop in the catalytic domain. Some bacterial and archaeal LeuRSs do not possess this insertion domain, including *H. pylori, B. subtilis* as well as *P. horikoshii* LeuRSs. Although the LSD has been shown to be critical to aminoacylation, it still remains unclear as to why some LeuRSs evolved to acquire this domain, whereas others did not. To gain better insight into the functional role of the LSD and its evolutionary advantage, we designed a chimeric swap of the *E. coli* LeuRS LSD into the *H. pylori* LeuRS, which lacks the domain altogether. Thus, we introduced the *E. coli* LeuRS LSD just upstream of the conserved 'KMSKS' sequence (Figure VI.3).

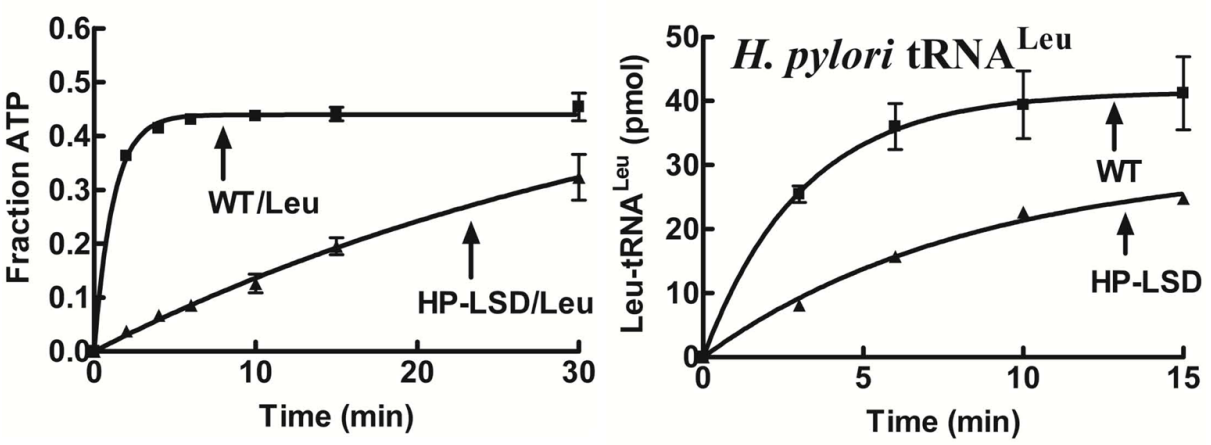

Figure VI.5. Enzymatic activities of chimeric *H. pylori* (HP-LSD) and wild type (WT) LeuRS. (Left) Activation of leucine. ATP/PPi exchange reactions were carried out with 1 mM leucine, 1 mM [^{32}P]-PP_i (100 μCi/mL), 1 mM ATP, and initiated with 1 μM enzyme. (Right) Aminoacylation of *H. pylori* $tRNA^{Leu}$. Reactions containing 4 μM transcribed *H. pylori* $tRNA^{Leu}$, 21 μM [^{3}H]-leucine (150 μCi/mL) and 100 nM enzyme were initiated with 4 mM ATP. Symbols are: (■) wild type (WT) *H. pylori* and (▲) chimeric HP-LSD LeuRS. Error bars for each time point result from each reaction repeated in triplicate.

The chimeric *H. pylori* LeuRS bearing the *E. coli* LSD (HP-LSD LeuRS) is active in leucine activation (Figure VI.5, left) and in aminoacylating the *H. pylori* $tRNA^{Leu}$ (Figure VI.5, right), albeit with less efficiency as compared to the wild type *H. pylori* LeuRS. However, HP-LSD LeuRS can hydrolyze mischarged *H. pylori* $tRNA^{Leu}$ similar to the wild type *H. pylori* LeuRS (Figure VI.6), suggesting that the LSD critically impacts aminoacylation activity, but not editing activity. This is consistent with the analysis of LSD mutants where deletion of the domain abolished aminoacylation by *E. coli* LeuRS (Vu and Martinis, 2007).

We tested LSD-dependent tRNA specificity by incorporating *E. coli* $tRNA^{Leu}$ transcript into aminoacylation reaction of the chimeric HP- LSD LeuRS. The insertion of the *E. coli* LeuRS LSD clearly stimulated aminoacylation of the chimeric enzyme compared to the wild type *H. pylori* LeuRS (Figure VI.7). The k_{cat}/K_M of HP-LSD LeuRS (5.2 $\mu M^{-1}sec^{-1}$) was increased 3-fold over the wild type *H. pylori* LeuRS (1.9 $\mu M^{-1}sec^{-1}$) for the *E. coli* $tRNA^{Leu}$ due to a decrease in K_M (Table VI.1). We also measured the K_D of *E. coli* $tRNA^{Leu}$

binding, which was 5-fold tighter for the chimeric HP-LSD LeuRS (1.2 μM) compared to the wild type *H. pylori* LeuRS (5.6 μM) (Figure VI.8, Table VI.1), suggesting significantly tighter enzyme-*E. coli* $tRNA^{Leu}$ binding interactions in presence of the LSD that originated from *E. coli* LeuRS.

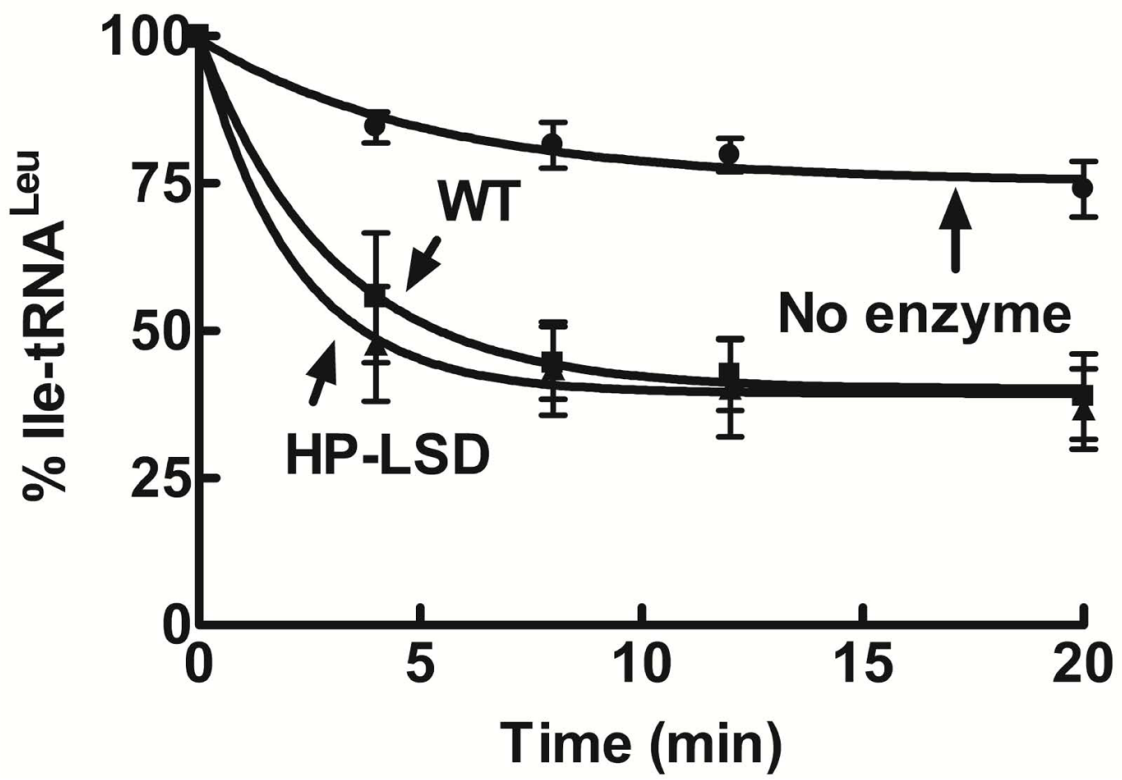

Figure VI.6. Deacylation activity of wild type and chimeric *H. pylori* LeuRSs. Hydrolysis of approximately 2 μM [^{3}H]-Ile-*H. pylori* $tRNA^{Leu}$ was initiated with 1 μM enzyme. Symbols are: (●) no enzyme; (■) wild type (WT) *H. pylori*; and (▲) chimeric HP-LSD LeuRS. Each reaction was measured in triplicate.

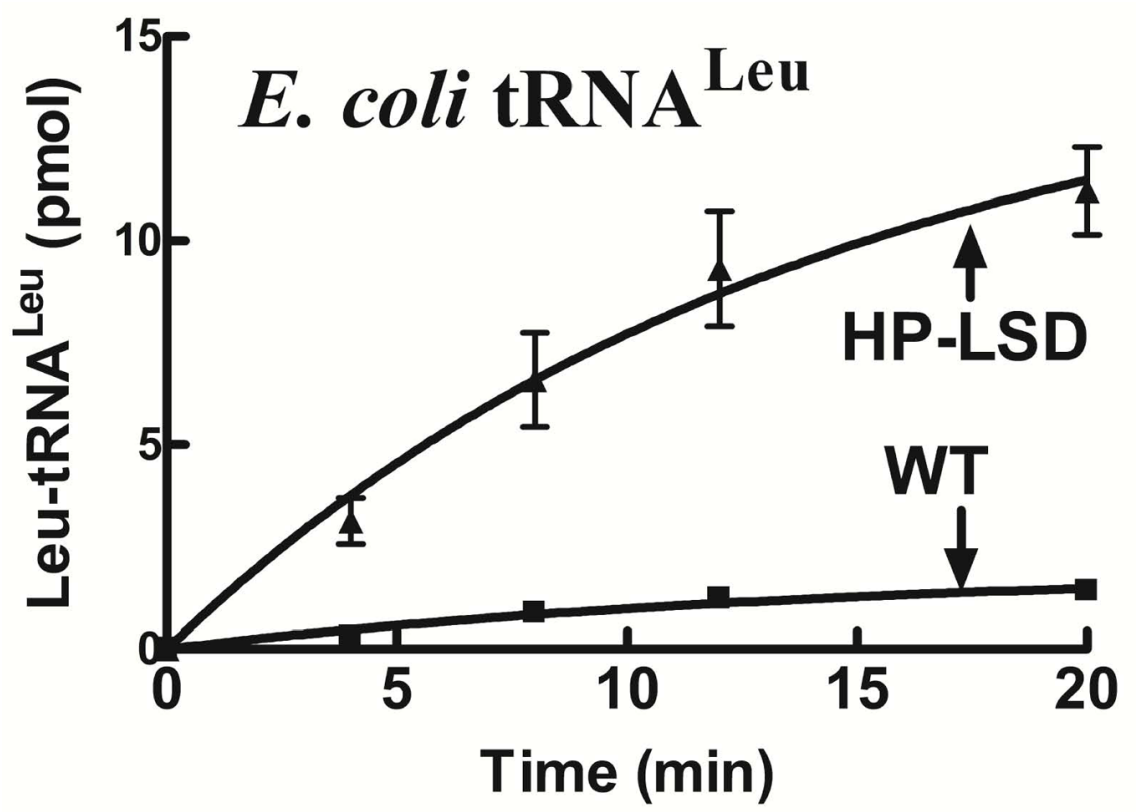

Figure VI.7. Aminoacylation of *E. coli* $tRNA^{Leu}$ by wild type and chimeric *H. pylori* LeuRSs. Reactions containing 4 μM transcribed $tRNA^{Leu}$, 21 μM [^{3}H]-leucine (150 μCi/mL) and 100 nM enzyme were initiated with 4 mM ATP. Symbols are: (■) wild type (WT) *H. pylori* and (▲) chimeric HP-LSD LeuRS. Error bars for each time point result from each reaction repeated in triplicate.

Based on our biochemical analysis, we hypothesize that the LSD enhances LeuRS-$tRNA^{Leu}$ interactions and binding and this provides an advantage in aminoacylating $tRNA^{Leu}$. The LSD was inserted in LeuRSs from some organisms, most likely to confer an advantage to tRNA recognition and thus catalysis. Although crystal structures for *P. horikoshii* and *T. thermophilus* LeuRS to date have failed to capture any direct contact between the LSD and the tRNA, a model of $tRNA^{Leu}$ docked to *T. thermophilus* LeuRS suggests LSD interactions with the base of the acceptor stem (Cusack, et al., 2000). Thus, it is possible the domain has important interactions to stabilize the 3´ end of $tRNA^{Leu}$ during a transient stage of the aminoacylation reaction. This might include substrate-binding, tRNA translocation and/or product release.

Table VI.1. Apparent aminoacylation kinetic parameters and binding constants of *E. coli* $tRNA^{Leu}$*

Enzyme	K_M (μM)	k_{cat} (sec^{-1})	k_{cat}/K_M ($\mu M^{-1}sec^{-1}$)	K_D (μM)
WT	1.1 ± 0.2	2.0 ± 0.01	1.9 ± 0.3	5.6 ± 1.0
HP-LSD	0.4 ± 0.05	1.8 ± 0.3	5.2 ± 1.7	1.2 ± 0.2

* $tRNA^{Leu}$ transcript concentrations ranged from 0.025 to 16 μM in aminoacylation reactions, and from 0.4 to 10 μM in binding assays.

In fact, the most recently solved *E. coli* LeuRS-$tRNA^{Leu}$ co-crystal structure (Palencia, 2012) captures direct interaction between the LSD and $tRNA^{Leu}$ in the editing conformation. This direct interaction is however lost when the enzyme transitions from the editing to the aminoacylation conformation, due to a major rotation of the LSD towards the synthetic active site.

In addition, the LSD may also impact the mobility of the neighboring catalytically critical 'KMSKS' loop (Vu and Martinis, 2007). The role of the mobile 'KMSKS' loop in amino acid activation and aminoacylation has been extensively studied in the class I synthetases, TyrRS (Kobayashi, et al., 2005), TrpRS (Retailleau, et al., 2007) and more recently in LeuRS (Palencia, 2012). The 'KMSKS' loop that directly interacts with $tRNA^{Leu}$ moves as an integral part of the LSD when the latter rotates during transition of LeuRS from the editing to the aminoacylation conformation. This movement brings the 'KMSKS' loop closer to the aminoacylation active site, enabling more intimate interactions with the $tRNA^{Leu}$ acceptor stem. These interactions between the 'KMSKS' loop and the tRNA optimally position the tRNA for transfer of the aminoacyl moiety. Furthermore, comparison of aminoacylation and editing structures of LeuRS-$tRNA^{Leu}$ reveals the 'KMSKS' loop to be in a relatively open or relaxed state in the editing conformation.

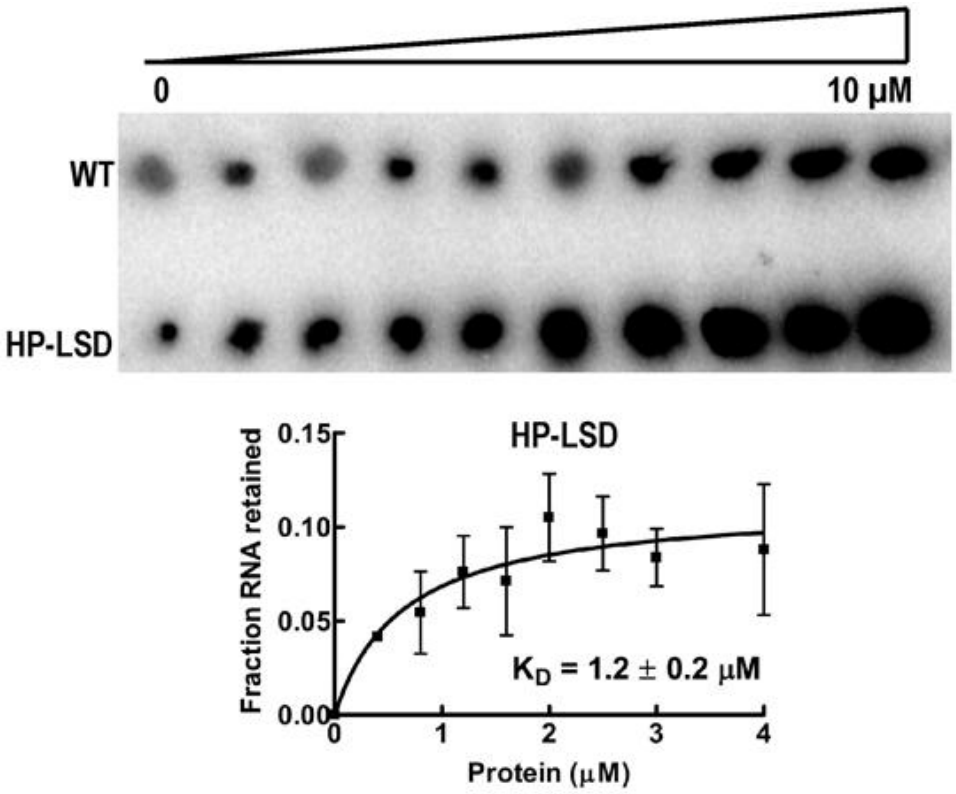

Figure VI.8. Binding of *E. coli* $tRNA^{Leu}$ to wild type or chimeric *H. pylori* LeuRS. (Top) Phosphorimage of a representative nitrocellulose membrane showing tRNA:protein complex formation when protein concentrations were varied from 0 to 10 µM. The chimeric HP-LSD LeuRS showed greater amount of complex formation with *E. coli* $tRNA^{Leu}$ than the wild type *H. pylori* LeuRS. (Bottom) Binding curve for the chimeric HP-LSD LeuRS. Error bars for each time point result from each reaction repeated in triplicate.

The crystal structure of the *E. coli* TyrRS catalytic domain in complex with tyrosine and a tyrosine adenylate analog has captured extensive local induced-fit local conformational changes. These conformational changes span over the flexible 'KMSKS' loop and within the substrate-binding pock. Such local flexibility is the basis for stabilizing ATP-binding and using the ATP-binding energy to activate amino acid (Kobayashi, et al., 2005). The events captured in this ensemble of snapshots include: tyrosine binding at the active site in the 'open' conformation of the KMSKS loop; ATP-binding at the active site inducing a transition of the KMSKS loop to the 'semi-open' conformation; adenylate formation in the 'closed' conformation of the KMSKS loop; the KMSKS loop reverting to the 'semi-open' conformation to allow entry of the 3′-end of the tRNA for transfer of the aminoacyl moiety,

because in the ‘closed’ conformation of the KMSKS loop, the 3′-adenosine of the tRNA cannot reach the catalytic site.

Thermodynamic calculations in the *B. stearothermophilus* TrpRS reveal modest enthalpy changes, consistent with the idea of entropy-driven ATP binding accompanying the induced-fit assembly at the substrate-binding site (Retailleau, et al., 2007). The same study also highlights the criticality of movements in the KMSKS loop in stabilization of transition state during the aminoacylation reaction.

The flexible LSD of LeuRS could assist in facilitating conformational changes of the KMSKS loop that are critical to aminoacylation. It is highly plausible that coordinated movements of the LeuRS LSD and the KMSKS loop not only orchestrate substrate binding for catalysis but also induce more intimate inertactions with $tRNA^{Leu}$.

Chapter VII: The Yeast Mitochondrial Leucyl-tRNA Synthetase CP1 Domain has Functionally Diverged to Accommodate RNA Splicing at the Expense of Hydrolytic editing

This research was originally published in J. Biol. Chem.

Jaya Sarkar, Kiranmai Poruri, Michal T. Boniecki, Katherine K. McTavish, and Susan A. Martinis. The yeast mitochondrial leucyl-tRNA synthetase CP1 domain has functionally diverged to accommodate RNA splicing at the expense of hydrolytic editing. *J. Biol. Chem.* 2012; doi:10.1074/jbc.M111.322412.

VII.1. Introduction

The diverse family of aminoacyl tRNA-synthetases (AARSs) have been recruited to host alternate activities in the cell (Lambowitz and Perlman, 1990; Martinis, et al., 1999) in addition to their housekeeping function in protein synthesis (Ibba and Söll, 2000). This includes aiding splicing of group I introns in the mitochondria, which is essential to certain lower eukaryotes. Two fungal mitochondrial AARSs, leucyl-tRNA synthetase (LeuRS or NAM2p) (Herbert, et al., 1988; Labouesse, et al., 1985; Labouesse, 1990) and tyrosyl-tRNA synthetase (TyrRS or CYT-18p) (Akins and Lambowitz, 1987; Paukstelis and Lambowitz, 2008) are required splicing factors to facilitate splicing of group I introns in *Neurospora crassa* and *Saccharomyces cerevisiae* respectively.

Yeast mitochondrial LeuRS (ymLeuRS) was originally implicated in group I intron splicing when suppressor mutations in LeuRS rescued RNA processing in the absence of a functional bI4 maturase (Labouesse, et al., 1987). In addition to the bI4 maturase (De La Salle, et al., 1982; Labouesse, et al., 1984) and also Mss116p (Huang, et al., 2005), LeuRS aids splicing of the related bI4 and aI4α group I introns from the mitochondrial genes encoding cytochrome b (*cob*) and the α subunit of cytochrome oxidase (*cox1α*). We have demonstrated that LeuRS and bI4 maturase bind independently to the bI4 intron and stimulate

RNA splicing (Rho and Martinis, 2000). However, the mechanistic details of how LeuRS promotes splicing remain unclear.

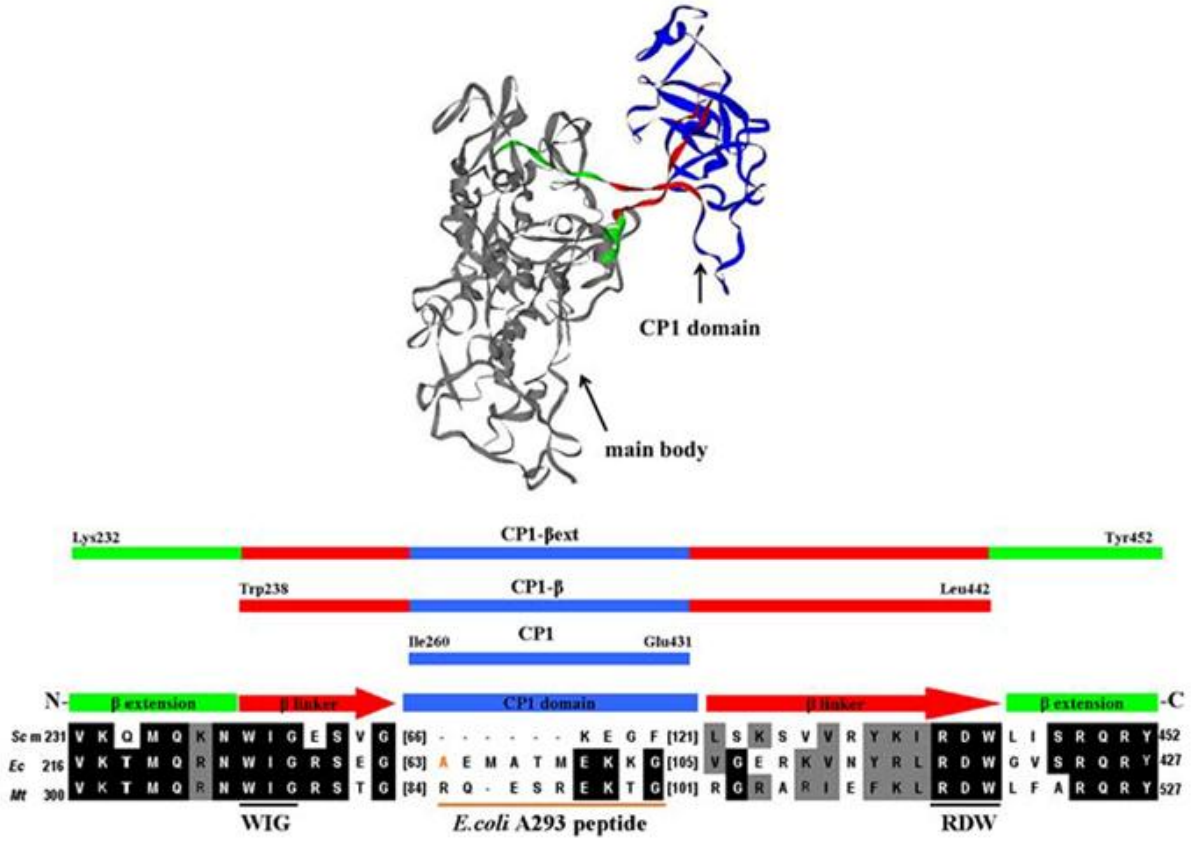

Figure VII.1. Primary and tertiary structure of the LeuRS CP1 domain. (Top) Homology model of ymLeuRS (Rho, et al., 2002). (Bottom) Multiple sequence alignment of LeuRS CP1 domain and flanking regions containing both the N and C-terminal β-strand linkers and extensions. The CP1 domain, β-strand linkers and β-strand extensions are shown in blue, red and green respectively. Bracketed numbers indicate the number of amino acids of a peptide insert. The *E. coli* LeuRS A293 residue (Li, et al., 1999; Williams and Martinis, 2006) is highlighted in orange and the corresponding peptide by an orange line. It is absent in the ymLeuRS. Each of the yeast mitochondrial CP1 domain constructs are indicated at the top of the figure as follows: CP1 (Ile260 to Glu431), CP1-β (Trp238 to Leu442) and CP1-βext (Lys232 to Tyr452). Abbreviations are: *Saccharomyces cerevisiae* mitochondrial (*Sc*m), *Escherichia coli* (*Ec*) and *Mycobacterium tuberculosis* (*Mt*).

The connective polypeptide 1 (CP1) domain (Hou, et al., 1991; Starzyk, et al., 1987) of LeuRS have been proposed to play a role in RNA splicing (Hsu, et al., 2006; Rho, et al., 2002). The approximately 170 amino acid CP1 insertion splits the ATP-binding Rossmann fold that characterizes the aminoacylation active site of class I AARSs (Hou, et al., 1991) and folds discretely into a separate domain. The CP1 domain is connected to the rest of the

enzyme via two flexible β-strands (Figure VII.1) (Cusack, et al., 2000). Although the LeuRS CP1 domain is best known for its role in proofreading or editing misacylated $tRNA^{Leu}$ (Betha, et al., 2007; Boniecki, et al., 2008), genetic rescue experiments identified splicing sensitive sites within and around the CP1 domain (Labouesse, et al., 1987; Li, et al., 1996). We had also shown that the isolated CP1 domain from ymLeuRS stimulated bI4 intron RNA splicing *in vivo* (Rho, et al., 2002).

Herein, we utilized a LeuRS-dependent *in vitro* splicing assay (Boniecki, et al., 2009) to isolate and characterize molecular determinants within the ymLeuRS CP1 domain and the connecting β-strands that directly impact splicing. We show how the LeuRS CP1 domain adapted to and functionally diverged to accommodate its dual essential activities in aminoacylation and splicing. In some cases, LeuRS adaptations for splicing appear to have evolved at some expense to the enzyme's housekeeping function in aminoacylation.

VII.2. Experimental methods

VII.2.A. Cloning, mutagenesis and plasmid construction

The plasmid pBETeCP1-2-35 (Betha, et al., 2007) contains the gene fragment encoding the CP1 domain of *E. coli* LeuRS and was used for *in vitro* expression of the protein ecCP1-βext LeuRS. The ymLeuRS gene fragment encoding the ymCP1-β LeuRS fragment was amplified in a 50 μL polymerase chain reaction (PCR) that contained 100 ng of pYM3-17 (Rho and Martinis, 2000) template plasmid DNA, 125 ng each of forward [ymCP1-β-Fwd(*Nde*I)(W238-L442)] and reverse [ymCP1-β-Rev(*Bam*HI)(W238-L442)] primer containing the *Nde*I and *Bam*HI restriction sites respectively, 0.05 mM dNTP mix and 0.05 U *Pfu* DNA polymerase in commercial buffer. The PCR products were digested with *Nde*I and *Bam*HI at 37 °C for 6 h. The restriction-digested PCR products were separated on a 1% agarose gel and gel-purified using the QIAquick gel extraction kit-250 (Qiagen Inc). The

vector pET-14b (Novagen, Gibbstown, NJ) was also cleaved with *Nde*I and *Bam*HI, followed by gel-extraction. Gel purified restriction digests of the PCR amplified gene fragment and the vector were ligated using T4 DNA ligase at 37 °C for 15 min to yield the plasmid p14MBymCP1+N+C(RDWL). The ligation reaction was used to transform *E. coli* strain DH5α. Plasmid DNA was isolated from a 3 mL overnight culture of a single transformant using the QIAprep Spin mini prep kit-250 (Qiagen Inc).

The plasmid p14MBymCP1+N+C(RDWL) was used as template to generate the plasmid p14JSymCP1-βext, encoding the LeuRS protein fragment ymCP1-βext. This site directed PCR-based insertion mutagenesis used primers ymCP1-βext-Cter-Fwd-(W238-R449), ymCP1-βext-Cter-Fwd-(W238-Y452), ymCP1-βext-Nter-Fwd-(Q235-Y452) and ymCP1-Nter-βext-Fwd-(K232-Y452). Mutations were introduced into the template plasmid as described above via PCR. The final PCR mixture was restriction digested with 0.8 U *Dpn*I for 4 h at 37 °C and then used to transform *E. coli* strain DH5α. The plasmid p14JSymCP1-βext, was used as template to introduce the W238C point mutation with primer ymCP1-βext-Fwd-(W238C) to generate plasmid p14JSymW238C-CP1-βext, encoding the ymCP1-βext LeuRS that contained a W238C mutation. Likewise, the wild type full length ymLeuRS encoding plasmid pYM3-17 (Rho and Martinis, 2000) was used as template to generate the plasmids pEXW238A, pEXW238C, pEXW238F and pEXW238Y, encoding the mutant proteins W238A, W238C, W238F and W238Y full length ymLeuRSs. Mutations were confirmed by DNA sequencing (UIUC Core Sequencing Facility, Urbana, IL or Seq Wright, Houston, TX).

For *in vivo* studies in yeast strains HM410 and HM402 (Li, et al., 1992; Seraphin, et al., 1987) the plasmid pKIRAN (Karkhanis, et al., 2006) and ymLeuRST (Houman, et al., 2000) were used to express wild type *E. coli* LeuRS and wild type ymLeuRS proteins, respectively. Both these plasmids contain a constitutive ADH promoter along with a 5′ tag

encoding a mitochondrial import sequence and also a TRP marker for their selection in the HM410 and HM402 yeast strains. The plasmid ymLeuRST was used in site directed PCR mutagenesis to generate the plasmids pMPW238A, pMPW238C, pMPW238F and pMPW238Y.

VII.2.B. *In vitro* transcription of yeast mitochondrial $tRNA^{Leu}$

Yeast mitochondrial $tRNA^{Leu}_{UAA}$ ($ymtRNA^{Leu}$) was transcribed from the plasmid $pymtDNA^{Leu}$ (Rho and Martinis, 2000) as described in Chapter II. The concentration of the tRNA was calculated spectrophotometrically on the basis of its extinction co-efficient (Table VII.1) as estimated by the online Ambion oligonucleotide calculator (http://www.ambion.com/techlib/misc/oligo_calculator.html).

VII.2.C. Precursor RNA Transcription

Plasmid pM96Δhj1-3 (Boniecki, et al., 2009) encodes the gene for the shortest bI4 intron deletion mutant, bI4Δ1168 precursor RNA (pre-RNA), that has been shown to be catalytically active *in vitro*. A custom made RNA ladder, ranging from 250 to 50 base pairs (Boniecki, et al., 2009) was used for analyzing the splicing products by gel electrophoresis. Plasmids pUC8MB-250, pUC8MB-200, pUC8MB-150, pUC8MB-100 and pUC8MB-50 (Boniecki, et al., 2009) encode specific RNAs ranging from 250-50 base pairs. Each plasmid was isolated from *E. coli* strain DH5α using a QIAGEN Plasmid Mega Prep kit-25 (Qiagen Inc). The isolated DNA was then restriction digested using 50 U *Bam*HI for the bI4Δ1168 RNA or *Sal*I for the ladder RNAs, overnight, at 37 °C. RNA was transcribed from the respective restriction digested DNA template using the MEGAscript T7 transcription kit (Ambion Inc., Austin, TX). Transcription reactions were carried out using 1 μg template

DNA in a 20 μL reaction mixture, at 37 °C, for 4 h, according to manufacturer's protocol. The transcribed RNA was radiolabeled by including 10 μCi [α-^{32}P]-UTP in the transcription

Table VII.1. Extinction Coefficients of protein and RNA

Protein/RNA	Extinction Coefficient (x 10^3 $M^{-1}cm^{-1}$)
ymtRNA$^{Leu}_{UAA}$	878.5[a]
bI4Δ1168 pre-RNA	4275.8[a]
Wild type ymLeuRS	145.48 [b]
W238X ymLeuRSs	139.23 [b]
ymCP1-β	24.20 [b]
ymCP1-βext	25.44 [b]
W238C ymCP1-βext	19.94 [b]
Wild type *E. coli* LeuRS	166.17 [b]
E. coli CP1-βext	39.55 [b]
N-terminal GST-tagged bI4 maturase	98.7[b]
N-terminal GST-cleaved bI4 maturase	55.8[b]

[a]Calculated by Ambion oligonucleotide calculator (http://www.ambion.com/techlib/misc/oligo_calculator.html)
[b]Calculated by ExPASy Protparam (http://ca.expasy.org/tools/protparam.html).

reaction. The bI4Δ1168 pre-RNA was isolated on Chroma Spin+TE-200 columns (Clontech, Mountain View, CA). RNA concentration was estimated spectrophotometrically, based on its extinction co-efficient, calculated by the online Ambion oligonucleotide calculator (http://www.ambion.com/techlib/misc/oligo_calculator.html) (Table VII.1). The bI4Δ1168 pre-RNA was folded *in vitro*, in the presence of 1 mM $MgCl_2$, at 50 °C for 2 min, followed by cooling at 32 °C for 10 min. The ladder RNAs were isolated by

phenol:chloroform:isoamyl alcohol [125:24:1] extraction, followed by ethanol precipitation. The recovered RNA pellet was washed with 70% ethanol, vacuum dried and then dissolved in 50-100 µL nuclease-free water (Ambion Inc., Austin, TX). A 2 µL aliquot of each RNA was visualized on denaturing analytical polyacrylamide gel to ensure successful transcription (Figure VII.2).

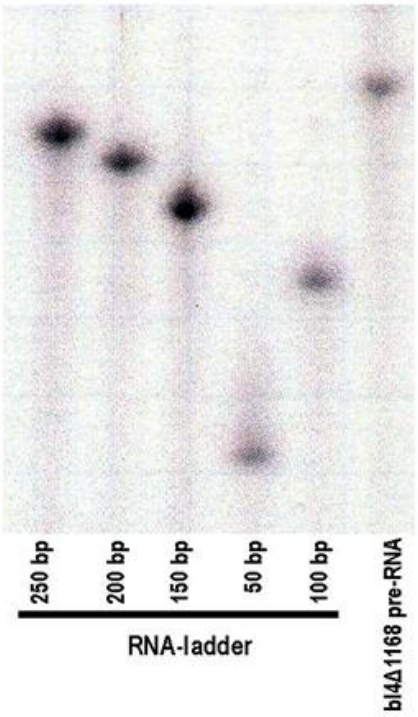

Figure VII.2. T7 RNA polymerase-based transcription of bI4Δ1168 pre-RNA and a custom-made RNA ladder ranging from 50 to 250 base pairs (bp).

VII.2.D. *In vitro* expression and purification of N-terminal six histidine-tagged proteins

Wild type and mutant proteins were expressed from their respective plasmids in *E. coli* strain BL21 (DE3) codon PLUS as described in Chapter II, except that both the buffers HAI and HAII contained 50 mM and 250 mM KCl, respectively. The final protein concentrations were determined spectrophotometrically at 280 nm using the respective

extinction coefficients, estimated by the ExPASy Protparam tool (http://ca.expasy.org/tools/protparam.html). (Table VII.1).

VII.2.E. *In vitro* expression and purification of GST-tagged bI4 maturase ptotein

The gene sequence encoding N-terminal GST-tagged bI4 maturase in the plasmid pGEX2T-MAT2 (Delahodde, et al., 1989) was corrected for a missing asparagine residue (Asn253) at the C-terminus of the bI4 maturase protein sequence, in a PCR reaction using the forward (Flong-fixN253) and reverse (Rlong-fixN253) primers to result in the final plasmid pGEX2T-MAT2-bI4matfix, which encodes the N-terminal GST-tagged bI4 maturase protein with a thrombin cleavage site at the junction of the GST tag and the N-terminus of the bI4 maturase protein.

E. coli strain Rosetta (DE3) was transformed with the plasmid pGEX2T-MAT2-bI4matfix and a single transformant used to inoculate 3 mL LB supplemented with 100 μg/mL Amp and 34 μg/mL Cm and then incubated at 37 °C overnight. In order to find out the optimal conditions for protein expression, the overnight culture was used to inoculate small 3 mL LB with antibiotics, cells grown at 37 °C until the OD_{600} reached 0.6 to 0.8, followed by induction with 0.5 or 1 mM IPTG. Expression was allowed for 45 min, 2 h, 4 h or overnight at room temperature or overnight at 37 °C. Cells were harvested by centrifugation in a table-top centrifuge, resuspended in 1X phosphate buffered saline (PBS; 140 mM NaCl, 10 mM Na_2HPO_4 and 1.8 mM KH_2PO_4), followed by cell lysis by sonication. The soluble fraction was separated from the cell debris or insoluble fraction by centrifugation. SDS-PAGE analysis of the soluble and the insoluble fractions (Figure VII.3) showed that optimal expression conditions for the N-terminal GST-tagged bI4 maturase protein was induction of protein expression with 1 mM IPTG, followed by expression at room temperature for 4 h to overnight.

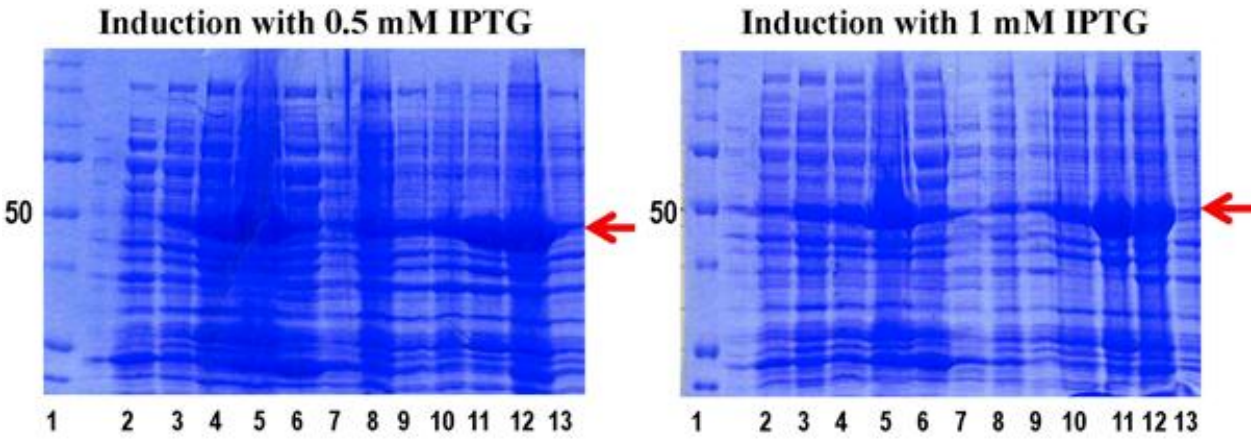

Figure VII.3. SDS-PAGE analysis of small scale expression of N-terminal GST-tagged bI4 maturase. (Left) Induction of protein expression with 0.5 mM IPTG. (Right) Induction of protein expression with 1 mM IPTG. The 56 kD bI4 maturase expression on the gel has been highlighted by red arrows. Lanes are: On both gels, lanes 2 to 7 contain soluble fractions and lanes 8 to 13 contain insoluble fractions of the cell lysate. Lane 1 corresponds to protein ladder, with the 50 kD band marked; (2 and 8), (3 and 9), (4 and 10), (5 and 11), and (6 and 12) correspond to protein expression for 45 min, 2 h, 4h, overnight at room temperature, and overnight at 37 °C, respectively; (7 and 13) correspond to non-induced.

The optimal conditions deduced from the small scale expression were used to express bI4 maturase on a large scale (4 x 0.5 L LB containing antibiotics). Cells were induced with 1 mM IPTG and protein expressed at room temperature for 5 h. Harvested cell pellets were resuspended in 1X PBS containing 1 mg/mL hen egg white lysozyme (Sigma-Aldrich, St Louis, MO), incubated on ice for 30 min followed by brief sonication. The cell lysate was centrifuged at 12,000 rpm for 30 min at 4 °C. The protein-containing supernatant was mixed with 4 mL of glutathione-agarose beads in water, pre-equilibrated with 1X PBS. Protein binding was allowed at 4 °C for 4 h. The protein-bound glutathione-agarose resin was washed with 30 mL 1X PBS and the GST-tagged bI4 maturase protein (56 kD) was eluted from the resin in four 1 mL fractions with 1X PBS containing 10 mg/mL (33 mM) glutathione in 50 mM Tris-HCl, pH 9.0 to 10.0 (Figure VII.4., left). Alternately, in order to isolate N-terminal GST-cleaved bI4 maturase (30 kD), the protein-bound glutathione-agarose resin was incubated with 20 U of thrombin protease in 2 mL buffer (10 mM tris-HCl, pH 7.5,

100 mM NaCl, 5 mM $MgCl_2$, 1 mM EDTA and 30% glycerol) with gentle rocking at room temperature overnight. The N-terminal GST-cleaved bI4 maturase-containing supernatant was collected and analyzed by SDS-PAGE to show the band corresponding to the protein (Figure VII.4, right). The GST tag (26 kD) bound to the glutathione-agarose resin was finally eluted by incubating the resin with 1 X PBS containing 10 mg/mL (33 mM) glutathione (Figure VII.4, right). In each case, protein concentration was measured spectrophotometrically at 280 nm using extinction coefficient as estimated by the ExPASy Protparam tool (http://ca.expasy.org/tools/protparam.html).

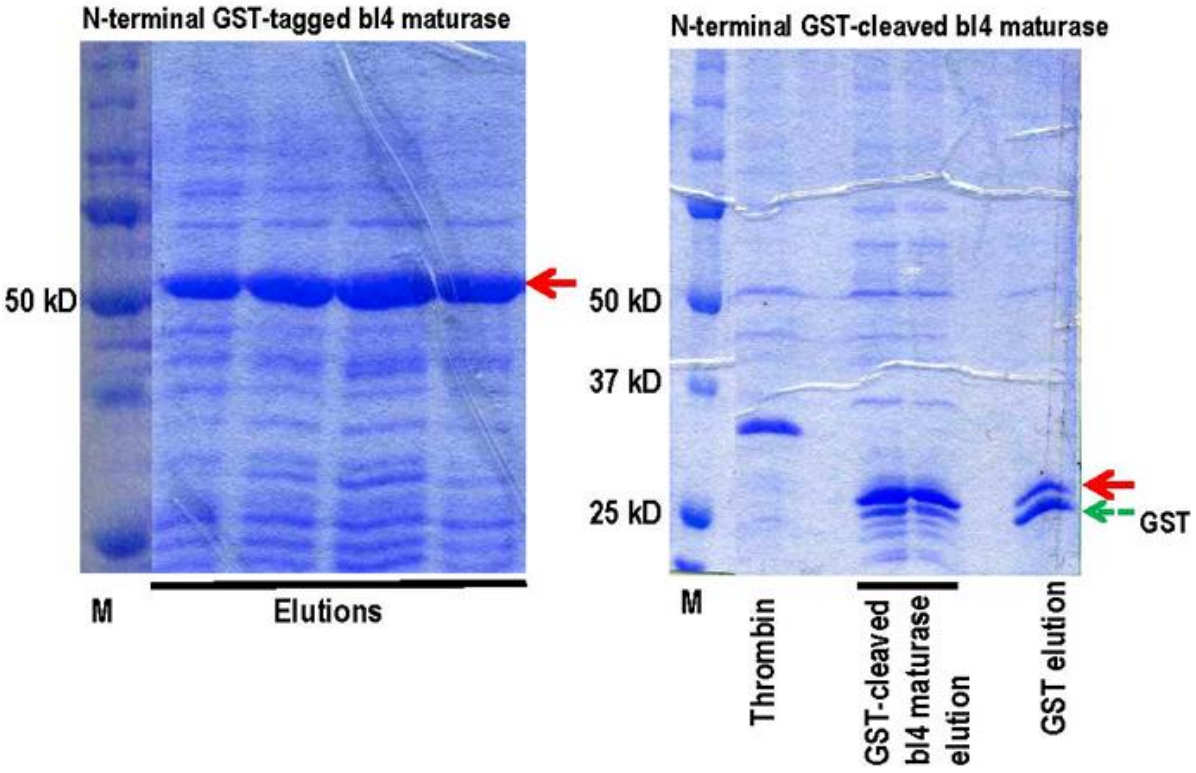

Figure VII.4. Purification of bI4 maturase. (Left) SDS-PAGE analysis of N-terminal GST-tagged bI4 maturase eluted from glutathione-agarose beads with 10 mg/mL glutathione in 50 mM Tris-HCl, pH 9 to 10. (Right) SDS-PAGE analysis of N-terminal GST-cleaved bI4 maturase by thrombin treatment. The solid red arrow corresponds to bI4 maturase with GST tag (56 kD, left) or without GST tag (30 kD, right). The green dashed arrow corresponds to GST (26 kD). A reference lane containing only thrombin protease has also been shown.

VII.2.F. Circular Dichroism

CD measurements were performed using a Jasco J-720 spectropolarimete. A sample containing 1 μM protein in 5 mM KP_i, pH 7.5 was measured in the far-ultraviolet region using a 0.1 cm path cell. Background signals from the cell and the buffer were subtracted from each spectrum.

VII.2.G. Aminoacylation assay

Each aminoacylation reaction contained 60 mM Tris, pH 7.5, 10 mM $MgCl_2$, 10 mM KCl, 1 mM dithiothreitol (DTT), 4 μM transcribed $ymtRNA^{Leu}$, 21 μM [^{3}H]-leucine (150 μCi/mL) and 1 μM enzyme. Each reaction was initiated with 4 mM ATP and performed as described in Chapter II.

VII.2.H. Isolation of mischarged Ile-$tRNA^{Leu}$

Misaminoacylation of $ymtRNA^{Leu}$ with isoleucine was carried out by incubating the following reaction mixture at 25 °C for 3 h: 60 mM Tris, pH 7.5, 10 mM $MgCl_2$, 10 mM KCl, 1 mM DTT, 8 μM transcribed $ymtRNA^{Leu}$, 23 μM [^{3}H]-isoleucine (300 μCi/mL), 1 μM editing defective *E. coli* LeuRS and 4 mM ATP and performed as described in Chapter II.

VII.2.I. Post-transfer editing deacylation assay

Deacylation reaction mixtures contained 60 mM Tris, pH 7.5, 10 mM $MgCl_2$, 10 mM KCl and approximately 2 μM [^{3}H]-Ile-$ymtRNA^{Leu}$. The reactions were initiated with 1 μM enzyme and were carried out at 25 °C as described in Chapter II.

VII.2.J. LeuRS-dependent *in vitro* splicing assay

The *in vitro* splicing reaction (Boniecki, et al., 2009) included 1 μM [^{32}P]-bI4Δ1168 pre-RNA (0.13 μCi/μL), 1 μM LeuRS, 150 mM KCl, Stop RNase inhibitor (5 Prime, Inc., Gaithersburg, MD) in 1X binding buffer (10 mM Tris, pH 7.5, 100 mM NaCl, 5 mM $MgCl_2$, 1 mM ethylenediaminetetraacetic acid (EDTA) and 10% glycerol. The reaction was carried out at 37 °C and initiated with 1 mM guanosine. Aliquots of 10 μL were quenched in 10 μL of 5 M urea, 30 mM EDTA and mixed with 5 μL of RNA-loading dye for incubation at 65 °C for 10 min.

Each aliquot was electrophoresed on a 6% denaturing urea-polyacrylamide gel, overnight at 10 mA, in 1X TBE buffer. The gel was dried and phosphorimaged using a FUJIFILM BAS Cassette 2040 (FUJIFILM Medical Systems, Stanford, CT) and products were visualized by scanning the images using a STORM 840 Molecular Dynamics scanner (Amersham Pharmacia Biotech, Piscataway, NJ). Images were quantified using ImageQuant software. Bands corresponding to the bI4Δ1168 precursor RNA, excised intron and ligated exons, for each time point were normalized by measuring the fraction of each relative to the sum of the intensities of the three bands for the respective time points. Background intensity was deducted, based on the zero time point. The fraction of bI4Δ1168 pre-RNA remaining and extent of reaction for both the products, bI4 and B4-B5 were plotted using the GraphPad Prism software.

VII.2.K. *In vivo* yeast complementation assay

The yeast complementation assays utilized the yeast strains HM410 and HM402 (Li, et al., 1996; Seraphin, et al., 1987). Both HM410 (*MATα ade2-1 his-11,15 leu2-3, 112 trp1-1 ura3-1 can1-100 nam2Δ::LEU2* [777-3A]) and HM402 (*MATα ade2-1 his-11,15 leu2-3, 112*

trp1-1 ura3-1 can1-100 nam2Δ::LEU2 [Δ introns]) are yeast null strains that contain a genomic/allelic disruption of the *nam2* gene, encoding ymLeuRS, but contain a LEU marker insertion. Wild type ymLeuRS fused to mitochondrial import sequence, is expressed via a maintenance plasmid YEpGMCO63 that bears a URA3 marker. The *ade2* mutation enables the cells to develop a red pigment when mitochondria are functional. The strain HM410 contains all thirteen mitochondrial introns. All of these introns have been deleted in HM402.

Yeast HM410 and HM402 competent cells were transformed with the plasmids pMPW238A, pMPW238C, pMPW238F or pMPW238Y, encoding the respective mutant ymLeuRSs or with pKIRAN, encoding the wild type *E. coli* LeuRS, fused to an N terminal mitochondrial import sequence. As positive and negative controls, yeast cells were also transformed with the plasmid ymLeuRST, encoding the wild type ymLeuRS, fused to a mitochondrial import sequence and the empty vector pQB153T, respectively. All these plasmids bear a TRP marker. Selection of transformants that contain both the maintenance plasmid YEpGMCO63 with a URA3 marker and the mutant or heterologous LeuRS expressing plasmid with a TRP marker was carried out on synthetic complete (SC) Leu^-Ura^- Trp^- dropout media. The selected transformants were then grown on glucose containing 5-flouroorotic acid (FOA). This negative selection step selects for cells that have lost the maintenance plasmid YEpGMCO63 with URA3 marker, expressing wild type ymLeuRS. Thus, cells that grow on glucose-FOA media are Ura^- segregants that now contain only the plasmid with TRP marker that express the mutant or heterologous LeuRSs. The FOA resistant colonies were then grown on SC Leu^- Trp^- dropout media, containing either 2% glucose or glycerol to test for complementation activity (Houman, et al., 2000).

VII.2.L. Northern blot analysis

Total cellular RNA was extracted from yeast null strain HM410, expressing wild type ymLeuRS and W238A, W238C mutant ymLeuRSs. The cells were selectively grown in 25 mL SC Leu^- Trp^- dropout media containing FOA until the OD_{600} reached 1.5. The cultures were then harvested and pellets washed with ice cold water. The washed pellets were resuspended in 400 μL TES (10 mM Tris, pH 7.5, 10 mM EDTA and 0.5% SDS) followed by hot acid phenol extraction at 65 °C for 1 h. The aqueous layer was extracted twice with chloroform. The recovered RNA was precipitated overnight with 40 μL 3 M CH_3COONa, pH 5.3 and 100% chilled ethanol (that was stored at -20 °C). This was followed by washing with 70% ethanol before drying the pellet and dissolving the same in nuclease-free water (Ambion Inc., Austin, TX).

Upto 100 μg of total cellular RNA were electrophoresed on a 1% agarose gel containing 1.85% formaldehyde and 40 mM 3-(N-morpholino) propanesulphonic acid (MOPS), 0.1 mM EDTA, 0.5 mM CH_3COONa MOPS buffer. The RNA was transferred to a nitrocellulose membrane in 5X sodium salt citrate (SSC: 0.75 M NaCl and 0.075 M $NaH_2C_6H_5O_7$) overnight. RNA was UV cross-linked to the nitrocellulose membrane for 1 min. The membrane was then prehybridized for 1 hr at 42 °C with 25 mL hybridization buffer (0.5 M NaP_i, pH 7.2, 7% SDS, 1% BSA and 0.04% EDTA).

A DNA oligomer that represents the ligated B4-B5 exon junction (5′-GAATATAGTTATCAGGATGACCTAAAGTATTAGGTGAATAG-3′) was radiolabeled in a reaction containing 0.3 μg of the oligo, 50 μCi [γ-^{32}P]-ATP and 10 U T4 polynucleotide kinase (Promega, Madison, WI). The radiolabeled probe was added to the prehybridized membrane and hybridization was carried out overnight at 42 °C. The membrane was then washed three times for 10 min with 1X SSC and 0.1% SDS, followed by drying. The dried membrane was exposed to FUJIFILM BAS Cassette 2040 (FUJIFILM Medical Systems,

Stanford, CT) and the image scanned using a STORM 840 Molecular Dynamics scanner (Amersham Pharmacia Biotech, Piscataway, NJ).

VII.2.M. RT-PCR detection of spliced product

Denaturation of 25 μg of total cellular RNA was carried out by incubation at 95 °C for 5 min. This was followed by an annealing reaction at 48 °C for 1 hr with 10 pmoles of forward (bI4-F-5′-GGCATTACATATTCATGGTTCATC-3′) and reverse (bI5-R-5′-GGTGTTACTAAAGGATTACCAGGAA-3′) primers followed by reverse transcription at 37 °C for 90 min using 10 U of AMV Reverse Transcriptase (Promega, Madison, WI). The PCR reaction was carried out by subsequent addition of 10 pmoles of forward and reverse primers along with 5 U of Go Taq Flexi DNA polymerase (Promega, Madison, WI). Subsequent to denaturation for 5 min at 95 °C, 30 cycles of PCR were carried out as follows: 94 °C, 1 min; 50 °C, 1 min; and 72 °C for 2 min with a final extension for 10 min at 72 °C.

The yeast complementation assays and Northern blot and RT-PCR analysis of the spliced products were performed by Kiranmai Poruri, alumnus of Professor Susan A. Martinis's research group.

VII.3. Results

Isolated ymCP1 domain splices in vitro, unlike its E. coli counterpart. The isolated ymLeuRS CP1 domain is sufficient to support *in vivo* splicing activity of the bI4 intron RNA (Rho, et al., 2002). To investigate CP1 adaptations that confer splicing activity *in vitro*, we designed three ymLeuRS protein fragments that contained the CP1 domain and various lengths of its flanking extensions (Figure VII.1). These constructions were based on available LeuRS crystal structures as well as biochemical investigations. Our goal was to

incorporate the LeuRS protein fragments into a recently developed *in vitro* splicing assay for the bI4 intron (Boniecki, et al., 2009) to distinguish adaptations of this housekeeping protein that are important to RNA splicing. The full-length wild type ymLeuRS was found to support splicing of the minimized bI4Δ1168 pre-RNA in this *in vitro* assay (Boniecki, et al., 2009), as shown by identification of the products on a denaturing polyacrylamide gel and also by quantification of the processing of the pre-RNA and formation of products – the spliced

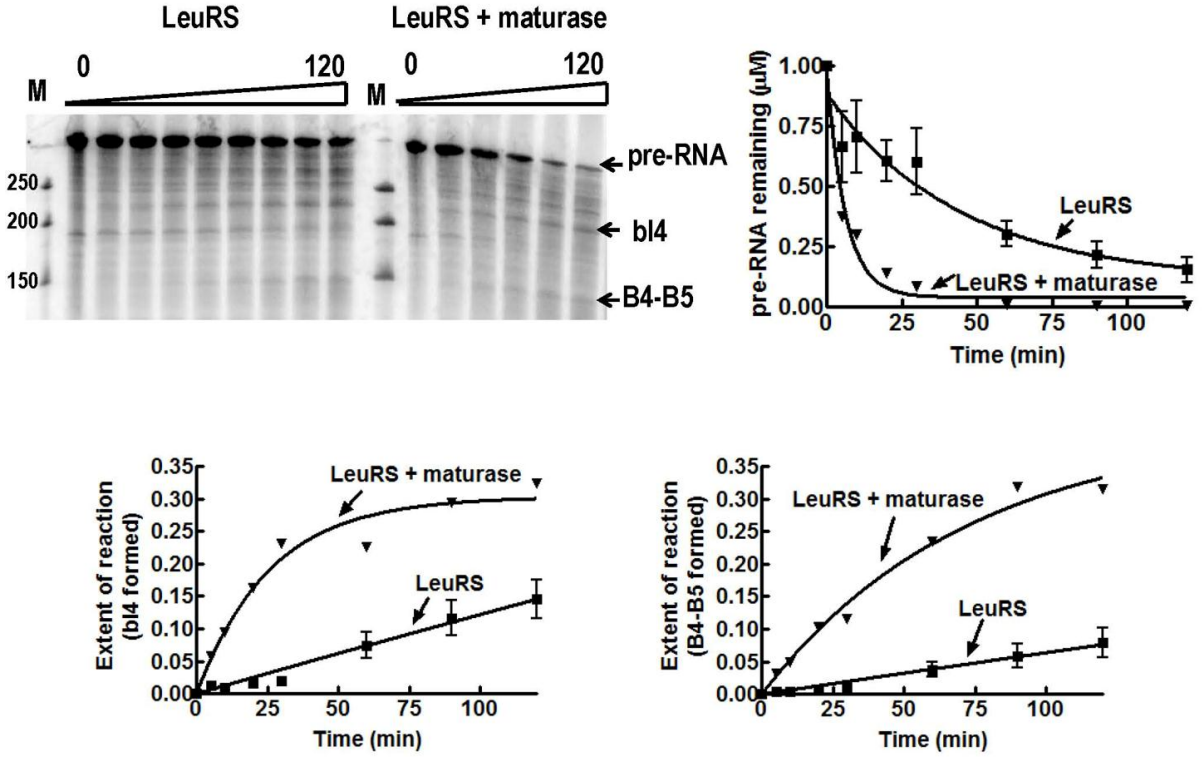

Figure VII.5. *In vitro* splicing activity of full-length wild type ymLeuRS in absence or presence of bI4 maturase. (Top left) Products of the *in vitro* splicing reaction were resolved on a 6% denaturing polyacrylamide gel and identified by comparing the position of the bands with a custom-made RNA marker ('M'). The pre RNA (B4-bI4-B5), and the products bI4 and B4-B5 have been marked by arrows. The splicing of 1 μM [^{32}P]-bI4Δ1168 pre-RNA (0.13 μCi/μL) in presence of proteins was initiated by addition of 1 mM guanosine and the reaction carried out at 37 °C for 120 min. (Top right) Processing of the bI4Δ1168 pre-RNA. (Bottom left) Extent of the splicing reaction with respect to excised bI4 intron formed. (Bottom right) Extent of the splicing reaction with respect to ligated B4-B5 exons formed. Symbols are: (■) LeuRS; (▼) LeuRS + bI4 maturase. Error bars for each time point result from each reaction repeated in triplicate.

bI4 intron and the B4-B5 ligated exons, albeit less efficiently as compared to splicing of the pre-RNA in presence of both LeuRS and bI4 maturase proteins (Figure VII.5).

The CP1 domain is defined as a polypeptide insertion that splits the ATP binding Rossmann fold (Starzyk, et al., 1987). However, several X-ray crystal structures show that

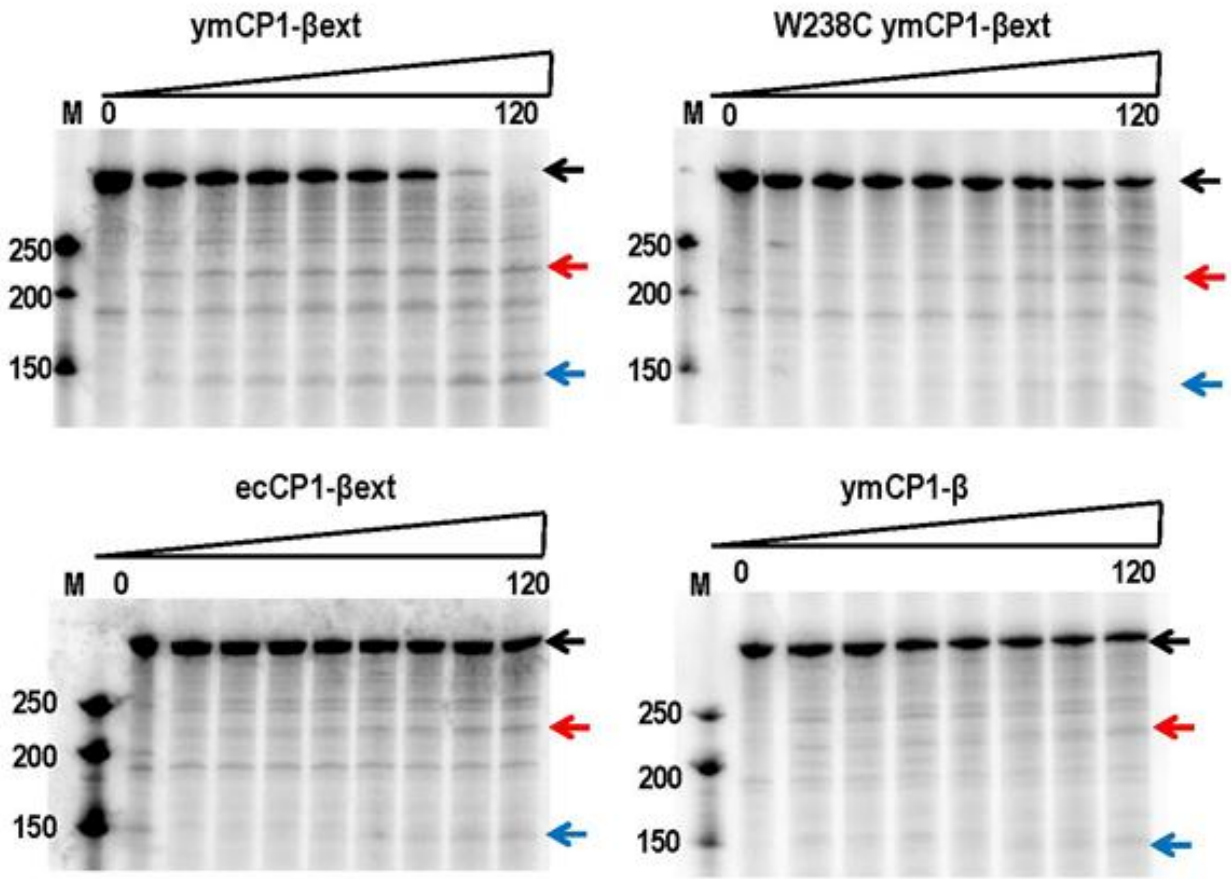

Figure VII.6. Representative isolated LeuRS CP1domain-dependent *in vitro* splicing reactions analyzed on 6% denaturing poyacrylamide gels. The excised bI4 intron and ligated B4-B5 exon were identified on the gel by comparison with a custom-made RNA marker ('M'). The pre-RNA, bI4 intron and B4-B5 ligated exon are marked by black, red and blue arrows, respectively.

the primary structure of CP1 folds as a discrete domain (Cusack, et al., 2000). The CP1 domain is linked to the LeuRS main body via the flexible N and C-terminal β-strands (Cusack, et al., 2000). In ymLeuRS, the isolated CP1 domain (CP1; Figure VII.1) extends

from Ile 260 to Glu 431. Previously, we showed that the β-strands are required for deacylation of mischarged tRNA in the *E. coli* enzyme (Betha, et al., 2007). Thus, we constructed a CP1-containing fragment that included the β-strands, extending from Trp 238 to Leu 446 (CP1- β; Figure VII.1). We had also determined that inclusion of short extensions

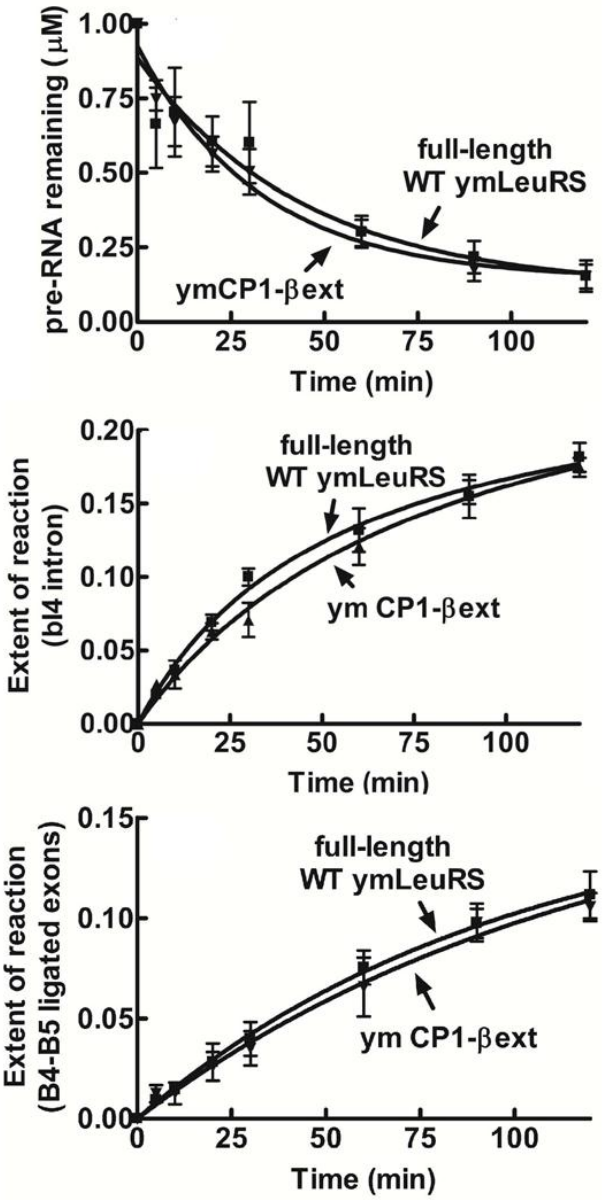

Figure VII.7. *In vitro* splicing activity of ymLeuRS. Evaluation of *in vitro* bI4Δ1168 pre-RNA splicing with respect to (A) processing of substrate pre-RNA, (B) fraction of bI4 excised intron and (C) fraction of the ligated B4-B5 exons. Splicing reactions incorporated 1 μM of substrate pre-RNA and 1 μM LeuRS and were initiated with 1 mM guanosine. Symbols are: full-length ymLeuRS (■) and isolated ymCP1-βext (▲). Error bars for each time point result from each reaction repeated in triplicate.

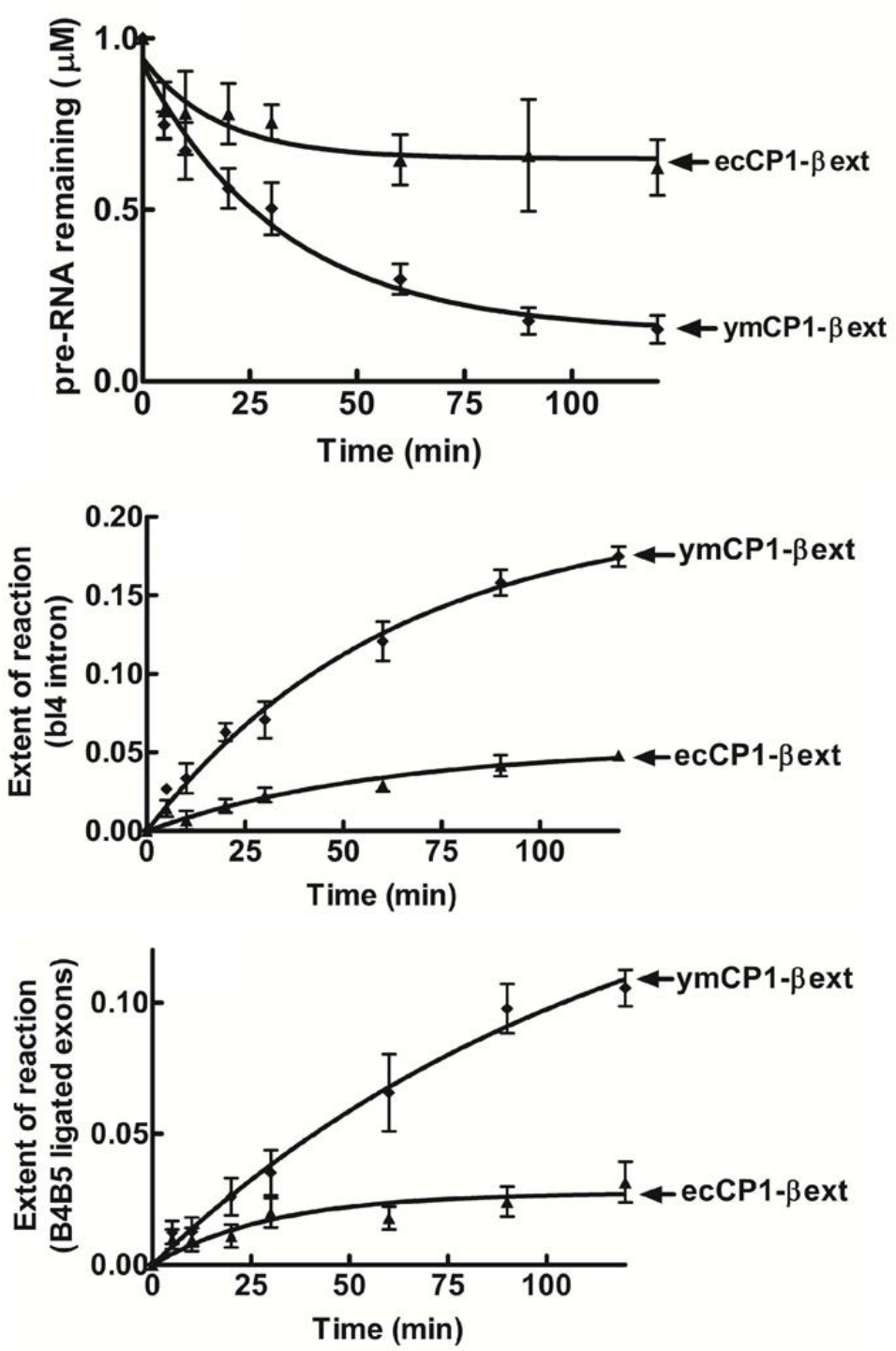

Figure VII.8. Species-specific LeuRS CP1 domain-dependent *in vitro* splicing of the bI4Δ1168 presursor RNA. The processing of the bI4Δ1168 presursor RNA (pre-RNA) was evaluated with respect to (Top) substrate pre-RNA processing, (Center) fraction of excised bI4 intron formed and (Bottom) fraction of ligated B4-B5 exons formed. Calculations were based on the intensity of the phosphorimaged bands for the substrate, products bI4 and B4-B5 as well as other alternate bands that emerged during the reaction. Splicing reactions incorporated 1 μM of pre-RNA and 1 μM LeuRS and were initiated with 1 mM guanosine. Symbols are: ecCP1-βext (▲) and ymCP1-βext (♦). Error bars for each time point are the result of each reaction repeated in triplicate.

from the β-strands to the aminoacylation core that contained conserved 'WIG' and 'RDW' motifs, enhanced tRNA deacylation by the isolated *E. coli* CP1 domain (Betha, et al., 2007). In addition to the β-strands, these extensions have been shown to be important for $tRNA^{Leu}$-protein interactions in *E. coli* LeuRS (Mascarenhas and Martinis, 2008; Nawaz, et al., 2007). We hypothesized that they might also be important for interacting with the bI4 intron RNA. Based on the *E. coli* LeuRS model (Betha, et al., 2007), we designed a similar fragment for the ymLeuRS CP1 domain that includes extensions of the β-strands (CP1-βext; Lys 232 to Tyr 452; Figure VII.1) to assess its contributions to RNA splicing.

We analyzed the LeuRS CP1 domain-dependent splicing activity *in vitro* using a minimized bI4 intron (bI4Δ1168) (Boniecki, et al., 2009) that was comprised primarily of its catalytic core. The isolated ymCP1-βext LeuRS that contained the CP1 domain, the β-strands and the extensions, was active in processing the bI4Δ1168 pre-RNA (Figure VII.6, top left; Figure VII.7, top) and produced the expected bI4 intron and fused B4-B5 exon products, comparable to the full-length wild type ymLeuRS (Figure VII.7). The extent of the splicing reaction based on relative yields of the excised intron bI4 (Figure VII.6, top left; Figure VII.7, middle) and the ligated exons B4-B5 (Figure VII.6, top left; Figure VII.7, bottom) were comparable.

LeuRSs from diverse origins can splice (Houman, et al., 2000) and because this includes LeuRSs that do not encounter group I introns in their natural environment, we also tested the homologous CP1-βext (Val 216 to Ala 430) construct from *E. coli* LeuRS. These two CP1 domain protein fragments from ymLeuRS and *E. coli* LeuRS share ~34% homology (Herbert, et al., 1988). The *E. coli* based ecCP1-βext LeuRS protein fragment, in contrast to its counterpart from ymLeuRS, showed significantly reduced processing of the bI4Δ1168 intron (Figure VII.6, bottom left; Figure VII.8). Thus, even though it has been suggested that LeuRS uses its broadly conserved evolutionarily features to function in RNA splicing

(Houman, et al., 2000), the ymLeuRS CP1 domain, as we hypothesized, is more highly adapted for RNA splicing.

Full length E. coli LeuRS supports splicing of bI4 RNA in vivo. Because the CP1 domain of *E. coli* LeuRS failed to support splicing of the bI4 intron *in vitro*, we wondered if the full length *E. coli* LeuRS could substitute for the yeast enzyme in RNA splicing, similar to other LeuRSs that originated from *M. tuberculosis* or human mitochondria (Houman, et al., 2000). We transformed yeast null strains, HM410 and HM402 that have an allelic disruption of the nuclear encoded gene for the endogenous ymLeuRS, with the plasmid expressing full length *E. coli* LeuRS fused to an N-terminal mitochondrial import sequence. The strain HM410 contains all thirteen mitochondrial introns and would require both the splicing and aminoacylation functions of LeuRS. In contrast, the intronless strain HM402 would require only aminoacylation for growth. The full length *E. coli* LeuRS supported growth of both HM410 and HM402 on glycerol media, indicating that the enzyme was active in both aminoacylation and splicing (Figure VII.9). The full-length *E. coli* protein was also active

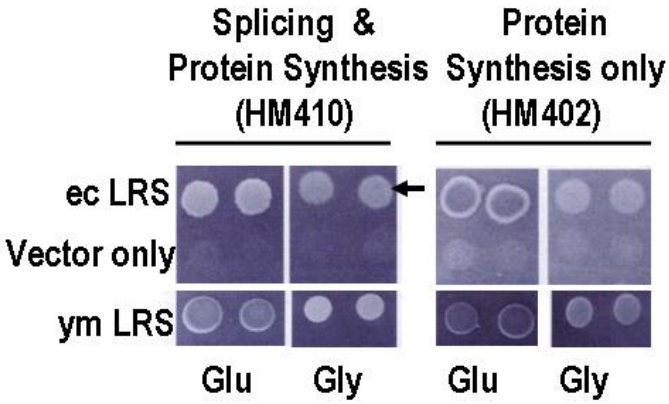

Figure VII.9. *In vivo* presursor RNA splicing activity of full length *E. coli* LeuRS. Complementation assays were performed using yeast null strains HM410 (with all 13 mitochondrial introns) and HM402 (intronless) (Li, et al., 1996). Complementation is indicated by darker colonies grown on glucose (Glu) media and by growth on glycerol (Gly) media. The arrow indicates that the full length *E. coli* LeuRS supports growth of HM410 on Gly media. Both stains were transformed with the parent vector pQB153T or with plasmids expressing the wild type ymLeuRS (pymLRST) or the wild type *E. coli* LeuRS (pKIRAN).

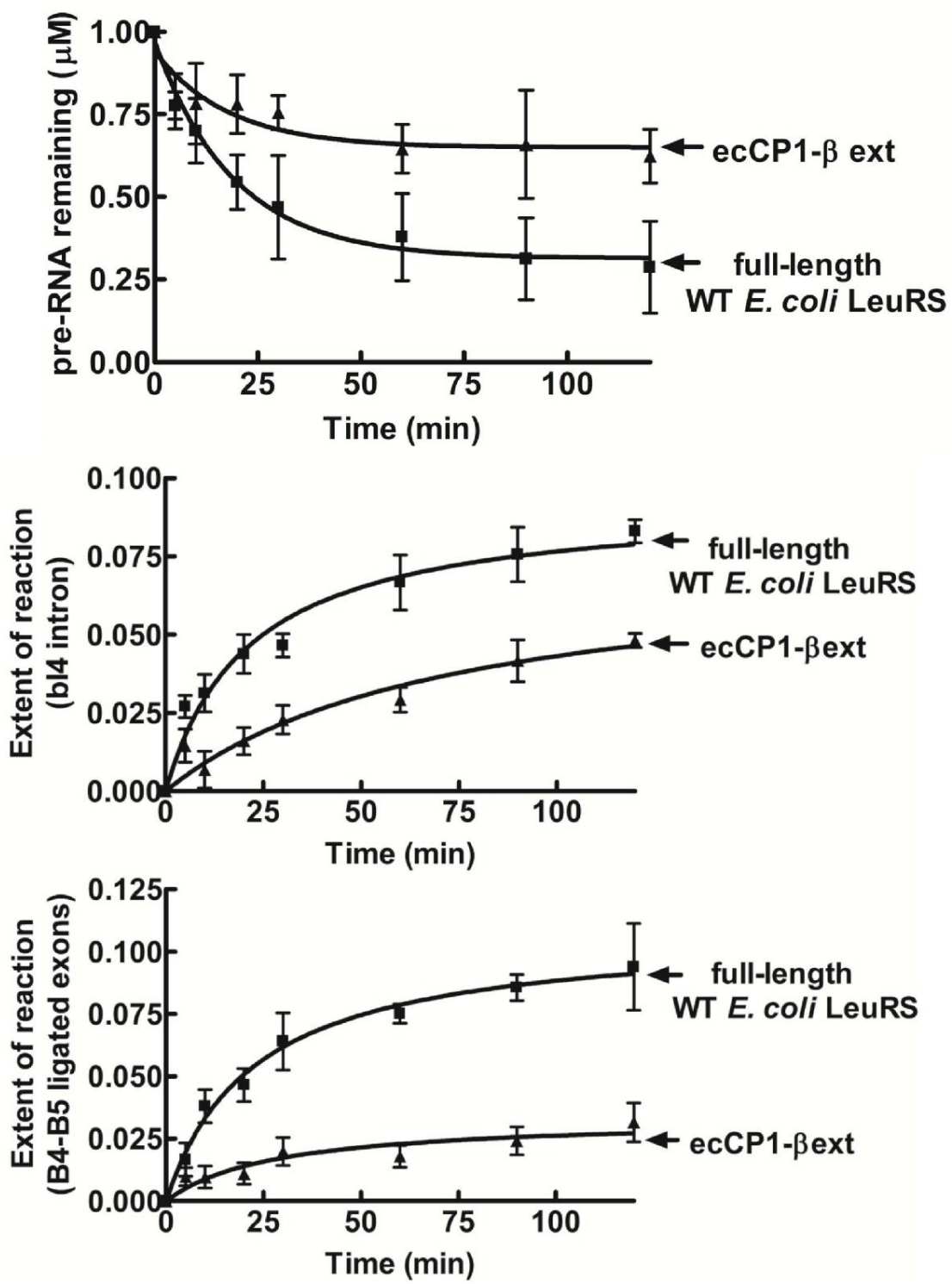

Figure VII.10. *In vitro* splicing activity of *E. coli* LeuRS. The processing of the bI4Δ1168 presursor RNA (pre-RNA) was evaluated with respect to (Top) substrate pre-RNA processing, (Center) fraction of excised bI4 intron formed and (Bottom) fraction of ligated B4-B5 exons formed. Splicing reactions incorporated 1 μM of substrate pre-RNA and 1 μM LeuRS and were initiated with 1 mM guanosine. Symbols are: full-length *E. coli* LeuRS (■) and isolated ecCP1-βext (▲). Error bars for each time point result from each reaction repeated in triplicate.

when incorporated in the *in vitro* splicing assay (Figure VII.10). Because the isolated *E. coli* LeuRS CP1 domain failed to support splicing *in vitro*, we hypothesize that the ymLeuRS contains evolutionary adaptations that are specific to the CP1 domain. This would allow its CP1 domain to be more robust in splicing in the absence of the full-length protein, compared to the *E. coli* CP1 domain.

Functional divergence of the LeuRS CP1 domain to accommodate RNA splicing and protein synthesis in yeast mitochondria. The CP1 domains from isoleucyl-tRNA synthetase

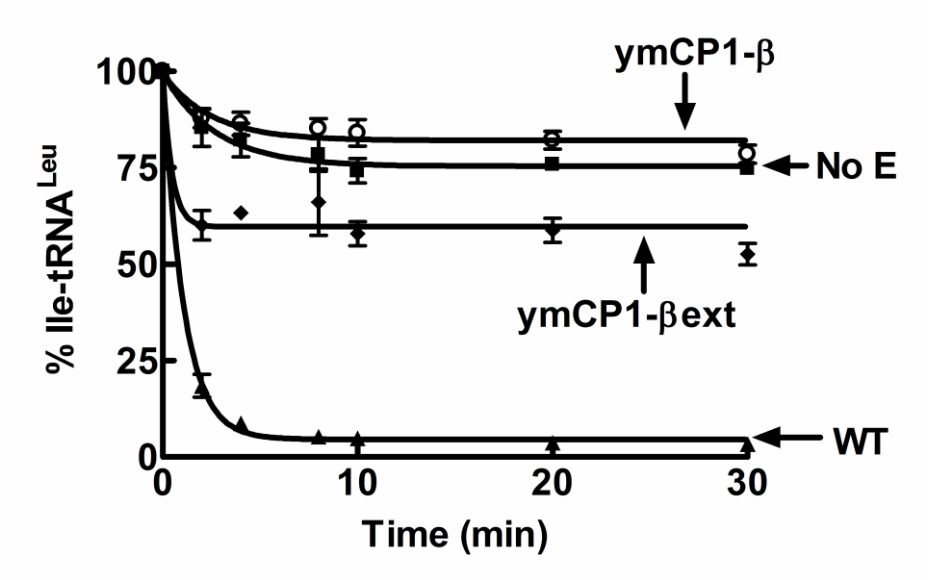

Figure VII.11. Deacylation activity of the ymLeuRS CP1 domain. Deacylation reactions included approximately 2 μM [^{3}H]-Ile-tRNA^{Leu} and 1 μM enzyme. Symbols are: wild type (▲), ymCP1-β (o), ymCP1-βext (♦) and no enzyme (■). Error bars for each time point are the result of each reaction repeated in triplicate.

(IleRS), valyl-tRNA synthetase (ValRS) and *E. coli* LeuRS that are independent from the rest of the enzyme, effectively clear misacylated tRNAs (Betha, et al., 2007; Lin, et al., 1996). The β-strands of the *E. coli* LeuRS CP1 domain are required for hydrolytic editing activity (Betha, et al., 2007). As highlighted above, short extensions of the β-strands into the main body significantly enhance the hydrolytic activity of the *E. coli* CP1 domain. They are

hypothesized to bind and position the 3′ end $tRNA^{Leu}$ for editing (Betha, et al., 2007). We tested whether the β-strands and extensions of the ymLeuRS CP1 domain were similarly important to deacylation activity. In contrast to the *E. coli* LeuRS CP1 domain, inclusion of the β-strands in the ymCP1-β LeuRS failed to confer deacylation activity to the CP1 domain (Figure VII.11), although both isolated protein fragments fold with overlapping significant α-helical character, as the wild type enzyme (Figure VII.12). The k_{obs} for deacylation by the ymCP1-β LeuRS was 0.3 ± 0.07 min^{-1} compared to 1.0 ± 0.11 min^{-1} for the full-length wild type ymLeuRS (Table VII.2).

Addition of the extensions in ymCP1-βext LeuRS only hydrolyzed misacylated Ile-$tRNA^{Leu}$ at low levels (k_{obs} = 0.3 ± 0.1 min^{-1} for 1 μM enzyme) (Table VII.2) compared to the full-length ymLeuRS, albeit the extension additions increase the extent of the reaction (Figure VII.11). Increasing enzyme concentrations up to 5 μM did not show any significant increase in the observed rate constants for deacylation (Table VII.2).

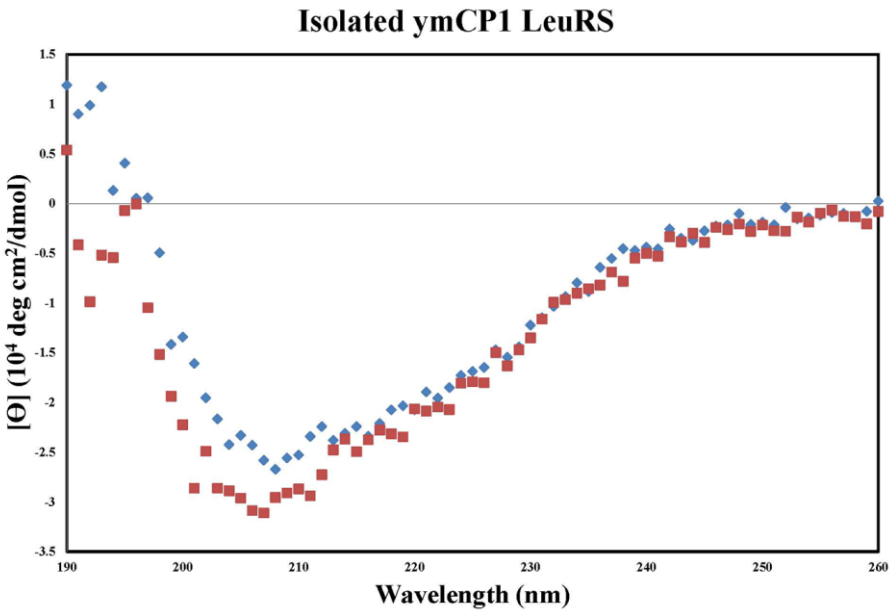

Figure VII.12. CD spectra of isolated ymCP1 constructs. The red squares represent the protein fragment ymCP1-β and the blue diamonds represent the protein fragment ymCP1-βext.

Table VII.2. Observed rate constants (k_{obs}) for deacylation of Ile-tRNA^{Leu} by full-length or isolated LeuRS CP1 protein constructs.

Enzyme	No enzyme	Full-length wild type ymLeuRS*	ymCP1-β*	ymCP1-βext		
				1 µM	2 µM	5µM
$\boldsymbol{k_{obs}}$ **(min^{-1})**	0.36 ± 0.17	1.0 ± 0.11	0.3 ± 0.07	0.3 ± 0.1	0.33 ± 0.16	0.37 ± 0.2

*Reported k_{obs} were measured using 1 µM enzyme. In addition, substrate preparations contain uncharged tRNA, as well as mischarged tRNA.

We hypothesize that the ymLeuRS has functionally diverged at the CP1 domain to facilitate RNA splicing. This may have occurred at a cost to the enzyme's CP1-based editing activity, since the full length ymLeuRS clears misacylated tRNA^{Leu} via its CP1 domain (Karkhanis, et al., 2006) (Figure VII.11). Interestingly, editing defects in yeast had minimal effects on cell viability and mitochondrial function, although they are lethal to *E. coli* (Karkhanis, et al., 2006). It is possible that the cell as well as the mitochondrial LeuRS have adapted to accommodate both translational fidelity requirements and RNA splicing which is essential to mitochondrial function. Although the β-strands failed to enable amino acid editing by the isolated CP1 domain from ymLeuRS, we wondered if they would be sufficient in stimulating RNA splicing *in vitro.* As shown in Figure VII.7., the ymCP1-βext LeuRS fragment, which includes the β-strands as well its extensions, is active in processing the bI4Δ1168 pre-RNA *in vitro,* comparable to the full-length wild type ymLeuRS. To determine if the β-strands alone can render the ymCP1 domain active in RNA splicing, we tested the ymCP1-β LeuRS protein fragment that includes only the β-strands, but not the extensions (Figure VII.1). It exhibited significantly reduced processing of the bI4Δ1168 pre-RNA as compared to the ymCP1-βext LeuRS fragment that includes both the β-strands and the extensions (Figure VII.13). The observed rate of formation of both the spliced bI4 intron (46×10^{-3} min^{-1}) and the ligated exons B4-B5 (26×10^{-3} min^{-1}) in presence of ymCP1-β were

2 to 3 fold decreased as compared to product formation in presence of ymCP1-βext (Table VII.3).

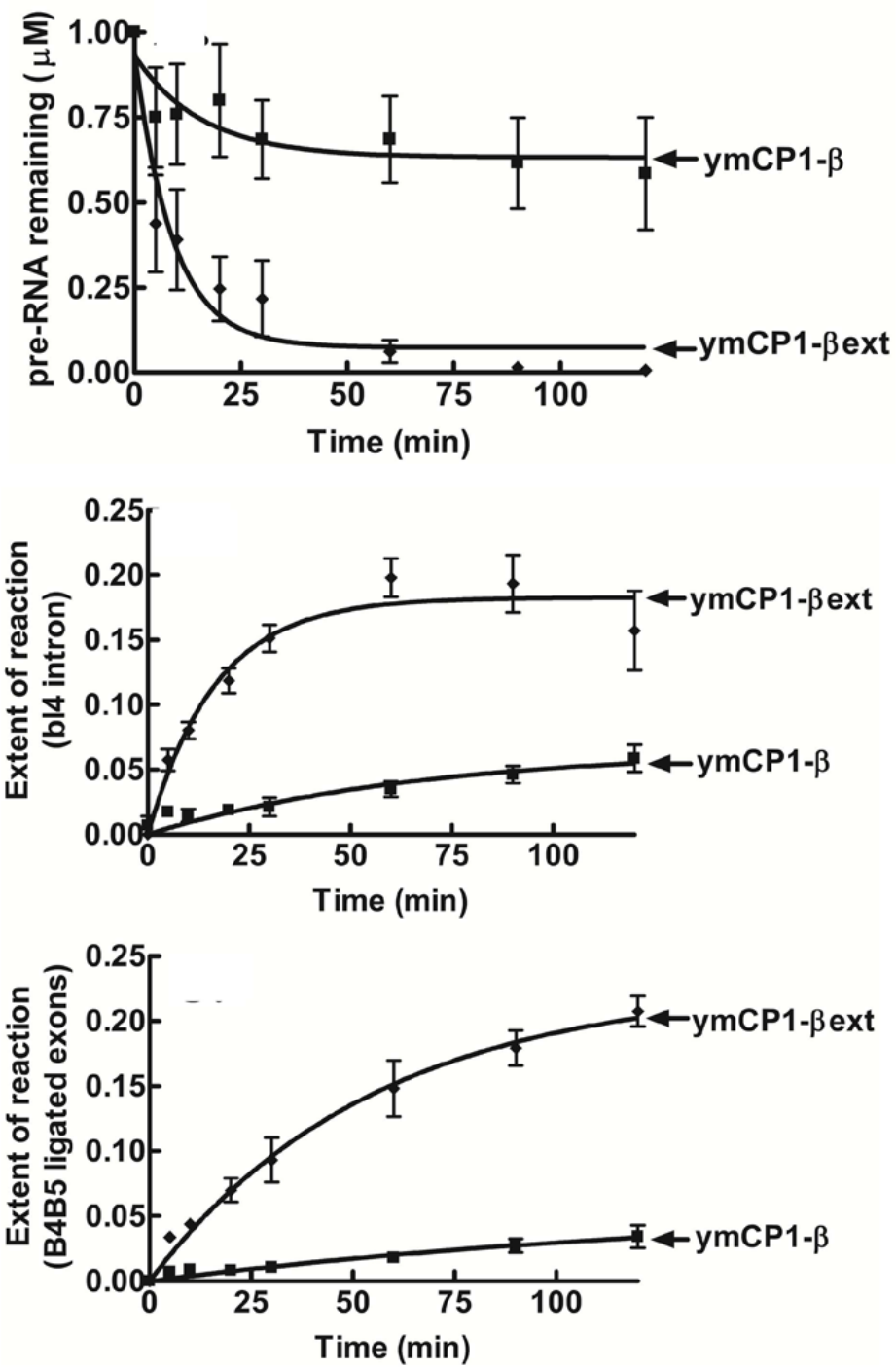

Figure VII.13. LeuRS CP1 domain extension-dependent splicing activity. *In vitro* bI4Δ1168 pre-RNA splicing was determined with respect to (Top) processing of the substrate pre-RNA, (Center) fraction of the excised bI4 intron formed and (Bottom) fraction of the ligated B4-B5 exons formed. Splicing reactions incorporated 1 μM of pre-RNA and 1 μM LeuRS and were initiated with 1 mM guanosine. Symbols are: ymCP1-β (■) and ymCP1-βext (♦). Error bars for each time point are the result of each reaction repeated in triplicate.

Table VII.3. Observed rates (k_{obs}) for splicing of bI4Δ1168 pre-RNA

Protein	Pre-RNA	bI4	B4-B5
		k_{obs} X 10^{-3} min^{-1}	
ymCP1-β	0.4 ± 0.03	46 ± 12	26 ± 9
ymCP1-βext	36 ± 16	128 ± 76	59 ± 18

It is noteworthy that the ymCP1-β LeuRS protein fragment contains the conserved 'WIG' and 'RDW' motifs at the end of the N and C-terminal β-strands respectively (Figure VII.1). Thus, although these motifs provide critical interactions with the tRNA (Nawaz, et al., 2007), they are not sufficient to confer optimal splicing activity to the ymLeuRS CP1 domain, isolated from the rest of the enzyme. Thus, we hypothesize that short extensions of the β-strands into the enzyme catalytic core domain are essential, not only to confer hydrolytic editing activity but also to confer RNA splicing activity to the isolated CP1 domain of LeuRS.

'WIG' peptide extension of ymLeuRS is adapted for RNA splicing. Genetic rescue experiments originally implicated Gly 240 as a critical factor in LeuRS's splicing activity (Li, et al., 1996). This site is located in a peptide that contains a conserved 'WIG' motif (Figure VII.14) (Hou, et al., 1991) in the extension of the N-terminal β-strand (Figure VII.1) that links the CP1 domain of LeuRS to its aminoacylation core. Mutation of Gly 240 to serine suppresses splicing defects when the bI4 maturase is inactivated (Herbert, et al., 1988; Labouesse, 1990). Mutation of the Trp 238 to cysteine in the 'WIG' motif abolishes splicing, but retains aminoacylation activity in the ymLeuRS (Li, et al., 1996).

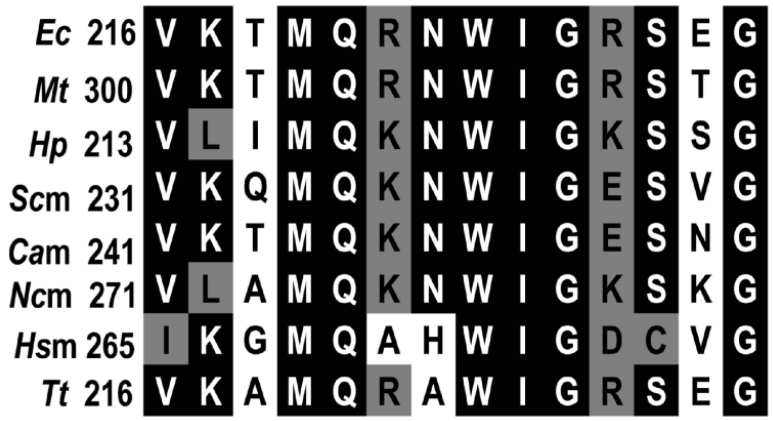

Figure VII.14. Primary sequence alignment of the 'WIG' peptide in LeuRS. Abbreviations are: *Escherichia coli* (*Ec*), *Mycobacterium tuberculosis* (*Mt*), *Helicobacter pylori* (*Hp*), *Saccharomyces cerevisiae* mitochondrial (*Sc*m), *Candida albicans* mitochondrial (*Ca*m), *Neurospora crassa* mitochondrial (*Nc*m), *Homo sapiens* mitochondrial (*Hs*m), *Thermus thermophilus* (Tt).

To distinguish the effects of Trp 238 on splicing and aminoacylation functions of LeuRS, we transformed wild type (HM410) and intronless (HM402) yeast strains with plasmids encoding the full length wild type, W238A, W238C, W238F and W238Y ymLeuRSs fused to an N-terminal mitochondrial import sequence. As expected, the full-length wild type and all the mutant ymLeuRS complemented growth of the intronless strain HM402 on glycerol media (Figure VII.15, top left), supporting that they are all active in aminoacylation. The full-length mutant W238F and W238Y ymLeuRSs also complemented the intron containing HM410 strain (Figure VII.15, top left). However, the full-length W238A and W238C ymLeuRS mutants failed to support growth of the wild type strain HM410 on glycerol media (Figure VII.15, top left, indicated by arrows). Analysis of cell extracts from HM410 expressing full length wild type or W238A or W238C ymLeuRSs, via RT-PCR (Figure VII.15, top right) and Northern blot (Figure VII.15, bottom left), failed to detect the B4-B5 spliced product. As would be expected from the complementation assays, the full-length W238A and W238C mutants retained aminoacylation activity *in vitro*, albeit at

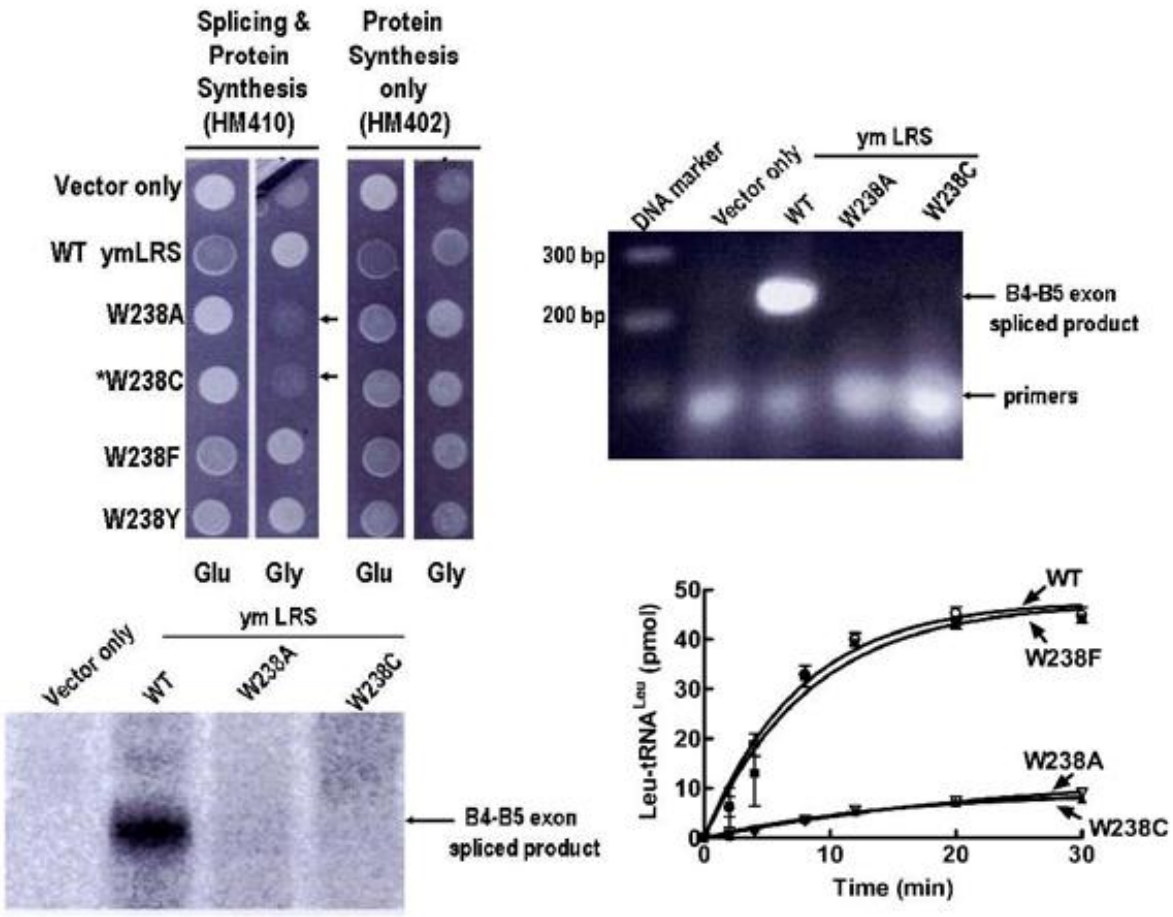

Figure VII.15. Analysis of ymLeuRS Trp238 mutants *in vivo* splicing activity. (Top left) Complementation assays used yeast null strains HM410 and HM402 and is indicated by darker colonies grown on glucose (Glu) media and by growth on glycerol (Gly) media. The arrows indicate that the W238A and W238C mutant ym LRSs can support growth of HM402, but not of HM410 on Gly media. Both strains were transformed with the parent vector pQB153T or with plasmids expressing the wild type (pymLRST) or W238A (pMPW238A), W238C (pMPW238C), W238F (pMPW238F) and W238Y (pMPW238Y) mutant ymLeuRSs. (Top right) RNA amplification via RT-PCR of total cellular RNA from yeast null strain HM410 expressing wild type and W238 mutant ymLRSs was carried out. A 250 base pair (bp) amplified product on a 1% agarose gel indicates the B4-B5 ligated exon product. (Bottom left) Northern blot of 100 μg of total cellular RNA isolated from HM410 yeast cells expressing wild type and W238 mutant ym LRSs. Hybridization was carried out with a [^{32}P]-labeled B4-B5 exon junction probe. Presence of the band indicates B4-B5 spliced product. (Bottom right) *In vitro* aminoacylation by the full-length wild type or Trp238 mutant ymLeuRSs. Aminoacylation reactions included 4 μM transcribed ymtRNA, 1 μM enzyme and 21 μM [^{3}H]-leucine (150 μCi/ml) and were initiated with 4 mM ATP. Symbols are: wild type (■), W238A (▼), W238C (Δ), and W238F (O). Error bars for each time point result from each reaction repeated in triplicate.

significantly lower levels than the wild type enzyme (Figure VII.15, bottom right). Thus, even these reduced levels of aminoacylation still meet an *in vivo* threshold that is necessary to support cell viability. It is also possible that the availability of appropriately modified native tRNA in the mitochondria elevates aminoacylation activity *in vivo* to an acceptable threshold levels.

Since the W238C ymLeuRS mutant failed to support mitochondrial splicing *in vivo,* we wondered if it would also compromise splicing in the isolated CP1 domain. We introduced the W238C mutation into ymCP1-βext LeuRS and tested its effect in our *in vitro* splicing assay. The W238C mutation significantly impeded processing of the bI4Δ1168 pre-RNA (Figure VII.16, top) and extent of formation of the products, bI4 (Figure VII.16, center) and B4-B5 (Figure VII.16, bottom), *in vitro.* Thus, the W238C mutation which abolished RNA splicing in the full length ymLeuRS, *in vivo,* is also critical to the isolated ymCP1 splicing domain. These combined results show that the Trp238 site in the splicing sensitive 'WIG' peptide requires a bulky aromatic residue for optimal interaction with the bI4 intron RNA. We hypothesize that the β-strand extension functionally diverged in ymLeuRS to adapt to its secondary alternate role in role in splicing, while maintaining essential aminoacylation activity at sufficient levels for allowing cell viability.

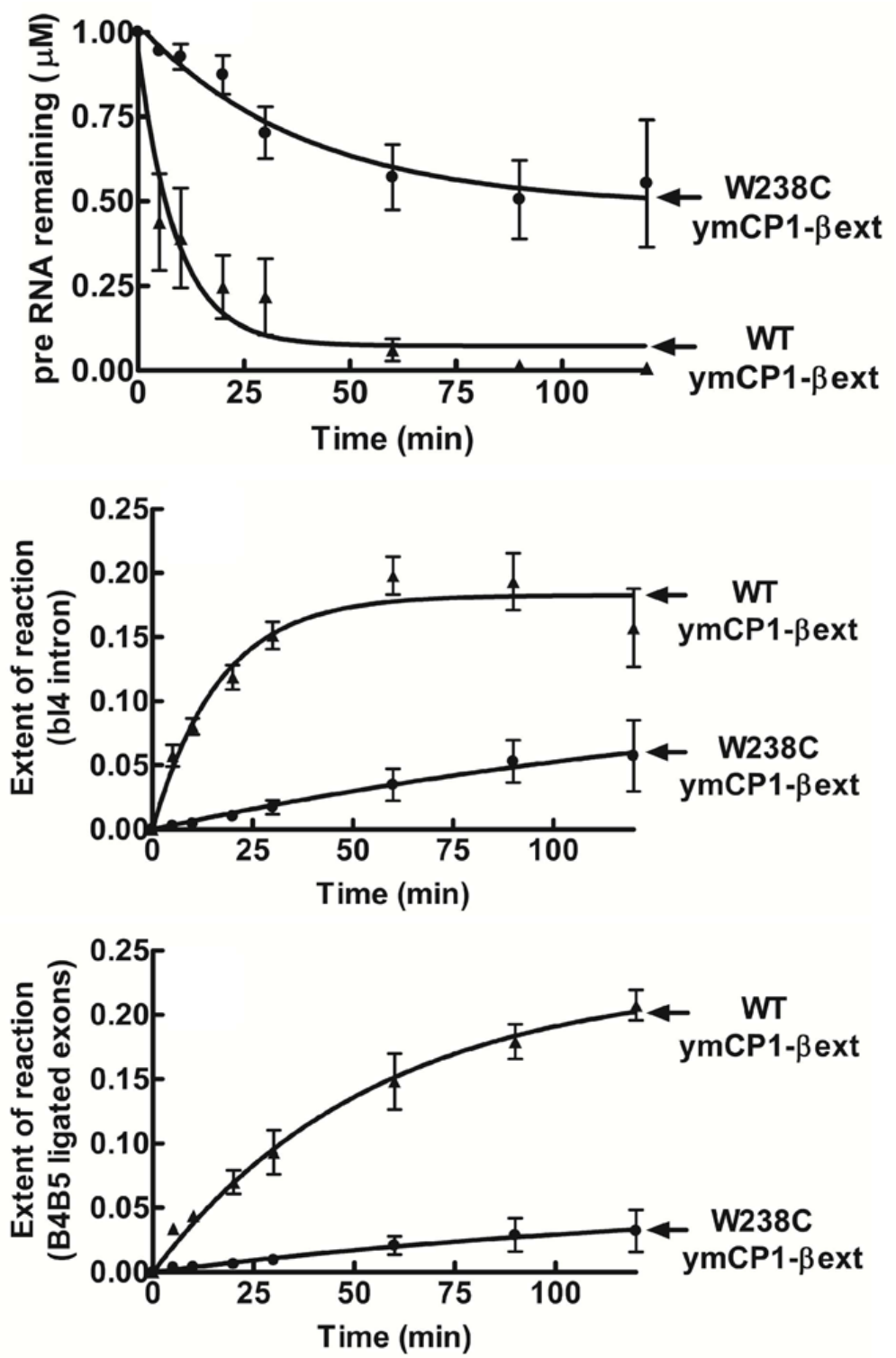

Figure VII.16. The Trp 238 mutation in the 'WIG' peptide abolishes splicing but maintains sufficient aminoacylation activity. Evaluation of *in vitro* bI4Δ1168 pre-RNA splicing with respect to (Top) processing of substrate pre-RNA, (Center) fraction of bI4 excised intron and (Bottom) fraction of the ligated B4-B5 exons. Splicing reactions incorporated 1 μM of substrate pre-RNA and 1 μM LeuRS and were initiated with 1 mM guanosine. Symbols are: WT ymCP1-βext (▲) and W238C ymCP1-βext (●). Error bars for each time point result from each reaction repeated in triplicate.

VII.4. Discussion

The bifunctional LeuRS is not only required for protein synthesis, but also as an auxiliary protein factor in the excision of two related bI4 and aI4α group I introns for the expression of the mitochondrial *cob* and *cox1α* genes. The nuclear encoded LeuRS and the intron encoded bI4 maturase work in concert in a ternary complex formed on the bI4 intron. A direct role of LeuRS in splicing of these two introns has been established, whereby LeuRS can independently bind to the bI4 intron and promote splicing (Rho and Martinis, 2000). Three different regions of the ymLeuRS have been reported to be important in the protein's RNA splicing activity: the CP1 amino acid editing domain (Rho, et al., 2002), the conserved 'WIG' signature sequence (Figure VII.1) (Li, et al., 1996) and the C-terminal domain (Hsu, et al., 2006; Li, et al., 1996) The yeast mitochondrial CP1 domain, isolated from the rest of the enzyme, has been shown to independently stimulate group I intron splicing *in vivo* (Rho, et al., 2002). We utilized the isolated CP1 domain from ymLeuRS with different lengths of its flanking β-strands to probe the adaptations of the protein that facilitate aminoacylation and RNA splicing.

The isolated ymCP1-βext LeuRS processed a minimized bI4 intron *in vitro*, unlike its counterpart from the *E. coli* enzyme. Interestingly however, the full-length *E. coli* LeuRS rescued bI4 intron splicing activity *in vivo*, similar to LeuRSs from other origins such as *M. tuberculosis* and human mitochondria (Houman, et al., 2000). Thus, although RNA splicing activity was proposed to be based on LeuRS's broadly conserved evolutionary features, the CP1 domain of the splicing ymLeuRS appears to be adapted to facilitate RNA processing compared to its non-splicing counterpart from *E. coli* LeuRS.

To accommodate its RNA splicing activity, our results suggested that the ymLeuRS CP1 domain had functional diverged. *In vitro*, the isolated ymCP1-β LeuRS failed to hydrolyze misacylated Ile-tRNA^{Leu}. Inclusion of the short β-extensions in the isolated

ymCP1-βext LeuRS enabled deacylation activity, but at significantly lower levels as compared to the editing active full-length protein. This contrasts with the homologous isolated CP1 construct from *E. coli* LeuRS (Betha, et al., 2007), where, inclusion of the β-strand extensions retained deacylation activity that was comparable to the full-length enzyme (Betha, et al., 2007). Previously, we showed that the robust and viable post-transfer editing activity of full-length ymLeuRS appears to be dispensable to cell viability (Karkhanis, et al., 2006). It is possible that yeast mitochondria have evolved to tolerate increased infidelity during translation. Alternatively, they may possess distinct alternate mechanisms to suppress mistakes, such as precisely controlling mitochondrial amino acid concentrations or increased discrimination between cognate and noncognate amino acids. Interestingly and unlike TyrRS (CYT18) (Cherniack, et al., 1990; Paukstelis, et al., 2008) LeuRS has not acquired an idiosyncratic domain or peptide insert that is dedicated to RNA splicing. Thus, we hypothesize that evolutionary pressures on ymLeuRS CP1 domain for dual functions in the cell compromised it amino acid editing to facilitate its secondary, but essential role of RNA splicing.

The β-strands and its extensions provide critical contacts between the discretely folded CP1 domain and the LeuRS main body (Cusack, et al., 2000). They also provide flexibility to the CP1 domain to facilitate transitions of the enzyme between the different stages of the aminoacylation reaction (Fukunaga and Yokoyama, 2005a; Tukalo, et al., 2005). In our investigation of the structure-function relationships that are responsible for LeuRS CP1-based adaptations for RNA splicing, we determined that the β-strand extensions of the CP1 domain significantly enhance *in vitro* RNA processing activity. Because inclusion of these short extensions had opposite effects on deacylation and RNA splicing in the ymCP1-βext LeuRS, we hypothesize that this region of LeuRS is differentially adapted to favor RNA splicing in ymLeuRS and in contrast, deacylation in the non-splicing *E. coli* LeuRS. Further mutational analysis in the aminoacylation-critical conserved 'WIG' peptide at the end of the

N-terminal β-strand, demonstrated that a bulky aromatic residue is a requirement at this site to maintain RNA splicing activity of the ymLeuRS CP1 domain.

Significantly, the mitochondrial and bacterial LeuRS conserved 'WIG' peptide was not sufficient to confer optimal splicing to the isolated ymCP1 domain and required the extensions of the β-strands into the canonical core to generate a splicing-active construct (ymCP1-βext). In the *E. coli* enzyme, these extensions contain flexible hinge motifs that have critical interactions with the tRNA during post-transfer editing (Tukalo, et al., 2005) and are essential to confer deacylation activity to the isolated CP1 domain (Betha, et al., 2007). In lieu of a splicing-specific peptide or domain in LeuRS, it is possible that the 'WIG' peptide and/or hinge regions intimately contact the intron RNA in the context of the isolated CP1 domain and full-length ymLeuRS. Direct or indirect interactions may facilitate RNA folding into a catalytically competent form. Because inclusion of these short extensions had only small effects on deacylation by ymCP1-βext LeuRS, yet significantly enhanced its RNA splicing activity, we hypothesize that this region of LeuRS is differentially adapted to favor RNA splicing in ymLeuRS. Significantly, this contrasts with our results with the non-splicing adapted *E. coli* LeuRS, which relied on these extensions for tRNA deacylation.

Previously, we had shown that the leucine-specific C-terminal domain (CTD) differentially adapted to accommodate RNA splicing and $tRNA^{Leu}$ aminoacylation (Hsu, et al., 2006). While in the non-splicing LeuRSs, deletion of the CTD abolishes aminoacylation, in the splicing ymLeuRS, the deletion enhances aminoacylation, but results in a splicing-inactive ternary complex of CTD-deletion mutant LeuRS : maturase : bI4 intron (Hsu, et al., 2006). Together, these results suggest that common regions of the protein, such as the β-strands, its extensions, the conserved 'WIG' peptide and the C-terminal domain are critical to interactions with both $tRNA^{Leu}$ and the bI4 intron and these have been the points where splicing LeuRSs have undergone differential adaptations.

The only other splicing-active AARS, TyrRS, uses newly acquired intron RNA-binding insertions to recognize highly conserved secondary and tertiary structural features of

group I introns. These insertions are distinct from the regions of the protein that bind $tRNA^{Tyr}$ (Paukstelis, et al., 2008). In contrast, LeuRS has not acquired any splicing-specific domain or peptide insertion. Key sites for editing remain intact. This LeuRS splicing factor relies on canonical features such as the CP1-domain-based 'WIG' peptide and the β-strand extensions, which are evolutionarily conserved among bacteria and mitochondrial LeuRSs (Figure VII.14). It is possible that within the pre-existing domains of LeuRS, splicing-sensitive molecular determinants are distinct from the ones that the protein uses for $tRNA^{Leu}$-binding. Interestingly also, while TyrRS is required for the splicing of a number of unrelated group I introns (Akins and Lambowitz, 1987; Cherniack, et al., 1990; Majumder, et al., 1989). LeuRS is required for the splicing of only two closely related yeast mitochondrial group I introns. Hence, it is possible that LeuRS recognizes idiosyncratic features of the bI4 and aI4α introns in addition to general structurally conserved features of the intron RNA substrate, facilitating formation of a catalytically-active RNA structure. Thus, to accommodate dual essential functions in aminoacylation and splicing, we propose that the ymLeuRS functionally diverged within the confines of the CP1 domain and other regions, including the C-terminal domain and the consensus 'WIG' motif.

Chapter VIII: Conclusion

Maintenenace of fidelity during protein synthesis involves the combined effort of several players, such as the AARSs (Mascarenhas, 2008) , EF-Tu (LaRiviere, et al., 2001) and the ribosome (Ogle, et al., 2002; Zaher and Green, 2009). Among these, the AARSs serve as the first and primary checkpoint. This ancient family of enzymes has remained conserved evolutionarily across species to perform the housekeeping functions of aminoacylating cognate tRNA (Ibba and Söll, 2000) and then when necessary, proofreading in order to ensure the production of correctly charged tRNAs (Mascarenhas, 2008). Although all AARSs essentially catalyze the aminoacylation reaction via overlapping 2-step reaction mechanisms, they are classified into class I and II enzymes, based on active site architectural and sequence differences (Arnez and Moras, 1997). Interestingly, several of the AARSs have also evolved to acquire secondary essential functions in the cell (Martinis, et al., 1999), such as the involvement of LeuRS and TyrRS in mitochondrial RNA splicing.

About half of the synthetases have evolved editing mechanisms that include both pre- (Baldwin and Berg, 1966; Fersht, 1977b) and post-transfer (Eldred and Schimmel, 1972; Fersht and Kaethner, 1976) editing. Interestingly, in LeuRSs across different species, distinct sets of molecular determinants drive the balance between pre- and post-transfer editing pathways (Martinis and Boniecki, 2010). My thesis research addressed key questions on the editing mechanisms and this balance between coexisting editing pathways in the ycLeuRS and also in the *E. coli* enzyme. In addition, I also studied the alternate but essential cellular role of the ymLeuRS in protein-assisted splicing of group I introns. Crystal structures (Cusack, et al., 2000) show that LeuRS possesses an exclusive domain, called the leucine-specific domain (LSD) that is critical in aminoacylation (Vu and Martinis, 2007). Utilizing a chimeric *H. pylori* LeuRS that contained the *E. coli* LSD, I also examined the interactions between this specific domain and $tRNA^{Leu}$ during aminoacylation.

LeuRSs contain a highly conserved threonine-rich editing pocket in the CP1 domain. Residues within this pocket serve as critical specificity determinants during the post-transfer editing reaction (Lincecum, et al., 2003; Mursinna, et al., 2001; Pang and Martinis, 2009; Zhai and Martinis, 2005). Mutations at specific sites within the conserved editing pocket give rise to editing-defective LeuRS mutants that lead to formation and accumulation of mischarged $tRNA^{Leu}$ and hence mistranslation. Accumulation of misfolded proteins have resulted in neurodegeneration in mouse (Lee, et al., 2006). Hence, in order to gain a better understanding of the intracellular effects of the editing defects in LeuRS, I devised a fluorescence-based *in vivo* assay that relies on split-GFP reassembly. The N- and C-terminal halves of GFP, each fused to a leucine zipper reassemble when expressed in *trans* in bacteria (Ghosh, 2000; Magliery, et al., 2005). The assay was designed such that proteins incorporated noncognate amino acids when the cells were grown on solid growth medium on Petri plates. The fluorescence of refolded GFP fragments was monitored in the presence of overexpressed LeuRS, either the wild type or an editing-defective mutant. In the case of the editing-defective LeuRS, mistranslation would lead to statistical substitutions of leucines within the leucine zippers by the noncognate amino acid that is incorporated in the growth medium. Since three of the four leucine positions absolutely require a leucine for dimerization of the zippers (Hu, et al., 1990), these statistical substitutions disrupt dimerization and hence, reassembly of the GFP fragments. This effect is manifested in decreased observable fluorescence.

Similar halo assays that rely on a zone of cell death around central wells filled with excess noncognate amino acids on solid growth media, have been previously used to study editing defects in LeuRS (Hellmann and Martinis, 2009; Karkhanis, et al., 2006; Rock, et al., 2007; Sarkar, et al., 2011). Importantly, these assays relied on an ‘all or none’ effect of LeuRS editing defects on cell viability. However, the GFP fluorescence-based halo assay

provides a more sophisticated and sensitive handle on studying a varied range of editing defective LeuRS mutants by allowing us to quantify the extent of mistranslation via fluorescence intensity changes. Furthermore, mass spectrometric analysis of the mistranslated leucine zipper peptides would furnish information about the products formed during such mistranslation. Thus the GFP fluorescence-based halo assay provides a valuable tool to quantitatively inspect the extent of editing defects for the different molecular determinants that are known to impact editing in LeuRS.

Drug design targeting the synthetases has exploited both the aminoacylation and the editing active sites of the enzymes. A novel class of benzoxaborole-based antifungals halts protein synthesis by targetting ycLeuRS. These new drugs are in clinical trials for the treatment of onychomycosis, a fungal disease of the toenail (Rock, et al., 2007). The conserved editing pocket of LeuRS also happens to be the drug-binding site for these antimicrobials. Our collaborators identified drug-resistant mutants within (Rock, et al., 2007) and outside (Sarkar, et al., 2011) the drug-binding/editing pocket. This provided us with the unique opportunity to dissect the role of elements outside the conserved core of the CP1 domain, in maintaining a functional editing activity in this enzyme.

My project focused on one such resistant site in the ycLeuRS, Asp 487 that lies outside the conserved editing/drug-binding pocket in a peptide insert, called I4 that is specific to fungal and archaeal LeuRSs, but absent in the bacterial enzymes. Biochemical experiments determined that drug-resistant mutants at this site (D487G and D487N) are also defective in hydrolyzing mischarged $tRNA^{Leu}$. In addition, while mutations at Asp 487 to positively charged arginine and lysine render the enzyme defunct in post-transfer editing, a homologous substitution by a glutamic acid rescues editing activity. Based on available crystal structures (Seiradake, et al., 2009) and our biochemical data, we identified a plausible salt-bridge interaction between Asp 487 and an arginine residue (Arg 316) within the editing

pocket. Double mutants that included charge swapping between these two positions rescued editing activity for only the D487K/R316D mutant ycLeuRS, suggesting that the longer side chains of an arginine or glutamic acid at either of these positions may juxtapose them in an orientation unsuitable for an effective salt-bridge interaction. From these results, I hypothesized that ycLeuRS relies on Asp 487 to form an electrostatic interaction with the arginine residue within the editing pocket, when the flexible I4 insert closes over the substrate-bound editing pocket in a cap-like fashion (Sarkar, et al., 2011).

Importantly, because the I4 insert is absent in the bacterial LeuRSs, this finding highlights a unique molecular determinant exclusively used by the fungal LeuRS and not by the bacterial enzyme. It also stresses the importance of evolutionarily acquired eukaryotic CP1 domain-based peptide insertions in finer mechanistic adaptations such as substrate stabilization within the CP1 domain editing pocket. Reliance of ycLeuRS on an idiosyncratic substrate stabilizing mechanism and plasticity within the editing/drug-binding pocket also presents exciting opportunities for designing more efficacious drugs that specifically target the pathogen editing pocket, while excluding the human counterpart.

Early reports suggested that while the *E. coli* LeuRS clears mistakes via the post-transfer editing pathway, ycLeuRS edits by the pre-transfer route. However, work in our's and other labs have shown that three distinct sets of mutations in the *E. coli* LeuRS, including one that completely deletes the CP1 editing domain, unmask an inherent pre-transfer editing activity in the enzyme (Boniecki, et al., 2008; Chen, et al., 2001; Williams and Martinis, 2006). On the other hand, the ycLeuRS effectively hydrolyzes mischarged $tRNA^{Leu}$ (Lincecum, et al., 2003). These findings raise questions about the redundancy of multiple coexisting editing pathways in the same enzyme. Which pathway, if any, predominates and what cellular cues or molecular determinants within these enzymes control the balance

between these editing pathways are important questions that need to be addressed in an enzyme and species-specific manner.

In a second project on the ycLeuRS editing pathways, I determined that the identity of the noncognate amino acid can dictate the shift between co-existing pre- and post-transfer editing pathways (Sarkar and Martinis, 2011). While, the ycleuRS misactivates both the noncognate isoleucine and methionine, the enzyme effectively clears $tRNA^{Leu}$ mischarged with isoleucine, but its post-transfer editing activity against $tRNA^{Leu}$ mischarged with methionine was significantly impaired *in vitro.* However, no significant accumulation of Met-$tRNA^{Leu}$ was detected *in vitro*. Instead, we observed robust enzyme-catalyzed pre-transfer editing activity against the methionyl-adenylate, in the absence of tRNA. The presence of cognate $tRNA^{Leu}$ increased the overall editing activity of ycLeuRS against methionine, but not against isoleucine.

Similar to the *E. coli* enzyme, the ycLeuRS also possesses functional pre- and post-transfer editing and we hypothesize that these multiple pathways are not redundant but provide multiple checkpoints to the cell to maintain fidelity against the chemically distinct noncognate amino acids that the enzyme misactivates. However, the location and the precise molecular determinants of pre-transfer editing in ycLeuRS remain unclear. Nonetheless, this finding reflects the immense diversity of editing activities in the ancient AARSs, acquired throughout a long evolutionary period. It is critical to decipher the cellular cues that regulate the balance between the multiple pathways, since that will provide us high resolution insights into the natural pressures of AARS evolution.

The ymLeuRS is one of the two AARSs known to assist group I intron splicing *in vivo* (Labouesse, 1990). The other splicing AARS is TyrRS (Akins and Lambowitz, 1987). Our lab has shown that the two proteins required for splicing group I introns, the nuclear-encoded ymLeuRS and the intron-encoded bI4 maturase, can independently bind to the group

I intron and stimulate splicing (Rho and Martinis, 2000). Several splicing-sensitive sites have been implicated in the ymLeuRS, including the CP1 domain (Rho, et al., 2002) and the C-terminal domain (Hsu, et al., 2006).

A part of my thesis research efforts was dedicated towards identifying and understanding the adaptations that the ymLeuRS has undergone in and around the CP1 domain to accommodate its dual roles of splicing and aminoacylation (Sarkar, et al., 2012). Previous work from our lab had shown that the isolated CP1 doamin stimulated RNA splicing *in vivo* (Rho, et al., 2002).

In my project, I determined that the connecting β-strands and its extensions into the LeuRS main body are absolutely essential to confer splicing activity to the isolated ymCP1 domain, possibly because these long extensions enable the intron RNA to fold or conform into a competent splicing-active structure. However, these linkers and the extensions failed to confer splicing activity to the homologous isolated *E. coli* CP1 domain, although the full-length *E. coli* enzyme rescued splicing activity, similar to other nonsplicing LeuRSs (Houman, et al., 2000). This suggested that although LeuRS uses its evolutionarily conserved features for splicing, the ymCP1 domain is specifically adapted to accommodate the secondary role.

Significantly however, the isolated ymCP1 domain was inactive in hydrolyzing mischarged $tRNA^{Leu}$, unlike its *E. coli* counterpart. The inclusion of the β-strands and its extensions only weakly stimulated the hydrolytic editing activity. We hypothesized that, in order to accommodate splicing, the ymCP1 has functionally diverged within the CP1 domain and the connecting β-strands and extensions, at some expense to the enzyme's hydrolytic editing activity.

We further scrutinized the conserved 'WIG' peptide at the N-terminal β strand, and determined that mutation of the tryptophan to a cysteine generated a splicing-inactive mutant

ymLeuRS (Li, et al., 1996) that maintained threshold levels of aminoacylation sufficient to support cell viability. I hypothesized that the 'WIG' peptide is critical to the ymLeuRS's splicing activity because it has important interactions with the intron RNA and also correlates with the β-strand enabled movements of the CP1 domain with respect to the main body. Thus, the 'WIG' peptide which has important interactions with the tRNA in nonsplicing LeuRSs, continues to be important in splicing. Interestingly however, in the splicing ymLeuRS, this peptide appears to be more critical to splicing than aminoacylation, unlike the nonsplicing LeuRSs where mutations within the 'WIG' peptide abolish aminoacylation. Thus, these results show that the ymLeuRS, which has not acquired any apparent splicing-specific insertion, relies upon its canonical features for its splicing activity and has undergone adaptations within the CP1 domain, the connecting β-strands and extensions and the conserved 'WIG' peptide to accommodate RNA splicing, while maintaining functional levels of aminoacylation.

Finally, I have worked on LeuRS-tRNA^{Leu} interactions via the LSD. Evolutionarily, the LSD was inserted in some bacterial LeuRSs just prior to the catalytically critical 'KMSKS' loop (Cusack, et al., 2000). Deletion of the LSD abolishes aminoacylation (Vu and Martinis, 2007). In this project I addressed the question as to what advantanges the LSD provides to those LeuRSs that acquired the domain as opposed to those which did not. The *H. pylori* LeuRS was selected as a model since this bacterial enzyme completely lacks the LSD. A chimeric *H. pylori* LeuRS was constructed that contained the LS domain from the *E. coli* enzyme. Biochemical analysis showed that insertion of the LSD provided a significant advantage to the chimeric *H. pylori* LeuRS in aminoacylating the non-native *E. coli* tRNA^{Leu}. Aminoacylation kinetic analysis and tRNA^{Leu} binding to the chimeric enzyme showed that enhanced aminoacylation was primarily due to an increased affinity of the *E. coli* tRNA^{Leu} to the enzyme. I hypothesized that insertion of the LSD may directly have stabilizing

interactions with the 3′-end of the tRNA or may indirectly impact the mobility of the neighboring 'KMKS' loop that is critical to ATP-binding and amino acid activation.

In summary, my PhD thesis research focused on LeuRS-based translational fidelity, drug-resistance and a novel RNA splicing reaction. In addition, critical enzyme-tRNA interactions during the aminoacylation reaction were also investigated in LeuRS. I have dissected the editing activities of LeuRS, in terms of substrate-binding mechanism, shifting balance between diverse editing pathways, and assay development to study the intracellular impact of specific editing defects. These studies provide valuable molecular level insights into the conservation, diversity and adaptations within the editing active site of LeuRS. My studies on LeuRS-assisted RNA splicing significantly enhance our understanding of the overlaps and the diversities that LeuRS acquired to accommodate its dual roles of RNA splicing and aminoacylation.

References

Ahel, I., Stathopoulos, C., Ambrogelly, A., Sauerwald, A., Toogood, H., Hartsch, T. and Söll, D. (2002) "Cysteine activation is an inherent *in vitro* property of prolyl-tRNA synthetases." J. Biol. Chem. 277(38): 34743-34748

Ahel, I., Korencic, D., Ibba, M. and Söll, D. (2003) "Trans-editing of mischarged tRNAs." Proc. Natl. Acad. Sci. U. S. A. 100(26): 15422-15427

Akins, R.A. and Lambowitz, A.M. (1987) "A protein required for splicing group I introns in *Neurospora* mitochondria is mitochondrial tyrosyl-tRNA synthetase or a derivative thereof." Cell. 50(3): 331-345

An, S. and Musier-Forsyth, K. (2005) "Cys-tRNA^{Pro} editing by *Haemophilus influenzae* YbaK via a novel synthetase●YbaK●tRNA ternary complex." J. Biol. Chem. 280(41): 34465-34472

Antonellis, A., Ellsworth, R.E., Sambuughin, N., Puls, I., Abel, A., Lee-Lin, S.Q., Jordanova, A., Kremensky, I., Christodoulou, K., Middleton, L.T., Sivakumar, K., Ionasescu, V., Funalot, B., Vance, J.M., Goldfarb, L.G., Fischbeck, K.H. and Green, E.D. (2003) "Glycyl tRNA synthetase mutations in Charcot-Marie-Tooth disease type 2D and distal spinal muscular atrophy type V." Am. J. Hum. Genet. 72(5): 1293-1299

Arnez, J.G., Harris, D.C., Mitschler, A., Rees, B., Francklyn, C.S. and Moras, D. (1995) "Crystal structure of histidyl-tRNA synthetase from *Escherichia coli* complexed with histidyl-adenylate." EMBO J. 14(17): 4143-4155

Arnez, J.G. and Steitz, T.A. (1996) "Crystal structures of three misacylating mutants of *Escherichia coli* glutaminyl-tRNA synthetase complexed with tRNA^{Gln} and ATP." Biochemistry. 35(47): 14725-14733

Arnez, J.G., Augustine, J.G., Moras, D. and Francklyn, C.S. (1997) "The first step of aminoacylation at the atomic level in histidyl-tRNA synthetase." Proc. Natl. Acad. Sci. U. S. A. 94(14): 7144-7149

Arnez, J.G. and Moras, D. (1997) "Structural and functional considerations of the aminoacylation reaction." Trends Biochem. Sci. 22(6): 211-216

Asahara, H., Himeno, H., Tamura, K., Hasegawa, T., Watanabe, K. and Shimizu, M. (1993) "Recognition nucleotides of *Escherichia coli* tRNA^{Leu} and its elements facilitating discrimination from tRNA^{Ser} and tRNA^{Tyr}." J. Mol. Biol. 231(2): 219-229

Asahara, H., Nameki, N. and Hasegawa, T. (1998) "*In vitro* selection of RNAs aminoacylated by *Escherichia coli* leucyl-tRNA synthetase." J. Mol. Biol. 283(3): 605-618

Baker, S.J., Zhang, Y.K., Akama, T., Lau, A., Zhou, H., Hernandez, V., Mao, W., Alley, M.R., Sanders, V. and Plattner, J.J. (2006) "Discovery of a new boron-containing antifungal agent, 5-fluoro-1,3-dihydro-1-hydroxy-2,1- benzoxaborole (AN2690), for the potential treatment of onychomycosis." J. Med. Chem. 49(15): 4447-4450

Baldwin, A.N. and Berg, P. (1966) "Transfer ribonucleic acid-induced hydrolysis of valyladenylate bound to isoleucyl ribonucleic acid synthetase." J. Biol. Chem. 241(4): 839-845

Banci, L., Bertini, I., Durazo, A., Girotto, S., Gralla, E.B., Martinelli, M., Valentine, J.S., Vieru, M. and Whitelegge, J.P. (2007) "Metal-free superoxide dismutase forms soluble oligomers under physiological conditions: a possible general mechanism for familial ALS." Proc. Natl. Acad. Sci. U. S. A. 104(27): 11263-11267

Bass, B.L. and Cech, T.R. (1986) "Ribozyme inhibitors: deoxyguanosine and dideoxyguanosine are competitive inhibitors of self-splicing of the *Tetrahymena* ribosomal ribonucleic acid precursor." Biochemistry. 25(16): 4473-4477

Beebe, K., Ribas De Pouplana, L. and Schimmel, P. (2003) "Elucidation of tRNA-dependent editing by a class II tRNA synthetase and significance for cell viability." EMBO J. 22(3): 668-675

Belrhali, H., Yaremchuk, A., Tukalo, M., Berthet-Colominas, C., Rasmussen, B., Bosecke, P., Diat, O. and Cusack, S. (1995) "The structural basis for seryl-adenylate and Ap4A synthesis by seryl-tRNA synthetase." Structure. 3(4): 341-352

Betha, A.K., Williams, A.M. and Martinis, S.A. (2007) "Isolated CP1 domain of *Escherichia coli* leucyl-tRNA synthetase is dependent on flanking hinge motifs for amino acid editing activity." Biochemistry. 46(21): 6258-6267

Beuning, P.J. and Musier-Forsyth, K. (2000) "Hydrolytic editing by a class II aminoacyl-tRNA synthetase." Proc. Natl. Acad. Sci. U. S. A. 97(16): 8916-8920

Biou, V., Yaremchuk, A., Tukalo, M. and Cusack, S. (1994) "The 2.9 Å crystal structure of *T. thermophilus* seryl-tRNA synthetase complexed with $tRNA^{Ser}$." Science. 263(5152): 1404-1410

Bishop, A.C., Nomanbhoy, T.K. and Schimmel, P. (2002) "Blocking site-to-site translocation of a misactivated amino acid by mutation of a class I tRNA synthetase." Proc. Natl. Acad. Sci. U. S. A. 99(2): 585-590

Björk, G.(1996) "*Escherichia coli* and *Samonella typhimurium*: Cellular and Molecular Biology. (Neidhardt, F., Ingraham, J., L., and Curtiss, R., eds). American Society for Microbiology Press, Washington, DC.

Boniecki, M.T., Vu, M.T., Betha, A.K. and Martinis, S.A. (2008) "CP1-dependent partitioning of pretransfer and posttransfer editing in leucyl-tRNA synthetase." Proc. Natl. Acad. Sci. U S A. 105(49): 19223-19228

Boniecki, M.T., Rho, S.B., Tukalo, M., Hsu, J.L., Romero, E.P. and Martinis, S.A. (2009) "Leucyl-tRNA synthetase-dependent and -independent activation of a group I intron." J. Biol. Chem. 284(39): 26243-26250

Borel, F., Vincent, C., Leberman, R. and Hartlein, M. (1994) "Seryl-tRNA synthetase from *Escherichia coli*: implication of its N-terminal domain in aminoacylation activity and specificity." Nucleic Acids Res. 22(15): 2963-2969

Breitschopf, K., Achsel, T., Busch, K. and Gross, H.J. (1995) "Identity elements of human $tRNA^{Leu}$: structural requirements for converting human $tRNA^{Ser}$ into a leucine acceptor *in vitro*." Nucleic Acids Res. 23(18): 3633-3637

Brown, M.J., Carter, P.S., Fenwick, A.S., Fosberry, A.P., Hamprecht, D.W., Hibbs, M.J., Jarvest, R.L., Mensah, L., Milner, P.H., O'Hanlon, P.J., Pope, A.J., Richardson, C.M., West, A. and Witty, D.R. (2002) "The antimicrobial natural product chuangxinmycin and some synthetic analogues are potent and selective inhibitors of bacterial tryptophanyl tRNA synthetase." Bioorg. Med. Chem. Lett. 12(21): 3171-3174

Buehner, M., Ford, G.C., Olsen, K.W., Moras, D. and Rossman, M.G. (1974) "Three-dimensional structure of D-glyceraldehyde-3-phosphate dehydrogenase." J. Mol. Biol. 90(1): 25-49

Bullock, T.L., Uter, N., Nissan, T.A. and Perona, J.J. (2003) "Amino acid discrimination by a class I aminoacyl-tRNA synthetase specified by negative determinants." J. Mol. Biol. 328(2): 395-408

Burke, J.M. (1988) "Molecular genetics of group I introns: RNA structures and protein factors required for splicing--a review." Gene. 73(2): 273-294

Caprara, M.G., Mohr, G. and Lambowitz, A.M. (1996) "A tyrosyl-tRNA synthetase protein induces tertiary folding of the group I intron catalytic core." J. Mol. Biol. 257(3): 512-531

Cavarelli, J., Eriani, G., Rees, B., Ruff, M., Boeglin, M., Mitschler, A., Martin, F., Gangloff, J., Thierry, J.C. and Moras, D. (1994) "The active site of yeast aspartyl-tRNA synthetase: structural and functional aspects of the aminoacylation reaction." EMBO J. 13(2): 327-337

Cavarelli, J., Delagoutte, B., Eriani, G., Gangloff, J. and Moras, D. (1998) "L-arginine recognition by yeast arginyl-tRNA synthetase." EMBO J. 17(18): 5438-5448

Cech, T.R. (1987) "The chemistry of self-splicing RNA and RNA enzymes." Science. 236(4808): 1532-1539

Cech, T.R. (1988) "Conserved sequences and structures of group I introns: building an active site for RNA catalysis--a review." Gene. 73(2): 259-271

Cech, T.R. (1990) "Self-splicing of group I introns." Annu. Rev. Biochem. 59(543-568

Cech, T.R., Damberger, S.H. and Gutell, R.R. (1994) "Representation of the secondary and tertiary structure of group I introns." Nat. Struct. Biol. 1(5): 273-280

Chadee, A.B., Bhaskaran, H. and Russell, R. (2010) "Protein roles in group I intron RNA folding: the tyrosyl-tRNA synthetase CYT-18 stabilizes the native state relative to a long-lived misfolded structure without compromising folding kinetics." J. Mol. Biol. 395(3): 656-670

Chen, J.F., Guo, N.N., Li, T., Wang, E.D. and Wang, Y.L. (2000) "CP1 domain in *Escherichia coli* leucyl-tRNA synthetase is crucial for its editing function." Biochemistry. 39(22): 6726-6731

Chen, J.F., Li, T., Wang, E.D. and Wang, Y.L. (2001) "Effect of alanine-293 replacement on the activity, ATP binding, and editing of *Escherichia coli* leucyl-tRNA synthetase." Biochemistry. 40(5): 1144-1149

Chen, X., Ma, J.J., Tan, M., Yao, P., Hu, Q.H., Eriani, G. and Wang, E.D. (2011) "Modular pathways for editing non-cognate amino acids by human cytoplasmic leucyl-tRNA synthetase." Nucleic Acids Res. 39(1): 235-247

Cherniack, A.D., Garriga, G., Kittle, J.D., Jr., Akins, R.A. and Lambowitz, A.M. (1990) "Function of *Neurospora* mitochondrial tyrosyl-tRNA synthetase in RNA splicing requires an idiosyncratic domain not found in other synthetases." Cell. 62(4): 745-755

Cusack, S., Berthet-Colominas, C., Hartlein, M., Nassar, N. and Leberman, R. (1990) "A second class of synthetase structure revealed by X-ray analysis of *Escherichia coli* seryl-tRNA synthetase at 2.5 Å." Nature. 347(6290): 249-255

Cusack, S. (1997) "Aminoacyl-tRNA synthetases." Curr Opin Struct Biol. 7(6): 881-889

Cusack, S., Yaremchuk, A. and Tukalo, M. (2000) "The 2 Å crystal structure of leucyl-tRNA synthetase and its complex with a leucyl-adenylate analogue." EMBO J. 19(10): 2351-2361

Davies, R.W., Waring, R.B., Ray, J.A., Brown, T.A. and Scazzocchio, C. (1982) "Making ends meet: a model for RNA splicing in fungal mitochondria." Nature. 300(5894): 719-724

De La Salle, H., Jacq, C. and Slonimski, P.P. (1982) "Critical sequences within mitochondrial introns: pleiotropic mRNA maturase and cis-dominant signals of the box intron controlling reductase and oxidase." Cell. 28(4): 721-732

Delahodde, A., Goguel, V., Becam, A.M., Creusot, F., Perea, J., Banroques, J. and Jacq, C. (1989) "Site-specific DNA endonuclease and RNA maturase activities of two homologous intron-encoded proteins from yeast mitochondria." Cell. 56(3): 431-441

Dhawale, S., Hanson, D.K., Alexander, N.J., Perlman, P.S. and Mahler, H.R. (1981) "Regulatory interactions between mitochondrial genes: interactions between two mosaic genes." Proc. Natl. Acad. Sci. U. S. A. 78(3): 1778-1782

Dock-Bregeon, A., Sankaranarayanan, R., Romby, P., Caillet, J., Springer, M., Rees, B., Francklyn, C.S., Ehresmann, C. and Moras, D. (2000) "Transfer RNA-mediated editing in threonyl-tRNA synthetase. The class II solution to the double discrimination problem." Cell. 103(6): 877-884

Dock-Bregeon, A.C., Rees, B., Torres-Larios, A., Bey, G., Caillet, J. and Moras, D. (2004) "Achieving error-free translation; the mechanism of proofreading of threonyl-tRNA synthetase at atomic resolution." Mol. Cell. 16(3): 375-386

Dulic, M., Cvetesic, N., Perona, J.J. and Gruic-Sovulj, I. (2010) "Partitioning of tRNA-dependent editing between pre- and post-transfer pathways in class I aminoacyl-tRNA synthetases." J. Biol. Chem. 285(31): 23799-23809

Eldred, E.W. and Schimmel, P.R. (1972) "Rapid deacylation by isoleucyl transfer ribonucleic acid synthetase of isoleucine-specific transfer ribonucleic acid aminoacylated with valine." J. Biol. Chem. 247(9): 2961-2964

Englisch, S., Englisch, U., von der Haar, F. and Cramer, F. (1986) "The proofreading of hydroxy analogues of leucine and isoleucine by leucyl-tRNA synthetases from *E. coli* and yeast." Nucleic Acids Res. 14(19): 7529-7539

Eriani, G., Delarue, M., Poch, O., Gangloff, J. and Moras, D. (1990) "Partition of tRNA synthetases into two classes based on mutually exclusive sets of sequence motifs." Nature. 347(6289): 203-206

Fersht, A.R. and Kaethner, M.M. (1976) "Enzyme hyperspecificity. Rejection of threonine by the valyl-tRNA synthetase by misacylation and hydrolytic editing." Biochemistry. 15(15): 3342-3346

Fersht, A.R.(1977a) "Enzyme structure and mechanism" W. H. Freeman and Company limited, 283

Fersht, A.R. (1977b) "Editing mechanisms in protein synthesis. Rejection of valine by the isoleucyl-tRNA synthetase." Biochemistry. 16(5): 1025-1030

Fersht, A.R. and Dingwall, C. (1979a) "Establishing the misacylation/deacylation of the tRNA pathway for the editing mechanism of prokaryotic and eukaryotic valyl-tRNA synthetases." Biochemistry. 18(7): 1238-1245

Fersht, A.R. and Dingwall, C. (1979b) "An editing mechanism for the methionyl-tRNA synthetase in the selection of amino acids in protein synthesis." Biochemistry. 18(7): 1250-1256

Fersht, A.R., Knill-Jones, J.W., Bedouelle, H. and Winter, G. (1988) "Reconstruction by site-directed mutagenesis of the transition state for the activation of tyrosine by the tyrosyl-tRNA synthetase: a mobile loop envelopes the transition state in an induced-fit mechanism." Biochemistry. 27(5): 1581-1587

First, E.A. and Fersht, A.R. (1995) "Analysis of the role of the KMSKS loop in the catalytic mechanism of the tyrosyl-tRNA synthetase using multimutant cycles." Biochemistry. 34(15): 5030-5043

Francklyn, C. and Schimmel, P. (1989) "Aminoacylation of RNA minihelices with alanine." Nature. 337(6206): 478-481

Fukai, S., Nureki, O., Sekine, S., Shimada, A., Tao, J., Vassylyev, D.G. and Yokoyama, S. (2000) "Structural basis for double-sieve discrimination of L-valine from L-isoleucine and L-threonine by the complex of $tRNA^{Val}$ and valyl-tRNA synthetase." Cell. 103(5): 793-803

Fukunaga, R. and Yokoyama, S. (2005a) "Aminoacylation complex structures of leucyl-tRNA synthetase and $tRNA^{Leu}$ reveal two modes of discriminator-base recognition." Nat. Struct. Mol. Biol. 12(10): 915-922

Fukunaga, R. and Yokoyama, S. (2005b) "Crystal structure of leucyl-tRNA synthetase from the archaeon *Pyrococcus horikoshii* reveals a novel editing domain orientation." J. Mol. Biol. 346(1): 57-71

Fukunaga, R. and Yokoyama, S. (2006) "Structural basis for substrate recognition by the editing domain of isoleucyl-tRNA synthetase." J. Mol. Biol. 359(4): 901-912

Fuller, A.T., Mellows, G., Woolford, M., Banks, G.T., Barrow, K.D. and Chain, E.B. (1971) "Pseudomonic acid: an antibiotic produced by *Pseudomonas fluorescens*." Nature. 234(5329): 416-417

Ghosh, I., Hamilton, A., D., and Regan, L. (2000) "Antiparallel leucine zipper-directed protein reassembly: application to green fluorescent protein." J. Am. Chem. Soc. 122(23): 5658-5659

Giegé, R., Sissler, M. and Florentz, C. (1998) "Universal rules and idiosyncratic features in tRNA identity." Nucleic Acids Res. 26(22): 5017-5035

Grandori, R., Struck, K., Giovanielli, K. and Carey, J. (1997) "A three-step PCR protocol for construction of chimeric proteins." Protein Eng. 10(9): 1099-1100

Gruic-Sovulj, I., Uter, N., Bullock, T. and Perona, J.J. (2005) "tRNA-dependent aminoacyl-adenylate hydrolysis by a nonediting class I aminoacyl-tRNA synthetase." J. Biol. Chem. 280(25): 23978-23986

Gruic-Sovulj, I., Rokov-Plavec, J. and Weygand-Durasevic, I. (2007) "Hydrolysis of non-cognate aminoacyl-adenylates by a class II aminoacyl-tRNA synthetase lacking an editing domain." FEBS Lett. 581(26): 5110-5114

Guo, M., Yang, X.L. and Schimmel, P. (2010) "New functions of aminoacyl-tRNA synthetases beyond translation." Nat. Rev. Mol. Cell. Biol. 11(9): 668-674

Hale, S.P., Auld, D.S., Schmidt, E. and Schimmel, P. (1997) "Discrete determinants in transfer RNA for editing and aminoacylation." Science. 276(5316): 1250-1252

Hati, S., Ziervogel, B., Sternjohn, J., Wong, F.C., Nagan, M.C., Rosen, A.E., Siliciano, P.G., Chihade, J.W. and Musier-Forsyth, K. (2006) "Pre-transfer editing by class II prolyl-tRNA synthetase: role of aminoacylation active site in "selective release" of noncognate amino acids." J. Biol. Chem. 281(38): 27862-27872

Hellmann, R.A. and Martinis, S.A. (2009) "Defects in transient tRNA translocation bypass tRNA synthetase quality control mechanisms." J. Biol. Chem. 284(17): 11478-11484

Hendrickson, T.L., Nomanbhoy, T.K., de Crecy-Lagard, V., Fukai, S., Nureki, O., Yokoyama, S. and Schimmel, P. (2002) "Mutational separation of two pathways for editing by a class I tRNA synthetase." Mol. Cell. 9(2): 353-362

Herbert, C.J., Labouesse, M., Dujardin, G. and Slonimski, P.P. (1988) "The NAM2 proteins from *S. cerevisiae* and *S. douglasii* are mitochondrial leucyl-tRNA synthetases, and are involved in mRNA splicing." EMBO J. 7(2): 473-483

Hopfield, J.J. (1974) "Kinetic proofreading: a new mechanism for reducing errors in biosynthetic processes requiring high specificity." Proc. Natl. Acad. Sci. U. S. A. 71(10): 4135-4139

Hou, Y.M., Shiba, K., Mottes, C. and Schimmel, P. (1991) "Sequence determination and modeling of structural motifs for the smallest monomeric aminoacyl-tRNA synthetase." Proc. Natl. Acad. Sci. U. S. A. 88(3): 976-980

Hou, Y.M., Westhof, E. and Giegé, R. (1993) "An unusual RNA tertiary interaction has a role for the specific aminoacylation of a transfer RNA." Proc. Natl. Acad. Sci. U. S. A. 90(14): 6776-6780

Houman, F., Rho, S.B., Zhang, J., Shen, X., Wang, C.C., Schimmel, P. and Martinis, S.A. (2000) "A prokaryote and human tRNA synthetase provide an essential RNA splicing function in yeast mitochondria." Proc. Natl. Acad. Sci. U. S. A. 97(25): 13743-13748

Hountondji, C., Dessen, P. and Blanquet, S. (1986) "Sequence similarities among the family of aminoacyl-tRNA synthetases." Biochimie. 68(9): 1071-1078

Hsu, J.L., Rho, S.B., Vannella, K.M. and Martinis, S.A. (2006) "Functional divergence of a unique C-terminal domain of leucyl-tRNA synthetase to accommodate its splicing and aminoacylation roles." J. Biol. Chem. 281(32): 23075-23082

Hsu, J.L. and Martinis, S.A. (2008) "A flexible peptide tether controls accessibility of a unique C-terminal RNA-binding domain in leucyl-tRNA synthetases." J. Mol. Biol. 376(2): 482-491

Hu, J.C., O'Shea, E.K., Kim, P.S. and Sauer, R.T. (1990) "Sequence requirements for coiled-coils: analysis with lambda repressor-GCN4 leucine zipper fusions." Science. 250(4986): 1400-1403

Huang, H.R., Rowe, C.E., Mohr, S., Jiang, Y., Lambowitz, A.M. and Perlman, P.S. (2005) "The splicing of yeast mitochondrial group I and group II introns requires a DEAD-box protein with RNA chaperone function." Proc. Natl. Acad. Sci. U. S. A. 102(1): 163-168

Hughes, J. and Mellows, G. (1978) "Inhibition of isoleucyl-transfer ribonucleic acid synthetase in *Escherichia coli* by pseudomonic acid." Biochem. J. 176(1): 305-318

Ibba, M., Hong, K.W., Sherman, J.M., Sever, S. and Söll, D. (1996) "Interactions between tRNA identity nucleotides and their recognition sites in glutaminyl-tRNA synthetase determine the cognate amino acid affinity of the enzyme." Proc. Natl. Acad. Sci. U. S. A. 93(14): 6953-6958

Ibba, M., Morgan, S., Curnow, A.W., Pridmore, D.R., Vothknecht, U.C., Gardner, W., Lin, W., Woese, C.R. and Söll, D. (1997) "A euryarchaeal lysyl-tRNA synthetase: resemblance to class I synthetases." Science. 278(5340): 1119-1122

Ibba, M. and Söll, D. (2000) "Aminoacyl-tRNA synthesis." Annu. Rev. Biochem. 69(617-650

Ibba, M., Francklyn, C., and Cusack, S., Eds.(2005) "Aminoacyl-tRNA Synthetases" Landes Bioscience, Georgetown, TX.

Jakubowski, H. (1999) "Misacylation of $tRNA^{Lys}$ with noncognate amino acids by lysyl-tRNA synthetase." Biochemistry. 38(25): 8088-8093

Jordanova, A., Irobi, J., Thomas, F.P., Van Dijck, P., Meerschaert, K., Dewil, M., Dierick, I., Jacobs, A., De Vriendt, E., Guergueltcheva, V., Rao, C.V., Tournev, I., Gondim, F.A., D'Hooghe, M., Van Gerwen, V., Callaerts, P., Van Den Bosch, L., Timmermans, J.P., Robberecht, W., Gettemans, J., Thevelein, J.M., De Jonghe, P., Kremensky, I. and

Timmerman, V. (2006) "Disrupted function and axonal distribution of mutant tyrosyl-tRNA synthetase in dominant intermediate Charcot-Marie-Tooth neuropathy." Nat. Genet. 38(2): 197-202

Karimova, G., Pidoux, J., Ullmann, A. and Ladant, D. (1998) "A bacterial two-hybrid system based on a reconstituted signal transduction pathway." Proc. Natl. Acad. Sci. U. S. A. 95(10): 5752-5756

Karkhanis, V.A., Boniecki, M.T., Poruri, K. and Martinis, S.A. (2006) "A viable amino acid editing activity in the leucyl-tRNA synthetase CP1-splicing domain is not required in the yeast mitochondria." J. Biol. Chem. 281(44): 33217-33225

Karkhanis, V.A., Mascarenhas, A.P. and Martinis, S.A. (2007) "Amino acid toxicities of *Escherichia coli* that are prevented by leucyl-tRNA synthetase amino acid editing." J. Bacteriol. 189(23): 8765-8768

Kim, H.Y., Ghosh, G., Schulman, L.H., Brunie, S. and Jakubowski, H. (1993) "The relationship between synthetic and editing functions of the active site of an aminoacyl-tRNA synthetase." Proc. Natl. Acad. Sci. U. S. A. 90(24): 11553-11557

Ko, Y.G., Kang, Y.S., Kim, E.K., Park, S.G. and Kim, S. (2000) "Nucleolar localization of human methionyl-tRNA synthetase and its role in ribosomal RNA synthesis." J. Cell. Biol. 149(3): 567-574

Kobayashi, T., Takimura, T., Sekine, R., Kelly, V.P., Kamata, K., Sakamoto, K., Nishimura, S. and Yokoyama, S. (2005) "Structural snapshots of the KMSKS loop rearrangement for amino acid activation by bacterial tyrosyl-tRNA synthetase." J. Mol. Biol. 346(1): 105-117

Konishi, M., Nishio, M., Saitoh, K., Miyaki, T., Oki, T., and Kawaguchi, H. (1989) "Cispentacin, a new antifungal antibiotic. I. Production, isolation, physico-chemical properties and structure." J. Antibiot.(Tokyo). 42(1749-1755

Konrad, I. and Roschenthaler, R. (1977) "Inhibition of phenylalanine tRNA synthetase from *Bacillus subtilis* by ochratoxin A." FEBS Lett. 83(2): 341-347

Kunst, C.B., Mezey, E., Brownstein, M.J. and Patterson, D. (1997) "Mutations in SOD1 associated with amyotrophic lateral sclerosis cause novel protein interactions." Nat. Genet. 15(1): 91-94

Kushner, J.P., Boll, D., Quagliana, J. and Dickman, S. (1976) "Elevated methionine-tRNA synthetase activity in human colon cancer." Proc. Soc. Exp. Biol. Med. 153(2): 273-276

Labouesse, M., Netter, P. and Schroeder, R. (1984) "Molecular basis of the 'box effect', A maturase deficiency leading to the absence of splicing of two introns located in two split genes of yeast mitochondrial DNA." Eur. J. Biochem. 144(1): 85-93

Labouesse, M., Dujardin, G. and Slonimski, P.P. (1985) "The yeast nuclear gene NAM2 is essential for mitochondrial DNA integrity and can cure a mitochondrial RNA-maturase deficiency." Cell. 41(1): 133-143

Labouesse, M., Herbert, C.J., Dujardin, G. and Slonimski, P.P. (1987) "Three suppressor mutations which cure a mitochondrial RNA maturase deficiency occur at the same codon in the open reading frame of the nuclear NAM2 gene." EMBO J. 6(3): 713-721

Labouesse, M. (1990) "The yeast mitochondrial leucyl-tRNA synthetase is a splicing factor for the excision of several group I introns." Mol. Gen. Genet. 224(2): 209-221

Lambowitz, A.M. and Perlman, P.S. (1990) "Involvement of aminoacyl-tRNA synthetases and other proteins in group I and group II intron splicing." Trends Biochem. Sci. 15(11): 440-444

Lambowitz, A.M., Caprara, M. G., Zimmerly, S., and Perlman, P. S.(1999) "Group I and group II ribozymes as RNPs: Clues to the past and guides to the future" In: The RNA World, 2nd ed. (Gesteland, R., F., Cech, T., R., and Atkins, J., F., eds), Cold Spring Harbor Laboratory Press, New York, 451-485

Landschulz, W.H., Johnson, P.F. and McKnight, S.L. (1988) "The leucine zipper: a hypothetical structure common to a new class of DNA binding proteins." Science. 240(4860): 1759-1764

LaRiviere, F.J., Wolfson, A.D. and Uhlenbeck, O.C. (2001) "Uniform binding of aminoacyl-tRNAs to elongation factor Tu by thermodynamic compensation." Science. 294(5540): 165-168

Larkin, D.C., Williams, A. M., Martinis, S. A., and Fox, G. E. (2002) "Identification of essential domains for *Escherichia coli* $tRNA^{Leu}$ aminoacylation and amino acid editing using minimalist RNA molecules." Nucleic Acids Res. 30(2103-2113

Lazowska, J., Jacq, C. and Slonimski, P.P. (1980) "Sequence of introns and flanking exons in wild-type and box3 mutants of cytochrome b reveals an interlaced splicing protein coded by an intron." Cell. 22(2 Pt 2): 333-348

Lee, J.W., Beebe, K., Nangle, L.A., Jang, J., Longo-Guess, C.M., Cook, S.A., Davisson, M.T., Sundberg, J.P., Schimmel, P. and Ackerman, S.L. (2006) "Editing-defective tRNA synthetase causes protein misfolding and neurodegeneration." Nature. 443(7107): 50-55

Leibundgut, M., Frick, C., Thanbichler, M., Böck, A. and Ban, N. (2005) "Selenocysteine tRNA-specific elongation factor SelB is a structural chimaera of elongation and initiation factors." EMBO J. 24(1): 11-22

Lévque F., P.P., Dessen P., Blanquet S. (1990) "Homology of lysS and lysU, the two *Escherichia coli* genes encoding distinct lysyl-tRNA synthetase species " Nucleic Acids Res. 18(305-312

Li, G.Y., Herbert, C.J., Labouesse, M. and Slonimski, P.P. (1992) "*In vitro* mutagenesis of the mitochondrial leucyl-tRNA synthetase of *S. cerevisiae* reveals residues critical for its *in vivo* activities." Curr Genet. 22(1): 69-74

Li, G.Y., Becam, A.M., Slonimski, P.P. and Herbert, C.J. (1996) "*In vitro* mutagenesis of the mitochondrial leucyl tRNA synthetase of *Saccharomyces cerevisiae* shows that the suppressor activity of the mutant proteins is related to the splicing function of the wild-type protein." Mol. Gen. Genet. 252(6): 667-675

Li, L., Boniecki, M.T., Jaffe, J.D., Imai, B.S., Yau, P.M., Luthey-Schulten, Z.A. and Martinis, S.A. (2011) "Naturally occurring aminoacyl-tRNA synthetases editing-domain mutations that cause mistranslation in *Mycoplasma* parasites." Proc. Natl. Acad. Sci. U. S. A. 108(23): 9378-9383

Li, T., Li, Y., Guo, N., Wang, E. and Wang, Y. (1999) "Discrimination of $tRNA^{Leu}$ isoacceptors by the insertion mutant of *Escherichia coli* leucyl-tRNA synthetase." Biochemistry. 38(28): 9084-9088

Lin, L., Hale, S.P. and Schimmel, P. (1996) "Aminoacylation error correction." Nature. 384(6604): 33-34

Lincecum, T.L., Jr., Tukalo, M., Yaremchuk, A., Mursinna, R.S., Williams, A.M., Sproat, B.S., Van Den Eynde, W., Link, A., Van Calenbergh, S., Grötli, M., Martinis, S.A. and Cusack, S. (2003) "Structural and mechanistic basis of pre- and posttransfer editing by leucyl-tRNA synthetase." Mol. Cell. 11(4): 951-963

Ling, J., Reynolds, N. and Ibba, M. (2009) "Aminoacyl-tRNA synthesis and translational quality control." Annu. Rev. Microbiol. 63(61-78

Liu, C.C. and Schultz, P.G. (2010) "Adding new chemistries to the genetic code." Annu. Rev. Biochem. 79(413-444

Loftfield, R.B. (1963) "The frequency of errors in protein biosynthesis." Biochem. J. 89(82-92

Low, B., Gates, F., Goldstein, T. and Söll, D. (1971) "Isolation and partial characterization of temperature-sensitive *Escherichia coli* mutants with altered leucyl- and seryl-transfer ribonucleic acid synthetases." J. Bacteriol. 108(2): 742-750

Lupas, A. (1996) "Coiled coils: new structures and new functions." Trends. Biochem. Sci. 21(10): 375-382

Magliery, T.J., Wilson, C.G., Pan, W., Mishler, D., Ghosh, I., Hamilton, A.D. and Regan, L. (2005) "Detecting protein-protein interactions with a green fluorescent protein fragment reassembly trap: scope and mechanism." J. Am. Chem. Soc. 127(1): 146-157

Majumder, A.L., Akins, R.A., Wilkinson, J.G., Kelley, R.L., Snook, A.J. and Lambowitz, A.M. (1989) "Involvement of tyrosyl-tRNA synthetase in splicing of group I introns in *Neurospora crassa* mitochondria: biochemical and immunochemical analyses of splicing activity." Mol. Cell. Biol. 9(5): 2089-2104

Mannella, C.A., Collins, R.A., Green, M.R. and Lambowitz, A.M. (1979) "Defective splicing of mitochondrial rRNA in cytochrome-deficient nuclear mutants of *Neurospora crassa*." Proc. Natl. Acad. Sci. U. S. A. 76(6): 2635-2639

Martin, F., Eriani, G., Eiler, S., Moras, D., Dirheimer, G. and Gangloff, J. (1993) "Overproduction and purification of native and queuine-lacking *Escherichia coli* $tRNA^{Asp}$. Role of the wobble base in $tRNA^{Asp}$ acylation." J. Mol. Biol. 234(4): 965-974

Martinis, S.A. and Schimmel, P. (1992) "Enzymatic aminoacylation of sequence-specific RNA minihelices and hybrid duplexes with methionine." Proc. Natl. Acad. Sci. U. S. A. 89(1): 65-69

Martinis, S.A. and Fox, G.E. (1997) "Non-standard amino acid recognition by *Escherichia coli* leucyl-tRNA synthetase." Nucleic Acids Symp. Ser. 36(125-128

Martinis, S.A., Plateau, P., Cavarelli, J. and Florentz, C. (1999) "Aminoacyl-tRNA synthetases: a family of expanding functions." EMBO J. 18(17): 4591-4596

Martinis, S.A. and Boniecki, M.T. (2010) "The balance between pre- and post-transfer editing in tRNA synthetases." FEBS Lett. 584(2): 455-459

Mascarenhas, A.P. and Martinis, S.A. (2008) "Functional segregation of a predicted "hinge" site within the beta-strand linkers of *Escherichia coli* leucyl-tRNA synthetase." Biochemistry. 47(16): 4808-4816

Mascarenhas, A.P. and Martinis, S.A. (2009) "A glycine hinge for tRNA-dependent translocation of editing substrates to prevent errors by leucyl-tRNA synthetase." FEBS Lett. 583(21): 3443-3447

Mascarenhas, A.P., Martinis, S. A., An, S., Rosen, A. E., and Musier-Forsyth, K. (2008) "Fidelity mechanisms of the aminoacyl-tRNA synthetases in: Protein engineering (Rajbhandary, U. L., and Koehrer, C., Eds.)." Springer-Verlag. 153-200

McClain, W.H., Chen, Y.M., Foss, K. and Schneider, J. (1988) "Association of transfer RNA acceptor identity with a helical irregularity." Science. 242(4886): 1681-1684

McClain, W.H. and Foss, K. (1988) "Changing the identity of a tRNA by introducing a G-U wobble pair near the 3' acceptor end." Science. 240(4853): 793-796

Mechulam, Y., Schmitt, E., Maveyraud, L., Zelwer, C., Nureki, O., Yokoyama, S., Konno, M. and Blanquet, S. (1999) "Crystal structure of *Escherichia coli* methionyl-tRNA synthetase highlights species-specific features." J. Mol. Biol. 294(5): 1287-1297

Michel, F., Hanna, M., Green, R., Bartel, D.P. and Szostak, J.W. (1989) "The guanosine binding site of the *Tetrahymena* ribozyme." Nature. 342(6248): 391-395

Michel, F. and Westhof, E. (1990) "Modelling of the three-dimensional architecture of group I catalytic introns based on comparative sequence analysis." J. Mol. Biol. 216(3): 585-610

Minajigi, A. and Francklyn, C.S. (2010) "Aminoacyl transfer rate dictates choice of editing pathway in threonyl-tRNA synthetase." J. Biol. Chem. 285(31): 23810-23817

Miyawaki, A., Llopis, J., Heim, R., McCaffery, J.M., Adams, J.A., Ikura, M. and Tsien, R.Y. (1997) "Fluorescent indicators for Ca^{2+} based on green fluorescent proteins and calmodulin." Nature. 388(6645): 882-887

Muramatsu, T., Nishikawa, K., Nemoto, F., Kuchino, Y., Nishimura, S., Miyazawa, T. and Yokoyama, S. (1988) "Codon and amino-acid specificities of a transfer RNA are both converted by a single post-transcriptional modification." Nature. 336(6195): 179-181

Mursinna, R.S., Lincecum, T.L., Jr. and Martinis, S.A. (2001) "A conserved threonine within *Escherichia coli* leucyl-tRNA synthetase prevents hydrolytic editing of leucyl-tRNA^{Leu}." Biochemistry. 40(18): 5376-5381

Mursinna, R.S., Lee, K.W., Briggs, J.M. and Martinis, S.A. (2004) "Molecular dissection of a critical specificity determinant within the amino acid editing domain of leucyl-tRNA synthetase." Biochemistry. 43(1): 155-165

Mursinna, R.S., and Martinis S. A. (2002) "Rational design to block amino acid editing of a tRNA synthetase." J. Am. Chem. Soc. 124(25): 7286-7287

Nangle, L.A., Motta, C.M. and Schimmel, P. (2006) "Global effects of mistranslation from an editing defect in mammalian cells." Chem. Biol. 13(10): 1091-1100

Nangle, L.A., Zhang, W., Xie, W., Yang, X.L. and Schimmel, P. (2007) "Charcot-Marie-Tooth disease-associated mutant tRNA synthetases linked to altered dimer interface and neurite distribution defect." Proc. Natl. Acad. Sci. U. S. A. 104(27): 11239-11244

Nass, G., Poralla, K., and Zahner, H. (1969) "Effect of the antibiotic borrelidin on the regulation of threonine biosynthetic enzymes in *E. coli*." Biochem. Biophys. Res. Commun. 34(84-91

Nawaz, M.H., Pang, Y.L. and Martinis, S.A. (2007) "Molecular and functional dissection of a putative RNA-binding region in yeast mitochondrial leucyl-tRNA synthetase." J. Mol. Biol. 367(2): 384-394

Nawaz, M.H., and Martinis, S.A. (2008) "Chemistry of aminoacyl-tRNA synthetases." Wiley Encyclopedia of Chem. Biol. 1-12

Nomanbhoy, T.K., Hendrickson, T.L. and Schimmel, P. (1999) "Transfer RNA-dependent translocation of misactivated amino acids to prevent errors in protein synthesis." Mol. Cell. 4(4): 519-528

Nordin, B.E. and Schimmel, P. (2003) "Transiently misacylated tRNA is a primer for editing of misactivated adenylates by class I aminoacyl-tRNA synthetases." Biochemistry. 42(44): 12989-12997

Normanly, J., Ogden, R.C., Horvath, S.J. and Abelson, J. (1986) "Changing the identity of a transfer RNA." Nature. 321(6067): 213-219

Nureki, O., Vassylyev, D.G., Katayanagi, K., Shimizu, T., Sekine, S., Kigawa, T., Miyazawa, T., Yokoyama, S. and Morikawa, K. (1995) "Architectures of class-defining and specific domains of glutamyl-tRNA synthetase." Science. 267(5206): 1958-1965

Nureki, O., Vassylyev, D.G., Tateno, M., Shimada, A., Nakama, T., Fukai, S., Konno, M., Hendrickson, T.L., Schimmel, P. and Yokoyama, S. (1998) "Enzyme structure with two catalytic sites for double-sieve selection of substrate." Science. 280(5363): 578-582

Ogilvie, A., Wiebauer, K. and Kersten, W. (1975) "Inhibition of leucyl-transfer ribonucleic acid synthetasymol." Biochem. J. 152(3): 511-515

Ogle, J.M., Murphy, F.V., Tarry, M.J. and Ramakrishnan, V. (2002) "Selection of tRNA by the ribosome requires a transition from an open to a closed form." Cell. 111(5): 721-732

Palencia, A., Crépin, T., Vu. M., T., Lincecum, T., L., Jr., Martinis, S., A., and Cusack, S. (2012) "Structural dynamics of the aminoacylation and proof-reading functional cycle of bacterial leucyl-tRNA synthetase." In press.

Palmer, J.D. and Logsdon, J.M., Jr. (1991) "The recent origins of introns." Curr. Opin. Genet. Dev. 1(4): 470-477

Palmer, J.L., Masui, S., Pritchard, S., Kalousek, D.K. and Sorensen, P.H. (1997) "Cytogenetic and molecular genetic analysis of a pediatric pleomorphic sarcoma reveals similarities to adult malignant fibrous histiocytoma." Cancer Genet. Cytogenet. 95(2): 141-147

Pang, Y.L. and Martinis, S.A. (2009) "A paradigm shift for the amino acid editing mechanism of human cytoplasmic leucyl-tRNA synthetase." Biochemistry. 48(38): 8958-8964

Park, H.S., Hohn, M.J., Umehara, T., Guo, L.T., Osborne, E.M., Benner, J., Noren, C.J., Rinehart, J. and Söll, D. (2011) "Expanding the genetic code of *Escherichia coli* with phosphoserine." Science. 333(6046): 1151-1154

Park, S.G., Schimmel, P. and Kim, S. (2008) "Aminoacyl tRNA synthetases and their connections to disease." Proc. Natl. Acad. Sci. U. S. A. 105(32): 11043-11049

Paukstelis, P.J., Chen, J.H., Chase, E., Lambowitz, A.M. and Golden, B.L. (2008) "Structure of a tyrosyl-tRNA synthetase splicing factor bound to a group I intron RNA." Nature. 451(7174): 94-97

Paukstelis, P.J. and Lambowitz, A.M. (2008) "Identification and evolution of fungal mitochondrial tyrosyl-tRNA synthetases with group I intron splicing activity." Proc. Natl. Acad. Sci. U. S. A. 105(16): 6010-6015

Pauling, L.(1958) "The probability of errors in the process of synthesis of protein molecules. Festschrift Arthur Stöll Siebzigsten Geburtstag." Birkhauser Verlag, Basel, Switzerland: 597-602

Pelletier, J.N., Campbell-Valois, F.X. and Michnick, S.W. (1998) "Oligomerization domain-directed reassembly of active dihydrofolate reductase from rationally designed fragments." Proc. Natl. Acad. Sci. U. S. A. 95(21): 12141-12146

Perlman, P.S. and Butow, R.A. (1989) "Mobile introns and intron-encoded proteins." Science. 246(4934): 1106-1109

Perona, J.J., Rould, M.A. and Steitz, T.A. (1993) "Structural basis for transfer RNA aminoacylation by *Escherichia coli* glutaminyl-tRNA synthetase." Biochemistry. 32(34): 8758-8771

Polycarpo, C., Ambrogelly, A., Ruan, B., Tumbula-Hansen, D., Ataide, S.F., Ishitani, R., Yokoyama, S., Nureki, O., Ibba, M. and Söll, D. (2003) "Activation of the pyrrolysine

suppressor tRNA requires formation of a ternary complex with class I and class II lysyl-tRNA synthetases." Mol. Cell. 12(2): 287-294

Putney, S.D. and Schimmel, P. (1981) "An aminoacyl tRNA synthetase binds to a specific DNA sequence and regulates its gene transcription." Nature. 291(5817): 632-635

Retailleau, P., Weinreb, V., Hu, M. and Carter, C.W., Jr. (2007) "Crystal structure of tryptophanyl-tRNA synthetase complexed with adenosine-5' tetraphosphate: evidence for distributed use of catalytic binding energy in amino acid activation by class I aminoacyl-tRNA synthetases." J. Mol. Biol. 369(1): 108-128

Rho, S.B. and Martinis, S.A. (2000) "The bI4 group I intron binds directly to both its protein splicing partners, a tRNA synthetase and maturase, to facilitate RNA splicing activity." RNA. 6(12): 1882-1894

Rho, S.B., Lincecum, T.L., Jr. and Martinis, S.A. (2002) "An inserted region of leucyl-tRNA synthetase plays a critical role in group I intron splicing." EMBO J. 21(24): 6874-6881

Ribas de Pouplana, L. and Schimmel, P. (2001) "Two classes of tRNA synthetases suggested by sterically compatible dockings on tRNA acceptor stem." Cell. 104(2): 191-193

Richards, F.M. and Vithayathil, P.J. (1959) "The preparation of subtilisin-modified ribonuclease and the separation of the peptide and protein components." J. Biol. Chem. 234(6): 1459-1465

Rock, F.L., Mao, W., Yaremchuk, A., Tukalo, M., Crepin, T., Zhou, H., Zhang, Y.K., Hernandez, V., Akama, T., Baker, S.J., Plattner, J.J., Shapiro, L., Martinis, S.A., Benkovic, S.J., Cusack, S. and Alley, M.R. (2007) "An antifungal agent inhibits an aminoacyl-tRNA synthetase by trapping tRNA in the editing site." Science. 316(5832): 1759-1761

Romby, P., Caillet, J., Ebel, C., Sacerdot, C., Graffe, M., Eyermann, F., Brunel, C., Moine, H., Ehresmann, C., Ehresmann, B. and Springer, M. (1996) "The expression of *E.coli* threonyl-tRNA synthetase is regulated at the translational level by symmetrical operator-repressor interactions." EMBO J. 15(21): 5976-5987

Ross, C.A. and Poirier, M.A. (2004) "Protein aggregation and neurodegenerative disease." Nat. Med. 10 Suppl(S10-17

Rossi, F., Charlton, C.A. and Blau, H.M. (1997) "Monitoring protein-protein interactions in intact eukaryotic cells by β-galactosidase complementation." Proc. Natl. Acad. Sci. U. S. A. 94(16): 8405-8410

Rossmann, M.G., Moras, D. and Olsen, K.W. (1974) "Chemical and biological evolution of nucleotide-binding protein." Nature. 250(463): 194-199

Rould, M.A., Perona, J.J., Söll, D. and Steitz, T.A. (1989) "Structure of *E. coli* glutaminyl-tRNA synthetase complexed with $tRNA^{Gln}$ and ATP at 2.8 Å resolution." Science. 246(4934): 1135-1142

Roy, H. and Ibba, M. (2006) "Phenylalanyl-tRNA synthetase contains a dispensable RNA-binding domain that contributes to the editing of noncognate aminoacyl-tRNA." Biochemistry. 45(30): 9156-9162

Ruan, B. and Söll, D. (2005) "The bacterial YbaK protein is a Cys-tRNA^{Pro} and Cys-tRNA^{Cys} deacylase." J. Biol. Chem. 280(27): 25887-25891

Sampson, J.R. and Uhlenbeck, O.C. (1988) "Biochemical and physical characterization of an unmodified yeast phenylalanine transfer RNA transcribed *in vitro*." Proc. Natl. Acad. Sci. U. S. A. 85(4): 1033-1037

Sankaranarayanan, R., Dock-Bregeon, A.C., Romby, P., Caillet, J., Springer, M., Rees, B., Ehresmann, C., Ehresmann, B. and Moras, D. (1999) "The structure of threonyl-tRNA synthetase-tRNA^{Thr} complex enlightens its repressor activity and reveals an essential zinc ion in the active site." Cell. 97(3): 371-381

Sarkar, J., Mao, W., Lincecum, T.L., Jr., Alley, M.R. and Martinis, S.A. (2011) "Characterization of benzoxaborole-based antifungal resistance mutations demonstrates that editing depends on electrostatic stabilization of the leucyl-tRNA synthetase editing cap." FEBS Lett. 585(19): 2986-2991

Sarkar, J. and Martinis, S.A. (2011) "Amino-acid-dependent shift in tRNA synthetase editing mechanisms." J. Am. Chem. Soc. 133(46): 18510-18513

Sarkar, J., Poruri, K., Boniecki, M.T., McTavish, K.K. and Martinis, S.A. (2012) "The yeast mitochondrial leucyl-tRNA synthetase CP1 domain has functionally diverged to accommodate RNA splicing at the expense of hydrolytic editing." J. Biol. Chem, in press.

Sauerwald, A., Zhu, W., Major, T.A., Roy, H., Palioura, S., Jahn, D., Whitman, W.B., Yates, J.R., 3rd, Ibba, M. and Söll, D. (2005) "RNA-dependent cysteine biosynthesis in archaea." Science. 307(5717): 1969-1972

Scheper, G.C., van der Klok, T., van Andel, R.J., van Berkel, C.G., Sissler, M., Smet, J., Muravina, T.I., Serkov, S.V., Uziel, G., Bugiani, M., Schiffmann, R., Krageloh-Mann, I., Smeitink, J.A., Florentz, C., Van Coster, R., Pronk, J.C. and van der Knaap, M.S. (2007) "Mitochondrial aspartyl-tRNA synthetase deficiency causes leukoencephalopathy with brain stem and spinal cord involvement and lactate elevation." Nat. Genet. 39(4): 534-539

Schimmel, P. (1987) "Aminoacyl tRNA synthetases: general scheme of structure-function relationships in the polypeptides and recognition of transfer RNAs." Annu. Rev. Biochem. 56(125-158

Schimmel, P. and Schmidt, E. (1995) "Making connections: RNA-dependent amino acid recognition." Trends Biochem. Sci. 20(1): 1-2

Schimmel, P., Tao, J., and Hill, J. (1998) "Aminoacyl tRNA synthetases as targets for anti-infectives." *FASEB J.* 12(15): 1599-1609

Schmidt, E. and Schimmel, P. (1994) "Mutational isolation of a sieve for editing in a transfer RNA synthetase." Science. 264(5156): 265-267

Schreier, A.A. and Schimmel, P.R. (1972) "Transfer ribonucleic acid synthetase catalyzed deacylation of aminoacyl transfer ribonucleic acid in the absence of adenosine monophosphate and pyrophosphate." Biochemistry. 11(9): 1582-1589

Seiradake, E., Mao, W., Hernandez, V., Baker, S.J., Plattner, J.J., Alley, M.R. and Cusack, S. (2009) "Crystal structures of the human and fungal cytosolic leucyl-tRNA synthetase editing domains: A structural basis for the rational design of antifungal benzoxaboroles." J. Mol. Biol. 390(2): 196-207

Senger, B., Auxilien, S., Englisch, U., Cramer, F. and Fasiolo, F. (1997) "The modified wobble base inosine in yeast $tRNA^{Ile}$ is a positive determinant for aminoacylation by isoleucyl-tRNA synthetase." Biochemistry. 36(27): 8269-8275

Seraphin, B., Boulet, A., Simon, M. and Faye, G. (1987) "Construction of a yeast strain devoid of mitochondrial introns and its use to screen nuclear genes involved in mitochondrial splicing." Proc. Natl. Acad. Sci. U. S. A. 84(19): 6810-6814

Sethi, A., O'Donoghue, P. and Luthey-Schulten, Z. (2005) "Evolutionary profiles from the QR factorization of multiple sequence alignments." Proc. Natl. Acad. Sci. U. S. A. 102(11): 4045-4050

Shiba, K. and Schimmel, P. (1992) "Functional assembly of a randomly cleaved protein." Proc. Natl. Acad. Sci. U. S. A. 89(5): 1880-1884

Silvian, L.F., Wang, J. and Steitz, T.A. (1999) "Insights into editing from an Ile-tRNA synthetase structure with $tRNA^{Ile}$ and mupirocin." Science. 285(5430): 1074-1077

Soma, A., Kumagai, R., Nishikawa, K. and Himeno, H. (1996) "The anticodon loop is a major identity determinant of *Saccharomyces cerevisiae* $tRNA^{Leu}$." J. Mol. Biol. 263(5): 707-714

Soma, A., Uchiyama, K., Sakamoto, T., Maeda, M. and Himeno, H. (1999) "Unique recognition style of $tRNA^{Leu}$ by *Haloferax volcanii* leucyl-tRNA synthetase." J. Mol. Biol. 293(5): 1029-1038

Splan, K.E., Ignatov, M.E. and Musier-Forsyth, K. (2008) "Transfer RNA modulates the editing mechanism used by class II prolyl-tRNA synthetase." J. Biol. Chem. 283(11): 7128-7134

Srinivasan, G., James, C.M. and Krzycki, J.A. (2002) "Pyrrolysine encoded by UAG in Archaea: charging of a UAG-decoding specialized tRNA." Science. 296(5572): 1459-1462

Starzyk, R.M., Webster, T.A. and Schimmel, P. (1987) "Evidence for dispensable sequences inserted into a nucleotide fold." Science. 237(4822): 1614-1618

Stehlin, C., Heacock, D.H., 2nd, Liu, H. and Musier-Forsyth, K. (1997) "Chemical modification and site-directed mutagenesis of the single cysteine in motif 3 of class II *Escherichia coli* prolyl-tRNA synthetase." Biochemistry. 36(10): 2932-2938

Sugimoto, N., Kierzek, R. and Turner, D.H. (1988) "Kinetics for reaction of a circularized intervening sequence with CU, UCU, CUCU, and CUCUCU: mechanistic implications from the dependence on temperature and on oligomer and Mg^{2+} concentrations." Biochemistry. 27(17): 6384-6392

Sylvers, L.A., Rogers, K.C., Shimizu, M., Ohtsuka, E. and Söll, D. (1993) "A 2-thiouridine derivative in $tRNA^{Glu}$ is a positive determinant for aminoacylation by *Escherichia coli* glutamyl-tRNA synthetase." Biochemistry. 32(15): 3836-3841

t Hart, L.M., Hansen, T., Rietveld, I., Dekker, J.M., Nijpels, G., Janssen, G.M., Arp, P.A., Uitterlinden, A.G., Jorgensen, T., Borch-Johnsen, K., Pols, H.A., Pedersen, O., van Duijn, C.M., Heine, R.J. and Maassen, J.A. (2005) "Evidence that the mitochondrial leucyl tRNA synthetase (LARS2) gene represents a novel type 2 diabetes susceptibility gene." Diabetes. 54(6): 1892-1895

Tanaka, K., Tamaki, M. and Watanabe, S. (1969) "Effect of furanomycin on the synthesis of isoleucyl-tRNA." Biochim. Biophys. Acta. 195(1): 244-245

Tang, Y. and Tirrell, D.A. (2001) "Biosynthesis of a highly stable coiled-coil protein containing hexafluoroleucine in an engineered bacterial host." J. Am. Chem. Soc. 123(44): 11089-11090

Tang, Y. and Tirrell, D.A. (2002) "Attenuation of the editing activity of the *Escherichia coli* leucyl-tRNA synthetase allows incorporation of novel amino acids into proteins *in vivo*." Biochemistry. 41(34): 10635-10645

Tang, Y., Wang, P., Van Deventer, J.A., Link, A.J. and Tirrell, D.A. (2009) "Introduction of an aliphatic ketone into recombinant proteins in a bacterial strain that overexpresses an editing-impaired leucyl-tRNA synthetase." Chembiochem. 10(13): 2188-2190

Tao, J., and Schimmel, P. (2000) "Inhibitors of aminoacyl-tRNA synthetases as novel anti-infectives." Expert. Opin. Investig. Drugs. 9(1767-1775

Tardif, K.D. and Horowitz, J. (2002) "Transfer RNA determinants for translational editing by *Escherichia coli* valyl-tRNA synthetase." Nucleic Acids Res. 30(11): 2538-2545

Tinoco, I., Jr. and Bustamante, C. (1999) "How RNA folds." J. Mol. Biol. 293(2): 271-281

Tocchini-Valentini, G., Saks, M.E. and Abelson, J. (2000) "tRNA leucine identity and recognition sets." J. Mol. Biol. 298(5): 779-793

Tsien, R.Y. (1998) "The green fluorescent protein." Annu. Rev. Biochem. 67(509-544

Tsui, W.C. and Fersht, A.R. (1981) "Probing the principles of amino acid selection using the alanyl-tRNA synthetase from *Escherichia coli*." Nucleic Acids Res. 9(18): 4627-4637

Tukalo, M., Yaremchuk, A., Fukunaga, R., Yokoyama, S. and Cusack, S. (2005) "The crystal structure of leucyl-tRNA synthetase complexed with $tRNA^{Leu}$ in the post-transfer-editing conformation." Nat. Struct. Mol. Biol. 12(10): 923-930

Vu, M.T. and Martinis, S.A. (2007) "A unique insert of leucyl-tRNA synthetase is required for aminoacylation and not amino acid editing." Biochemistry. 46(17): 5170-5176

Vu, M.T. (2008) "Characterization of molecular structure-function relationship of *E. coli* LeuRS".

Wakasugi, K. and Schimmel, P. (1999) "Two distinct cytokines released from a human aminoacyl-tRNA synthetase." Science. 284(5411): 147-151

Wakasugi, K., Slike, B.M., Hood, J., Ewalt, K.L., Cheresh, D.A. and Schimmel, P. (2002a) "Induction of angiogenesis by a fragment of human tyrosyl-tRNA synthetase." J. Biol. Chem. 277(23): 20124-20126

Wakasugi, K., Slike, B.M., Hood, J., Otani, A., Ewalt, K.L., Friedlander, M., Cheresh, D.A. and Schimmel, P. (2002b) "A human aminoacyl-tRNA synthetase as a regulator of angiogenesis." Proc. Natl. Acad. Sci. U. S. A. 99(1): 173-177

Webster, T., Tsai, H., Kula, M., Mackie, G.A. and Schimmel, P. (1984) "Specific sequence homology and three-dimensional structure of an aminoacyl transfer RNA synthetase." Science. 226(4680): 1315-1317

Werner, R.G., Thorpe, L.F., Reuter, W. and Nierhaus, K.H. (1976) "Indolmycin inhibits prokaryotic tryptophanyl-tRNA ligase." Eur. J. Biochem. 68(1): 1-3

Williams, A.M. and Martinis, S.A. (2006) "Mutational unmasking of a tRNA-dependent pathway for preventing genetic code ambiguity." Proc. Natl. Acad. Sci. U. S. A. 103(10): 3586-3591

Wilson, C.G., Magliery, T.J. and Regan, L. (2004) "Detecting protein-protein interactions with GFP-fragment reassembly." Nat. Methods. 1(3): 255-262

Wong, F.C., Beuning, P.J., Nagan, M., Shiba, K. and Musier-Forsyth, K. (2002) "Functional role of the prokaryotic proline-tRNA synthetase insertion domain in amino acid editing." Biochemistry. 41(22): 7108-7115

Wong, F.C., Beuning, P.J., Silvers, C. and Musier-Forsyth, K. (2003) "An isolated class II aminoacyl-tRNA synthetase insertion domain is functional in amino acid editing." J. Biol. Chem. 278(52): 52857-52864

Yanagisawa, T., Lee, J.T., Wu, H.C. and Kawakami, M. (1994) "Relationship of protein structure of isoleucyl-tRNA synthetase with pseudomonic acid resistance of *Escherichia coli*. A proposed mode of action of pseudomonic acid as an inhibitor of isoleucyl-tRNA synthetase." J. Biol. Chem. 269(39): 24304-24309

Yarus, M. (1972) "Phenylalanyl-tRNA synthetase and isoleucyl-tRNA^{Phe} : a possible verification mechanism for aminoacyl-tRNA." Proc. Natl. Acad. Sci. U. S. A. 69(7): 1915-1919

Zaher, H.S. and Green, R. (2009) "Quality control by the ribosome following peptide bond formation." Nature. 457(7226): 161-166

Zaug, A.J., Grabowski, P.J. and Cech, T.R. (1983) "Autocatalytic cyclization of an excised intervening sequence RNA is a cleavage-ligation reaction." Nature. 301(5901): 578-583

Zhai, Y. and Martinis, S.A. (2005) "Two conserved threonines collaborate in the *Escherichia coli* leucyl-tRNA synthetase amino acid editing mechanism." Biochemistry. 44(47): 15437-15443

Zhai, Y., Nawaz, M.H., Lee, K.W., Kirkbride, E., Briggs, J.M. and Martinis, S.A. (2007) "Modulation of substrate specificity within the amino acid editing site of leucyl-tRNA synthetase." Biochemistry. 46(11): 3331-3337

Zhu, B., Yao, P., Tan, M., Eriani, G. and Wang, E.D. (2009) "tRNA-independent pretransfer editing by class I leucyl-tRNA synthetase." J. Biol. Chem. 284(6): 3418-3424

Appendix. Plasmid Constructs

Alias	Plasmid name	Parent vector	Description
pJSyc1	pJSycD487G	pHAPPY-1-1-0-1	Asp487 mutated to Gly
pJSyc2	pJSycD487N	pHAPPY-1-1-0-1	Asp487 mutated to Asn
pJSyc3	pJSycD487A	pHAPPY-1-1-0-1	Asp487 mutated to Ala
pJSyc4	pJSycD487K	pHAPPY-1-1-0-1	Asp487 mutated to Lys
pJSyc5	pJSycD487R	pHAPPY-1-1-0-1	Asp487 mutated to Arg
pJSyc6	pJSycD487E	pHAPPY-1-1-0-1	Asp487 mutated to Glu
pJSyc7	pJSycD487G/T319A	pJSycD487G	Asp487 mutated to Gly; Thr319 mutated to Ala
pJSyc8	pJSycD487N/T319A	pJSycD487N	Asp487 mutated to Asn; Thr319 mutated to Ala
pJSyc9	pJSycD487A/T319A	pJSycD487A	Asp487 mutated to Ala; Thr319 mutated to Ala
pJSyc10	pJSycD487K/R316D	pJSycD487K	Asp487 mutated to Lys; Arg316 mutated to Asp
pJSyc11	pJSycD487K/R316E	pJSycD487K	Asp487 mutated to Lys; Arg316 mutated to Glu
pJSyc12	pJSycD487R/R316D	pJSycD487R	Asp487 mutated to Arg; Arg316 mutated to Asp
pJSyc13	pJSycD487R/R316E	pJSycD487R	Asp487 mutated to Arg; Arg316 mutated to Glu
pJSyc14	pJS-pTrc-(*EcoRI*)-yctRNA$^{Leu}_{CAA}$-(*BamHI*)	pTrc	Wild type yc tRNA$^{Leu}_{CAA}$ cloned in pTrc vector between EcoRI and BamH1
pJSGFP15	pJS-Duet1-NZGFP(MCS1)	pETDuet-1	$(His)_6$-NZGFP cloned in MCS1 of pDuet1 vector between BamHI and EcoRI
pJSGFP16	pJS-Duet1-NZGFPexact(MCS1)	pETDuet-1	Specific amino acid deletions (Ref. Chapter V, Section V.2.A, p102) in NZGFP fragment within pDuet1 vector to mimic the same fragment in pET11a vector (Regan Lab, Yale)
pJSGFP17	pJS-Duet1-NZGFPexact(MCS1)-modified	pETDuet-1	BamHI site generated in MCS2 of pDuet1; XhoI site within the NZGFP sequence removed by conservative mutations (Ref. Chapter V, Section V.2.A, p103)
pJSGFP18	pJS-Duet1-NZGFPexact(MCS1)-WTecLRS(MCS2)	pETDuet-1	$(His)_6$-NZGFP and wild type *E. coli* LeuRS cloned in MCS1 and MCS2 of pDuet1 vector, respectively

Appendix. Plasmid Constructs (continued)

Alias	Plasmid name	Parent vector	Description
pJSGFP19	pJS-Duet1-NZGFPexact(MCS1)-YDDecLRS(MCS2)	pETDuet-1	$(His)_6$-NZGFP and YDD editing defective *E. coli* LeuRS cloned in MCS1 and MCS2 of pDuet1 vector, repectively
pJSspl20	p14JSymCP1-βext	pET14b	Isolated ymCP1-βext protein fragment: ym CP1 domain including the β-strands and extensions (Lys232 to Tyr452)
pJSspl21	p14JSymW238C-CP1-βext	pET14b	Isolated ymCP1-βext protein fragment bearing the mutation W238C
pJSspl22	pGEX2T-MAT2-bI4matfix	pGEX2T-MAT2	bI4 maturase gene corrected for missing Asn253